

UNCLASSIFIED

AD NUMBER

AD377064

CLASSIFICATION CHANGES

TO: UNCLASSIFIED

FROM: CONFIDENTIAL

LIMITATION CHANGES

TO:  
Approved for public release; distribution is unlimited.

FROM:  
Distribution authorized to U.S. Gov't. agencies and their contractors; Critical Technology; 15 SEP 1966. Other requests shall be referred to Air Force Rocket Propulsion Laboratory, Attn: STINFO, Edwards AFB, CA 93523. This document contains export-controlled technical data.

AUTHORITY

20 Dec 1985 per document markings; AFRPL ltr,  
20 Dec 1985

THIS PAGE IS UNCLASSIFIED

AD 377064

AUTHORITY:

AFRPL

14c 20 DEC 85



# **SECURITY**

---

# **MARKING**

**The classified or limited status of this report applies to each page, unless otherwise marked.**

**Separate page printouts MUST be marked accordingly.**

---

**THIS DOCUMENT CONTAINS INFORMATION AFFECTING THE NATIONAL DEFENSE OF THE UNITED STATES WITHIN THE MEANING OF THE ESPIONAGE LAWS, TITLE 18, U.S.C., SECTIONS 793 AND 794. THE TRANSMISSION OR THE REVELATION OF ITS CONTENTS IN ANY MANNER TO AN UNAUTHORIZED PERSON IS PROHIBITED BY LAW.**

**NOTICE: When government or other drawings, specifications or other data are used for any purpose other than in connection with a definitely related government procurement operation, the U. S. Government thereby incurs no responsibility, nor any obligation whatsoever; and the fact that the Government may have formulated, furnished, or in any way supplied the said drawings, specifications, or other data is not to be regarded by implication or otherwise as in any manner licensing the holder or any other person or corporation, or conveying any rights or permission to manufacture, use or sell any patented invention that may in any way be related thereto.**

**CONFIDENTIAL**

31

AFRPL-TR-66-301

(Unclassified Title)

**ADVANCED THRUST CHAMBER FOR SPACE**

**MANEUVERING PROPULSION**

**Task I System Studies  
Final Report**

**H. G. Diem**

**Rocketdyne  
A Division of North American Aviation, Inc.  
Canoga Park, California**

September 1966

**Group 4  
Downgraded at 3-Year Intervals  
Declassified After 12 Years**

THIS MATERIAL CONTAINS INFORMATION AFFECTING THE NATIONAL DEFENSE OF THE UNITED STATES WITHIN THE MEANING OF THE ESPIONAGE LAWS, TITLE 18 U.S.C., SECTIONS 793 AND 794, THE TRANSMISSION OR REVELATION OF WHICH IN ANY MANNER TO AN UNAUTHORIZED PERSON IS PROHIBITED BY LAW.



**In addition to security requirements which must be met, this document is subject to special export controls and each transmittal to foreign governments or foreign nationals may be made only with prior approval of AFRPL, Edwards, California 93523.**

**Air Force Rocket Propulsion Laboratory  
Research and Technology Division  
Edwards Air Force Base, California  
Air Force Systems Command  
United States Air Force**

**CONFIDENTIAL**

37064

**CONFIDENTIAL**

AFRPL-TR-66-501

(Unclassified Title)

**ADVANCED THRUST CHAMBER FOR SPACE**

**MANEUVERING PROPULSION**

**Task I System Studies**

**Final Report**

September 1966

**Group 4  
Downgraded at 3-Year Intervals  
Declassified After 12 Years**

THIS MATERIAL CONTAINS INFORMATION AFFECTING THE NATIONAL DEFENSE OF THE UNITED STATES WITHIN THE MEANING OF THE ESPIONAGE LAWS, TITLE 18 U.S.C., SECTIONS 793 AND 794, THE TRANSMISSION OR REVELATION OF WHICH IN ANY MANNER TO AN UNAUTHORIZED PERSON IS PROHIBITED BY LAW.

In addition to security requirements which must be met, this document is subject to special export controls and each transmittal to foreign governments or foreign nationals may be made only with prior approval of AFRPL, Edwards, California 93523.

**Air Force Rocket Propulsion Laboratory  
Research and Technology Division  
Edwards Air Force Base, California  
Air Force Systems Command  
United States Air Force**

**CONFIDENTIAL**

## FOREWORD

- (U) This technical report presents the results of the Task I study effort of the program titled "Advanced Thrust Chamber for Space Maneuvering Propulsion." The Task I studies of the program were conducted during the period 16 May to 15 August 1966. The Task II and III experimental phases of the program are scheduled for completion by 15 April 1967. The program was authorized by the USAF Rocket Propulsion Laboratory under Contract AFO4(611)-11617. The Air Force Program Manager is Mr. W. W. Wells, RPREC.
- (U) This publication was prepared by Rocketdyne, a Division of North American Aviation, Inc., as Report R-6730.
- (U) This technical report has been reviewed and is approved.

W. W. Wells, AFRLPL Program Manager

# CONFIDENTIAL

## ABSTRACT

- (C) The previous study results of Contract AF04(611)-10745 are extended to investigate the capabilities of increased gross weight Maneuvering Space Propulsion Systems (MSPS) using  $\text{LF}_2/\text{LH}_2$ ,  $\text{LO}_2/\text{LH}_2$ , and  $\text{N}_2\text{O}_4/\text{N}_2\text{H}_4$ -UDMH (50-50) propellants. The range of stage gross weights considered was based on the payload capabilities of Titan III-C and Saturn I-B and several growth versions of these launch vehicles. Maneuvering space propulsion system gross weights ranging from 20,000 to 50,000 pounds were shown to result in velocity increment capabilities up to 29,000 ft/sec for the 2000-pound payload  $\text{LF}_2/\text{LH}_2$  system.
- (C) The concentric aerodynamic spike/bell engine configuration was selected for the  $\text{LF}_2/\text{LH}_2$  and  $\text{LO}_2/\text{LH}_2$  system design thrust levels investigated. The configuration selected for the  $\text{N}_2\text{O}_4/\text{N}_2\text{H}_4$ -UDMH (50-50) consisted of one larger primary bell nozzle engine and two small secondary bell nozzle engines.
- (C) The orbit storage life capabilities of the three propellant combinations were determined and compared for a 20,000-pound-gross weight stage. The  $\text{LF}_2/\text{LH}_2$  system provided higher  $\Delta V$  capabilities than the other propellants for orbital storage times up to 2 years with full propellant tanks. The  $\Delta V$  advantage for the  $\text{LF}_2/\text{LH}_2$  systems is also maintained when mission duty cycles result in partial propellant loads for the major portion of the storage duration.

## CONTENTS

Foreword . . . . .	iii
Abstract . . . . .	v
<u>Section I</u> . . . . .	1
Introduction . . . . .	1
<u>Section II</u> . . . . .	3
Summary . . . . .	3
<u>Section III</u> . . . . .	5
Launch Vehicle Payload Capability Determination . . . . .	5
Candidate Launch Vehicle Description . . . . .	5
Ground Rules and Methods of Analysis . . . . .	9
Parametric MSPS Stage Description . . . . .	9
MSPS Velocity Capability . . . . .	10
Effect of Common MSPS Size on In-Orbit Velocity Capability. . . . .	27
<u>Section IV</u> . . . . .	45
Maneuvering Space Propulsion System Vehicle Configuration	
Selection and Optimization . . . . .	45
Definition of Propulsion System Requirements . . . . .	45
$LF_2/LH_2$ Systems . . . . .	46
$LO_2/LH_2$ Systems . . . . .	66
$N_2O_4/N_2H_4$ -UDMH (50-50) Systems . . . . .	81
Propulsion System Comparison . . . . .	119
<u>Section V</u> . . . . .	149
Maneuvering Space Propulsion System Orbital	
Life Investigation . . . . .	149
Ground Rules . . . . .	149
Vehicle Description . . . . .	152
Thermal Analysis . . . . .	152
Cryogenic Systems . . . . .	156
$N_2O_4/N_2H_4$ -UDMH (50-50) Systems . . . . .	185
Storage Life Comparison . . . . .	197
Storage System Sensitivity Analysis . . . . .	214
<u>Section VI</u> . . . . .	237
Conclusions . . . . .	237

<u>Appendix I</u>	
MSPS Mission Performance Exchange Factors . . . . .	239
<u>Appendix II</u>	
A Survey of High Performance Thermal Insulation . . . . .	243
<u>Appendix III</u>	
Internal Heating Effects . . . . .	257
<u>Appendix IV</u>	
Thermal Heat Short Analysis for the $LF_2/LH_2$ Vehicle . . . . .	261
<u>Appendix V</u>	
Temperature Control Surfaces for Use in Earth Orbital Environment . . . . .	267
<u>Appendix VI</u>	
Selection of Hydrogen Pressurant Injection Temperature . . . . .	269
<u>Appendix VII</u>	
Thermal Conditioning System . . . . .	273
<u>Appendix VIII</u>	
Correlation of Calculated Propellant Boiloff Rates With Test Data . . . . .	279
References . . . . .	283

# CONFIDENTIAL

## ILLUSTRATIONS

1. Uprated Titan Configurations . . . . .	6
2. Saturn IB Configurations . . . . .	7
3. Comparison of MSPS Performance with Titan III-C Launch Vehicle . . . . .	11
4. Suborbital Firing Effects on $F_2/H_2$ MSPS . . . . .	12
5. Comparison of MSPS Performance with Titan III-C Launch Vehicle . . . . .	13
6. Comparison of MSPS Performance with Titan III Seven-Segment 120-Inch Solids . . . . .	16
7. Comparison of MSPS Performance with Titan III Seven-Segment 120-Inch Solids . . . . .	17
8. Comparison of MSPS Performance with Titan III Three-Segment 156-Inch Solids . . . . .	18
9. Comparison of MSPS Performance with Titan III Three-Segment 156-Inch Solids . . . . .	19
10. Comparison of MSPS Performance with Saturn IB . . . . .	20
11. Comparison of MSPS Performance with Saturn IB . . . . .	21
12. Comparison of MSPS Performance with Saturn IB/Minuteman . . . . .	22
13. Comparison of MSPS Performance with Saturn IB/Minuteman . . . . .	23
14. Comparison of Nominal Titan and Saturn Launch Vehicles . . . . .	24
15. Comparison of Titan Launch Vehicles . . . . .	25
16. Comparison of Saturn Launch Vehicles . . . . .	26
17. Size Comparison of Selected Gross Weights for 5000- and 2000-Pound-Payload Fluorine-Hydrogen MSPS . . . . .	33
18. Effect of System Gross Weight and Design Thrust Level on Overall Throttling Requirements . . . . .	47
19. Advanced Engines Selected for Further Analysis . . . . .	49
20. Chamber Pressure-Expansion Area Ratio Optimization for Fluorine/Hydrogen 30,000 lbf Aerodynamic Spike Engine . . . . .	53
21. Chamber Pressure-Expansion Area Ratio Optimization for Fluorine-Hydrogen 50,000 lbf Aerodynamic Spike Engine . . . . .	54
22. Chamber Pressure-Expansion Area Ratio Optimization for Fluorine-Hydrogen 75,000 lbf Aerodynamic Spike Engine . . . . .	55

# CONFIDENTIAL

23.	Effect of Throttling on 30,000 lbf Aerodynamic Spike Engine Fluorine-Hydrogen Propellant with a 10:1 Throttling Ratio . . . . .	57
24.	Duty Cycle Influence on Design Parameter Selection for 30,000-Pound-Thrust $F_2/H_2$ Aerodynamic Spike Engine . . . . .	57
25.	Chamber Pressure-Expansion Area Ratio Optimization for Fluorine-Hydrogen 3,300 lbf Bell Engine . . . . .	61
26.	Chamber Pressure-Expansion Area Ratio Optimization for Fluorine-Hydrogen 5,000 lbf Bell Engine . . . . .	62
27.	Chamber Pressure-Expansion Area Ratio Optimization for Fluorine-Hydrogen 7,500 lbf Bell Engine . . . . .	63
28.	Throttling Effects on Chamber Pressure-Expansion Area Ratio Optimization for Liquid Fluorine-Hydrogen 3300 lbf Bell Engine, 10:1 Throttled Operation . . . . .	65
29.	Duty Cycle Influence on Design Parameter Selection for 3300-Pound-Thrust $F_2/H_2$ Bell Engine . . . . .	67
30.	Chamber Pressure-Expansion Area Ratio Optimization for Oxygen-Hydrogen 30,000 lbf Aerodynamic Spike Engine . . . . .	71
31.	Chamber Pressure-Expansion Area Ratio Optimization for Oxygen-Hydrogen 50,000 lbf Aerodynamic Spike Engine . . . . .	72
32.	Chamber Pressure-Expansion Area Ratio Optimization for Oxygen-Hydrogen 75,000 lbf Aerodynamic Spike Engine . . . . .	73
33.	Throttling Effect on Chamber Pressure-Expansion Area Ratio Optimization for Liquid Oxygen-Hydrogen 30,000 lbf Aerospike Engine . . . . .	74
34.	Duty Cycle Influence on 30,000-Pound-Thrust $O_2/H_2$ Aerodynamic Spike Engine . . . . .	76
35.	Chamber Pressure-Expansion Area Ratio Optimization for Oxygen-Hydrogen 3300 lbf Bell Engine . . . . .	77
36.	Chamber Pressure-Expansion Area Ratio Optimization for Oxygen-Hydrogen 5,000 lbf Bell Engine . . . . .	78
37.	Chamber Pressure-Expansion Area Ratio Optimization for Oxygen-Hydrogen 7500 lbf Bell Engine . . . . .	79
38.	Throttling Effects on Chamber Pressure-Expansion Area Ratio Optimization for Liquid Oxygen-Hydrogen 3,300 lbf Bell Engine . . . . .	80
39.	Duty Cycle Influence on Design Parameter Selection for 3300-Pound-Thrust $O_2/H_2$ Bell Engine . . . . .	82

x

# CONFIDENTIAL

# CONFIDENTIAL

40. Minimum Area Ratio for Attaching a Radiation Cooled Nozzle . . .	85
41. Regenerative Coolant Jacket Pressure Drops . . . . .	86
42. Throttling Limits for a Regeneratively Cooled Storable Propellant Thrust Chamber . . . . .	88
43. Throttling Limits for a Regeneratively Cooled, 25,000-Pound- Thrust $N_2O_4/N_2H_4$ -UDMH(50-50) Propellant Thrust Chamber . . . .	89
44. Throttling Limits for a Regenerative Cooled $N_2O_4/N_2H_4$ - UDMH(50-50) 5000-Pound-Thrust Propellant Thrust Chamber . . . .	90
45. Throttling Limits for a Regeneratively Cooled $N_2O_4/N_2H_4$ - UDMH (50-50) Propellant Thrust Chamber . . . . .	91
46. Throttling Limits for a Regenerative Cooled $N_2O_4/N_2H_4$ - UDMH(50-50) Propellant Thrust Chamber . . . . .	92
47. Effect of Nominal Thrust Level on Maximum Feasible Throttle Ratio . . . . .	93
48. Film Cooling Requirements for Conventional Bell Nozzle Thrust Chamber . . . . .	95
49. Ablative Material Thickness vs Burning Duration . . . . .	97
50. Chamber Pressure-Expansion Area Ratio Optimization for $N_2O_4/N_2H_4$ -UDMH (50-50)25,700-Pound-Thrust Bell Engine at Full Thrust . . . . .	111
51. Chamber Pressure-Expansion Area Ratio Optimization for $N_2O_4/N_2H_4$ -UDMH (50-50) 42,900-Pound-Thrust Bell Engine at Full Thrust . . . . .	112
52. Chamber Pressure-Expansion Area Ratio Optimization for $N_2O_4/N_2H_4$ -UDMH (50-50) 64,300-Pound-Thrust Bell Engine at Full Thrust . . . . .	113
53. Chamber Pressure-Expansion Area Ratio Optimization for $N_2O_4/N_2H_4$ -UDMH (50-50) 25,700-Pound-Thrust Bell Engine . . . .	114
54. Chamber Pressure-Expansion Area Ratio Optimization for $N_2O_4/N_2H_4$ -UDMH (50-50) 42,900-Pound-Thrust Bell Engine . . . .	115
55. Chamber Pressure-Expansion Area Ratio Optimization for $N_2O_4/N_2H_4$ -UDMH (50-50) 64,300-Pound-Thrust Bell Engine . . . .	116

# CONFIDENTIAL

56. Chamber Pressure-Expansion Area Ratio Optimization for $N_2O_4/N_2H_4$ -UDMH (50-50) 5,370-Pound-Thrust Bell Engine at Full Thrust . . . . .	117
57. Chamber Pressure-Expansion Area Ratio Optimization for $N_2O_4/N_2H_4$ -UDMH (50-50) 5,370-Pound Thrust Bell Engine . . . . .	118
58. 50,000-Pound-Thrust $LF_2/LH_2$ MSPS Engine Performance . . . . .	124
59. $LH_2/LF_2$ MSPS, 36,000-Pound Gross Weight, 50,000-Pound-Thrust . . . . .	125
60. 50,000-Pound-Thrust $LO_2/LH_2$ MSPS Performance . . . . .	132
61. $LO_2/LH_2$ MSPS, 36,000-Pound Gross Weight, 50,000-Pound-Thrust . . . . .	135
62. 50,000-Pound-Thrust $N_2O_4/N_2H_4$ -UDMH (50-50) MSPS Performance . . . . .	142
63. $N_2O_4/N_2H_4$ -UDMH (50-50) Engine MSPS, 36,000-Pound Gross Weight, 50,000-Pound-Thrust . . . . .	143
64. Orbital Orientations . . . . .	150
65. Temperature History During Boost Phase for Nominal Vehicle Launched by Titan III-C From WTR . . . . .	155
66. $LF_2/LH_2$ Alternate Mission Vehicle . . . . .	157
67. Maximum and Minimum Possible Outer Wall Temperatures for a Vehicle in any 100 n mi Circular Earth Orbit in the Limit of Negligible Heat Transfer to the Propellants . . . . .	161
68. Ullage Requirement as a Function of Allowable Vapor Pressure for Liquid Hydrogen, Fluorine, and Oxygen . . . . .	163
69. Specific Heat Input to Tank by Radiation as a Function of Insulation Thickness . . . . .	164
70. Percentage of Liquid Fluorine Remaining as a Function of Percentage Used for First Firing for $LF_2/LH_2$ Vehicle (Helium Pressurant) . . . . .	166
71. Total Fluorine Tank Pressure as a Function of Percentage of Initial Propellant Loading Used for First Firing for $LF_2/LH_2$ Vehicle (Helium Pressurant) . . . . .	167
72. Fluorine Vapor Pressure as a Function of Time in Orbit for Various Preorbital Conditions . . . . .	168
73. Percentage of Liquid Fluorine Remaining as a Function of Storage Time for 10-Percent Remaining on First Day for $LF_2/LH_2$ Vehicle (Helium Pressurant) . . . . .	169

# CONFIDENTIAL

74.	Total Fluorine Tank Pressure as a Function of Storage Time for 10-Percent of Original Propellant Loading Remaining as a Liquid on the First Day for $LF_2/LH_2$ Vehicle (Helium Pressurant) . . . . .	170
75.	Hydrogen Vapor Pressure as a Function of Propellant Usage for First Firing for $LF_2/LH_2$ Vehicle . . . . .	172
76.	Percentage of Liquid Hydrogen Remaining as a Function of Percentage Used for First Firing for $LF_2/LH_2$ Vehicle (Hydrogen Pressurant) . . . . .	173
77.	Hydrogen Vapor Pressure as a Function of Time for Various Pre-orbital Conditions . . . . .	174
78.	Percentage of Liquid Hydrogen Remaining as a Function of Orbital Storage Time and Hydrogen Pressurant Temperature . . . . .	175
79.	Hydrogen Vapor Pressure as a Function of Storage Time and Hydrogen Pressurant Temperature for 10 Percent of Hydrogen Remaining After the First Day . . . . .	176
80.	Hydrogen Vapor Pressure as a Function of Propellant Used for First Firing, No Preorbital Heating, Hydrogen Pressurant, for $LF_2/LH_2$ Vehicle . . . . .	177
81.	Percentage of Liquid Hydrogen Remaining as a Function of Initial Propellant Loading Used for First Firing . . . . .	178
82.	Percentage of Hydrogen Vented to Space as a Function of Orbital Storage Time for Various Preorbital Conditions for $LF_2/LH_2$ Vehicle . . . . .	180
83.	Percentage of Liquid Oxygen Remaining as a Function of Propellant Used for First Firing . . . . .	181
84.	Total Oxygen Tank Pressure as a Function of Propellant Used for First Firing for $LO_2/LH_2$ Vehicle (Helium Pressurant) . . . . .	182
85.	Percentage of Liquid Oxygen Remaining as a Function of Storage Time, for 10 Percent Remaining on First Day (Helium Pressurant) . . . . .	183
86.	Total Oxygen Tank Pressure as a Function of Storage Time, for 10 Percent Remaining on First Day (Helium Pressurant) . . . . .	184

# CONFIDENTIAL

87.	Percentage of Liquid Hydrogen Remaining as a Function of Percentage Used for First Firing for $\text{LO}_2/\text{LH}_2$ Vehicle (Hydrogen Pressurant) . . . . .	186
88.	Hydrogen Vapor Pressure as a Function of Initial Propellant Loading Used for First Firing for $\text{LO}_2/\text{LH}_2$ Vehicle . . . . .	187
89.	Hydrogen Vapor Pressure as a Function of Time in Orbit for Various Pre-Orbital Conditions . . . . .	188
90.	Percentage of Liquid Hydrogen Remaining as a Function of Orbital Storage Time, for 10 Percent Remaining on First Day, Hydrogen Pressurant . . . . .	189
91.	Hydrogen Vapor Pressure as a Function of Storage Time, for 10 Percent Remaining on First Day, Hydrogen Pressurant . . . . .	190
92.	Storable Propellant Alternate Mission Vehicle, 5000-Pound Payload . . . . .	191
93.	Wall Temperature Ranges for a Vehicle in 100 n mi Circular Earth Orbit . . . . .	194
94.	Vehicle Outer Wall Temperature as a Function of Orbital Position . . . . .	196
95.	Required Insulation for NT0/50-50 Vehicle, 2% Ullage in Both Tanks . . . . .	198
96.	Design Point Ullage as a Function of Time for Performance Comparison . . . . .	205
97.	Point Design Insulation Thickness as a Function of Required Storage Time . . . . .	206
98.	Point Design Insulation Thickness as a Function of Required Storage Time . . . . .	208
99.	Point Design Insulation Thickness as a Function of Required Storage Time for the $\text{N}_2\text{O}_4/\text{N}_2\text{H}_4$ -UDMH (50-50) Vehicle . . . . .	209
100.	Full Tank Cycle Pressure History (Hydrogen) . . . . .	210
101.	90/10 Cycle Pressure History (Hydrogen) . . . . .	211
102.	Vehicle Performance Comparison for Full Tank Complete Depletion Mission . . . . .	213
103.	Vehicle Performance Comparison for 90/10 Duty Cycle Mission . . . . .	215
104.	Insulation Thickness Required to Perform 14-Day Mission as a Function of Thermal Resistivity for an Unvented Vehicle . . . . .	217

# CONFIDENTIAL

105.	Relative Velocity Increment as a Function of Effective Thermal Resistivity of Wall-to-Tank Connections, 14-Day Mission . . . . .	218
106.	Maximum Unvented Storage Time as a Function of Thermal Resistivity for Perfect Insulation and for Six Inches of Insulation . . . . .	220
107.	Relative Velocity Increment as a Function of $\rho k$ Product of Thermal Insulation for the $LF_2/LH_2$ Vehicle on a 14-Day Mission . . . . .	221
108.	Required Insulation Thickness as a Function of Outer Wall Absorptivity-to-Emissivity Ratio for the $LF_2/LH_2$ Vehicle on a 14-Day Mission . . . . .	222
109.	Vehicle Performance as a Function of Outer Wall Absorptivity-to-Emissivity Ratio for the $LF_2/LH_2$ Vehicle on a 14-Day Mission . . . . .	223
110.	Performance of $LF_2/LH_2$ Vehicle with Different Hydrogen Tank Pressurant Temperatures . . . . .	224
111.	Vehicle Performance for a 14-Day Mission as a Function of Pressurant Vent Pressure for $LF_2/LH_2$ Vehicle . . . . .	226
112.	Storage Time Limits as a Function of Pressurant Vent Pressure . . . . .	227
113.	Performance Comparison of $LF_2/LH_2$ Vehicle with and Without a Propellant Utilization System . . . . .	229
114.	Performance Comparison of $LF_2/LH_2$ Vehicle With and Without a Propellant Utilization System . . . . .	230
115.	Required Insulation as a Function of Ullage for the $LF_2/LH_2$ Vehicle on a 14-Day Mission . . . . .	231
116.	Maximum Unvented Storage Time for $LF_2/LH_2$ Vehicle Hydrogen Tank as a Function of Ullage Volume . . . . .	232
117.	Required Insulation Thickness for 14-Day Mission as a Function of Propellant Loading . . . . .	234
118.	Maximum Unvented Storage Time as a Function of Propellant Loading for Perfect Insulation and for Six Inches of Insulation for $F_2/H_2$ Vehicle . . . . .	235

# CONFIDENTIAL

119.	Effect of Structure Weight Change on $\Delta V$ Capability for 2000-Pound and 5000-Pound Payloads . . . . .	240
120.	Methods of Attachment . . . . .	246
121.	Cross Section of Three Installed Button Blankets . . . . .	248
122.	Insulation Systems . . . . .	251
123.	Effects of Hydrogen Pressurant Temperature and Insulation on Hydrogen Boiloff for 90/10 Duty Cycle . . . . .	271
124.	Hydrogen Tank Pressurant Inlet Temperature and Insulation Optimization, 90/10 Duty Cycle . . . . .	272
125.	Conceptual Thermal Conditioning Systems . . . . .	275
126.	Boiloff Rate vs $\alpha/\epsilon$ . . . . .	281
127.	Boiloff Rate vs $\alpha/\epsilon$ . . . . .	282

# CONFIDENTIAL

## TABLES

I. Selected Engine Design Parameters . . . . .	4
II. Titan III Launch Vehicle Descriptions . . . . .	8
III. Launch Vehicle Comparison Chart for 2000-Pound Payload $LF_2/LH_2$ MSPS . . . . .	28
IV. $LF_2/LH_2$ MSPS Performance Characteristics for 2000-Pound Payload . . . . .	29
V. Launch Vehicle Comparison Chart for 5000-Pound Payload $LF_2/LH_2$ MSPS . . . . .	31
VI. $LF_2/LH_2$ MSPS Performance Characteristics for 5000-Pound Payload . . . . .	32
VII. Performance Comparison Between 2000- and 5000-Pound Payloads ( $LF_2/LH_2$ MSPS) . . . . .	34
VIII. Launch Vehicle Comparison Chart for 2000-Pound Payload ( $LO_2/LH_2$ ) . . . . .	35
IX. $LO_2/LH_2$ MSPS Performance Characteristics for 2000-Pound Payload . . . . .	36
X. Launch Vehicle Comparison Chart for 5000-Pound Payload ( $LO_2/LH_2$ ) . . . . .	37
XI. $LO_2/LH_2$ MSPS Performance Characteristics for 5000-Pound Payload . . . . .	38
XII. Launch Vehicle Comparison Chart for 2000-Pound Payload ( $N_2O_4/N_2H_4$ -UDMH (50-50)) . . . . .	40
XIII. $N_2O_4/N_2H_4$ -UDMH (50-50) MSPS Performance Characteristics for 2000-Pound Payload . . . . .	41
XIV. Launch Vehicle Comparison Chart for 5000-Pound Payload ( $N_2O_4/N_2H_4$ -UDMH, 50-50) . . . . .	42
XV. $N_2O_4/N_2H_4$ -UDMH (50-50) MSPS Performance Characteristics For 5000-Pound Payload . . . . .	43
XVI. Main Engine Selection Criteria . . . . .	48
XVII. $LF_2/LH_2$ System Operating Characteristics . . . . .	52
XVIII. Optimum Operating Parameters for $LF_2/LH_2$ Aerodynamic Spike Thrust Chambers for Continuous Operation at Full Thrust . . . . .	50

# CONFIDENTIAL

XIX.	Design Parameter Selection for $LF_2/LH_2$ Propulsion Systems . . . . .	60
XX.	$LO_2/LH_2$ System Operating Characteristics . . . . .	69
XXI.	Design Parameter Selection for $LO_2/LH_2$ Propulsion Systems . . . . .	81
XXII.	Candidate Propulsion Systems Selected for Evaluation . . . . .	99
XXIII.	Engine Selection Criteria . . . . .	102
XXIV.	Engine Selection Evaluation . . . . .	105
XXV.	$N_2O_4/N_2H_4$ -UDMH (50-50) Bell Nozzle Engines System Operating Characteristics . . . . .	110
XXVI.	$N_2O_4/N_2H_4$ -UDMH (50-50) Engine Parameter Selection . . . . .	120
XXVII.	50,000-Pound-Thrust $LF_2/LH_2$ MSPS Engine Operating Characteristics . . . . .	123
XXVIII.	$LF_2/LH_2$ MSPS Vehicle Weight Summary . . . . .	127
XXIX.	Mission Performance Capabilities for $LF_2/LH_2$ MSPS . . . . .	129
XXX.	50,000-Pound-Thrust $LO_2/LH_2$ MSPS Engine Operating Characteristics . . . . .	131
XXXI.	$LO_2/LH_2$ MSPS Weight Summary . . . . .	137
XXXII.	Mission Performance Capabilities for $LO_2/LH_2$ MSPS . . . . .	139
XXXIII.	50,000-Pound-Thrust $N_2O_4/N_2H_4$ -UDMH (50-50) MSPS Engine Operating Characteristics . . . . .	141
XXXIV.	$N_2O_4/N_2H_4$ -UDMH (50-50) MSPS Vehicle Weight Summary . . . . .	146
XXXV.	Mission Performance Capabilities for $N_2O_4/N_2H_4$ -UDMH (50-50) MSPS . . . . .	147
XXXVI.	Vehicle Characteristics . . . . .	153
XXXVII.	System Operating Limits . . . . .	185
XXXVIII.	Centaur Launch Countdown Atlas-Centaur No. 5, March 1965 Launch . . . . .	200
XXXIX.	Maneuvering Propulsion System Thermal Protection Design . . . . .	201
XL.	Propulsion System Description . . . . .	203
XLI.	Specific Impulse Gain Factors . . . . .	241
XLII.	Design of Superinsulations . . . . .	244
XLIII.	Properties of Superinsulation . . . . .	245
XLIV.	Design Requirements . . . . .	247
XLV.	Insulation Systems . . . . .	253

**CONFIDENTIAL**

XLVI.	Substrate Material Properties . . . . .	254
XLVII.	Feed Lines . . . . .	262
XLVIII.	Vent Lines . . . . .	263
XLIX.	Fill Lines . . . . .	264
L.	Total Thermal Resistivity . . . . .	265
LI.	Radiation Properties of Coatings . . . . .	268
LII.	Component Parameters . . . . .	276
LIII.	Storage Characteristics of Selected Cryogenic Propellants . . . . .	280

# CONFIDENTIAL

## SECTION I

### INTRODUCTION

- (C) A study was conducted under Contract AF04(611)-10745 to define an advanced  $LF_2/LH_2$  Maneuvering Space Propulsion System (MSPS). For adaptability to the Titan III-C launch vehicle, the gross weight was selected to be 20,000 pounds. The study concluded that the optimum concept for the main engine was a 30,000-pound-thrust toroidal aerospike thrust chamber with a 3300-pound-thrust bell thrust chamber in the center of the toroid. This engine configuration offers the advantages of high performance over a wide throttle range and thrust alignment through the vehicle center-of-gravity for both chambers.
- (C) Because of the potential mission performance capability gains of the system, the analyses of the previous study were extended under this program, Contract AF04(611)-11617, to define the advantages offered by increasing the stage weight above 20,000 pounds for application with Titan III-C and Saturn IB launch vehicles and growth versions of these launch vehicles. Maximum payload capabilities of the launch vehicles for polar launches from the Western Test Range with payload injection into a 100 nautical mile orbit were to be determined. Optimum MSPS gross weights and configurations to maximize  $\Delta V$  for the propellant combinations of  $LF_2/LH_2$ ,  $LO_2/LH_2$  and  $N_2O_4/N_2H_4$ -UDMH (50-50) were then to be defined for each of the candidate launch vehicles.
- (U) An additional objective of the study was to determine the orbital life capabilities of the 20,000-pound gross weight systems beyond the previously studied requirement of 14 days. The  $LF_2/LH_2$ ,  $LO_2/LH_2$  and  $N_2O_4/N_2H_4$ -UDMH (50-50) system configurations defined in Contract AF04(611)-10745 (Ref. 2) were to be used for this analysis and their capabilities compared.
- (U) The above studies have been defined as Task I of the current program. Tasks II and III of the program are experimental efforts which are directed to verify the performance, regenerative cooling capability, and structural integrity of the 30,000-pound-thrust toroidal thrust chamber. The Task II and III efforts will be completed by April 1967 and will be reported separately.

# CONFIDENTIAL

## SECTION II

### SUMMARY

- (C) The launch vehicle payload studies defined the range of Maneuvering Space Propulsion System gross weights of interest for the Titan III-C and Saturn IB launch vehicles, and their growth versions. Two MSPS payloads, 2000 and 5000 pounds, were used in the analysis. MSPS vehicles using three different propellant combinations,  $\text{LF}_2/\text{LH}_2$ ,  $\text{LO}_2/\text{LH}_2$ , and  $\text{N}_2\text{O}_4/\text{N}_2\text{H}_4$ -UDMH (50-50), were investigated.
- (C) The studies have shown that as MSPS gross weight is increased, for the various launch vehicles and payloads considered, greater orbital maneuvering  $\Delta V$  can be achieved up to the point where suborbital burn of the MSPS is required (5 to 58 percent increase referred to a 20,000-pound gross weight system). For most cases of launch vehicles and payloads, the  $\Delta V$  advantage obtained as a result of the sub-orbital firing is slight (0 to 3 percent). For the nominal Titan III-C and Saturn I-B vehicles, however, the 5000-pound payload  $\text{LF}_2/\text{LH}_2$  MSPS achieved significant increases in  $\Delta V$  (14 percent) with suborbital burn and increasing gross weight.
- (U) Based on the results of the launch vehicle payload capability analyses, a single gross weight MSPS was selected for each propellant combination and MSPS payload. Use of the selected gross weight MSPS with each of the launch vehicles resulted in near maximum  $\Delta V$  capabilities, particularly for the cryogenic systems. The maximum loss, which was for the storable propellant system, was 8 percent. Losses for other conditions were generally much lower. It was found that the two payloads considered required two relatively different thrust levels and gross weights to achieve near-maximum  $\Delta V$  values. It is possible to select a compromise gross weight and thrust level which would accommodate either payload, but this may be done only with a small  $\Delta V$  penalty for each payload.
- (U) Configuration selection and design parameter optimization studies were conducted in parallel with the launch vehicle payload capability studies to determine the most efficient propulsion systems for each of the propellant combinations, MSPS gross weights within the applicable range, and corresponding design thrust levels. Design layouts, stage weights, and performance of the optimized propulsion systems were compared, as were the mission performance capabilities for each of the systems in conjunction with each of the launch vehicles.
- (C) The concentric aerodynamic spike/bell propulsion system was selected for the  $\text{LF}_2/\text{LH}_2$  and  $\text{LO}_2/\text{LH}_2$  propellants and for design thrust levels of 30,000 to 75,000 pounds. The selected  $\text{N}_2\text{O}_4/\text{N}_2\text{H}_4$ -UDMH (50-50) propulsion system for the range of design thrust levels of interest was a single primary bell nozzle engine flanked by two, lower-thrust, secondary bell nozzle engines. The maximum performance design parameters were determined for each of these engines. These are shown in Table I for the range of design thrust levels.

# CONFIDENTIAL

TABLE I  
SELECTED ENGINE DESIGN PARAMETERS

LF <sub>2</sub> /LH <sub>2</sub> System						
System Design Thrust, lb x 10 <sup>3</sup>	Aerospike			Bell		
	Thrust, lb x 10 <sup>3</sup>	Chamber Pressure, psia	Expansion Ratio Area	Thrust, lb x 10 <sup>3</sup>	Chamber Pressure, psia	Expansion Ratio Area
30	30	650	63	3.3	500	100
50	50	700	100	5.0	625	200
75	75	800	100	7.5	740	200

LO <sub>2</sub> /LH <sub>2</sub> System						
System Design Thrust, lb x 10 <sup>3</sup>	Aerospike			Bell		
	Thrust, lb x 10 <sup>3</sup>	Chamber Pressure, psia	Expansion Ratio Area	Thrust, lb x 10 <sup>3</sup>	Chamber Pressure, psia	Expansion Ratio Area
30	30	800	100	3.3	500	100
50	50	800	100	5.0	625	200
75	75	800	100	7.5	740	200

N <sub>2</sub> O <sub>4</sub> /N <sub>2</sub> H <sub>4</sub> -UDMH (50-50) System						
System Design Thrust, lb x 10 <sup>3</sup>	Primary Engine			Secondary Engine		
	Thrust, lb x 10 <sup>3</sup>	Chamber Pressure, psia	Expansion Ratio Area	Thrust, lb x 10 <sup>3</sup>	Chamber Pressure, psia	Expansion Ratio Area
30	25.7	1000	50	2.15	500	200
50	42.8	1000	50	3.6	500	200
75	64.3	1000	50	5.33	800	200

- (C) The orbital storage capabilities were determined for each of the propellant combinations to define the system velocity increment capabilities as a function of storage time in orbit. The 20,000-pound-gross weight systems of the previous studies (Ref. 2) define the thermal model. Ground hold, boost phase heating, and the earth orbital conditions combined with the vehicle internal heat sources were considered to describe the thermal environment of the vehicle. Storage system requirements such as insulation, ullage volume, and propellant losses were determined. The engines, vehicle parameters, and mission duty cycles were analyzed to determine their effects on the orbital storage life.
- (C) Results of the orbital propellant storage life comparison for the nominal 20,000 pound gross weight system indicate that the LF<sub>2</sub>/LH<sub>2</sub> MSPS has the greatest ΔV capability for orbital storage times of up to 2 years with full propellant tanks. This storage time is achieved by tanking at a mixture ratio below the operating mixture ratio of 13:1 to allow for hydrogen venting losses during the storage period. Utilizing a tanking mixture ratio the same as the operating mixture ratio of 13:1 would reduce the orbital storage life capabilities of both cryogenic systems. This suggests that a propellant utilization system would be beneficial for extended orbital storage periods.
- (C) For the severe 90/10 mission duty cycle, where 90 percent of the propellants are burned the first day and the remaining 10 percent are burned after the orbital storage period, the LF<sub>2</sub>/LH<sub>2</sub> mission performance ΔV capability is superior to that of the N<sub>2</sub>O<sub>4</sub>/N<sub>2</sub>H<sub>4</sub>-(50-50) system for at least 115 days and never falls below the LO<sub>2</sub>/LH<sub>2</sub> system. A system sensitivity analysis was also conducted, and areas of new technology where further design effort may provide methods of improving long term orbital storage capabilities were identified.

# CONFIDENTIAL

## SECTION III

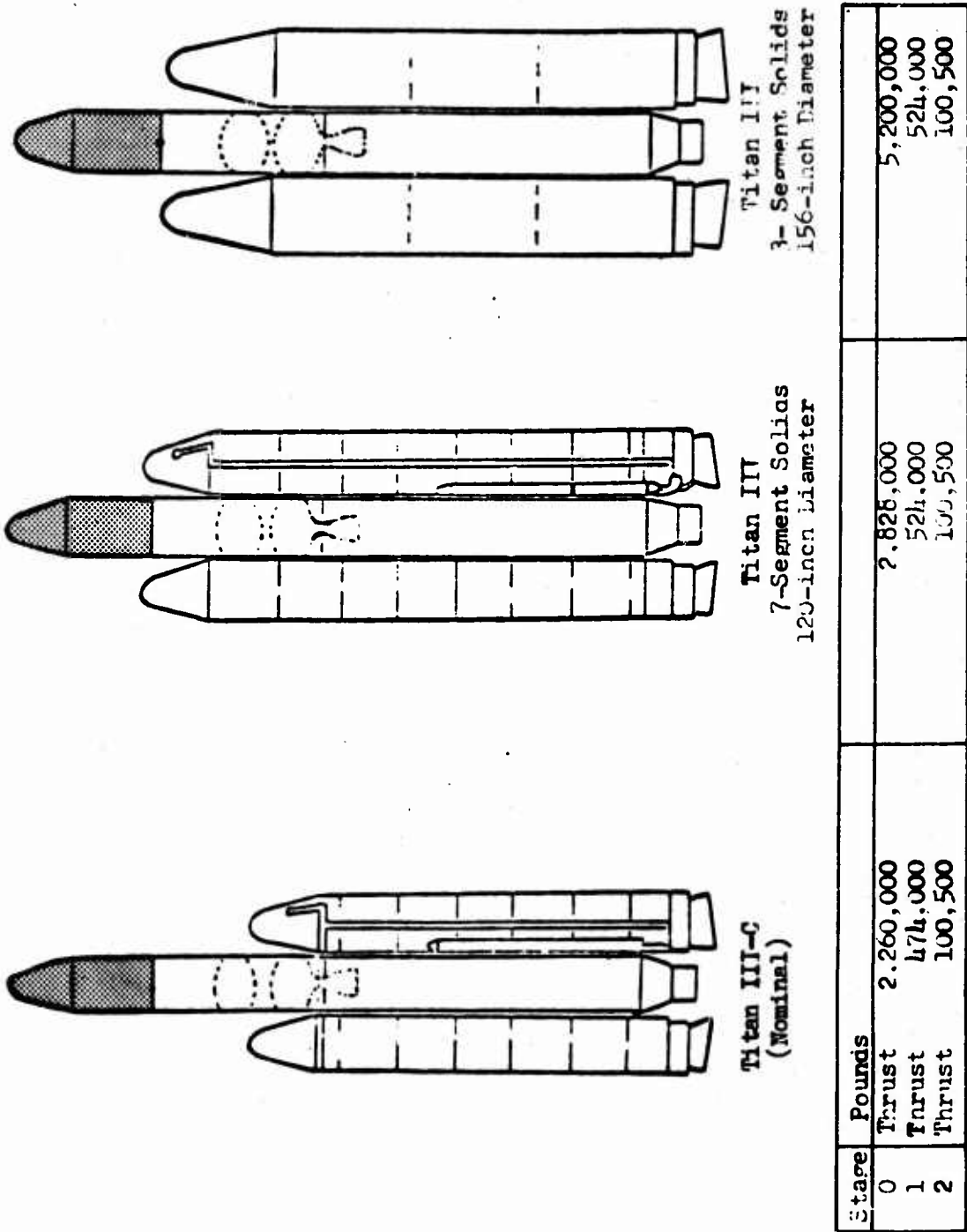
### LAUNCH VEHICLE PAYLOAD CAPABILITY DETERMINATION

- (C) The payload capability of the candidate booster vehicles that may be used to place the Maneuvering Space Propulsion System (MSPS) into orbit defines the potential size range for the maneuvering stage. In this study, an investigation was made of the relative capabilities of the nominal versions and several growth versions of the Titan III-C and the Saturn I-B launch vehicles for a wide range of gross weights of the MSPS. Preorbital burn of the MSPS was included for gross weight versions above the launch vehicle payload capabilities. Maneuvering Space Propulsion Systems designed for 2000- and 5000-pound payloads and using  $LF_2/LH_2$ ,  $LO_2/LH_2$ , and  $N_2O_4/N_2H_4$ -UDMH (50-50) propellants were investigated in conjunction with each candidate launch vehicle. The mission objective was to place the MSPS in a 100-nautical mile polar orbit from the Western Test Range (WTR). The results are presented in the form of the in-orbit  $\Delta V$  capability of the MSPS vs system gross weight. Typical increased gross weight maximum  $\Delta V$  systems are selected for each payload investigated. Further studies are presented to describe more exactly the capabilities of these example systems.

#### 1. CANDIDATE LAUNCH VEHICLE DESCRIPTION

- (U) Boost vehicles considered in the study were the nominal versions and selected growth versions of the Titan III-C and the Saturn I-B. A description of the two nominal vehicles is given in Fig. 1 and 2. The solid strap-on versions of these vehicles were the Titan III with seven-segment, 120-inch solids, the Titan III with three-segment, 156-inch solids, and the Saturn I-B with four Minuteman strap-on solids. The Transtage was not used on any of the Titan launch vehicles because the higher energy MSPS stage is available for the upper stage as required. Based upon information obtained from the Martin Co., the Titan vehicle can support payload weights as high as 70,000 pounds without the Transtage. Higher payload weights mounted on top of the Titan launch vehicle may create structural problems. Since the Transtage was not used, MSPS gross weights were limited to 70,000 pounds. The weight and performance information required for the analysis of the Saturn vehicles was obtained from Ref. 1. A description of each launch vehicle is presented in Fig. 1 and 2, and the stage weights and performance data is presented in Fig. 2 and Table II. The Titan launch vehicle configurations and the weight and performance data for these vehicles were obtained from cognizant Air Force Space Systems Division personnel. The launch vehicles specified were indicated to be those of prime interest for future Air Force missions. The growth version of the Saturn IB with Minuteman strap-ons was selected to provide payloads in the range of interest for MSPS.

CONFIDENTIAL

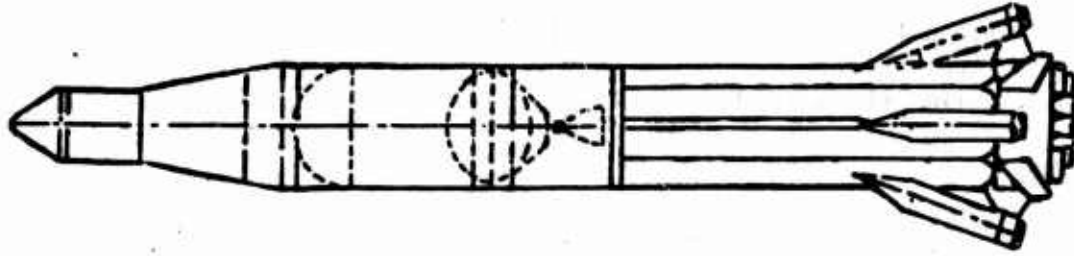


Payload in 100-nautical mile Polar Orbit

Figure 1. Upgraded Titan Configurations

6  
CONFIDENTIAL

S-IB/Minuteman



38,000 pounds

SECOND STAGE

Thrust = 205,000 Pounds\*

Propellant Weight = 228,340 Pounds

Specific Impulse = 428 Seconds\*

\*Programmed Mixture Ratio Operation

FIRST STAGE

Thrust = 1,640,000 Pounds

Propellant Weight = 883,950 Pounds

Specific Impulse = 264 Seconds

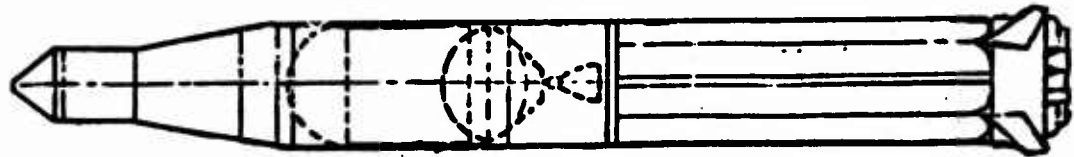
ZERO STAGE  
Minuteman

Thrust = 880,000 Pounds

Propellant Weight = 184,000 Pounds

Payload Capability in 100-nautical mile  
Polar Orbit

Nominal 9-IB



30,760 pounds

Figure 2. Saturn IB Configurations

# CONFIDENTIAL

TABLE II

## TITAN III LAUNCH VEHICLE DESCRIPTIONS

Titan III With Five-Segment, 120-Inch Solids (Existing)	Titan III With Seven-Segment, 120-Inch Solids	Titan III With Three-Segment, 156-Inch Solids	
<u>Zero Stage</u>			
Thrust (sea level), pounds	2,260,000	2,828,000	5,200,000
Propellant Weight, pounds	830,000	1,192,000	2,060,000
Specific Impulse (Sea Level), seconds	227	237	240
<u>First Stage</u>			
Thrust (vacuum), pounds	474,000	524,000	524,000
Propellant Weight, pounds	249,000	284,000	284,000
Specific Impulse (vacuum), pounds	286	299	299
<u>Second Stage</u>			
Thrust, pounds	100,500	100,500	100,500
Propellant Weight, pounds	67,900	67,900	67,900
Specific Impulse, seconds	310	313	313

# CONFIDENTIAL

## 2. GROUND RULES AND METHODS OF ANALYSIS

- (C) The basic ground rules established for the study were: (1) WTR launch into a 100-nautical mile polar orbit, and (2) a minimum desired MSPS thrust-to-weight ratio of 1.5 in orbit. The orbital thrust-to-weight ratio was evaluated in the optimization studies of Ref. 3. Thrust-to-weight ratio at suborbital ignition of the MSPS is, therefore, less than 1.5 since more propellant is on board at ignition.
- (C) The payload-in-orbit capabilities of the launch vehicles were calculated with the aid of Rocketdyne's Satellite Ascent Trajectory Simulation Program. The launch vehicle mission profile consists of a continuously powered trajectory to a 100-nautical mile polar orbit from the Western Test Range. The trajectory consists of a vertical rise for 10 seconds followed by a programmed kickover and gravity turn thrust steering program. The gravity turn is terminated when dynamic pressure decays to 50 lb/sq ft and is followed by a calculus-of-variations optimized thrust steering program into orbit. When the orbital payload capabilities of the specific launch vehicles were exceeded by higher gross weight MSPS configurations, suborbital firing of the MSPS was utilized.

## 3. PARAMETRIC MSPS STAGE DESCRIPTION

- (C) To determine the  $\Delta V$  capability of the MSPS for a range of gross weight values, parametric stage weight and performance data were required for the three propellant combinations. This information was obtained from propulsion system optimization studies conducted in parallel with this study effort. The stage inert weight data used in the stage performance calculations were based upon information generated in the previous MSPS studies for the alternate mission vehicles described in Ref. 2. These data were obtained for  $LF_2/LH_2$ ,  $LO_2/LH_2$ , and  $N_2O_4/N_2H_4$ -UDMH(50-50) propellants as a function of propellant weight. Engine weight and specific impulse data were obtained from preliminary results of the system optimization studies and reflects optimum configurations at each of the design thrust levels. Engine weight of the optimized systems increased nearly linearly with thrust.
- (C) Specific impulse for the  $LF_2/LH_2$  and  $LO_2/LH_2$  systems increase with thrust up to a design thrust level of 50,000 pounds and remain constant for higher thrust levels. This increase was primarily due to the improved regenerative cooling capabilities of the engines with increasing thrust which permitted increased  $P_c - \epsilon$  combinations for the primary engines. The optimized  $N_2O_4/N_2H_4$ -UDMH (50-50) systems were found to have a nearly constant specific impulse with increasing thrust. It should be noted that the system  $\Delta V$  comparisons are for continuous operation at full thrust and, therefore, only the maximum thrust specific impulse was used for the comparisons of this portion of the study.

9  
CONFIDENTIAL

# CONFIDENTIAL

## 4. MSPS VELOCITY CAPABILITY

(C) The results of the launch vehicle payload analysis are presented as MSPS relative  $\Delta V$  capability in orbit vs the total MSPS gross weight (including propellant consumed during suborbital firing). The launch-vehicle payload capabilities are thus translated directly to MSPS  $\Delta V$  capabilities, the information of primary interest. The results are referenced to the nominal 20,000-pound gross weight  $LF_2/LH_2$  MSPS of Ref. 2 which has a  $\Delta V$  capability of 23,150 ft/sec for continuous operation at full thrust. The nominal Titan III-C boost vehicle is discussed first and is followed by the two growth versions of this vehicle. The capabilities of the nominal and growth version of the Saturn I-B are then presented. Maneuvering space propulsion systems using  $LF_2/LH_2$ ,  $LO_2/LH_2$  and  $N_2O_4/N_2H_4$ -UDMH (50-50) are shown for each launch vehicle. Relative comparisons with the various launch vehicles are then presented for the MSPS.

### a. Titan Vehicles

(C) The  $\Delta V$  capability in orbit of the 2000-pound-payload MSPS using the Titan III-C boost vehicle is shown in Fig. 3. A weight of 21,700 pounds can be put into a 100-nautical mile orbit by the Titan III-C. For MSPS gross weights larger than 21,700 pounds, suborbital firing of the MSPS is required. The  $\Delta V$  capability increases with suborbital burn; a maximum increase of 800 ft/sec for the  $LF_2/LH_2$  MSPS occurs at a total gross weight of 38,000 pounds. The  $\Delta V$  capability of the  $LO_2/LH_2$  is only slightly improved, and the  $N_2O_4/N_2H_4$ -UDMH (50-50) MSPS is not improved with a suborbital firing because the lower specific impulse results in a larger amount of propellant being consumed during the suborbital firing, thus diminishing the amount of propellant available for the in-orbit maneuvers. As the gross weight is increased, this effect is accentuated, causing the curves for the various propellants to diverge. The curves representing the  $LO_2/LH_2$  and  $N_2O_4/N_2H_4$ -UDMH (50-50) propellant combinations peak at lower total gross weights for the same reason.

(U) The relatively small increase in  $\Delta V$  capability with suborbital firing and increasing gross weight can be explained by referring to Fig. 4. The sum of the gross weight in orbit and propellant weight used in the suborbital (bottom two curves) firing equals the total MSPS gross weight. The suborbital propellant weight increases at a faster rate than the gross weight in orbit. Hence, as total gross weight increases, a greater portion of it is used in suborbital burn, which increases weight in orbit at a lower rate. Vehicle burnout weight increases with total gross weight, which makes the quotient:

$$\frac{\text{gross weight in orbit}}{\text{burnout weight}} = R$$

(U) increase slightly and eventually decrease, as shown in the top curve. Since  $\Delta V$  is equal to  $I_s g \ln R$ , with  $I_s$  essentially constant and  $R$  varying very slightly, the net result is a small variation of the in-orbit  $\Delta V$  capability vs maneuvering system gross weight.

CONFIDENTIAL

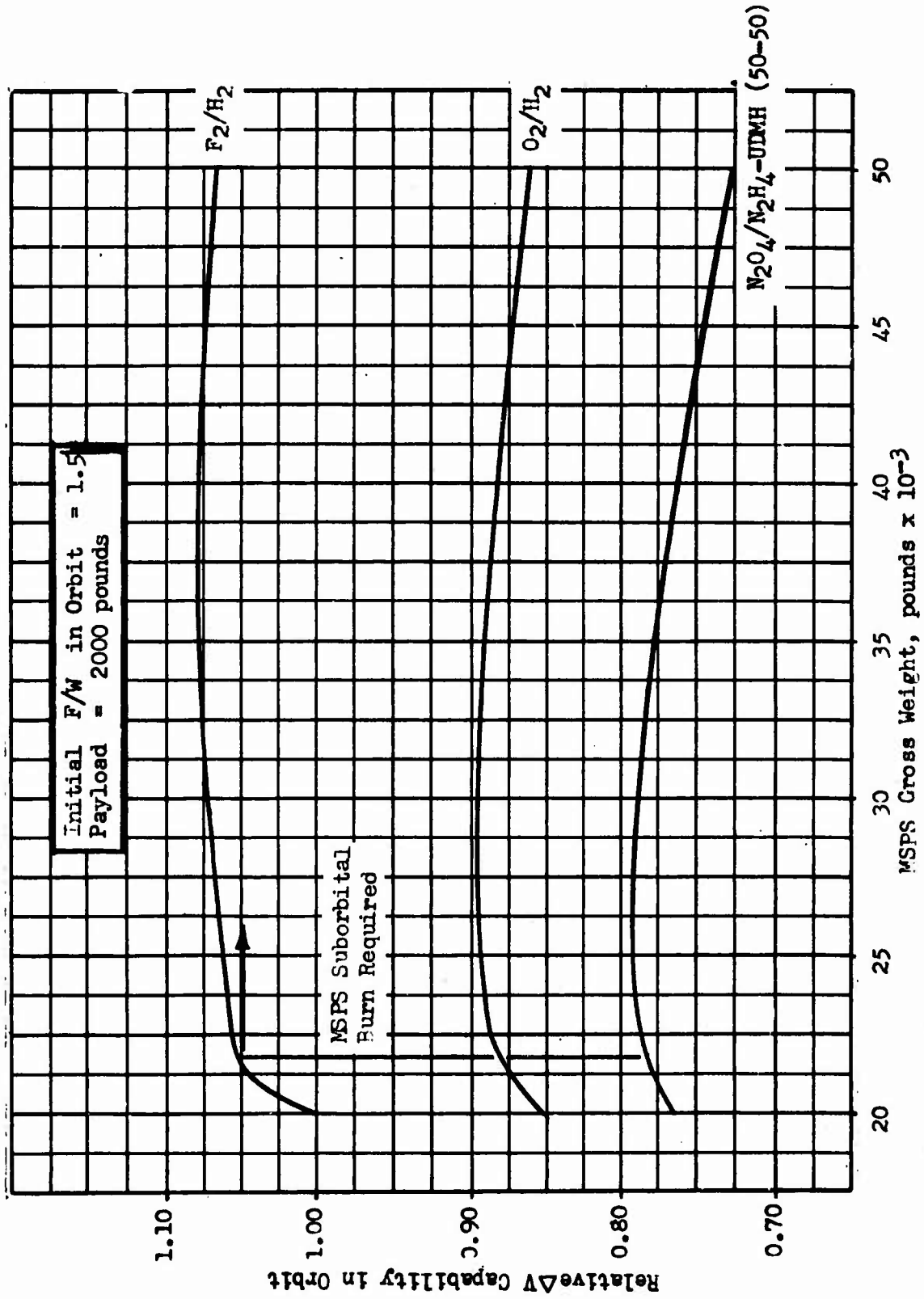


Figure 3 . Comparison of MSPS Performance with Titan III-C Launch Vehicle

CONFIDENTIAL

CONFIDENTIAL

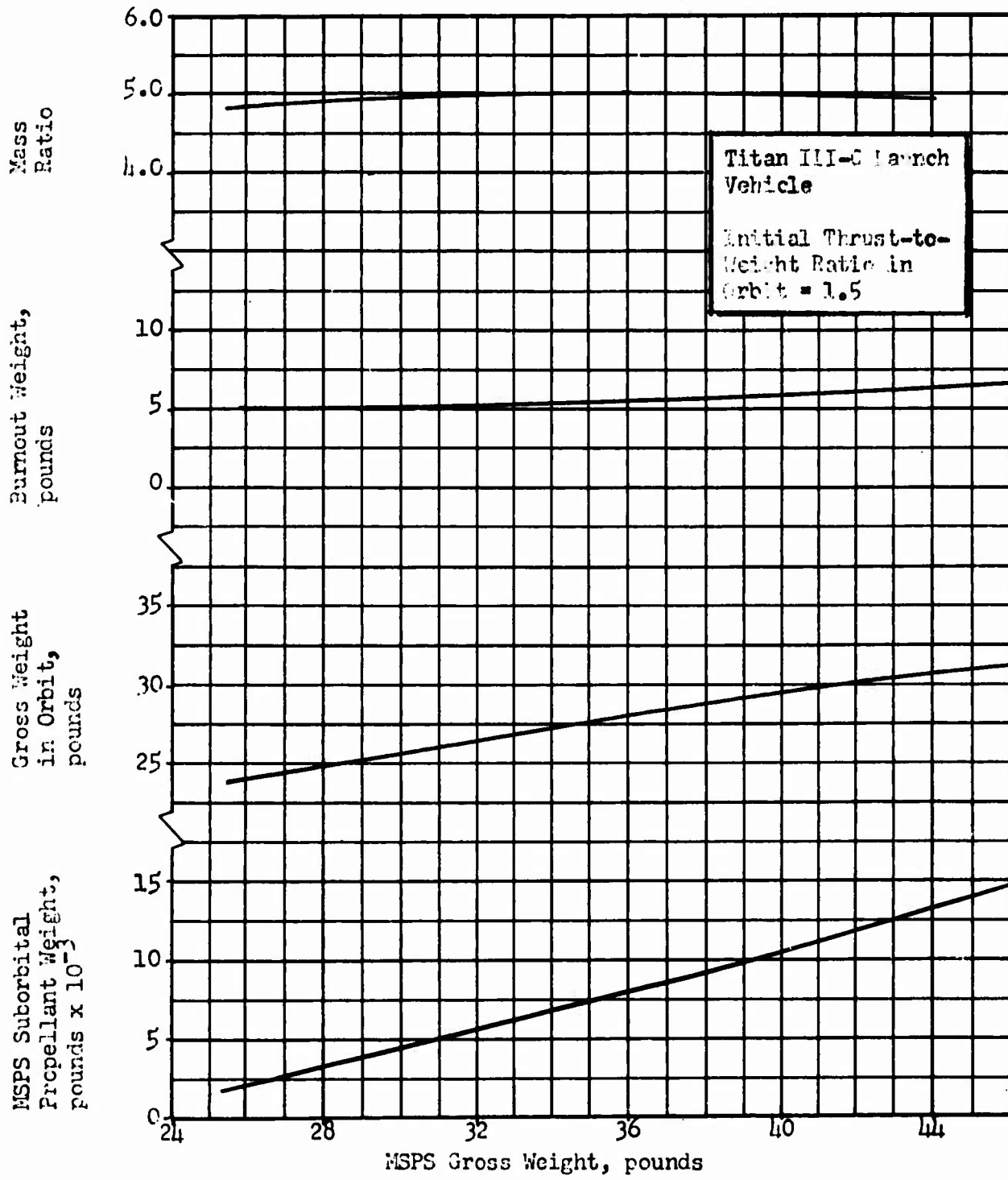


Figure 4. Suborbital Firing Effects on F<sub>2</sub>/H<sub>2</sub> MSPS

CONFIDENTIAL

CONFIDENTIAL

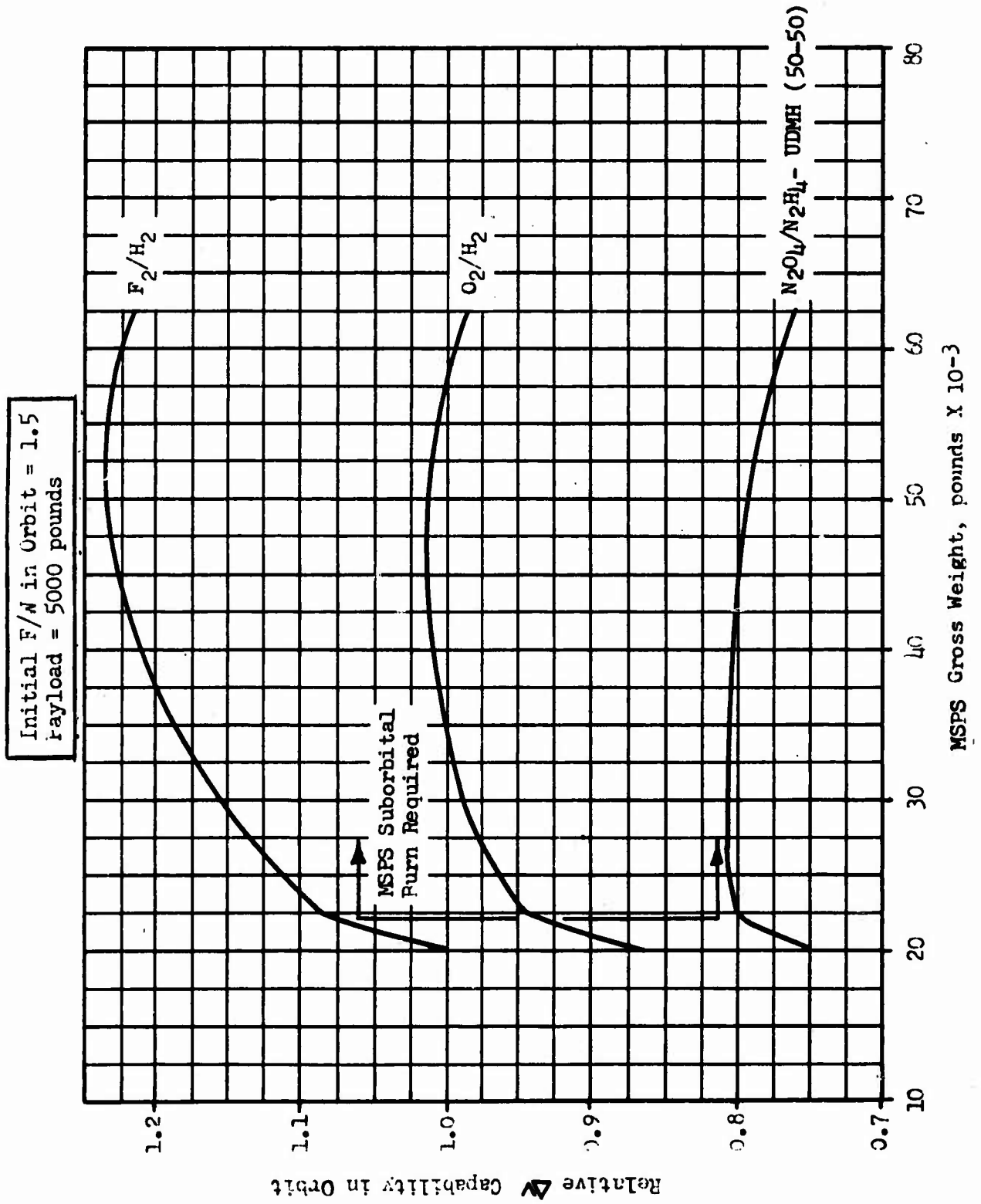


Figure 5 . Comparison of MSPS Performance with Titan III-C Launch Vehicle

CONFIDENTIAL

# CONFIDENTIAL

- (C) The ground rule requiring an initial thrust-to-weight ratio of 1.5 in orbit results in a thrust-to-weight ratio of less than 1.5 for the suborbital firing. The effect of this restriction was investigated to determine if a higher thrust-to-weight ratio for the suborbital firing would improve the in-orbit  $\Delta V$  capability of the MSPS. The results showed that gross weight in orbit and the propellant weight used in the suborbital firing were virtually unaffected by varying the initial in-orbit thrust-to-weight ratio over a fairly wide range. The net result indicates that the in-orbit  $\Delta V$  capability of the MSPS is insensitive to reasonable variations in the suborbital firing thrust-to-weight ratio.
- (C) The 5000-pound-payload MSPS  $\Delta V$  in-orbit capabilities are shown in Fig. 5 for the nominal Titan III-C launch vehicle. These results, when compared with the 2000-pound-payload system in Fig. 3, indicate a more rapid increase in  $\Delta V$  capability for the 5000-pound-payload MSPS in the range of gross weights where suborbital burn is not required. It is also noted that, after suborbital burn is required, there is a more significant increase in  $\Delta V$  capability with increasing gross weight, and the gross weight at which maximum  $\Delta V$  occurs is higher than for the 2000-pound-payload MSPS. This effect can be explained by examining the derivative of the familiar  $\Delta V$  equation with respect to gross weight:

$$\Delta V = I_s g \ln R$$

where the mass ratio  $R$  can be expressed as the gross weight ( $W_G$ ) over the burnout weight ( $W_{BO}$ ). The derivative can then be found as:

$$\frac{d(\Delta V)}{d W_G} = I_s g \left[ \frac{1}{W_G} - \frac{1}{W_{BO}} \left( 1 - \frac{1}{1+K} \right) \right]$$

where  $K$  is the propellant-dependent inert weight factor which is essentially constant over the range of gross weights investigated. It can then be seen that the slope of the  $\Delta V$  vs gross weight curve at any selected value of gross weight is dependent upon the burnout weight. When burnout weight increases, as it does with increasing payload weight, the slope of the  $\Delta V$  curve increases. In essence, this means that an increase in gross weight, of which the greater portion is propellant weight (the remainder is made up of propellant-dependent inert weight to accommodate the additional propellant), provides a greater benefit to the lower propellant weight or higher payload system. In the region of the curve where suborbital burn is required, the gross weight in the derivative expression is actually the gross weight in orbit. However, the same trend applies, thus explaining the more significant increase in  $\Delta V$  with gross weight and the higher maximum  $\Delta V$  gross weight value for the 5000-pound-payload systems. The explanation of some of the trends exhibited in the results for the nominal Titan vehicle also applies to the results for the other launch vehicles because the influencing factors are general or common to all the systems.

# CONFIDENTIAL

- (C) Maneuvering Space Propulsion System  $\Delta V$  capabilities for the Titan III with seven-segment, 120-inch solids are shown in Fig. 6 and 7 for the 2000- and 5000-pound-payload MSPS, respectively. This growth version of the Titan III launch vehicle can place 31,600 pounds into orbit; higher MSPS gross weights require suborbital burn. The 2000-pound-payload systems do not benefit from a suborbital burn. The 5000-pound-payload  $LF_2/LH_2$  MSPS shows a slight  $\Delta V$  advantage with increasing gross weight and suborbital burn.
- (C) The Titan III with three-segment, 156-inch solids can place a 43,000-pound-payload weight in orbit as indicated in Fig. 8 and 9 for the 2000- and 5000-pound-payload MSPS, respectively. There is only a slight increase in  $\Delta V$  capability for the 5000-pound-payload,  $LF_2/LH_2$  MSPS with suborbital burn when this launch vehicle is used. For the 2000-pound payload and alternate propellant systems, there is no  $\Delta V$  advantage in higher gross weight systems where suborbital burn is required.

## b. Saturn Vehicles

- (C) The nominal Saturn I-B is capable of placing a 30,760-pound payload in a 100-nautical mile polar orbit. The MSPS  $\Delta V$  trends are shown in Fig. 10 and 11. Since the Saturn I-B is a larger vehicle (greater payload or  $\Delta V$  capability) than the nominal Titan, the Saturn has more nearly obtained orbital velocity at the initiation of MSPS operation so that the payload is not increased noticeably by the suborbital firing of the MSPS stage. Therefore, the  $\Delta V$  is not improved as much for the Saturn as for the nominal Titan.
- (C) The uprated Saturn I-B with Minuteman strap-ons will orbit approximately 38,000 pounds without a suborbital firing of the MSPS. The  $\Delta V$  capabilities of the MSPS in conjunction with this launch vehicle are shown in Fig. 12 and 13 for the 2000- and 5000-pound payloads, respectively.

## c. Vehicle Comparisons

- (C) Comparisons of the various launch vehicles are presented in Fig. 14, 15, and 16. These curves are duplications of the 2000-pound-payload,  $LF_2/LH_2$  MSPS in conjunction with the various launch vehicles. The relative capabilities of the nominal Titan III-C and Saturn I-B are shown in Fig. 14. Both curves peak at an MSPS gross weight of approximately 38,000 pounds.
- (C) A comparison of the three Titan launch vehicles is shown in Fig. 15. The increase in  $\Delta V$  capability with suborbital firing and increasing gross weight for the Titan launch vehicles with lower payload capabilities is primarily due to the increasing specific impulse of the  $LF_2/LH_2$  propulsion system. The specific impulse of the optimized  $LF_2/LH_2$  system increased with thrust up to a design thrust level of 50,000 pounds and remained constant for higher design levels.

The two Saturn launch vehicles are compared in Fig. 16.

CONFIDENTIAL

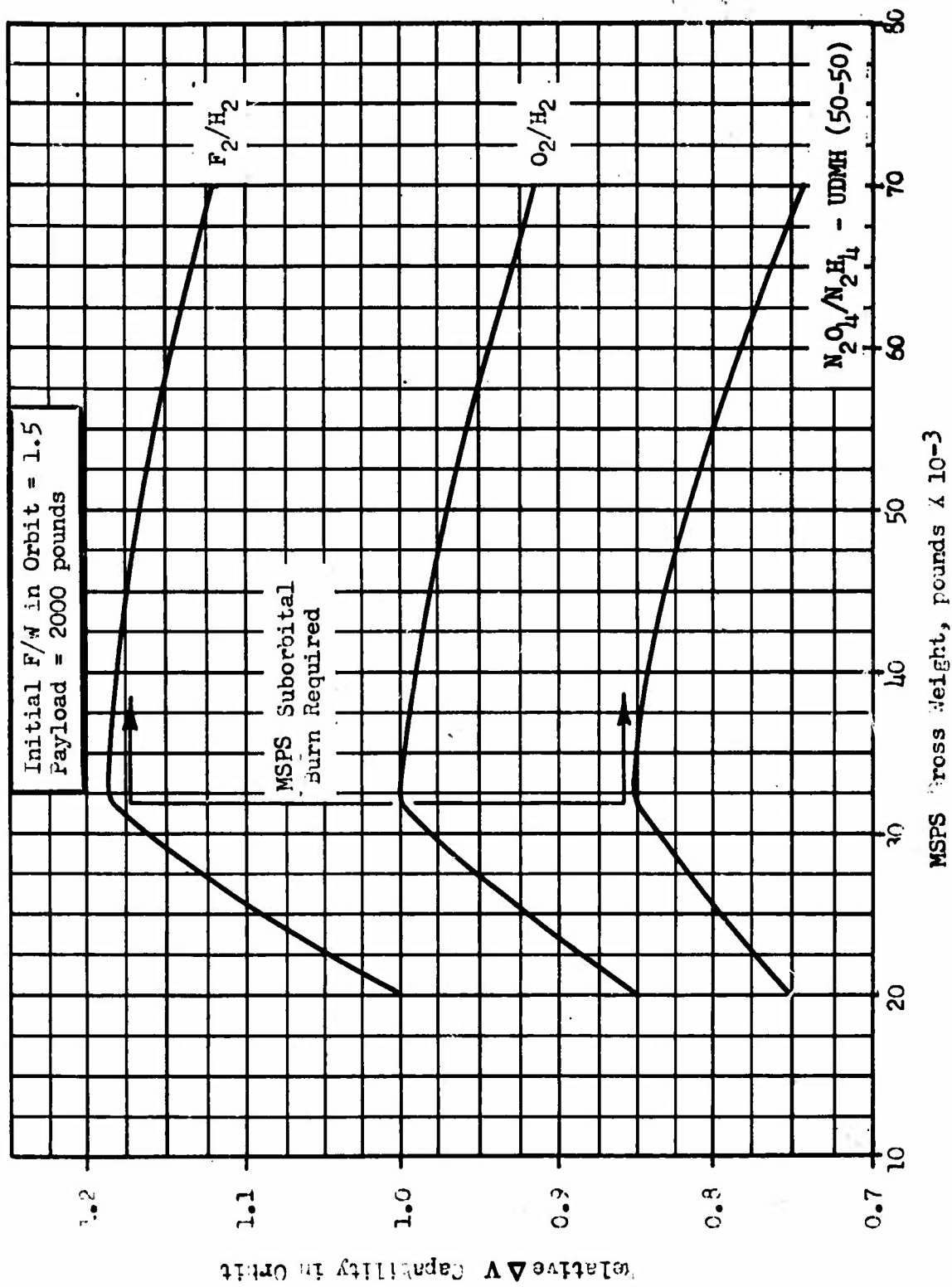


Figure 6 . Comparison of MSPS Performance with Titan III Seven-Segment 120-Inch Solids

CONFIDENTIAL

CONFIDENTIAL

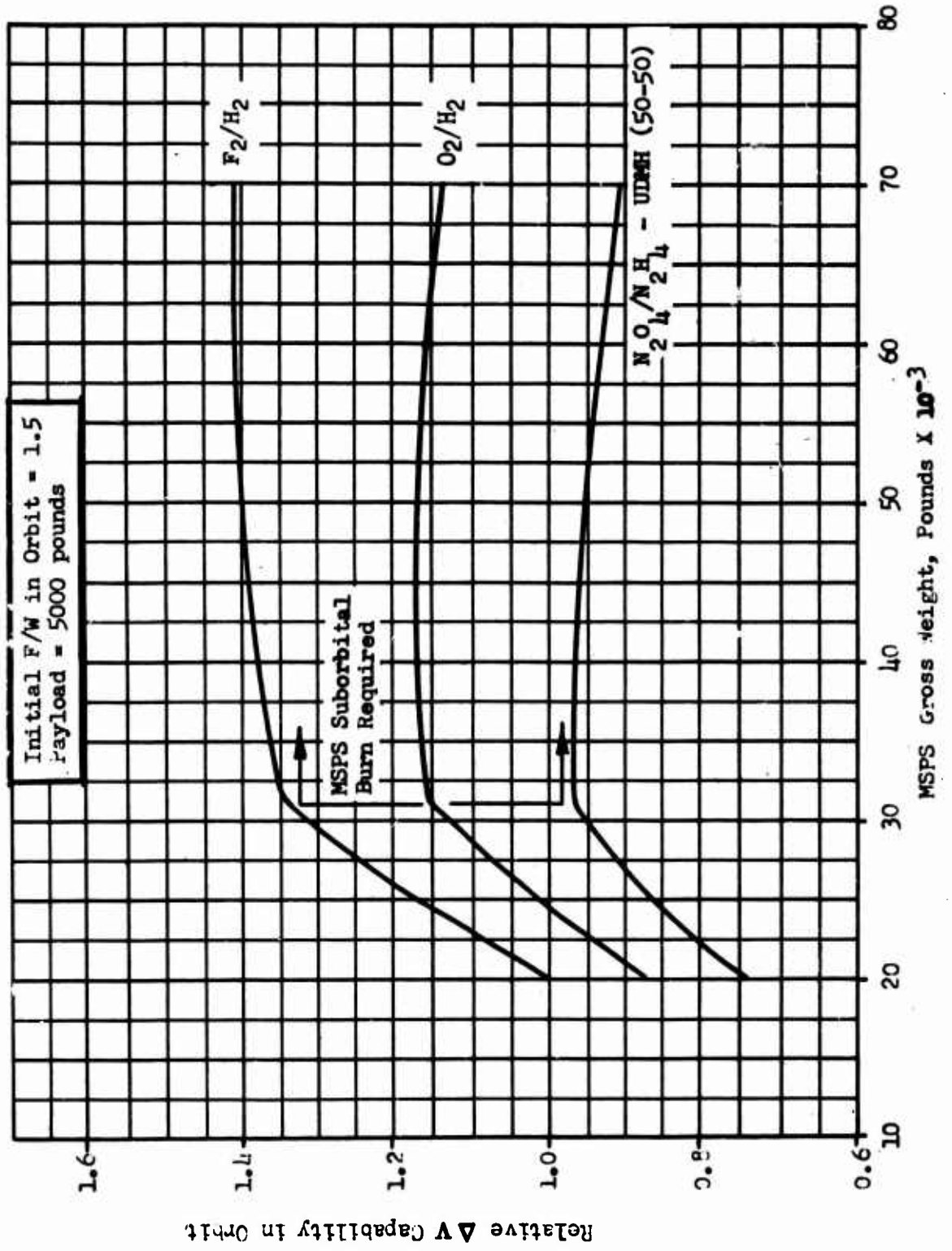


Figure 7 . Comparison of MSPS Performance with Titan III Seven-Segment 120-Inch Solids

CONFIDENTIAL

CONFIDENTIAL

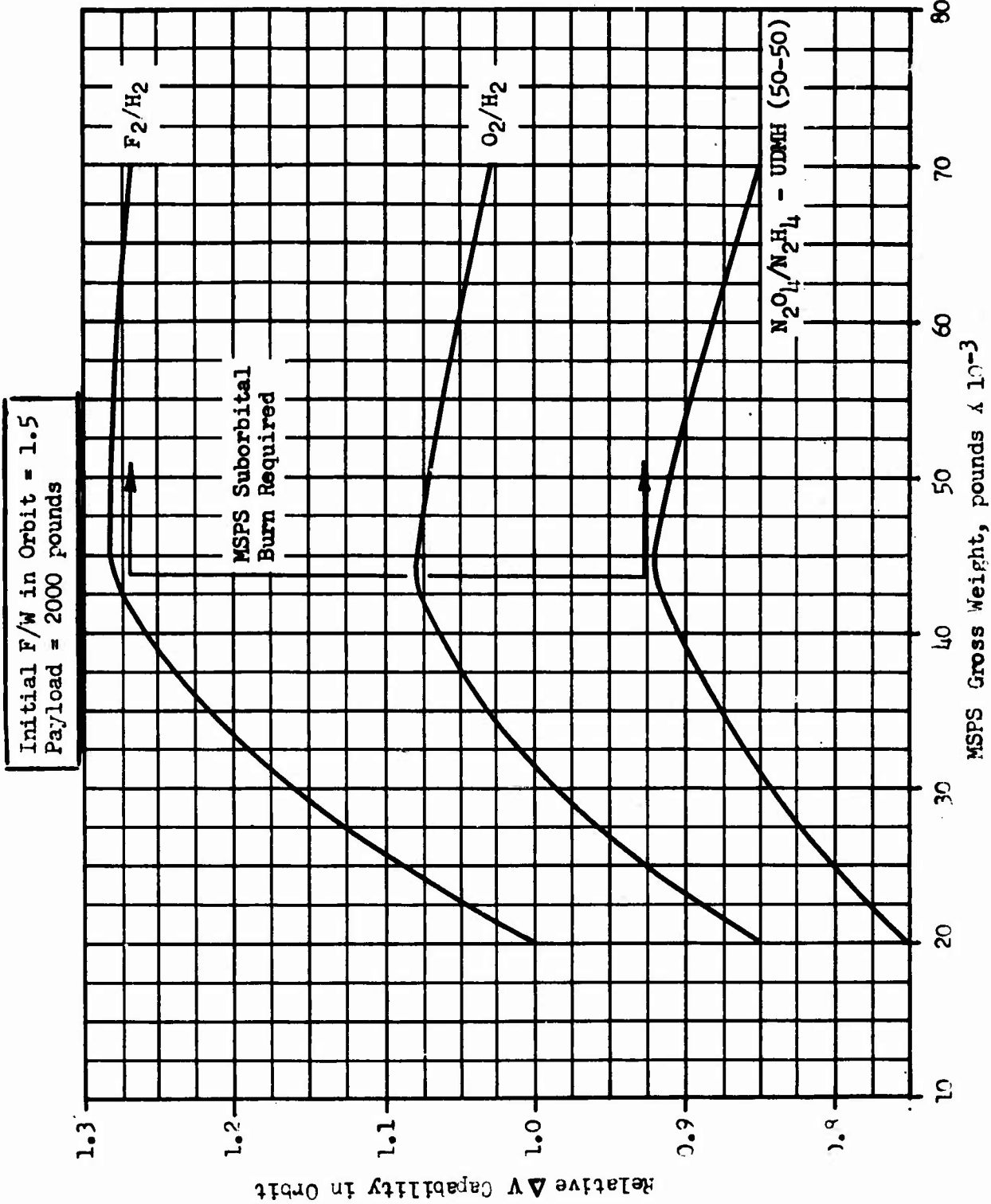


Figure 8 . Comparison of MSPS Performance with Titan III Three-Segment 156-Inch Solids

18  
CONFIDENTIAL

CONFIDENTIAL

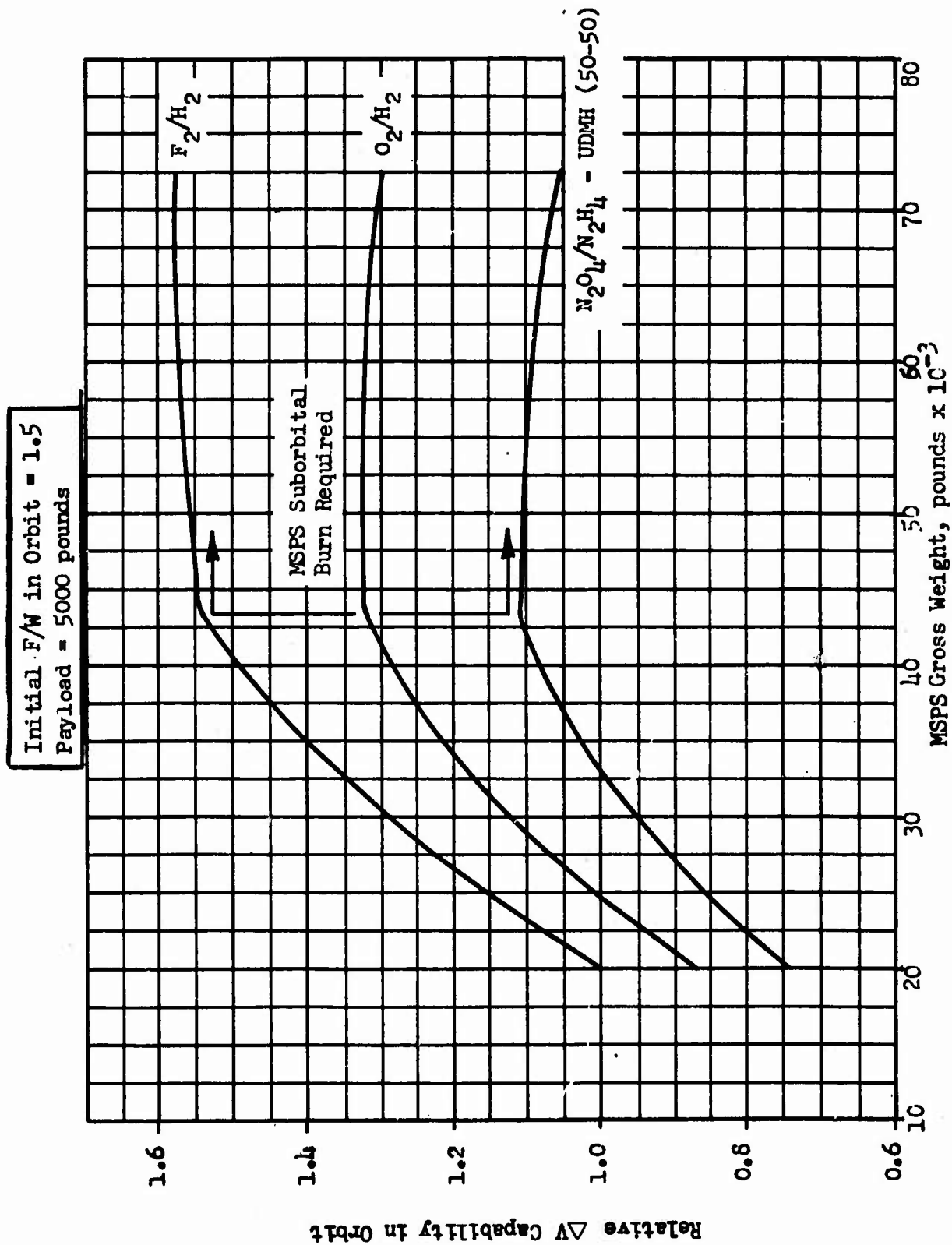


Figure 9 . Comparison of MSPS Performance with Titan III Three-Segment 156-Inch Solids

CONFIDENTIAL

CONFIDENTIAL

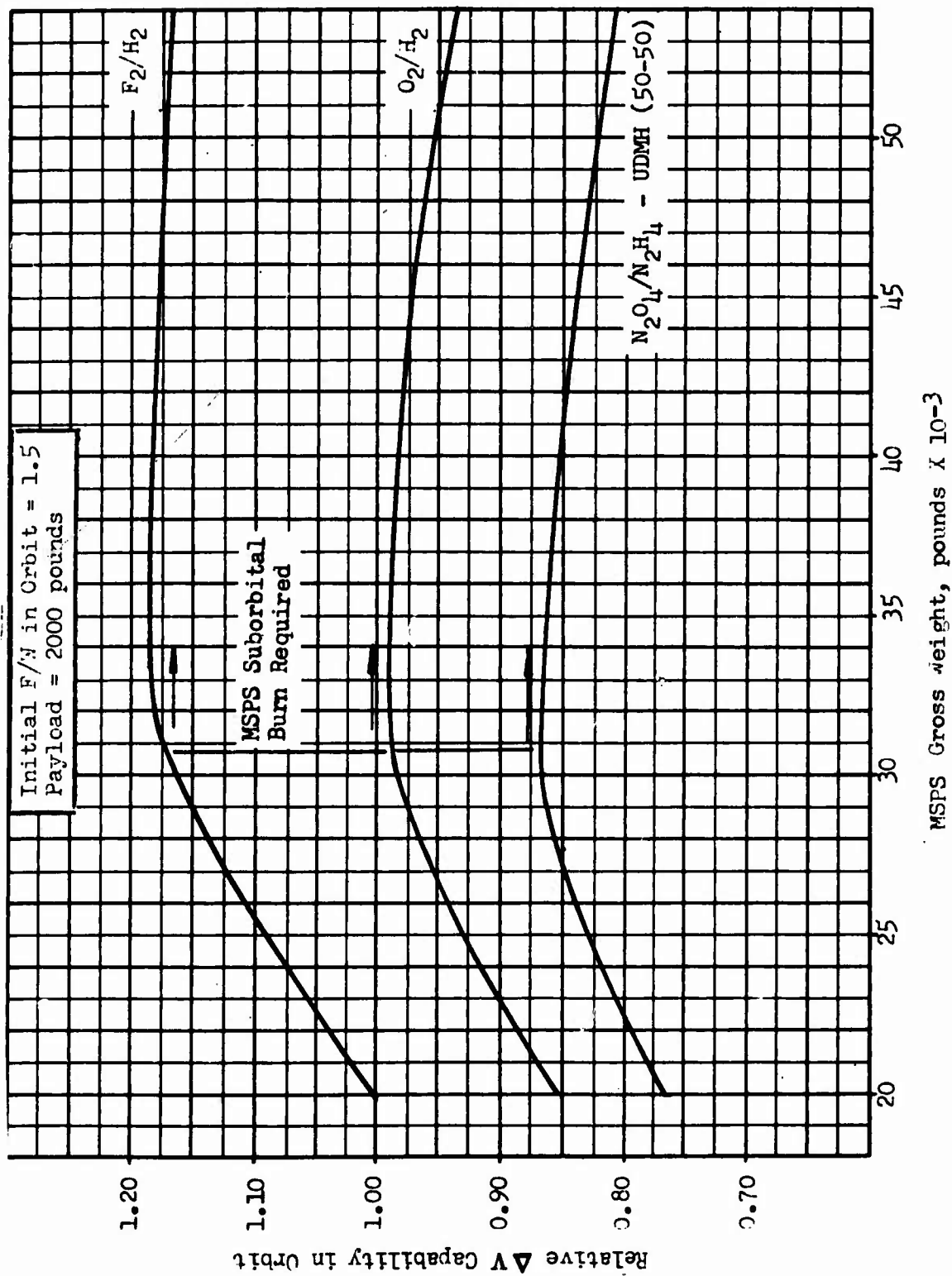


Figure 10. Comparison of MSPS Performance with Saturn IB

20  
CONFIDENTIAL

CONFIDENTIAL

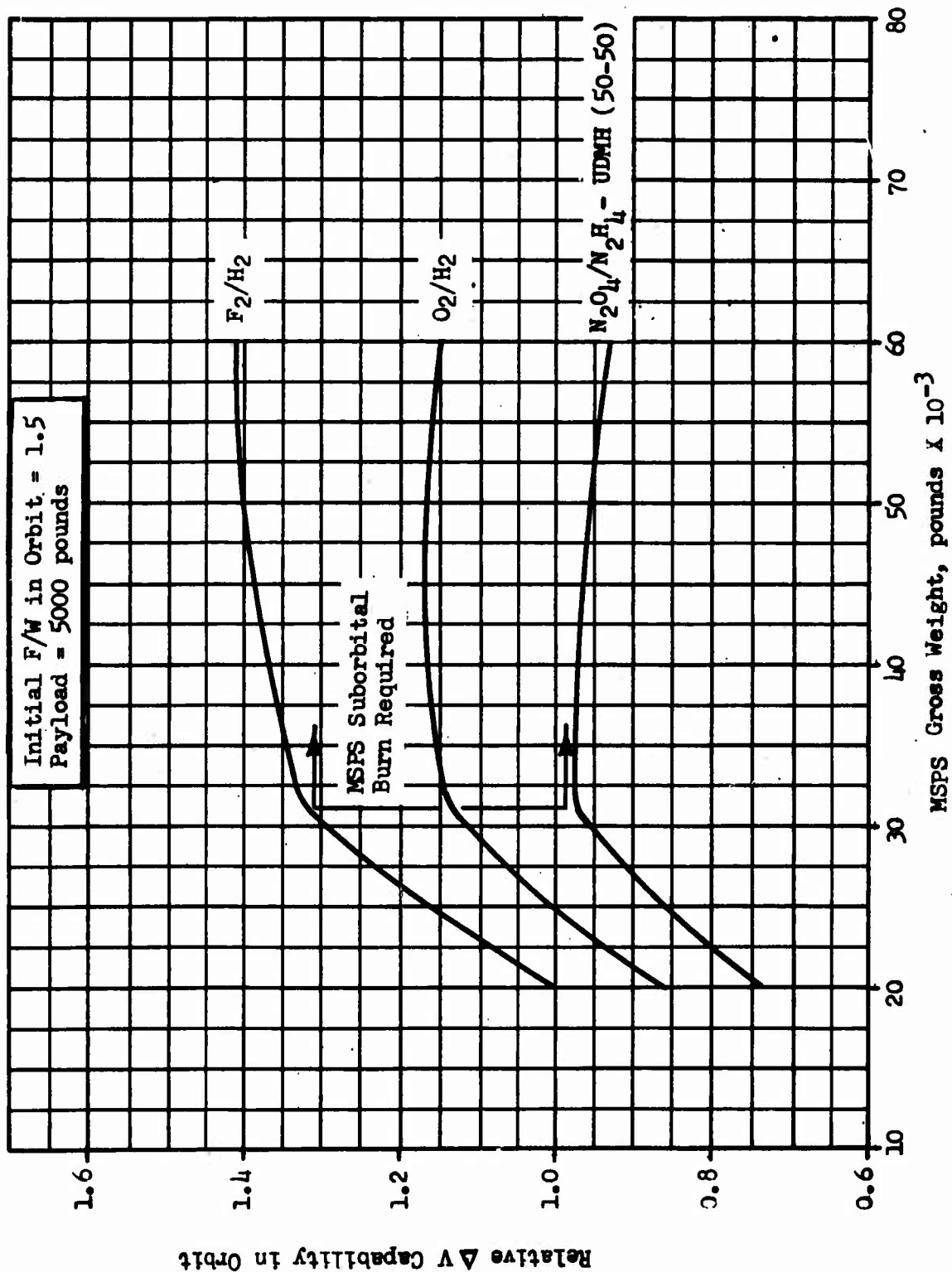


Figure 11 . Comparison of MSFS Performance with Saturn IB

21  
CONFIDENTIAL

CONFIDENTIAL

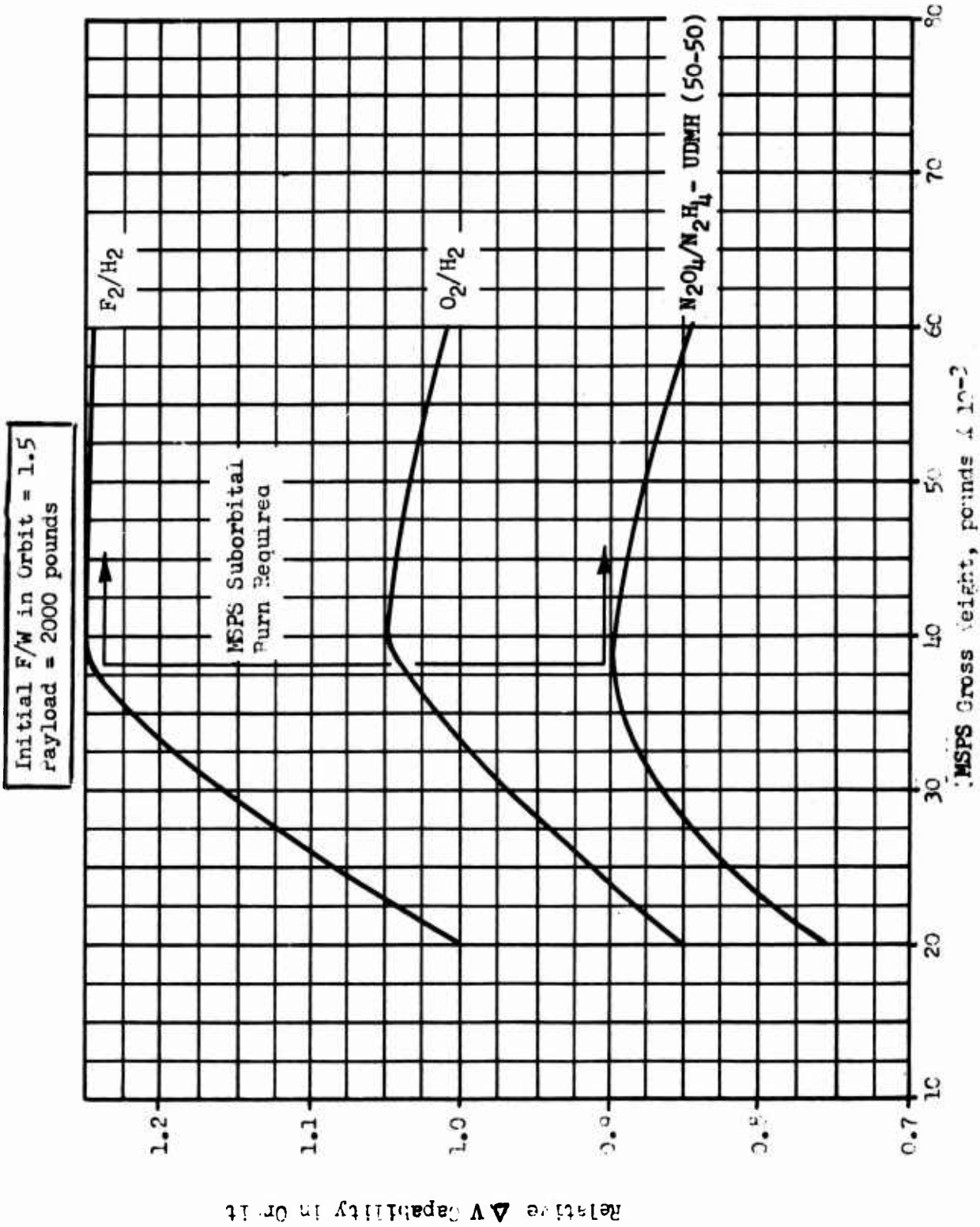


Figure 12. Comparison of MSPS Performance with Saturn IR/Minuteman

CONFIDENTIAL

CONFIDENTIAL

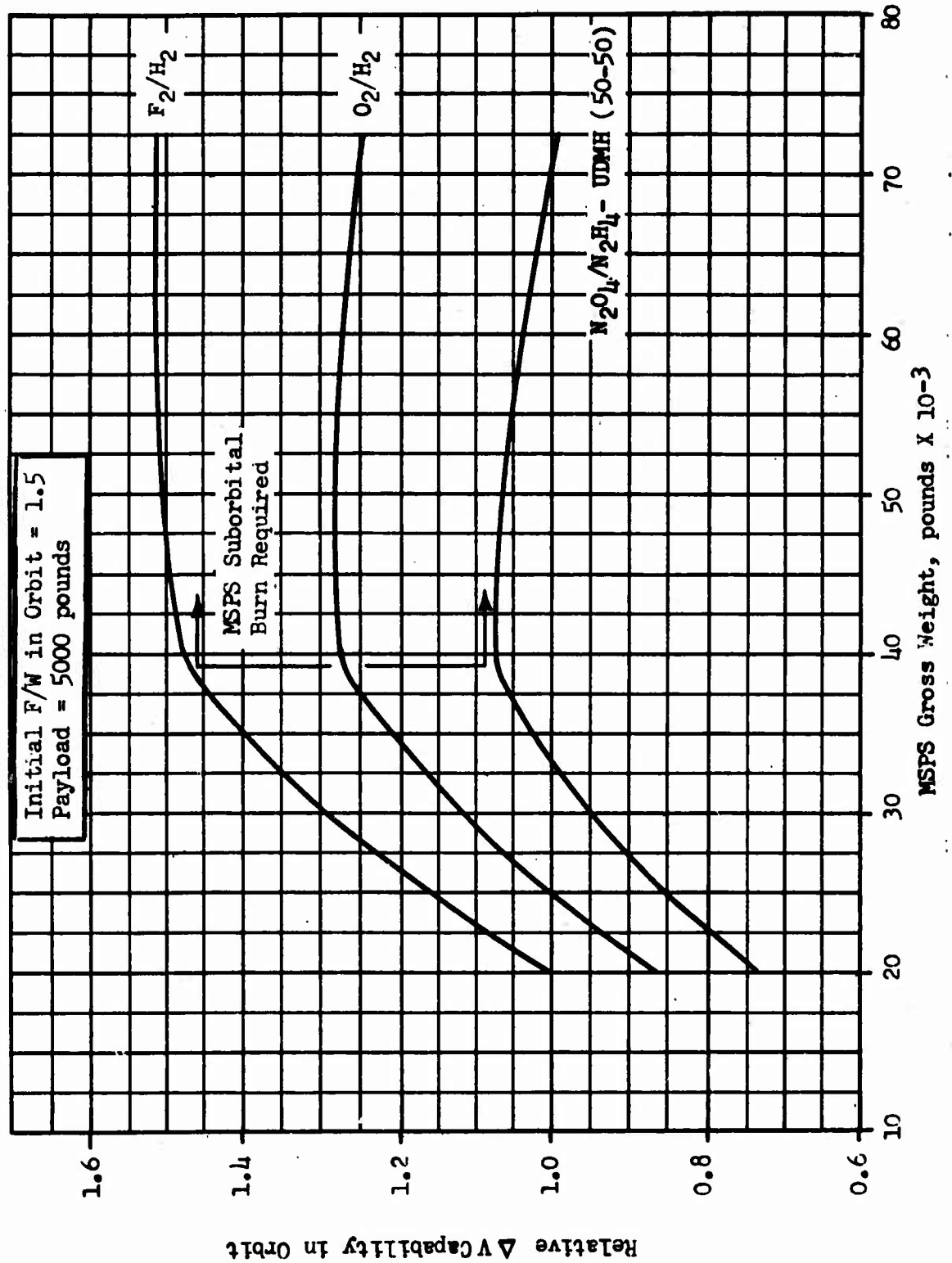


Figure 13. Comparison of MSPS Performance with Saturn IB/Minuteman

CONFIDENTIAL

CONFIDENTIAL

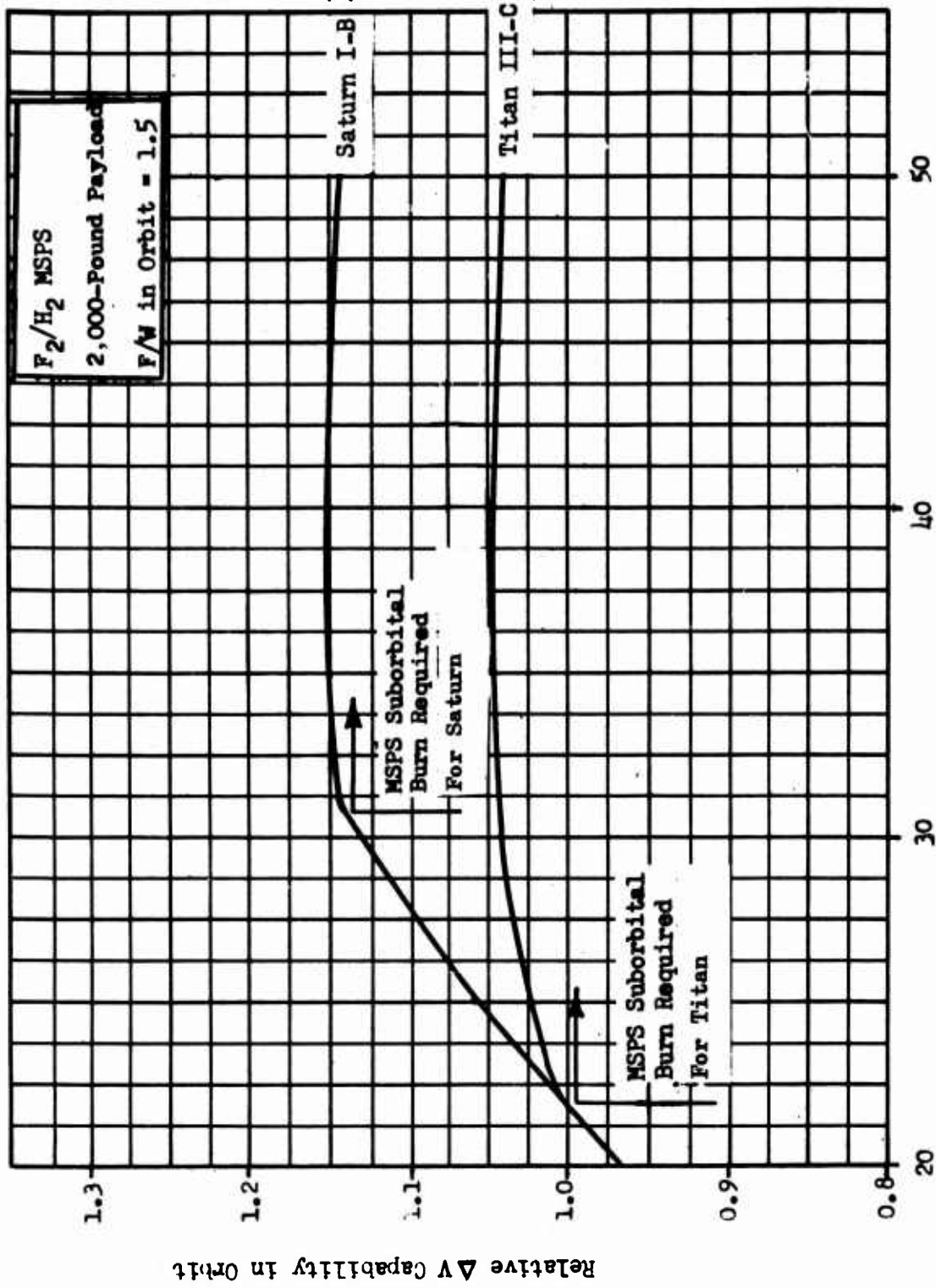
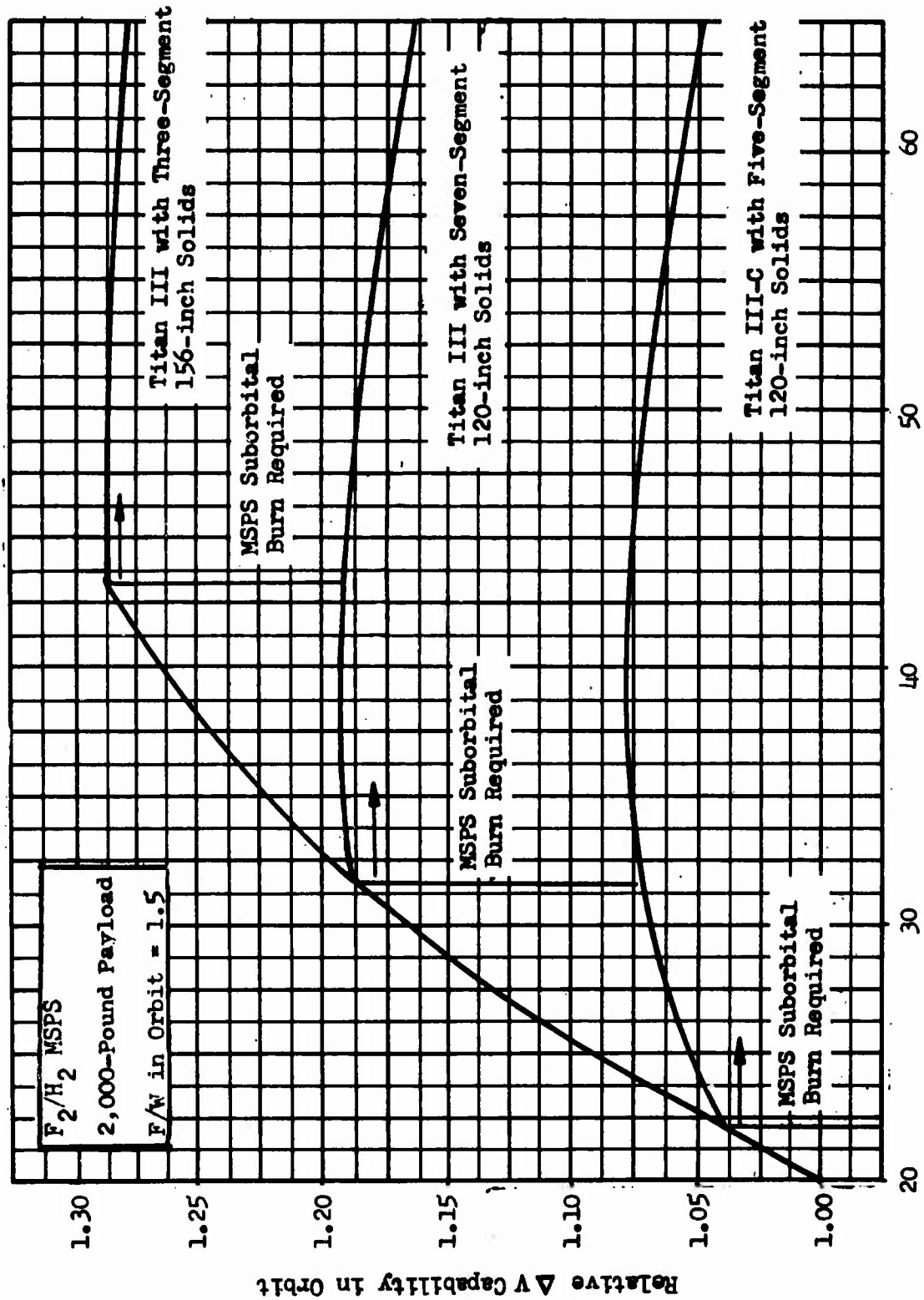


Figure 14 . Comparison of Nominal Titan and Saturn Launch Vehicles

24  
CONFIDENTIAL

CONFIDENTIAL



MSPS Gross Weight, pounds  $\times 10^{-3}$

Figure 15. Comparison of Titan Launch Vehicles

CONFIDENTIAL

CONFIDENTIAL

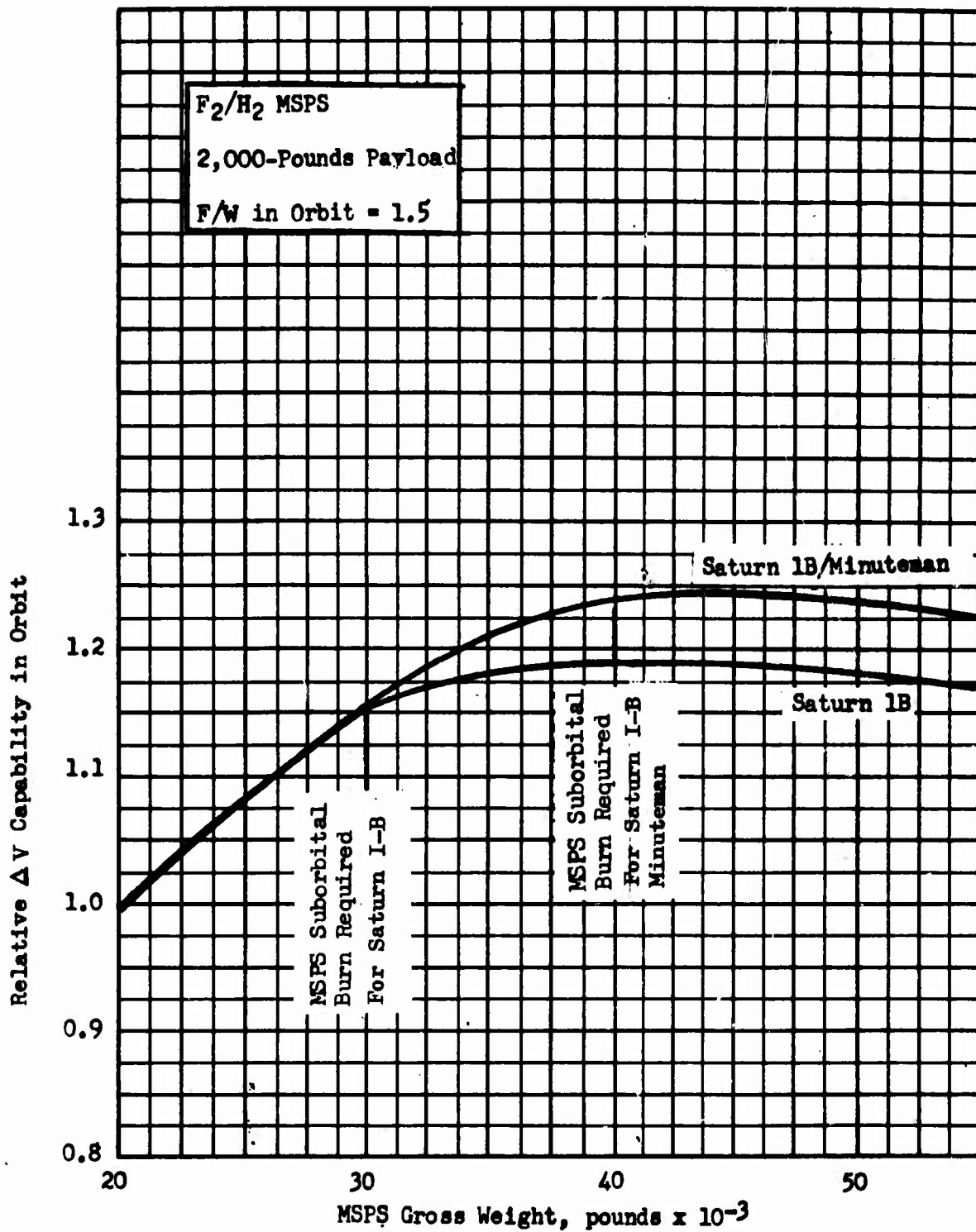


Figure 16. Comparison of Saturn Launch Vehicles

CONFIDENTIAL

# CONFIDENTIAL

## 5. EFFECT OF COMMON MSPS SIZE ON IN-ORBIT VELOCITY CAPABILITY

- (C) An evaluation of the results presented for the various launch vehicles was accomplished to define an MSPS gross weight and thrust level that would provide near-maximum  $\Delta V$  capability when used with any of the candidate launch vehicles. This was performed for the 2000- and 5000-pound-payload MSPS using  $LF_2/LH_2$ ,  $LO_2/LH_2$ ,  $N_2O_4/N_2H_4$ -UDMH (50-50) propellants. The  $\Delta V$  curves for each launch vehicle were reviewed to determine an MSPS gross weight range corresponding to a 0.2 percent loss in  $\Delta V$  capability. This value was arbitrarily selected as a maximum desirable degradation in performance for a common gross weight MSPS. From this gross weight range, corresponding in-orbit gross weights can be determined for each launch system. Then, by maintaining the required initial thrust-to-weight ratio of 1.5 in orbit, the engine design thrust level is defined. These comparisons are discussed in the following paragraphs.

### a. $LF_2/LH_2$ Systems

- (C) For the 2000-pound-payload  $LF_2/LH_2$  MSPS, the range of MSPS gross weights which will yield 99.8 percent of the optimum  $\Delta V$  is shown in Table III. The corresponding initial weights in orbit and thrust levels are also presented. Based on these data, a total gross weight of 36,000 pounds was selected as typical of the range of gross weights indicated. This gross weight is within the desirable range for the launch vehicles of primary interest (nominal Titan and Saturn and the Titan with seven-segment, 120-inch solids) and slightly below the desirable gross weight range for the remaining two launch vehicles. An engine design thrust level of 50,000 pounds was also selected as typical of the range of thrust requirements. The approximate maximum MSPS  $\Delta V$  is also shown. With these selected values of gross weight and thrust, Table IV was prepared to illustrate the range of thrust-to-weight ratios in orbit and  $\Delta V$  capabilities that could be achieved by the various launch vehicles. With a 36,000-pound gross weight MSPS, the Titan III with the three-segment, 156-inch solids and the uprated Saturn do not require suborbital burn of the MSPS, thus the initial in-orbit, thrust-to-weight ratio is lower than was specified. These systems with thrust-to-weight values below the required 1.5 will achieve this value as soon as a small amount of propellant is consumed. The 36,000-pound gross weight system achieves  $\Delta V$ 's within 4.7 percent of the maximum capability for each launch vehicle.
- (C) An identical evaluation was also conducted for the 5000-pound-payload,  $LF_2/LH_2$  MSPS, and the results are presented in Tables V and VI. Higher gross weights are found to be desirable for this payload. The selected common MSPS gross weight was 52,000 pounds and the thrust was 60,000 pounds. In this case, the selected common gross weight of 52,000 pounds provides a  $\Delta V$  capability within 0.8 percent of the maximum for each launch vehicle. These comparisons illustrate that for a specified payload weight, a common MSPS gross weight can be selected that will give near-maximum  $\Delta V$  capability when used on conjunction with any of the launch vehicles considered. A size comparison of the two selected MSPS

27  
CONFIDENTIAL

CONFIDENTIAL

TABLE III

LAUNCH VEHICLE COMPARISON CHART FOR 2000-POUND PAYLOAD  $LF_2/LH_2$  MSPS

Launch Vehicle	Maximum $\Delta V$ ,* (in Orbit), ft./sec	Gross Weight for $\Delta V=99.8$ Percent Maximum, pounds	Initial Gross Weight in Orbit, pounds	Maximum Engine Thrust, pounds
Nominal Titan III-C	24,200	36,000 to 42,000	28,000 to 30,000	42,000 to 45,000
Titan III-C With Seven-Segment, 120- Inch Solids	26,000	32,000 to 39,000	32,000 to 35,000	48,000 to 52,500
Titan III-C With Three-Segment, 156- Inch Solids	29,000	43,000 to 50,000	43,000 to 46,500	63,000 to 69,800
Nominal Saturn I-B	26,650	35,000 to 41,000	33,000 to 35,700	49,500 to 53,600
Saturn I-B With Minuteman	28,200	39,500 to 46,000	39,500 to 42,000	59,200 to 63,300

\*Single burn at maximum thrust

CONFIDENTIAL

TABLE IV

LF<sub>2</sub>/LH<sub>2</sub> MSPS PERFORMANCE CHARACTERISTICS FOR 2000-POUND PAYLOAD\*

Launch Vehicle	Initial Thrust-to-Weight Ratio in Orbit	Percent $\Delta V$ Maximum	$\Delta V^{**}$ (in Orbit), in./sec
Titan III-C (Nominal)	1.78	99.9	24,175
Titan III With Seven-Segment, 120-Inch Solids	1.48	100.0	26,600
Titan III With Three-Segment, 156-Inch Solids	1.39	95.3	27,625
Saturn I-B (Nominal)	1.49	100.0	26,650
Saturn I-B With Minuteman Strap-On	1.39	98.0	27,600

\*Gross weight = 36,000 pounds; thrust = 50,000 pounds

\*\*Single burn at maximum thrust

3  
CONFIDENTIAL

# CONFIDENTIAL

gross weights is presented in Fig. 17. To maintain the desired 10-foot stage diameter limit, a cylindrical section must be used in the LH<sub>2</sub> tanks to accommodate the increased LH<sub>2</sub> volume weight in comparison with the nominal 20,000-pound gross weight system. For the 52,000-pound gross weight stage, a cylindrical section in the LF<sub>2</sub> tank is also required.

- (C) Because of the gross weight and thrust differences between the two resulting vehicles, a comparison (Table VII) was made of the  $\Delta V$  capability of the selected 2000-pound-payload vehicle (gross weight = 36,000 pounds, thrust = 50,000 pounds) carrying the 5000-pound-payload (column 1) and the  $\Delta V$  capability of the selected 5000-pound-payload vehicle (gross weight = 52,000 pounds, thrust = 60,000 pounds) when carrying the 2000-pound payload.

The Titan III with 156-inch solids and the Saturn I-B Minuteman can place payloads greater than 36,000 pounds in orbit without a suborbital firing; therefore, these launch vehicles would be off-loaded (propellant removed) when used to place the MSPS gross weight of 36,000 pounds in orbit. Alternately these launch vehicles may be used with full propellant loads to provide higher orbit altitude or orbital plane changes at injection if required. Full propellant capacity is required for each of the launch vehicles to place the larger MSPS (52,000 pound) in orbit.

## b. LO<sub>2</sub>/LH<sub>2</sub> Systems

- (C) Comparisons and examples of MSPS gross weight and thrust level for LO<sub>2</sub>/LH<sub>2</sub> systems with the 2000 pound MSPS payload are presented in Tables VIII and IX. The range of gross weights and thrust levels shown in Table VIII to result in greater than 99.8 percent of the optimum  $\Delta V$  are seen to be slightly lower than the corresponding values for the LF<sub>2</sub>/LH<sub>2</sub> systems shown in Table III. This is a result of the lower specific impulse of the LO<sub>2</sub>/LH<sub>2</sub> systems compared to the LF<sub>2</sub>/LH<sub>2</sub> systems as discussed under Item 4.a. Comparisons of the ranges of near-optimum gross weights and thrust levels resulted in selecting values of 34,000 pounds and 48,000 pounds for the gross weight and thrust level respectively for the common LO<sub>2</sub>/LH<sub>2</sub>, 2000 pound payload MSPS. Although the selected gross weight is the 99.8 percent optimum  $\Delta V$  value shown in Table VIII for the MSPS used with the nominal Titan, the MSPS thrust level selected results in a greater than nominal thrust-to-weight ratio. Thus the orbital injection is more efficiently completed and the in-orbit  $\Delta V$  capability is improved by 0.2 percent. For these selected values the greatest  $\Delta V$  loss (6 percent) is experienced by the Titan III with 156 inch solid strap-ons. Selection of a larger and higher thrust MSPS would benefit this configuration but would result in degradation of the configurations using the nominal launch vehicles.

Similar results are shown in Tables X and XI for the 5000 pound payload MSPS. The selected common MSPS gross weight of 49,000 pounds and thrust level of 56,000 pounds result in payloads for all configurations which are within 0.4 percent of the maximum values obtainable for each configuration.

CONFIDENTIAL

TABLE V  
 LAUNCH VEHICLE COMPARISON CHART FOR 5000-POUND PAYLOAD  
 $\frac{L_F}{L_H}$  MSPS

Launch Vehicle	Maximum $\Delta V^*$ (in Orbit), ft/sec	Gross Weight for $\Delta V=99.8$ Percent Maximum, pounds	Initial Gross Weight in Orbit, pounds	Maximum Engine Thrust, pounds
Nominal Titan III-C	18,700	47,500 to 52,500	32,000 to 33,000	48,000 to 49,500
Titan III-C With Seven-Segment, 120- Inch Solids	21,400	55,000 to 65,000	40,700 to 43,400	61,000 to 65,000
Titan III-C With Three-Segment, 156- Inch Solids	24,000	62,000 to 75,000	50,500 to 53,200	76,000 to 80,000
Nominal Saturn I-B	21,400	52,500 to 62,500	40,000 to 42,700	60,000 to 64,000
Saturn I-B With Minuteman	23,100	58,000 to 68,000	46,800 to 49,500	70,000 to 74,200

\*Single burn at maximum thrust

31  
 CONFIDENTIAL

CONFIDENTIAL

TABLE VI

LF<sub>2</sub>/LH<sub>2</sub> MSPS PERFORMANCE CHARACTERISTICS FOR 5000-POUND PAYLOAD\*

Launch Vehicle	Initial Thrust-to-Weight Ratio in Orbit	Percent $\Delta V$ Maximum	$\Delta V^{**}$ (in Orbit), in./sec
Titan III-C (Nominal)	1.82	100	18,700
Titan III With Seven Segments	1.5	99.9	21,380
Titan III With Three-Segments 156-Inch Solids	1.28	99.2	23,800
Saturn I-B (Nominal)	1.5	99.7	21,330
Saturn I-B With Minuteman Strap-Ons	1.33	99.6	23,000

\*Gross weight = 52,000 pounds; thrust = 60,000 pounds

\*\*Single burn at maximum thrust

CONFIDENTIAL

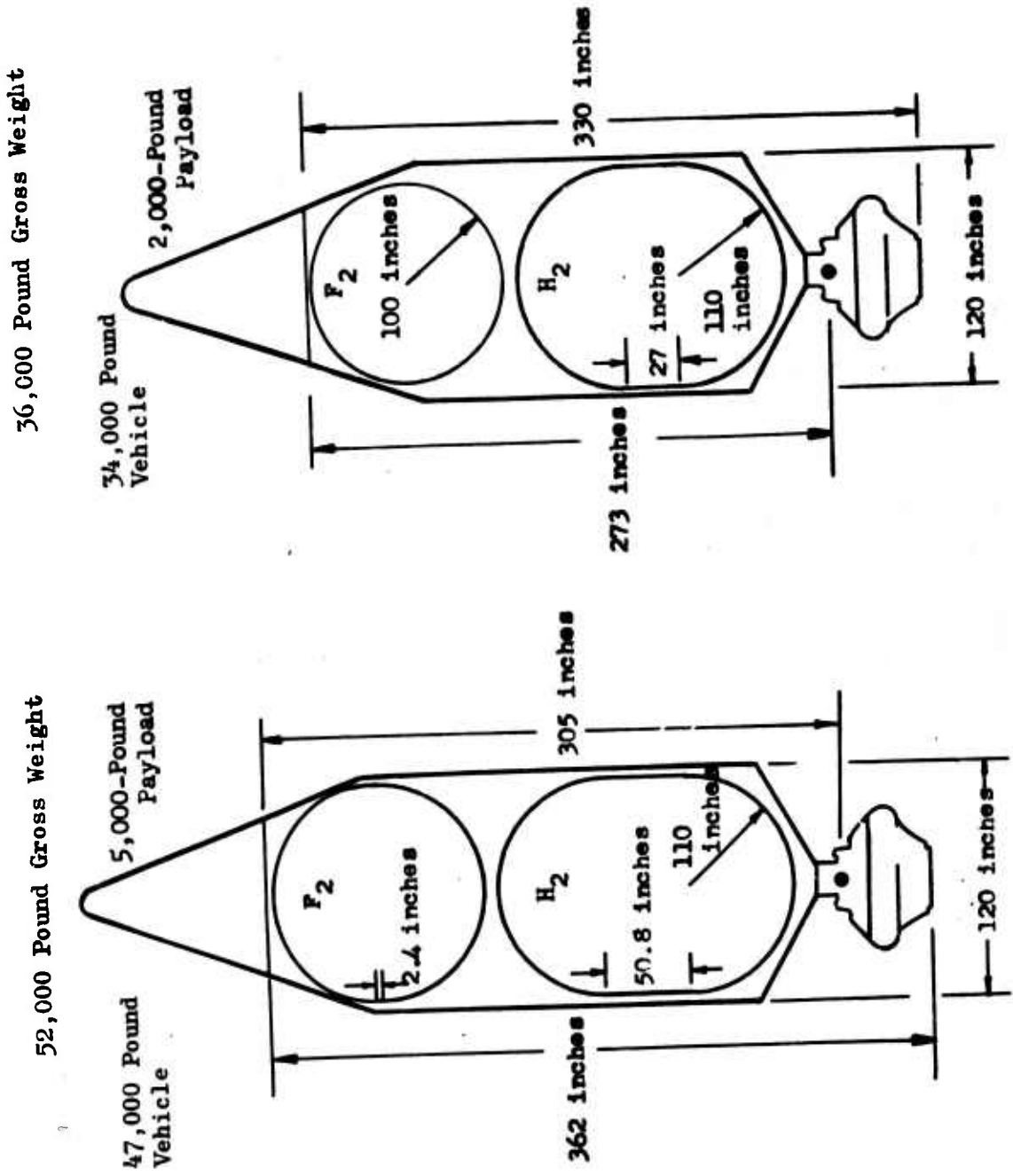


Figure 17 . Size Comparison of Selected Gross Weights for 5000- and 2000-Pound-Payload Fluorine-Hydrogen MSFS

# CONFIDENTIAL

TABLE VII

PERFORMANCE COMPARISON BETWEEN  
2000- AND 5000-POUND PAYLOADS\*  
( $LF_2/LH_2$  MSPS)

Launch Vehicle	Percent of Maximum $\Delta V$ for 5000-Pound-Payload Using 2000-Pound-Payload Vehicle	Percent of Maximum $\Delta V$ for 2000-Pound-Payload Using 5000-Pound-Payload Vehicle
Titan III-C (Nominal)	96.6	99.0
Titan III With Seven-Segment, 120-Inch Solids	96.3	98.1
Titan III With Three-Segment, 156-Inch Solids	90.0	99.7
Saturn I-B (Nominal)	96.3	99.1
Saturn I-B With Minuteman Strap-Ons	93.9	99.6

\*2000-pound-payload vehicle: gross weight = 36,000 pounds; thrust = 50,000 pounds

5000-pound-payload vehicle: gross weight = 52,000 pounds; thrust = 60,000 pounds

CONFIDENTIAL

TABLE VIII  
 LAUNCH VEHICLE COMPARISON CHART FOR 2000-POUND PAYLOAD ( $LO_2/LH_2$ )

Launch Vehicle	Maximum $\Delta V^*$ (in Orbit), ft/sec	Gross Weight for $\Delta V=99.8$ Percent Maximum, pounds	Initial Gross Weight in Orbit, pounds	Maximum Engine Thrust, pounds
Nominal Titan III-C	19,950	26,000 to 34,000	23,400 to 26,300	35,000 to 39,500
Titan III With Seven- Segment, 120-Inch Solids	22,430	31,500 to 34,500	31,600 to 32,900	47,500 to 49,400
Titan III With Three- Segment, 156-Inch Solids	24,300	43,000 to 45,000	43,000 to 44,200	64,500 to 66,300
Nominal Saturn I-B	22,370	31,200 to 35,000	31,000 to 32,400	46,500 to 48,500
Saturn I-B With Minuteman Strap-Ons	23,700	39,000 to 42,500	39,000 to 40,200	56,500 to 60,300

\*Single burn in orbit at maximum thrust

33  
 CONFIDENTIAL

# CONFIDENTIAL

TABLE IX

LO<sub>2</sub>/LH<sub>2</sub> MSPS PERFORMANCE CHARACTERISTICS  
FOR 2000-POUND PAYLOAD\*

Launch Vehicle	Initial Thrust-to-Weight Ratio in Orbit	Percent $\Delta V$ Maximum
Nominal Titan III-C	1.82	100
Titan III With Seven-Segment, 120-Inch Solids	1.47	99.9
Titan III With Three-Segment, 156-Inch Solids	1.41	94
Nominal Saturn I-B	1.50	99.8
Saturn I-B With Minuteman Strap-Ons	1.41	96.5

\*Gross weight = 34,000 pounds; thrust = 48,000 pounds

CONFIDENTIAL

TABLE X  
LAUNCH VEHICLE COMPARISON CHART FOR 5000-POUND PAYLOAD ( $LO_2/LH_2$ )

Launch Vehicle	Maximum $\Delta V$ (in Orbit), ft./sec	Gross Weight for $\Delta V=99.8$ Percent Maximum, pounds	Initial Gross Weight in Orbit, pounds	Maximum Engine Thrust, pounds
Nominal Titan III-C	15,200	37,500 to 49,000	27,500 to 31,800	41,300 to 47,600
Titan III With Seven- Segment, 120-Inch Solids	17,800	40,000 to 52,500	33,500 to 39,500	50,200 to 59,200
Titan III With Three- Segment, 156-Inch Solids	20,200	45,000 to 58,000	44,200 to 49,400	66,300 to 74,000
Nominal Saturn I-B	17,800	39,000 to 49,000	33,800 to 37,500	50,800 to 56,000
Saturn I-B With Minute- Man Strap-Ons	19,450	44,000 to 53,800	40,800 to 44,400	61,000 to 66,600

CONFIDENTIAL

# CONFIDENTIAL

TABLE XI

LO<sub>2</sub>/LH<sub>2</sub> MSPS PERFORMANCE CHARACTERISTICS  
FOR 5000-POUND PAYLOAD\*

Launch Vehicle	Initial Thrust-to-Weight Ratio in Orbit	Percent $\Delta V$ Maximum
Nominal Titan III-C	1.76	99.6
Titan III With Seven-Segment, 120-Inch Solids	1.46	100
Titan III With Three-Segment, 156-Inch Solids	1.22	100
Nominal Saturn I-B	1.49	99.7
Saturn I-B With Minute-man Strap-Ons	1.31	100

\*Gross weight = 49,000 pounds; thrust = 56,000 pounds

# CONFIDENTIAL

c. N<sub>2</sub>O<sub>4</sub>/N<sub>2</sub>H<sub>4</sub>-UDMH (50-50) Systems

- (C) Selections of MSPS gross weights and thrust levels were made for N<sub>2</sub>O<sub>4</sub>/N<sub>2</sub>H<sub>4</sub>-UDMH (50-50) systems. The results for the 2000 pound payload configuration are shown in Tables XII and XIII. Again, the lower specific impulse of the N<sub>2</sub>O<sub>4</sub>/N<sub>2</sub>H<sub>4</sub>-UDMH (50-50) MSPS results in lower maximum performance gross weights because of the inefficiency of using the MSPS for suborbital firing. The selected common gross weight and thrust level are 28,000 and 42,000 pounds, respectively. Selection of these parameters results in an 8 percent loss for the large Titan launch vehicle. A larger MSPS would reduce the losses for the uprated launch vehicles, but would increase the losses for configurations using the nominal Titan and Saturn launch vehicles.
- (C) Applicable MSPS gross weight and thrust ranges for the N<sub>2</sub>O<sub>4</sub>/N<sub>2</sub>H<sub>4</sub>-UDMH (50-50) system with 5000 pound payload are shown in Table XIV. The selected value of MSPS gross weight (36,000 pounds) and thrust (48,000 pounds) is shown in Table XV to result in very near-optimum  $\Delta V$ 's when used with the nominal launch vehicles and with the Titan III which uses 120-inch solid strap-ons. A 6.5 percent reduction from the maximum attainable value results when the common MSPS is used with the Titan III with 156 inch strap-ons.

CONFIDENTIAL

TABLE XII

LAUNCH VEHICLE COMPARISON CHART FOR 2000-POUND PAYLOAD ( $N_2O_4/N_2H_4$ -UDMH, 50-50)

Launch Vehicle	Maximum $\Delta V$ (in Orbit), ft/sec	Gross Weight for $\Delta V$ 99.8 Percent Maximum, pounds	Initial Gross Weight in Orbit, pounds	Maximum Engine Thrust, pounds
Nominal Titan III-C	17,500	21,800 to 28,000	21,800 to 23,200	32,700 to 34,900
Titan III-C With Seven-Segment, 120-Inch Solids	19,200	31,500 to 33,800	31,600 to 32,100	47,500 to 48,200
Titan III-C With Three-Segment, 156-Inch Solids	20,700	42,500 to 45,000	42,500 to 43,800	63,900 to 65,800
Nominal Saturn I-B	19,600	30,500 to 32,500	30,500 to 31,200	45,700 to 46,900
Saturn I-B With Minute- man Strap-Ons	20,280	38,000 to 39,000	38,000 to 38,900	57,000 to 58,200

CONFIDENTIAL

# CONFIDENTIAL

TABLE XIII

$N_2O_4/N_2H_4$ -UDMH (50-50) MSPS PERFORMANCE CHARACTERISTICS  
FOR 2000-POUND PAYLOAD\*

Launch Vehicle	Initial Thrust-to-Weight Ratio in Orbit	Percent $\Delta V$ Maximum
Nominal Tital III-C	1.81	100
Titan III-C With Seven-Segment, 120-Inch Solids	1.50	96.9
Titan III-C With Three-Segment, 156-Inch Solids	1.50	92.0
Nominal Saturn I-B	1.50	97.5
Saturn I-B With Minuteman Strap-Ons	1.50	93.9

\* Gross Weight = 28,000 pounds; Thrust = 42,000 pounds

CONFIDENTIAL

TABLE XIV

LAUNCH VEHICLE COMPARISON CHART FOR 5000-POUND PAYLOAD ( $N_2O_4/N_2H_4$ -UDMH, 50-50)

Launch Vehicle	Maximum $\Delta V$ (in Orbit), ft/sec	$\Delta V=99.8$ Percent Maximum, pounds	Gross Weight for $\Delta V=99.8$ Percent Maximum, pounds	Initial Gross Weight in Orbit, pounds	Maximum Engine Thrust, pounds
Nominal Titan III-C	12,300	27,500 to 36,000	23,000 to 25,000	34,500 to 37,500	
Titan III With Seven-Segment, 120- Inch Solids	14,820	31,500 to 37,500	31,500 to 33,000	47,500 to 49,500	
Titan III With Three- Segment, 156-Inch Solids	16,900	43,000 to 48,000	43,000 to 44,500	64,500 to 66,900	
Nominal Saturn I-B	14,780	33,800 to 40,000	31,500 to 32,800	47,200 to 49,300	
Saturn I-B With Minute- man Strap-Ons	16,300	38,500 to 42,500	38,500 to 39,600	57,800 to 59,500	

CONFIDENTIAL

# CONFIDENTIAL

TABLE XV

$N_2O_4/N_2H_4$ -UDMH (50-50) MSPS PERFORMANCE CHARACTERISTICS  
FOR 5000-POUND PAYLOAD\*

Launch Vehicle	Initial Thrust-to-Weight Ratio in Orbit	Percent $\Delta V$ Maximum
Nominal Titan III-C	1.92	99.9
Titan III With Seven-Segment, 120-Inch Solids	1.47	99.8
Titan III With Three-Segment, 156-Inch Solids	1.33	93.5
Nominal Saturn I-B	1.50	100
Saturn I-B With Minute man Strap-Ons	1.33	97.3

\*Gross weight = 36,000 pounds; thrust = 48,000 pounds

# CONFIDENTIAL

## SECTION IV

### MANEUVERING SPACE PROPULSION SYSTEM VEHICLE CONFIGURATION SELECTION AND OPTIMIZATION

- (U) Increased gross weight versions of the Maneuvering Space Propulsion System (MSPS) using  $\text{LF}_2/\text{LH}_2$ ,  $\text{LO}_2/\text{LH}_2$ , and  $\text{N}_2\text{O}_4/\text{N}_2\text{H}_4$ -UDMH (50-50) propellants were analyzed to determine their optimum configurations. This analysis was conducted in parallel with the work described in the preceding section and, therefore, a range of MSPS gross weights was selected based upon the preliminary results of the launch vehicle studies.
- (C) An engine configuration selection study was conducted to determine the most desirable propulsion system for each propellant combination and stage gross weight of interest. The selection was based upon the maneuvering propulsion system requirements for a satellite intercept and fast response reconnaissance-type missions. Maximum use was therefore made of the previous comprehensive selection studies of Ref. 3.
- (U) An optimization analysis was conducted for the selected engine configurations for each of the propellant combinations and selected stage gross weights. The engine operating and design parameters were optimized at the full-thrust and throttled operating conditions to determine the design configuration providing maximum  $\Delta V$  capability. Regenerative cooling limits, engine envelope restrictions, and operational duty cycle effects were combined with the optimization results to determine the selected engine design parameters.
- (U) An illustrative comparison of the  $\text{LF}_2/\text{LH}_2$ ,  $\text{LO}_2/\text{LH}_2$ , and  $\text{N}_2\text{O}_4/\text{N}_2\text{H}_4$ -UDMH (50-50) MSPS was then made based upon a selected system gross weight determined by the launch vehicle payload capability studies and the results of the configuration selection and optimization studies. This comparison includes engine system performance over the operating thrust range, system weights, and inboard profile drawings to indicate component arrangement and configuration size. The velocity capability of the specific MSPS is presented for each launch vehicle and several mission applications including continuous operation at maximum thrust, continuous operation at minimum thrust, and a series of nonevasive target satellite rendezvous maneuvers.

#### 1. DEFINITION OF PROPULSION SYSTEM REQUIREMENTS

- (C) A range of stage gross weights was selected for the propulsion system evaluation studies based upon the preliminary results from launch vehicle payload capability studies. It has been shown that payload capabilities for the nominal and growth versions of the Saturn I-B and Titan III-C range from 20,000 to 50,000 pounds. In view of the many possible launch vehicle and mission variations, stage gross weights of 20,000, 33,300, and 50,000 pounds were selected for the initial configuration selection and optimization analysis.

# CONFIDENTIAL

- (C) The requirement for a maximum thrust-to-weight ratio of 1.5 (Ref. 3) then defined the design thrust levels for each stage gross weight. The mission/propulsion system requirements also specify a minimum thrust-to-weight ratio at burnout of 0.1. These thrust-to-weight ratio requirements combined with the stage gross weight, payload, and inert weight characteristics define the required system overall throttling ratio. The effects of stage gross weight and propellant fraction ( $\lambda_p$ ) on the overall system throttling ratio are illustrated in Fig. 18 for the 2000-pound-payload case. It can be seen that the throttling ratio requirement increases with both increases in system gross weight and propellant fraction. In the current study, the throttling ratio was varied with the system gross weight, as described in Fig. 18. It should also be noted that the payload value affects the required throttling ratio. The lower value of payload (2000 pounds) coupled with the minimum thrust-to-weight ratio of 0.1 results in the highest propulsion system throttling ratio requirement.
- (U) A maximum overall propulsion system diameter of 10 feet was maintained for the range of design thrust levels investigated. This diameter limit was maintained for consistency with the Titan launch vehicle diameter and the maximum diameter of the MSPS.

## 2. $LF_2/LH_2$ SYSTEMS

### a. Engine Configuration Selection

- (U) The engine configuration selection for the  $LF_2/LH_2$  systems consisted primarily of a review of the major system configurations considered in the previous study of Ref. 3. A summary of the advanced engine systems selected for further analysis is shown in Fig. 19. The selection criteria used in the relative evaluation of these systems are presented in Table XVI. The increased thrust level of the systems to be considered in the present study is the only change to the basic ground rules (Ref. 3) used in the original configuration selection. A review of the selection criteria showed that the primary effect of the increased thrust level was to result in higher  $P_c - \epsilon$  combinations for the aerodynamic spike engine systems. This results in an increase in the specific impulse capabilities of the aerodynamic spike engine relative to the other engine configurations.

The engine configuration selection criteria established in Ref. 3 resulted in the concentric aerodynamic spike/bell nozzle propulsion system as the most favorable system for this application. Because the increased design thrust levels benefit the aerodynamic spike engine, the original selection results of the previous study (Ref. 3) are valid for the increased gross weight systems.

- (U) The selected  $LF_2/LH_2$  propulsion system consists of an aerodynamic spike engine designed to satisfy the maximum thrust requirement. The overall system throttling ratio is divided equally between the primary engine and the secondary engine. The secondary engine is a bell nozzle thrust chamber with a design thrust equal to the minimum thrust of the primary

CONFIDENTIAL

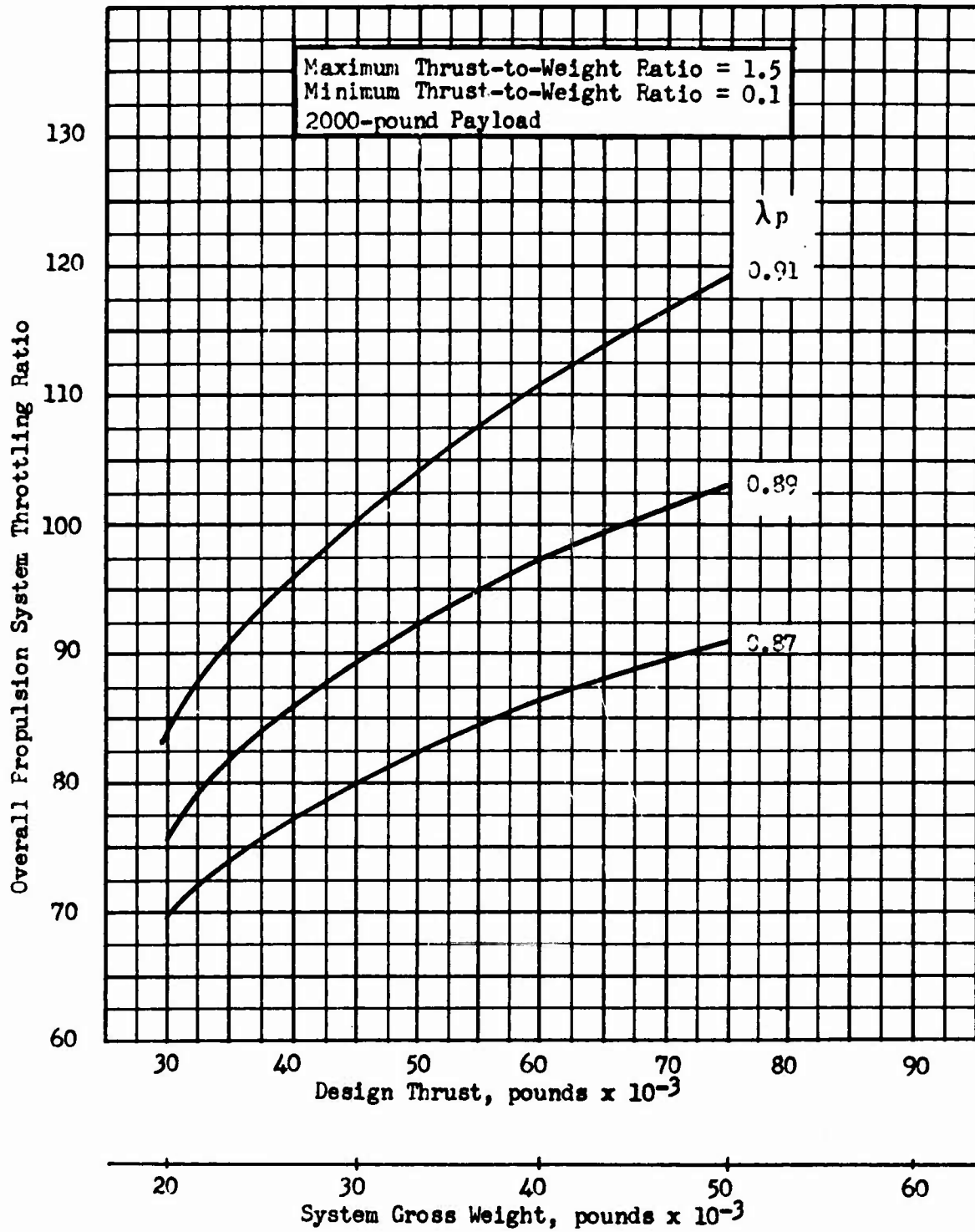


Figure 18 . Effect of System Gross Weight and Design Thrust Level on Overall Throttling Requirements

CONFIDENTIAL

**TABLE XVI**  
**MAIN ENGINE SELECTION CRITERIA**  
**(Ref. 3)**

**1. Performance**

**Specific Impulse (overall)**  
**Weight**

**2. Operational Suitability**

**Throttling**  
**Depth**  
**Adaptability**  
**Engine Length (interstage)**  
**Transient Losses**  
**Number of Throttling Control Operations**  
**Engine Mounting Adaptability**

**3. Complexity and Reliability Considerations**

**Number of Major Components**  
**Number of Critical Components**

**4. Development Considerations**

**Ease of Development**  
**Number of Engines to Be Developed**  
**Fabrication**  
**Segment Development**  
**Experience**  
**Technological Areas for Development**

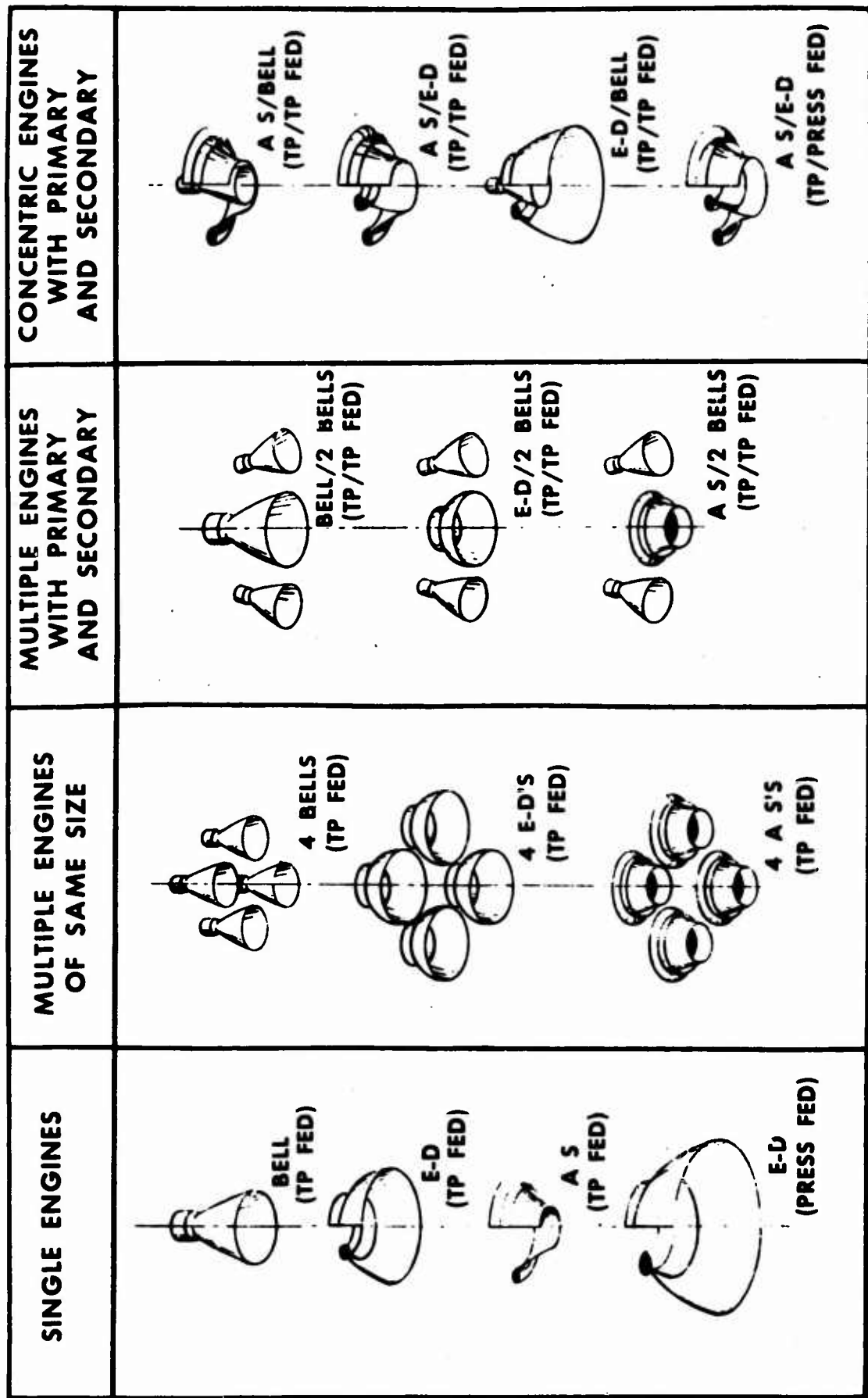


Figure 19 Advanced Engines Selected for Further Analysis

# CONFIDENTIAL

engine and is located in the center of the larger aerodynamic spike engine. Both engines are pump fed (individual turbopumps) using combustion chamber tapoff gases for turbine drive.

## b. Engine System Optimization Procedure

- (U) An engine-operating and design parameter optimization was conducted for the selected engine configuration at each of the design thrust levels. The optimization analysis results in design and operating parameters that provide maximum mission performance based upon a tradeoff between system weight and performance (delivered specific impulse). The results of the optimization analysis in conjunction with heat transfer and system considerations provide the basis for the selection of the design and operating parameters for the final propulsion system configurations.
- (C) Design thrust levels of 30,000, 50,000, and 75,000 pounds were chosen for the aerodynamic spike engines and 3300, 5000, and 7500 for the bell nozzle engines. The two thrust chambers of the composite systems operate at different times and are interdependent only in the control systems, envelope restrictions, and the equal and constant engine mixture ratio requirement. In view of these considerations, each engine may be optimized separately.
- (C) The optimization was conducted treating  $\Delta V$  as the dependent parameter and assuming stage gross weight values of 20,000, 33,300, and 50,000 pounds and a payload of 2000 pounds. The design chamber pressure and expansion area ratio were the independent parameters to be optimized.
- (C) An engine mixture ratio of 13:1 was selected for the  $LF_2/LH_2$  systems. This selection was based upon previous optimization studies that have included the effects of stage inert weight, performance, heat transfer capabilities, and throttling requirements. A detailed mixture ratio selection study for the  $LF_2/LH_2$  MSPS engine is reported in Ref. 3.
- (U) A 20-percent length nozzle contour was selected for the nozzle weight and performance calculations of the aerodynamic spike engines. An 80-percent nozzle length was selected for the bell nozzle thrust chambers. These values are consistent with the optimization results presented in Ref. 3.
- (U) The optimization analysis was conducted for continuous operation at both maximum thrust and minimum thrust. This analysis describes the two limiting operating conditions and, thus, the extremes in the optimum operating parameters which are combined to make the final selection of operating parameters.
- (1) (U) Engine Performance. Parametric engine performance data used in the optimization analysis were generated by performing engine system balances for a range of chamber pressures and area ratios for each of the selected thrust levels and thrust chamber configurations. Nozzle expansion efficiencies used in the system balance were obtained from the parametric data presented in Ref. 3 and other recent work. These efficiencies include

## CONFIDENTIAL

nozzle divergence losses and nozzle drag losses. The nozzle efficiencies were determined at the full-thrust and throttled operating conditions for each combination of chamber pressure and area ratio considered in the optimization analysis.

- (U) Theoretical propellant performance was based upon the equilibrium performance model, and theoretical propellant kinetic efficiencies were used to correct for the kinetic performance losses in the nozzle. The kinetic efficiencies were obtained for the full-thrust and throttled operating conditions and for parametric values of chamber pressure and area ratio.
- (C) For both engines, the turbopumps are powered by hot gases tapped from the combustion chamber. The aerodynamic spike utilizes two parallel turbines, one for each pump, and the bell nozzle engine has one turbine driving both pumps. Nominal pump and turbine efficiencies and other system operating characteristics used in establishing the parametric performance data for full-thrust and throttled operating conditions are presented in Table XVII for the aerodynamic spike and bell nozzle engines.
- (U) Oxidizer and fuel pump discharge pressure estimates were based upon the nominal values presented in Ref. 4. The ratio of the  $\Delta P/P_c$  for each of the system components (injector, cooling jacket, lines and valves) was held constant for a given operating thrust level. For the throttled operating condition, the pressure drops were varied based on flowrate scaling factors.
- (2) (U) Stage Weight. Parametric stage inert weight data used in the optimization analysis were obtained from stage designs conducted for the optimized  $LF_2/LH_2$  MSPS propulsion system. These stage weight data were also used in the optimization of the alternate mission propulsion systems presented in Ref. 2.
- (U) Parametric engine weight data were generated for the various engine configurations using existing Rocketdyne computer programs. The weight analysis was based upon past design and fabrication experience and provides a component-by-component evaluation of the overall engine system. These parametric weights were generated for the aerodynamic spike and bell nozzle engines for the range of operating parameters considered in the optimization.

### c. Aerodynamic Spike Engine Results

- (C) The results of the fluorine/hydrogen aerodynamic spike engine optimization are presented in Fig. 20 through 23 for continuous operation at three selected design thrust levels. As shown in the curves, variations of expansion ratio and chamber pressure over the range indicated, affected relative velocity capability by a maximum of approximately 1 percent. From these curves, it can be seen that a design chamber pressure of 700 to 800 psia and an area ratio of 100:1 provide near-maximum mission performance for all three design thrust levels. The inclusion of the regenerative cooling capabilities of these systems results in a slight adjustment in the selected

# CONFIDENTIAL

TABLE XVII  
 $LF_2/LH_2$  SYSTEM OPERATING CHARACTERISTICS

	Aerodynamic Spike Engine		Bell Nozzle Engine	
	Maximum Thrust	Minimum Thrust	Maximum Thrust	Minimum Thrust
Combustion Efficiency	0.99	0.98	0.99	0.98
Engine Mixture Ratio	13:1	13:1	13:1	13:1
Tapoff System Mixture Ratio	1.21	1.21	1.21	1.21
Tapoff Gas Temperature, R	1960	1960	1960	1960
Tapoff Gas Specific Heat Ratio ( $\lambda$ )	1.374	1.374	1.374	1.374
Tapoff Gas $C_p$	1.744	1.744	1.744	1.744
Oxidizer Pump Efficiency	0.76	0.718	0.55	0.519
Fuel Pump Efficiency	0.45	0.407	0.30	0.27
Oxidizer Turbine Efficiency	0.276	0.07	0.41	0.112
Fuel Turbine Efficiency	0.546	0.202	--	--
Oxidizer Turbine Pressure Ratio	15:1	13.7:1	15.0	13.7:1
Fuel Turbine Pressure Ratio	15:1	13.7:1	--	--

CONFIDENTIAL

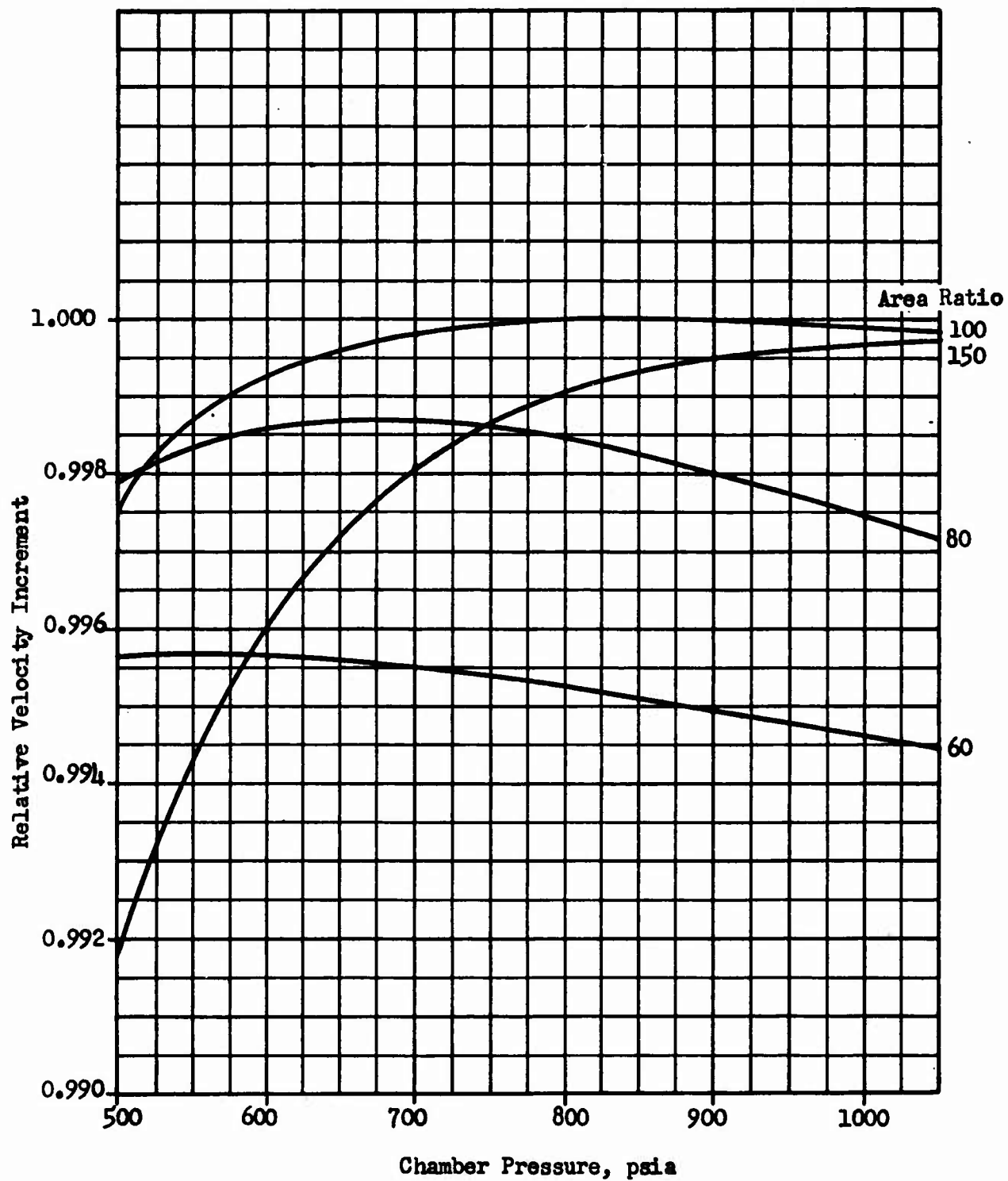


Figure 20. Chamber Pressure - Expansion Area Ratio Optimization for Fluorine/Hydrogen 30,000 lbf Aerodynamic Spike Engine

CONFIDENTIAL

CONFIDENTIAL

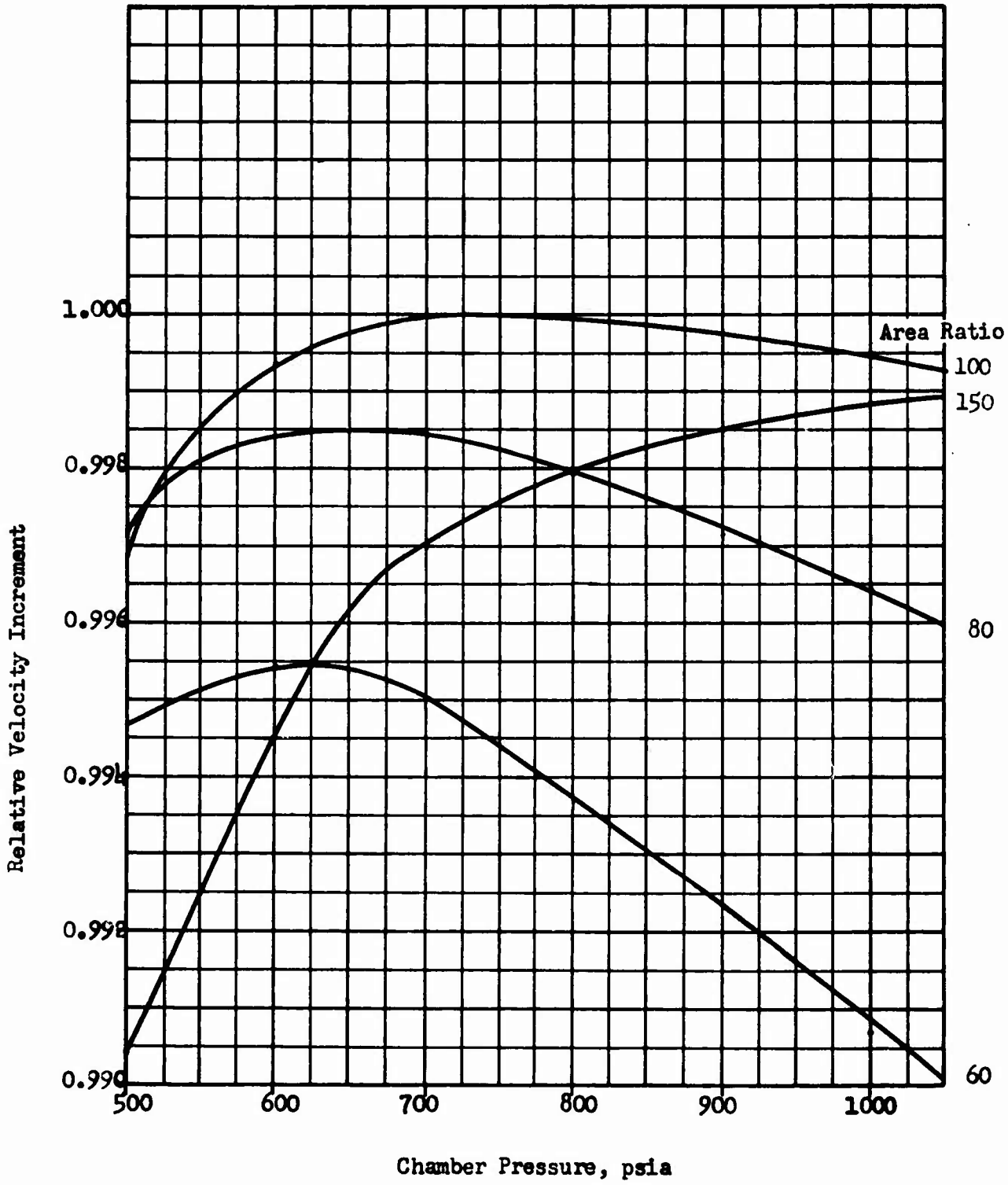


Figure 21. Chamber Pressure - Expansion Area Ratio Optimization for Fluorine-Hydrogen 50,000 lbf Aerodynamic Spike Engine

54  
CONFIDENTIAL

CONFIDENTIAL

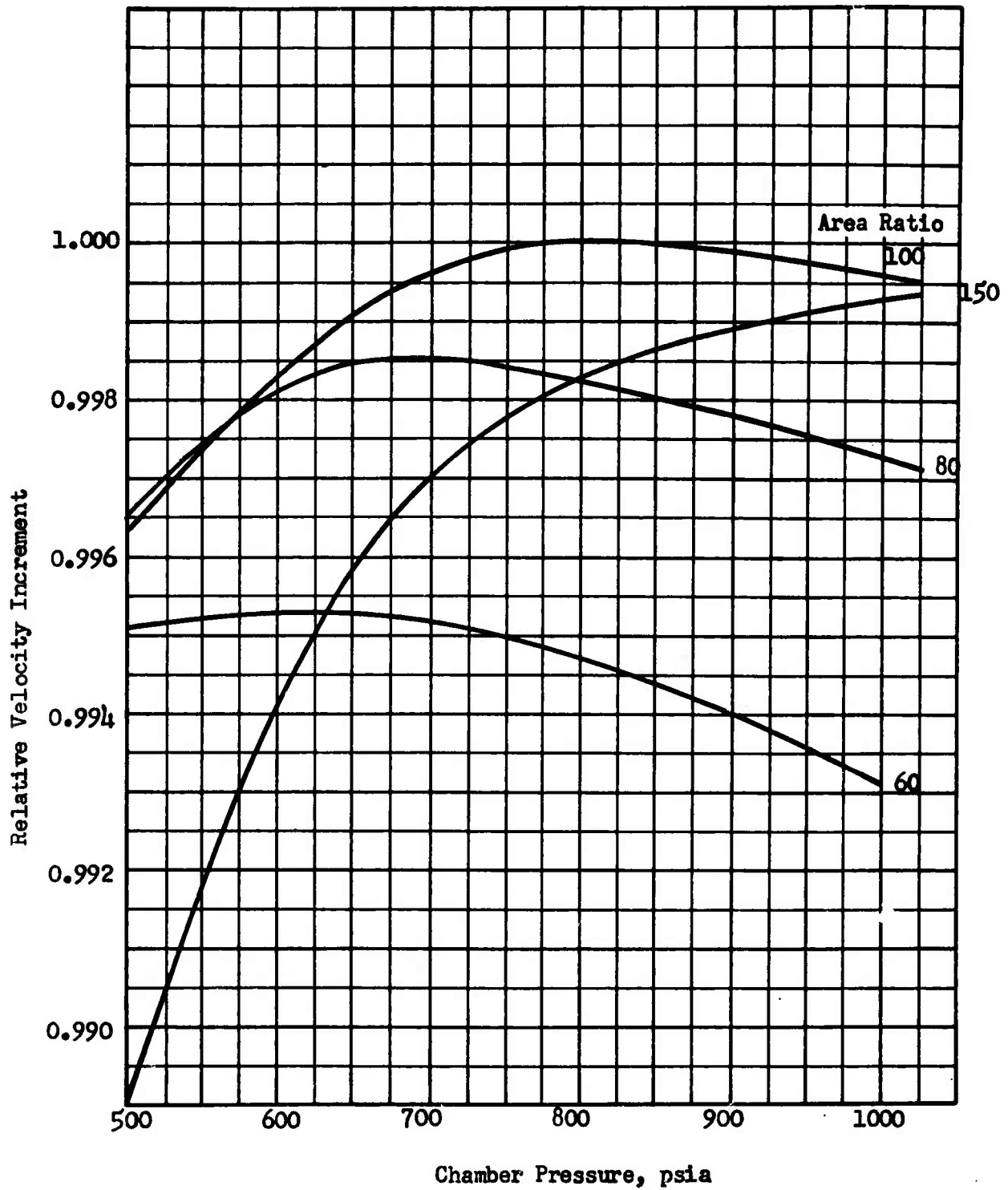


Figure 22. Chamber Pressure - Expansion Area Ratio Optimization for Fluorine-Hydrogen 75,000 lbf Aerodynamic Spike Engine

CONFIDENTIAL

# CONFIDENTIAL

chamber pressure and area ratio values; however, the overall velocity capability is affected only slightly (less than 0.2 percent for the 30,000 pound thrust level and 0 percent for the 50,000 and 75,000 pound thrust levels). The selected values of chamber pressure and expansion ratio are shown in Table XVIII.

TABLE XVIII

OPTIMUM OPERATING PARAMETERS FOR  $LF_2/LH_2$   
AERODYNAMIC SPIKE THRUST CHAMBERS FOR  
CONTINUOUS OPERATION AT FULL THRUST

<u>Thrust,</u> <u>pounds</u>	<u>Chamber</u> <u>Pressure,</u> <u>psia</u>	<u><math>\epsilon</math></u>
30,000	580	80
50,000	700	100
75,000	800	100

- (C) The selected chamber pressure value for the 30,000-pound design thrust level is slightly lower than the value determined in Ref. 3. This is primarily because of revised turbomachinery operating characteristics that evolved from the studies reported in the design phase (Ref. 4). These detailed studies resulted in refined turbine and pump efficiencies for a throttleable engine.
- (C) Because of the similarity of the full-thrust optimization results over the range of design thrust levels investigated, the optimization analysis at the throttled operating condition was conducted for the 30,000-pound-thrust system only. The results are typical for the range of design thrust levels of interest and will indicate the effect of the throttled engine performance on the selection of the maximum performance design parameters.
- (C) The throttled optimization results for the 30,000-pound-thrust  $LF_2/LH_2$  aerodynamic spike engine are shown in Fig. 23. As shown in the figure, continuous operation at the throttled condition makes higher chamber pressure more desirable. With the consideration of the regenerative cooling, the maximum performance design parameters for continuous operation at the throttled operating condition would be a full-thrust design chamber pressure of 680 psia and expansion area ratio of 60:1. The optimization was conducted at a throttled operating conditions of 10:1. This throttle ratio approximates the throttling requirement of the aerodynamic spike engine for each of the assumed full-thrust systems and also greatly simplified the analysis.
- (1) (U) Operating Parameter Selection for  $LF_2/LH_2$  Systems. The final selection of the operating parameters for the engines depends upon a compromise between the maximum performance parameters for continuous operation at full thrust and the throttled operating conditions. This selection is influenced by mission or throttling duty-cycle considerations. For those

CONFIDENTIAL

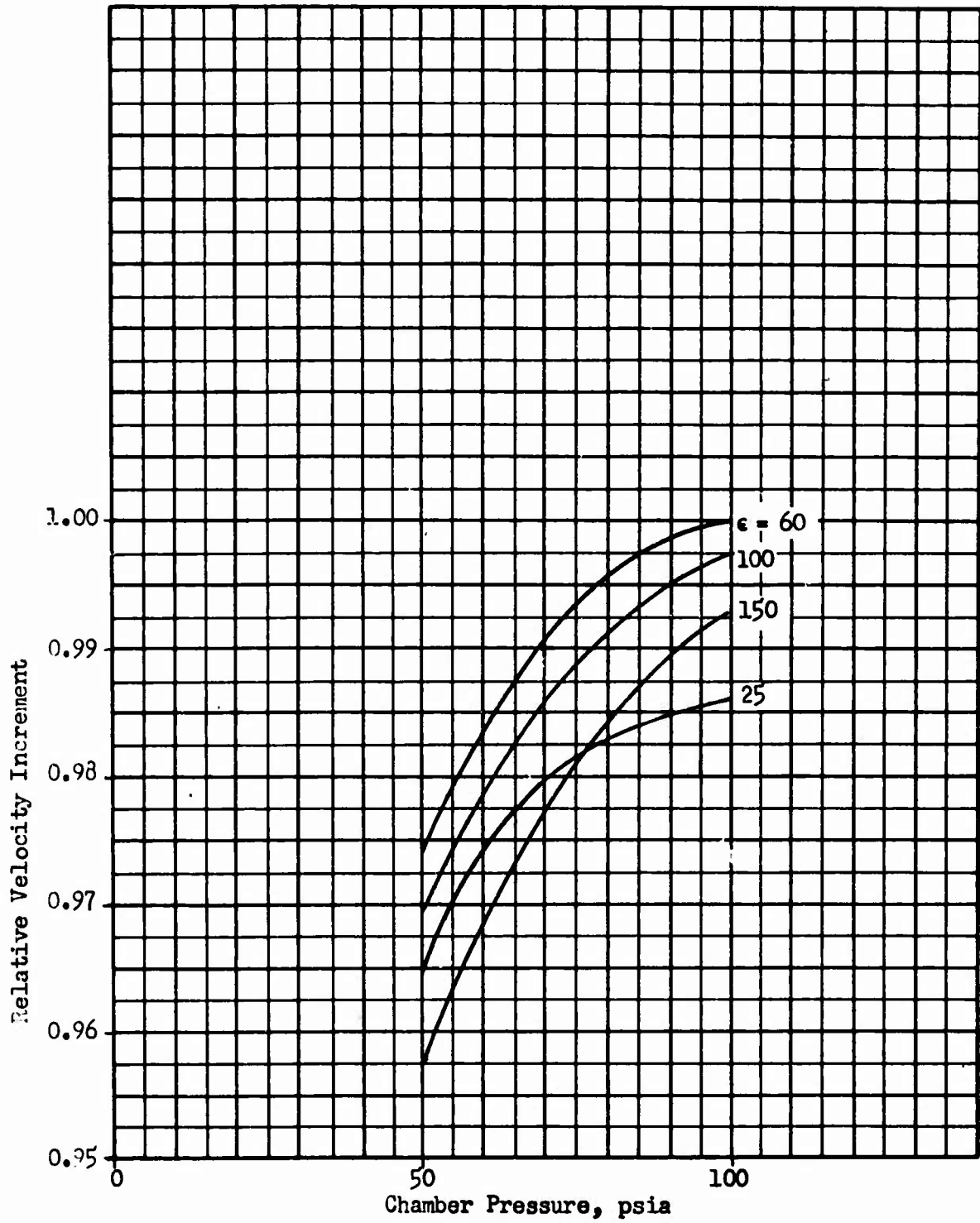


Figure 23. Effect of Throttling on 30,000 lbf Aerodynamic Spike Engine Fluorine-Hydrogen Propellant with a 10:1 Throttling Ratio

CONFIDENTIAL

# CONFIDENTIAL

missions where the major portion of the velocity increment is accomplished at or near full-thrust operating conditions, the maximum performance engine design parameters would correspond to the optimum values for continuous operation at full thrust. As a greater portion of the mission is accomplished at throttled operating conditions, greater overall mission performance is obtained with engine design parameters biased toward the optimum values for continuous throttled operation.

- (C) The effects of mission duty cycle on the design parameter selection were obtained by combining the results of the optimization analysis for continuous operation at both full thrust and minimum thrust. The procedure used in combining the results of the optimization analysis is illustrated in Fig. 24. In these curves, the relative total velocity increment is plotted vs the fraction of the total  $\Delta V$  that is achieved at full thrust. These results are for the 30,000-pound-thrust  $LF_2/LH_2$  aerodynamic spike engine. Where the fraction of full thrust  $\Delta V$  is zero, the entire velocity increment is achieved at the throttled operating condition. As the value of the fraction increases, a greater percentage of the mission is performed at full thrust. The curves are plotted for selected combinations of chamber pressure and expansion area ratio ranging from the full-thrust optimum to the throttled optimum design parameters. The results of the comparison shown in Fig. 24 indicate that the throttled engine performance has the dominant influence on the selection of the engine design parameters. However, it is also shown that the overall mission performance is only slightly affected as the design parameters are perturbed between the two optimum conditions. Based upon these results, it was concluded that near-maximum mission performance could be obtained for any operating thrust level by selecting the throttled optimum design parameters ( $P_c = 680$ ,  $\epsilon = 60$ ) for the 30,000-pound-thrust  $LF_2/LH_2$  aerodynamic spike engine.
- (C) These results are in very close agreement with the design parameters selected for the  $LF_2/LH_2$  engine in Ref. 3 ( $P_c = 650$ ,  $\epsilon = 63$ ). Therefore, the system improvements evolved since the earlier optimization study have been shown to have an insignificant effect on selection of engine design parameters.
- (U) Based upon these results, the design parameters for the higher-thrust  $LF_2/LH_2$  aerodynamic spike engines were selected and are summarized in Table XIX.

#### d. Bell Nozzle Engine Results

- (U) The  $P_c - \epsilon$  optimization for the bell nozzle  $LF_2/LH_2$  engines is presented in Fig. 25 through 27 for continuous operation at the selected design thrust levels.
- (C) In the selected concentric aerodynamic spike/bell engine configuration, the bell nozzle engine is located in the central base region of the aerodynamic spike, thus limiting the total diameter of the bell nozzle. These limits were determined for the assembly of the 3300-, 5000-, and 7500-pound-thrust bell nozzle engines with the 30,000-, 50,000-, and

CONFIDENTIAL

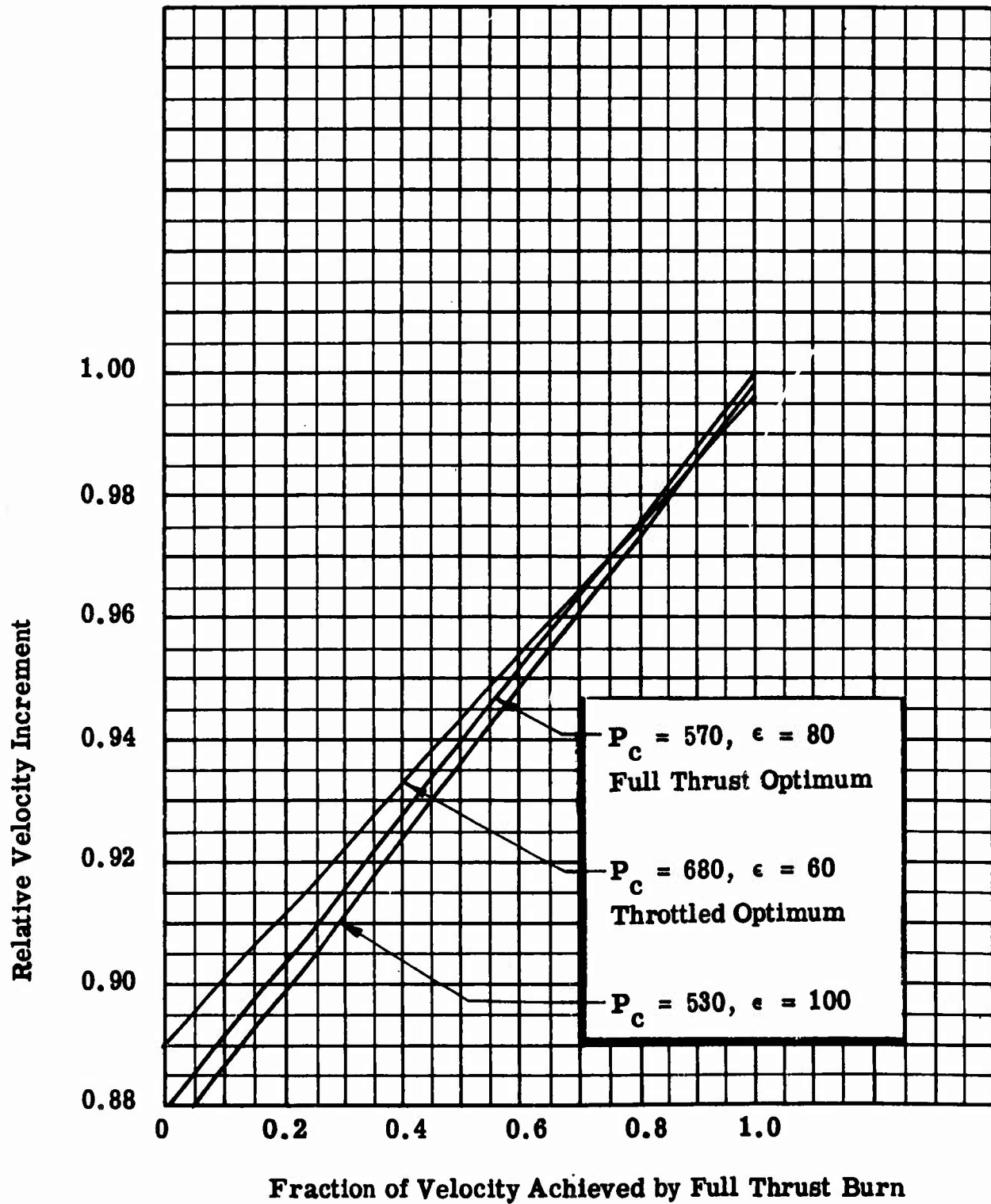


Figure 24. Duty Cycle Influence on Design Parameter Selection for 30,000-Pound-Thrust  $F_2/H_2$  Aerodynamic Spike Engine.

CONFIDENTIAL

# CONFIDENTIAL

TABLE XIX

DESIGN PARAMETER SELECTION  
FOR  $LF_2/LH_2$  PROPULSION SYSTEMS\*

Engine	Design Thrust, pounds	Chamber Pressure, psia	$\epsilon$
Aerodynamic Spike	30,000	650	63
	50,000	700	100
	75,000	800	100
Bell	3300	500	100
	5000	625	200
	7500	740	200

\* Mixture ratio = 13:1

CONFIDENTIAL

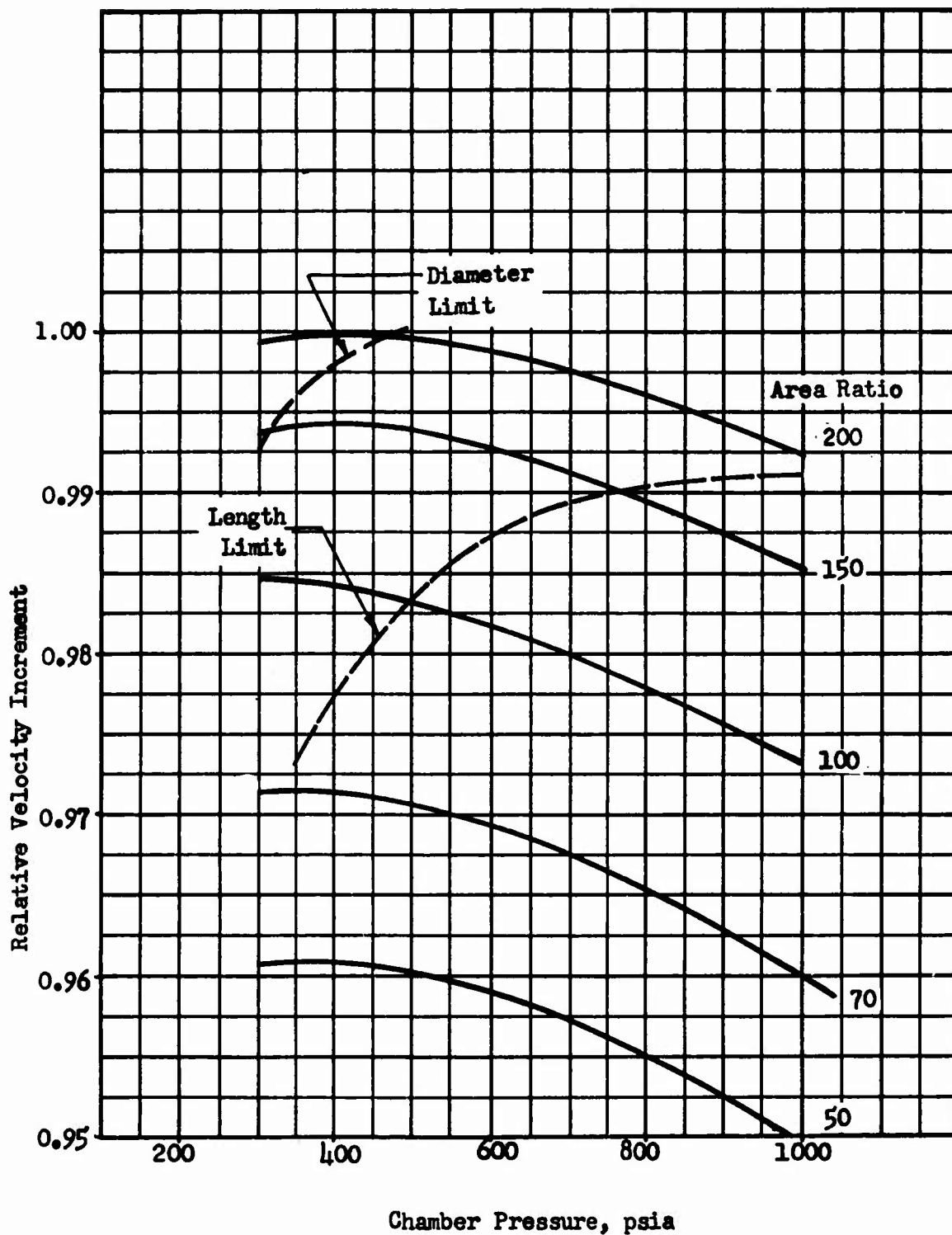


Figure 25. Chamber Pressure - Expansion Area Ratio Optimization for Fluorine-Hydrogen 3,300 lbf Bell Engine

CONFIDENTIAL

CONFIDENTIAL

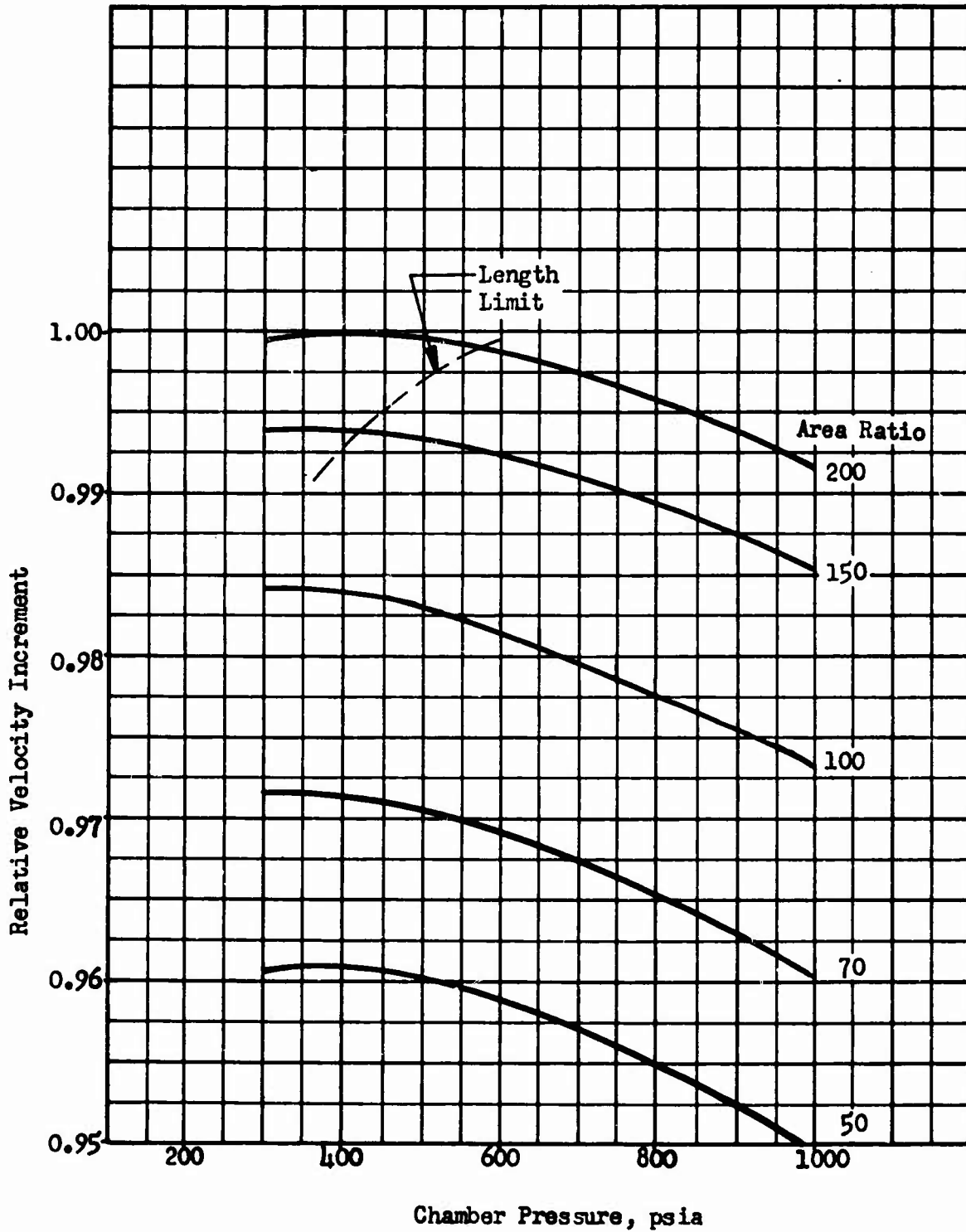


Figure 26. Chamber Pressure - Expansion Area Ratio Optimization for Fluorine-Hydrogen 5,000 lbf Bell Engine

CONFIDENTIAL

CONFIDENTIAL

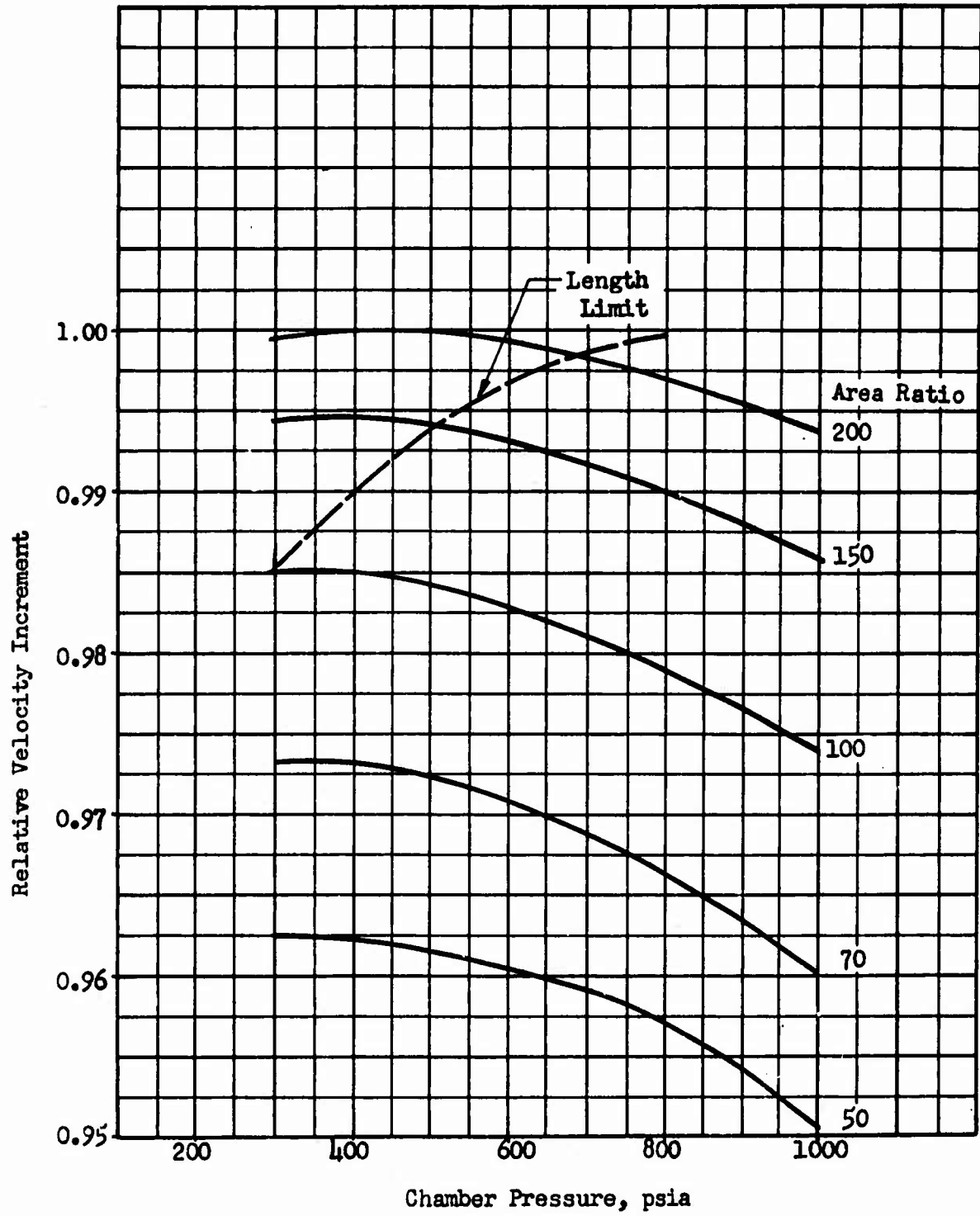


Figure 27. Chamber Pressure - Expansion Area Ratio Optimization for Fluorine-Hydrogen 7,500 lbf Bell Engine

CONFIDENTIAL

# CONFIDENTIAL

75,000-pound-thrust aerodynamic nozzles. The diameter limits are shown in the figures as a function of chamber pressure. An engine length restriction for the bell nozzle engines was also established. The position of the exit of the bell nozzle was restricted relative to the exit of the aerodynamic spike nozzle to avoid impingement of the hot gases from the outer nozzle on the bell nozzle. Since a single gimbal point is desired for both the inner and outer engines, the position of the bell thrust chamber is restricted to allow an efficient thrust mount and gimbal design as well as convenient component packaging. For these parametric studies, these design limits were established to maintain the same ratio of aerodynamic spike engine length to bell engine length as designed in the original 30,000-pound-thrust  $LF_2/LH_2$  propulsion system (Ref. 4). By maintaining this ratio, the overall propulsion package, mounting structure, and gimbal system design remain unaltered. This length limitation is illustrated for the previously described propulsion system assemblies in the respective figures. The design parameters selected for the aerodynamic spike engines were used in establishing the engine length limits. The regions to the right of the limit curves of Fig. 25, 26 and 27 are the desirable design areas.

- (U) It can be seen that the length limitation is much more restrictive than the diameter limit and thus will define the engine envelope restriction in selecting the engine design and operating parameters. As a result of this length restriction, the optimum chamber pressure values will be at higher values than the unrestricted optimum. As shown in the figures, the bell nozzle optimization is much more strongly affected by the expansion area ratio than by chamber pressure. Over the range of chamber pressures, a variation in relative velocity increment of approximately 1 percent occurs. Over the range of expansion area ratios, a relative velocity increment difference of approximately 4 percent exists. Although the addition of the length limit results in higher optimum chamber pressures, the relative velocity increment is reduced only slightly because of this restriction.
- (C) An optimization was also conducted for the 3300-pound-thrust  $LF_2/LH_2$  bell nozzle engine for continuous operation at one-tenth of the design thrust. The results are shown in Fig. 28. The nozzle length limitation is indicated on the curves. These results indicate that the throttled operating condition tends to result in much higher optimum chamber pressure values. Nozzle area ratio has a very slight effect on overall system performance because of the high nozzle drag losses that occur during throttled operation. The higher optimum chamber pressure is primarily a result of the kinetic performance losses associated with throttled operation of  $LF_2/LH_2$  systems.
- (1) (U) Operating Parameter Selection. The selection of the parameters for the secondary bell nozzle engines was based upon a mission weighted evaluation of the full-thrust and minimum-thrust optimization results and the engine envelope restrictions. Turbomachinery design considerations were also included in the final design parameter selection.

CONFIDENTIAL

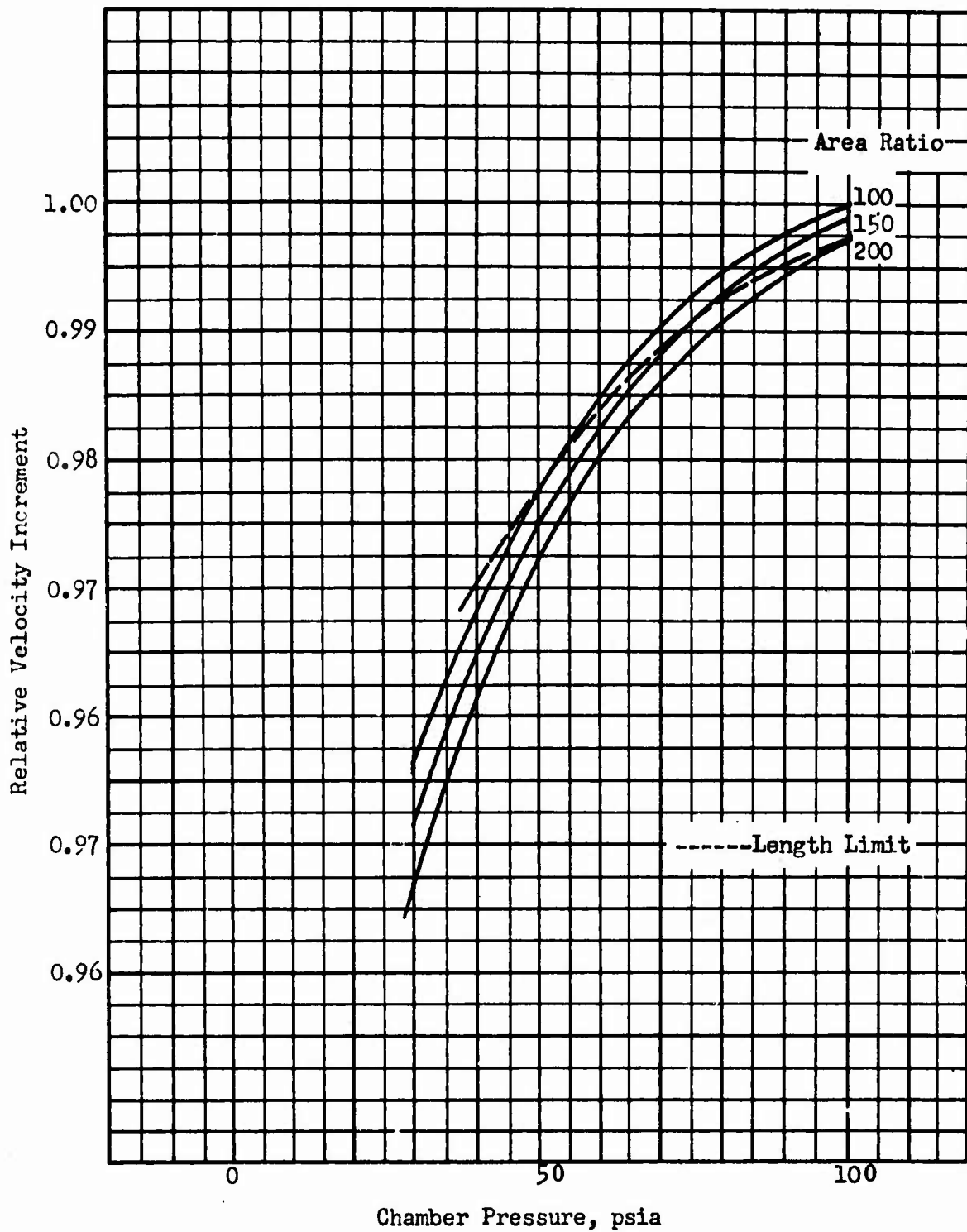


Figure 28. Throttling Effects on Chamber Pressure-Expansion Area Ratio Optimization for Liquid Fluorine-Hydrogen 3300 lbf Bell Engine, 10:1 Throttled Operation

CONFIDENTIAL

# CONFIDENTIAL

- (C) The mission effects were examined by selecting values of chamber pressure and area ratio in a region bracketed by the full-thrust and minimum-thrust optimum values. The mission weighted optimizations are shown in Fig. 29 for the 3300-pound-thrust  $LF_2/LH_2$  bell nozzle engine. These curves were constructed in the same manner as those for the aerodynamic spike engine optimization results. In essence, they combine the results of the full-thrust and throttled optimizations. From these results, it is shown that a relatively large range in the design values of chamber pressure and area ratio have only a minor effect on the overall mission performance.
- (U) A review of the parameter optimization results of Fig. 29 indicates that higher chamber pressures and area ratios are desired for maximum performance. In evaluating the pump design considerations for the small bell engine, however, it was found that considerable simplicity in the  $LH_2$  pump design can be realized (fewer stages) by selecting a lower value of chamber pressure. Because the loss in mission performance capability is slight for the lower chamber pressures, a chamber pressure of 500 psia and area ratio of 100:1 were selected. These parameters result in a performance capability reduction of only 1/2 percent and 1-1/2 percent at respectively the full thrust burn and minimum thrust burn conditions.
- (U) A summary of the selected design parameters for the  $LF_2/LH_2$  bell nozzle engines is presented in Table XIX.

## 3. $LO_2/LH_2$ SYSTEMS

### a. Engine Configuration Selection

- (U) In selecting a propulsion system configuration for the  $LO_2/LH_2$  propellant combination, the results of the  $LF_2/LH_2$  system selection study presented in Ref. 3 were reviewed to determine the differences that may occur in the selection criteria and in the relative ranking of the potential propulsion system configurations caused by the change in the oxidizer propellant. The major differences were found to exist in the areas of thrust chamber cooling and component development. However, these considerations would not affect the relative standing of the four top-ranking advanced propulsion system configurations.
- (U) The lower mixture ratios typical of the  $LO_2/LH_2$  systems result in a significant increase in  $LH_2$  available for thrust chamber cooling. This permits cooling at higher  $P_c - \epsilon$  combinations in comparison with the equivalent  $LF_2/LH_2$  systems. This factor will result in an increase in the relative ranking of those systems employing the aerodynamic spike engine concept.
- (U) In view of these considerations, the concentric aerodynamic spike-bell nozzle engine configuration selected in Ref. 3 and in this study for  $LF_2/LH_2$  propellants is also the most favorable propulsion configuration for the  $LO_2/LH_2$  systems. This conclusion also applies to the higher-thrust systems since increased thrust also benefits the aerodynamic spike engine configuration.

CONFIDENTIAL

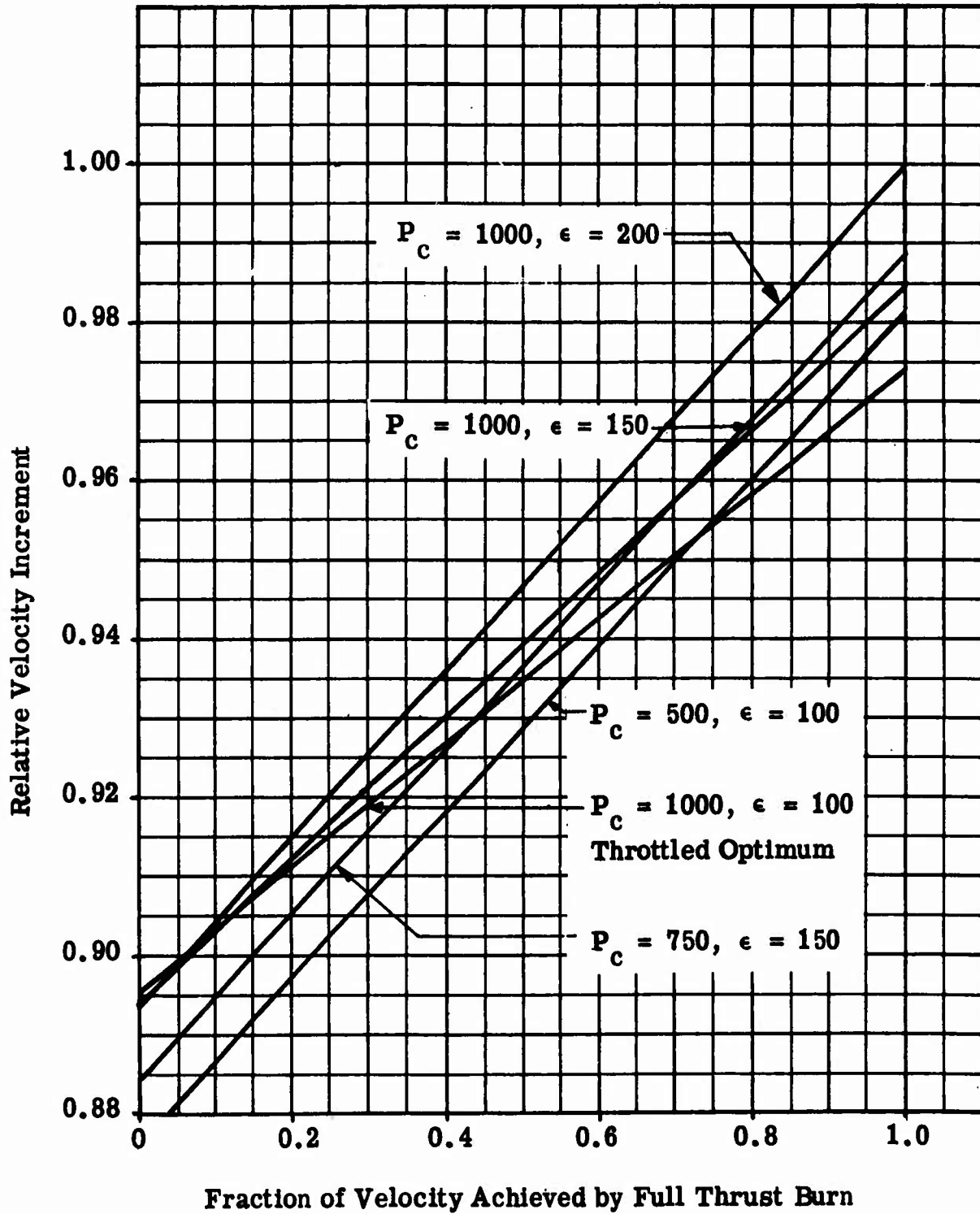


Figure 29. Duty Cycle Influence on Design Parameter Selection for 3300-Pound-Thrust  $F_2/H_2$  Bell Engine

CONFIDENTIAL

# CONFIDENTIAL

## b. Engine System Optimization Procedure

- (U) The selected engine configuration for the  $LO_2/LH_2$  MSPS is identical to that chosen for the  $LF_2/LH_2$  MSPS; therefore, the optimization analysis was conducted in exactly the same manner. Each thrust chamber was optimized separately, and design parameters were selected to ensure that the primary and secondary engines were compatible and could be assembled to provide the highest-performing overall propulsion system. Regenerative-cooling capabilities were investigated along with other engine design limitations. Throttled operating effects were also examined.
- (U) Previous studies of space propulsion systems have indicated that a propellant mixture ratio of 6:1 provides near-optimum performance for the oxygen/hydrogen combination. These studies include the effect of both engine specific impulse and the vehicle structural weight. Therefore, for the current investigation, the engine mixture ratio of 6:1 was selected.
- (C) Design thrust levels of 30,000, 50,000, and 75,000 pounds were chosen for the aerodynamic spike engines to correspond to the selected values of MSPS gross weight. Based upon the anticipated overall throttling requirements and the decision to divide this throttling ratio equally between the primary and secondary engines, design thrust levels of 3300, 5000, and 7500 pounds were selected for the bell nozzle engines.
- (U) An optimization analysis was conducted for each of these engines for continuous operation at full thrust and for continuous operation at one-tenth of the design thrust level.
- (1) (U) Engine Performance. Parametric engine performance data for the  $LO_2/LH_2$  optimization analysis were generated using exactly the same procedure as for the  $LF_2/LH_2$  systems. An engine system balance was conducted for a range of chamber pressures and area ratios for each of the selected thrust levels and thrust chamber configurations.
- (U) Nozzle expansion efficiency data including kinetic, divergence, and boundary layer drag losses were generated for the selected nozzle contours and exhaust gas properties. Both the full-thrust and throttled operating conditions were considered.
- (U) Theoretical propellant performance was based upon the equilibrium performance model. An analysis was conducted to determine kinetic efficiency associated with the nozzle expansion process for the complete range of operating conditions. Nozzle contours were selected to provide near-optimum performance. A 20-percent length nozzle was chosen for the aerodynamic spike contours and an 80-percent length bell nozzle was analyzed for the secondary engines.
- (U) The turbines of the primary and secondary engines are powered by hot gases tapped off from the combustion chambers. The aerodynamic spike uses two parallel turbines, one for each pump, and the bell nozzle engine has one turbine driving both pumps. Nominal pump and turbine efficiencies and

# CONFIDENTIAL

TABLE XX

## LO<sub>2</sub>/LH<sub>2</sub> SYSTEM OPERATING CHARACTERISTICS

	Aerodynamic Spike Engine		Bell Nozzle Engine	
	Maximum Thrust	Minimum Thrust	Maximum Thrust	Minimum Thrust
Combustion Efficiency	0.99	0.98	0.99	0.98
Engine Mixture Ratio	6.0:1	6.0:1	6.0:1	6.0:1
Tapoff System Mixture Ratio	1.12	1.12	1.12	1.12
Tapoff Gas Temperature, R	1960	1960	1960	1960
Tapoff Gas Specific Heat Ratio ( $\gamma$ )	1.348	1.348	1.348	1.348
Tapoff Gas C <sub>p</sub>	1.802	1.802	1.802	1.802
Oxidizer Pump Efficiency	0.76	0.718	0.55	0.519
Fuel Pump Efficiency	0.45	0.407	0.30	0.270
Oxidizer Turbine Efficiency	0.276	0.07	0.41	0.112
Fuel Turbine Efficiency	0.546	0.202	0.41	0.112
Oxidizer Turbine Pressure Ratio	15:1	13.7:1	15:1	13.7:1
Fuel Turbine Pressure Ratio	15:1	13.7:1	15:1	13.7:1

# CONFIDENTIAL

other system-operating characteristics used in establishing the parametric performance data are presented in Table XX. Both full-thrust and throttled operating conditions are shown for the aerodynamic spike and bell engines.

- (U) Oxidizer and fuel pump discharge pressure values were based upon the detailed analysis conducted for the  $LF_2/LH_2$  systems and other related system studies. Scaling procedures used to extend these data to cover the range of design parameters and operating conditions were as described for the  $LF_2/LH_2$  systems.
- (2) (U) Stage Weight. Parametric stage inert weight data used in the optimization analysis were obtained from stage design studies conducted for the  $LO_2/LH_2$  RL-10 stage and alternate mission vehicles presented in Ref. 3 and 4.
- (U) Engine weight data were obtained from a computerized analysis which determines the individual engine component weights based upon a correlation with past detailed hardware experience.

## c. Aerodynamic Spike Engines

- (C) The results of the  $LO_2/LH_2$  aerodynamic spike engine optimizations for continuous operations at full thrust are presented in Fig. 30 through 32 for each of the selected thrust levels. The optimum chamber pressures for these  $LO_2/LH_2$  systems are seen to occur in the 500- to 700-psi region. The overall effect of the variation of area ratio and chamber pressure on the relative velocity increment can be seen to be more significant than those observed in the fluorine/hydrogen systems for full-thrust operations. This is caused by the operation of the oxygen/hydrogen system at a mixture ratio of 6:1 and the resulting lower stage inert weight efficiency. A design chamber pressure and area ratio of 700 psia and 150:1 respectively, are seen to provide near-maximum mission performance throughout the range of thrust levels examined. The regenerative-cooling capabilities are well above the optimum chamber pressure and therefore do not influence the selection of the design parameters for the full-thrust case.
- (C) The optimization results for the 30,000-pound-thrust  $LO_2/LH_2$  aerodynamic spike operating at a 10:1 throttled condition are shown in Fig. 33. Because of the kinetic performance losses and increased drag losses associated with throttled operation, higher maximum performance values of chamber pressure occur. However, with the consideration of the regenerative cooling capabilities, a design chamber pressure of approximately 800 psia (80 psia at 10:1 throttled operating condition) provides maximum mission performance for continuous operation at the throttled operating condition.
- (1) (U) Operating and Design Parameter Selection. The method used in evaluating the combined optimization results for the  $LO_2/LH_2$  engines is identical with that used for the  $LF_2/LH_2$  engines in that the final selection of the engine design parameters was based upon a compromise between the maximum performance design parameters for continuous operation at full-thrust and at minimum-thrust.

CONFIDENTIAL

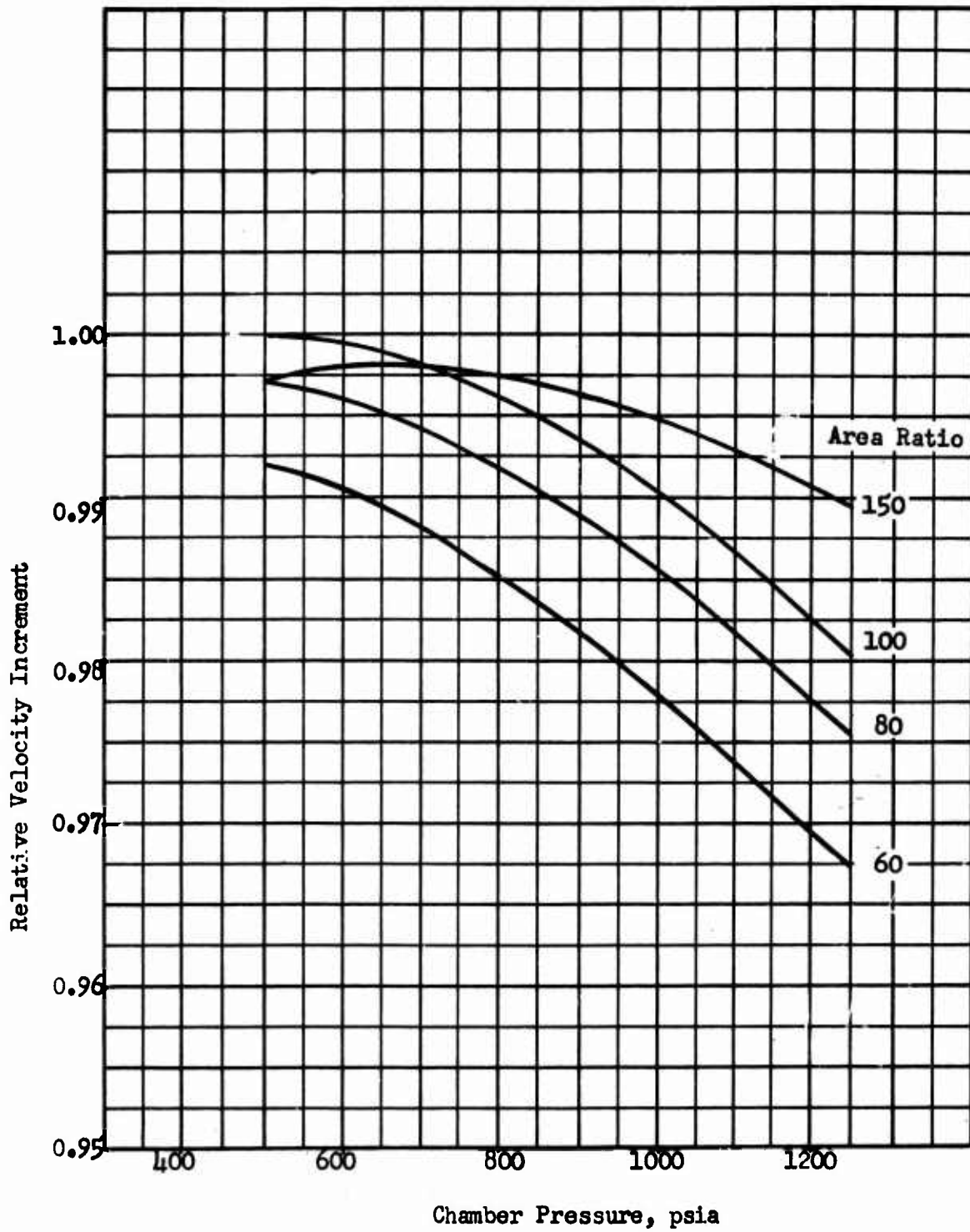


Figure 30. Chamber Pressure - Expansion Area Ratio Optimization for Oxygen-Hydrogen 30,000 lbf Aerodynamic Spike Engine

CONFIDENTIAL

CONFIDENTIAL

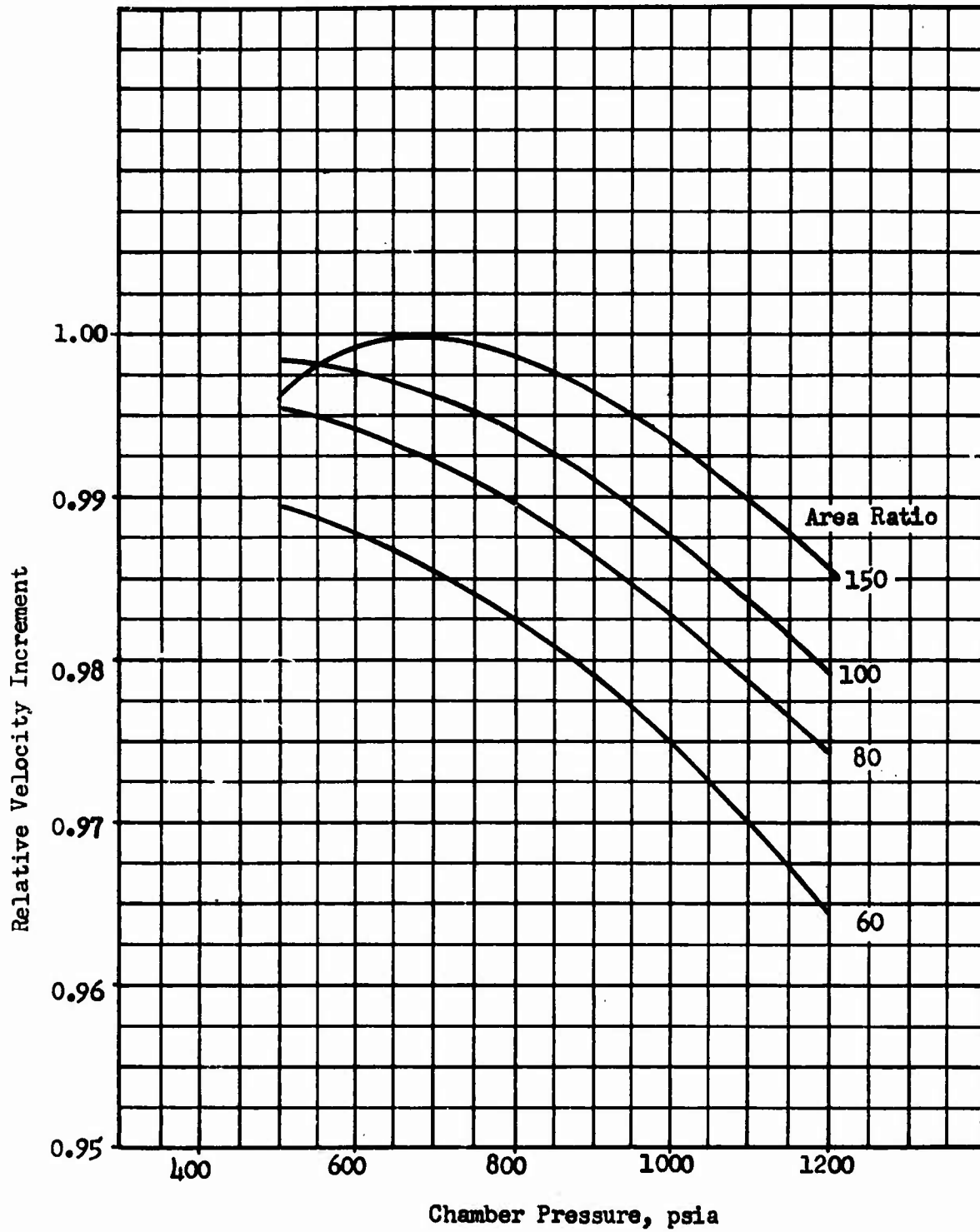


Figure 31. Chamber Pressure - Expansion Area Ratio Optimization for Oxygen-Hydrogen 50,000 lbf Aerodynamic Spike Engine

CONFIDENTIAL

CONFIDENTIAL

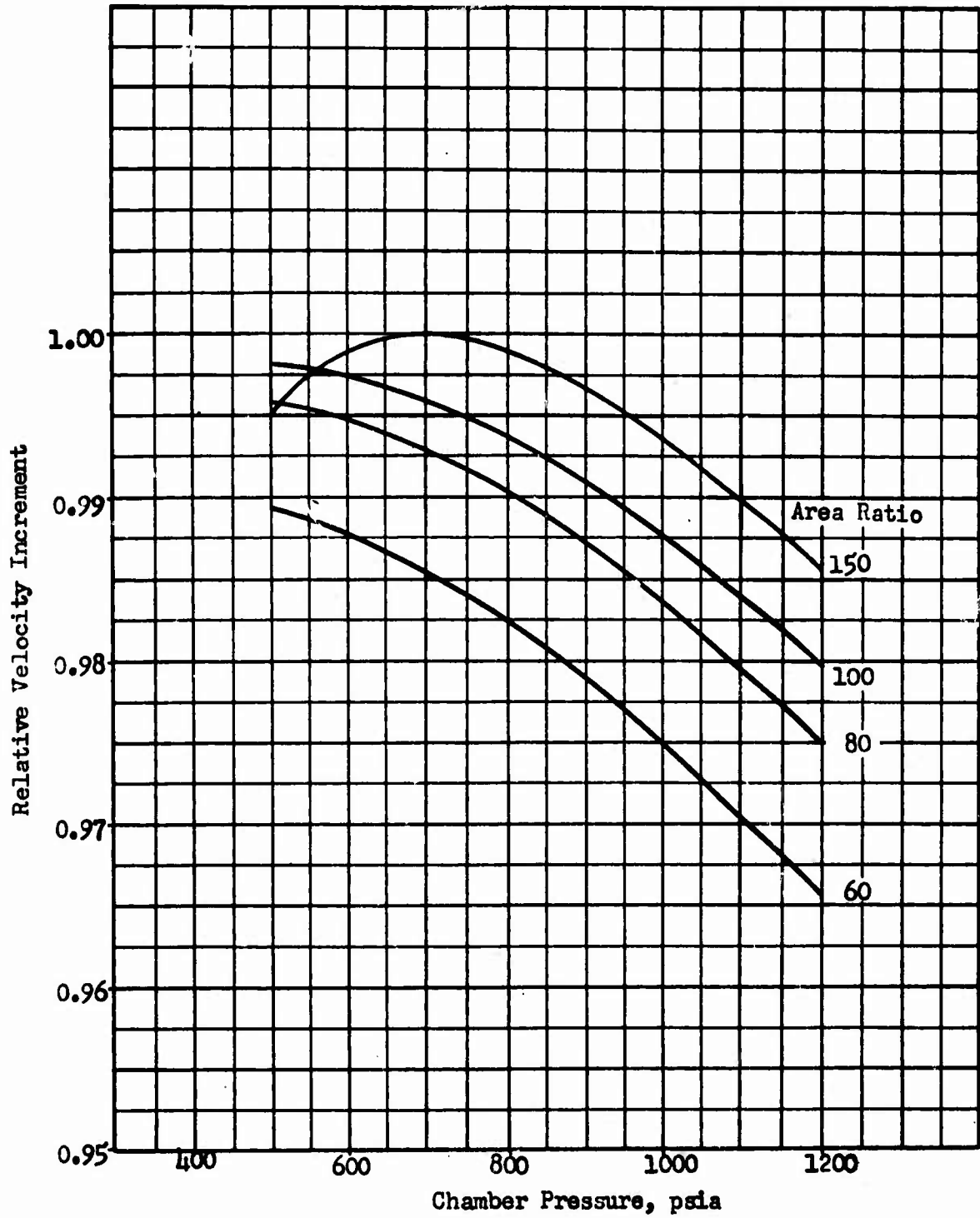


Figure 32. Chamber Pressure - Expansion Area Ratio Optimization for Oxygen-Hydrogen 75,000 lbf Aerodynamic Spike Engine

CONFIDENTIAL

**CONFIDENTIAL**

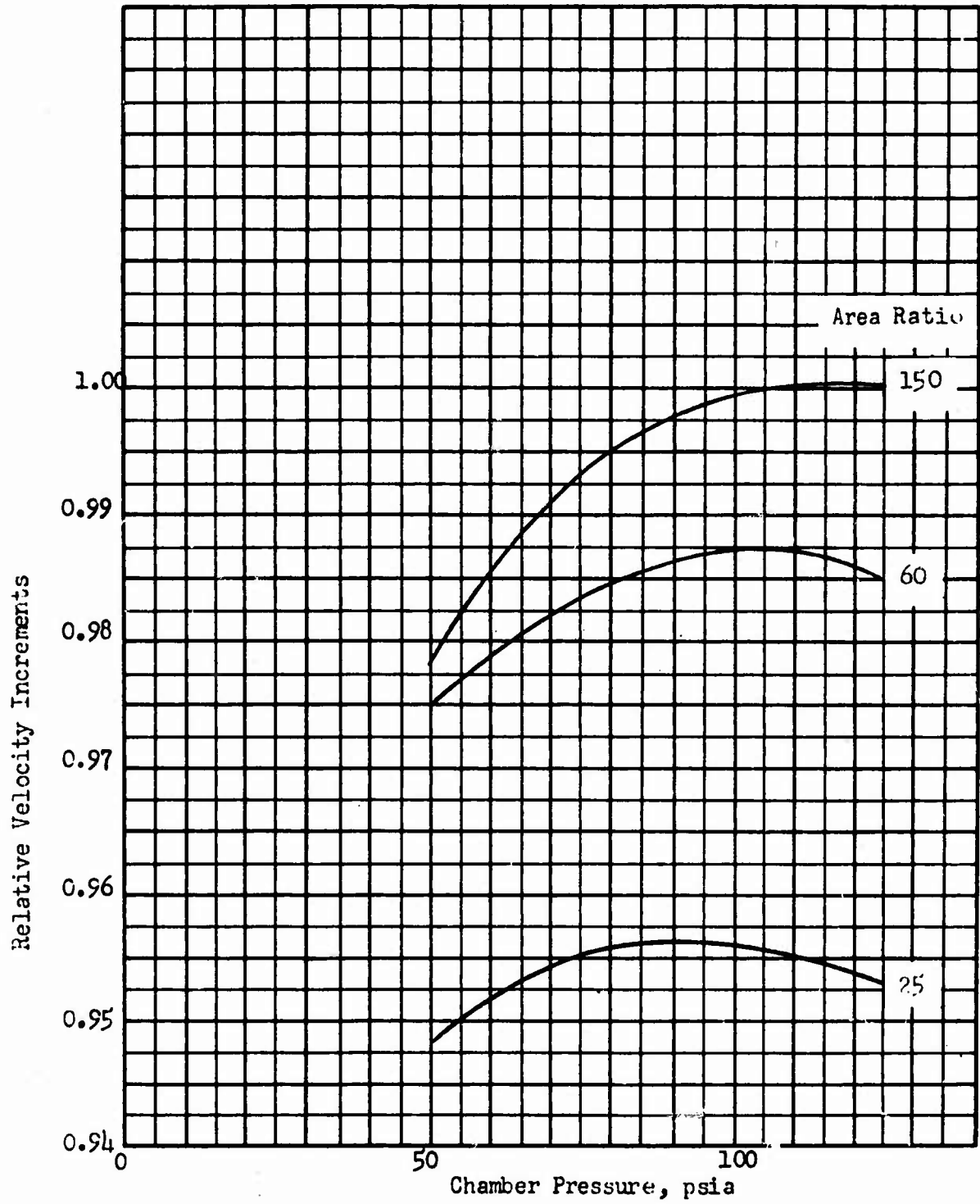


Figure 33. Throttling Effect on Chamber Pressure - Expansion Area Ratio Optimization for Liquid Oxygen - Hydrogen 30,000 lbf Aerospike Engine

**CONFIDENTIAL**

# CONFIDENTIAL

- (C) The weighted mission effects on the  $\text{LO}_2/\text{LH}_2$  aerodynamic spike engine are shown in Fig. 34 for  $P_c - \epsilon$  combinations ranging among the optimum values obtained for continuous operation at full and minimum thrust. The relative  $\Delta V$  vs the fraction of  $\Delta V$  accomplished at full thrust is shown. These results again indicate that, on an overall basis, the throttled optimum values of chamber pressure and area ratio provide near-maximum mission performance. It should be noted that only slight variations in the maximum  $\Delta V$  capability result for the entire range of  $P_c - \epsilon$  combinations. The combined results of the mission-weighted optimization results led to the selection of 800 psia chamber pressure and 100:1 area ratio for the  $\text{LO}_2/\text{LH}_2$  aerodynamic spike engines for the range of design thrust levels from 30,000 to 75,000 pounds.
- (U) A summary of the selected design values of chamber pressure and area ratio are shown in Table XXI for the  $\text{LO}_2/\text{LH}_2$  aerodynamic spike engines.

d. Bell Nozzle Engine

- (C) The optimization analysis for the  $\text{LO}_2/\text{LH}_2$  bell nozzle engine system at continuous full-thrust operation is presented in Fig. 35 through 37 for the three selected thrust levels. The length restrictions for the appropriate engine combinations are indicated on the respective curves. These length restrictions were established by the same method as those for the  $\text{LF}_2/\text{LH}_2$  bell nozzle engine. The length limit line shown defines the maximum bell nozzle engine length that will maintain the ratio of the bell nozzle engine length to the aerodynamic spike engine length equal to that of the original 30,000-pound-thrust  $\text{LF}_2/\text{LH}_2$  propulsion system. This relative engine length provides an efficient overall propulsion system package with respect to mounting structure and component arrangement and prevents aerodynamic spike hot-gas impingement on the bell engine. Engine diameter restrictions were outside the range of parameters of interest. These results indicate that the nozzle length restriction will have a significant influence on the selection of the design chamber pressure for near-maximum mission performance.
- (C) The effect of throttled operation on the optimization results for the 3300-pound-thrust  $\text{LO}_2/\text{LH}_2$  engine is shown in Fig. 38. The performance losses associated with throttled operation tend to force the maximum performance chamber pressure to higher values. These results indicate that a full-thrust design chamber pressure of approximately 1000 psi would provide the maximum  $\Delta V$  capability for continuous 10:1 throttled operation. These values are well above the nozzle length limit (high chamber pressure results in shorter nozzle length).
- (2) (U) Operating Parameter Selection. Factors influencing selection of the design parameters for the  $\text{LO}_2/\text{LH}_2$  bell nozzle engines are identical with those for the  $\text{LF}_2/\text{LH}_2$  bell nozzle engines. Final selection of the design parameters is based upon a compromise between the full-thrust and throttled optimization results, together with envelope and turbomachinery design considerations.

CONFIDENTIAL

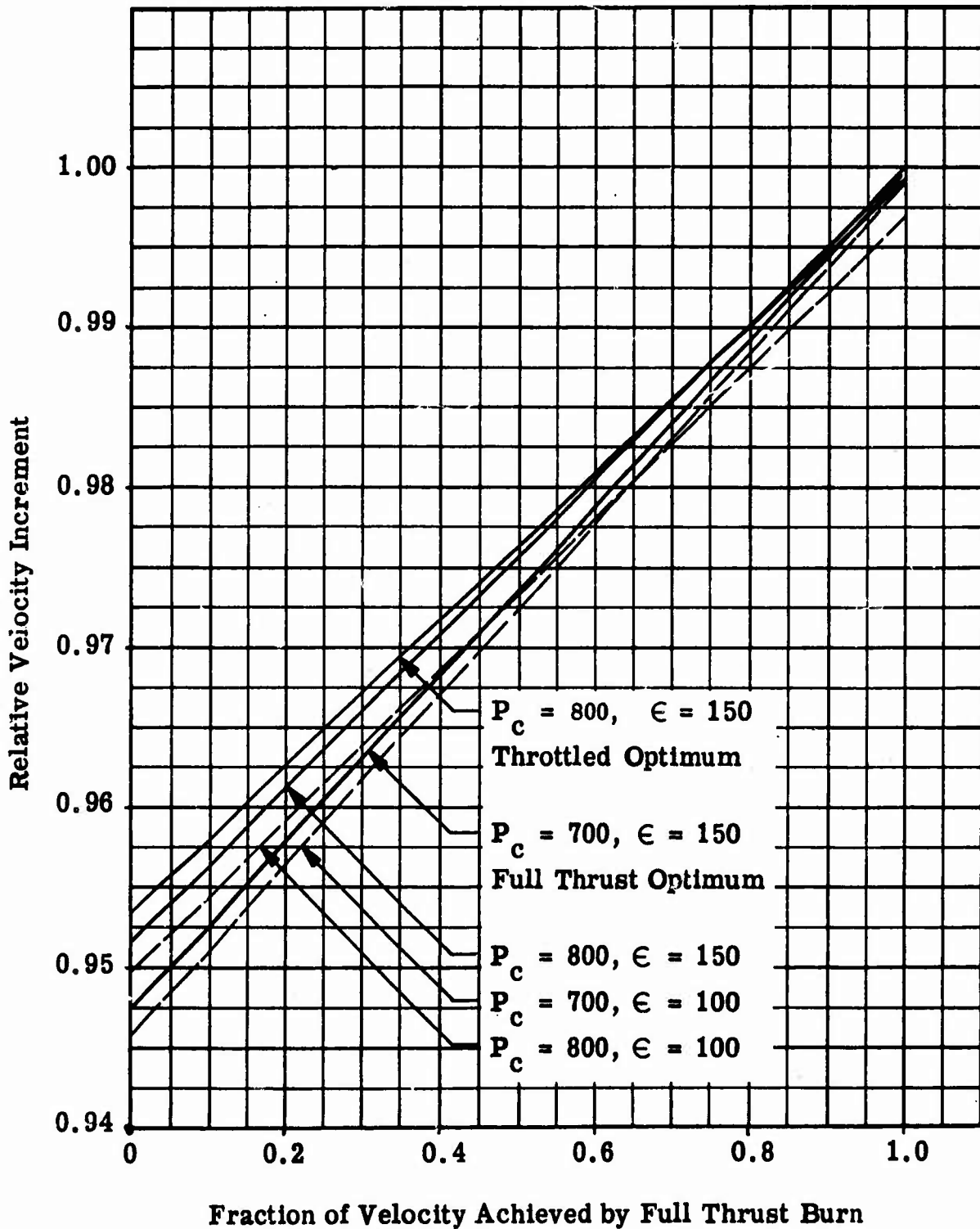


Figure 34. Duty Cycle Influence on 30,000-Pound-Thrust O<sub>2</sub>/H<sub>2</sub> Aerodynamic Spike Engine

CONFIDENTIAL

CONFIDENTIAL

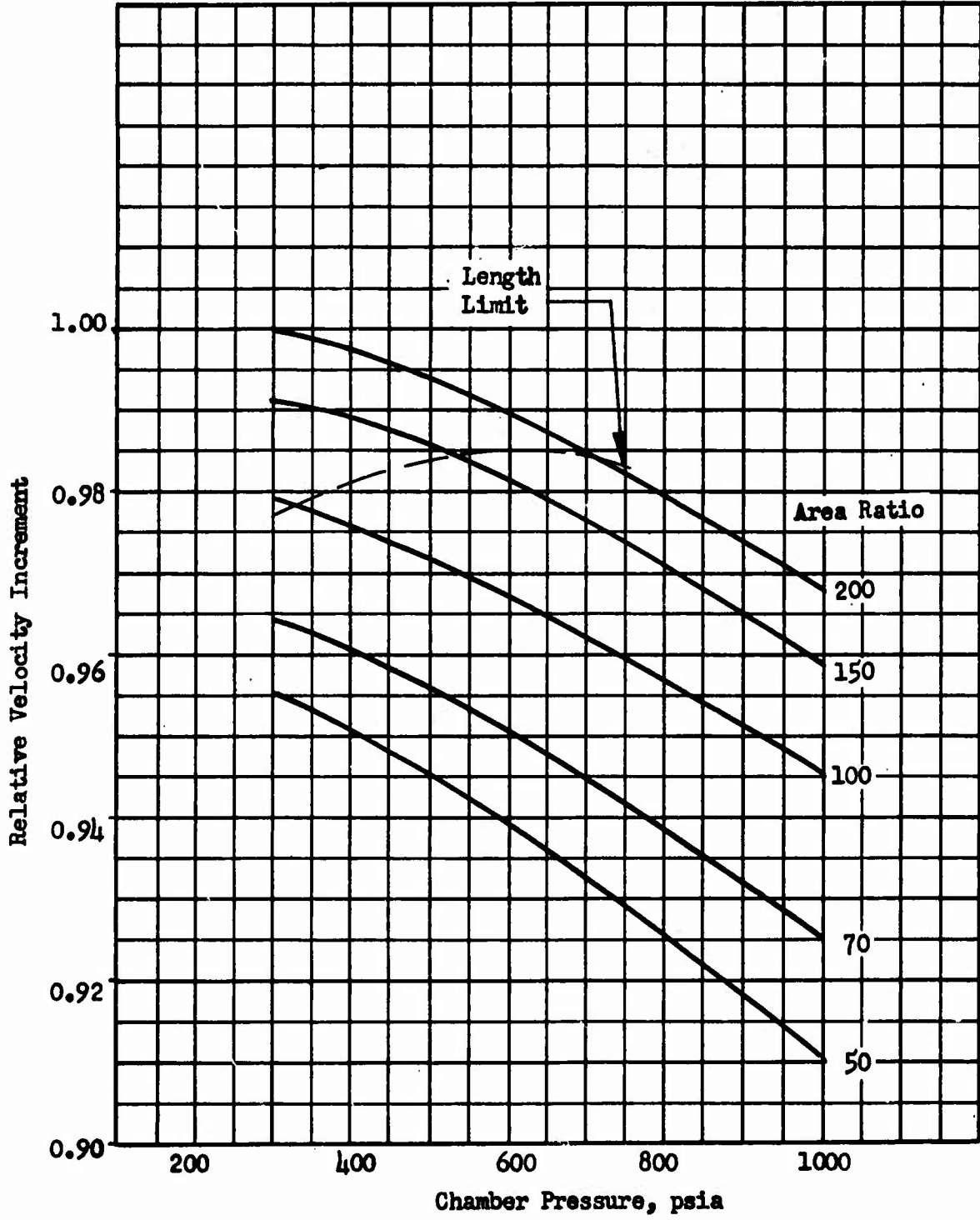


Figure 35. Chamber Pressure - Expansion Area Ratio Optimization for Oxygen-Hydrogen 3300 lbf Bell Engine

CONFIDENTIAL

CONFIDENTIAL

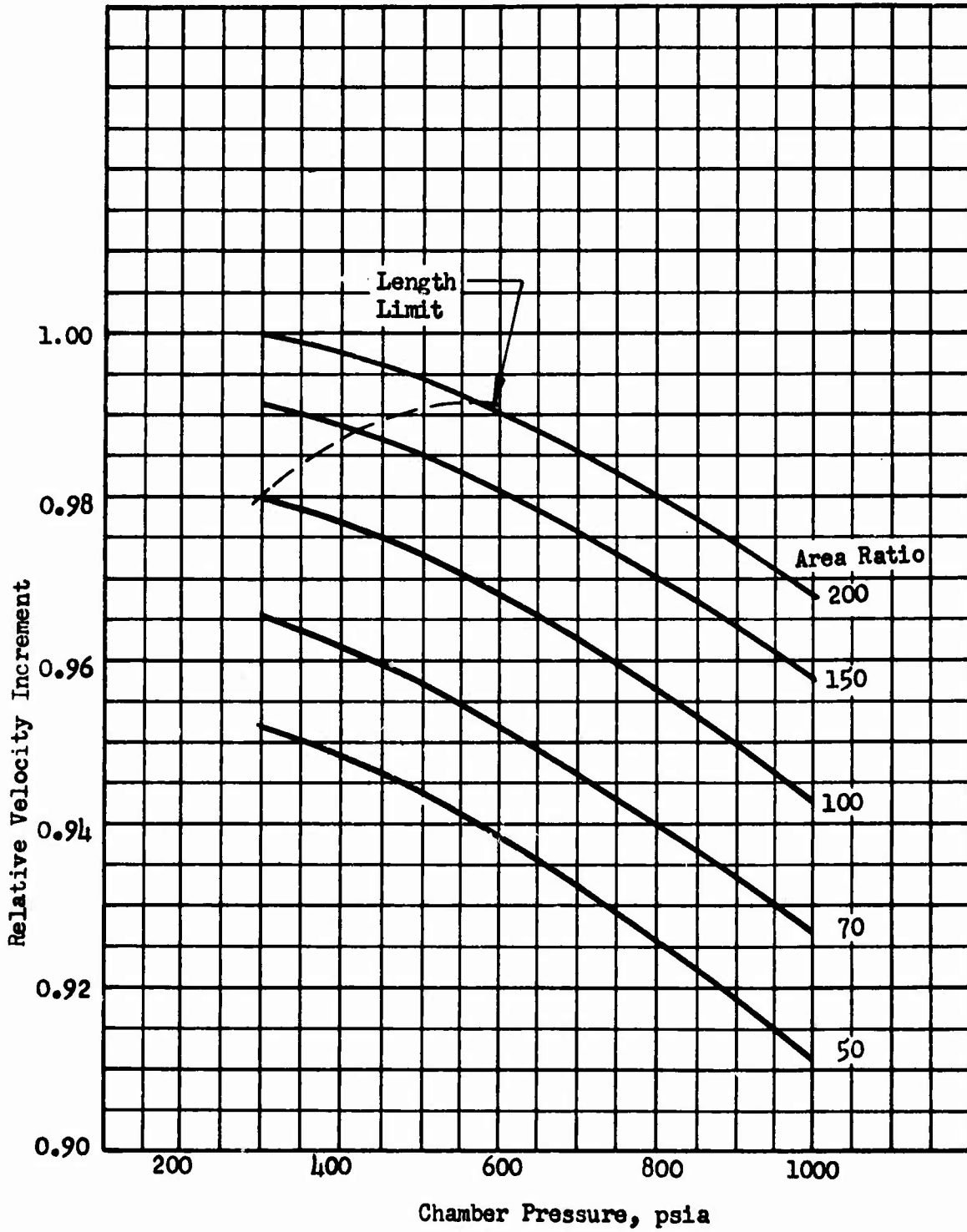


Figure 36. Chamber Pressure - Expansion Area Ratio Optimization for Oxygen-Hydrogen 5,000 lbf Bell Engine

CONFIDENTIAL

CONFIDENTIAL

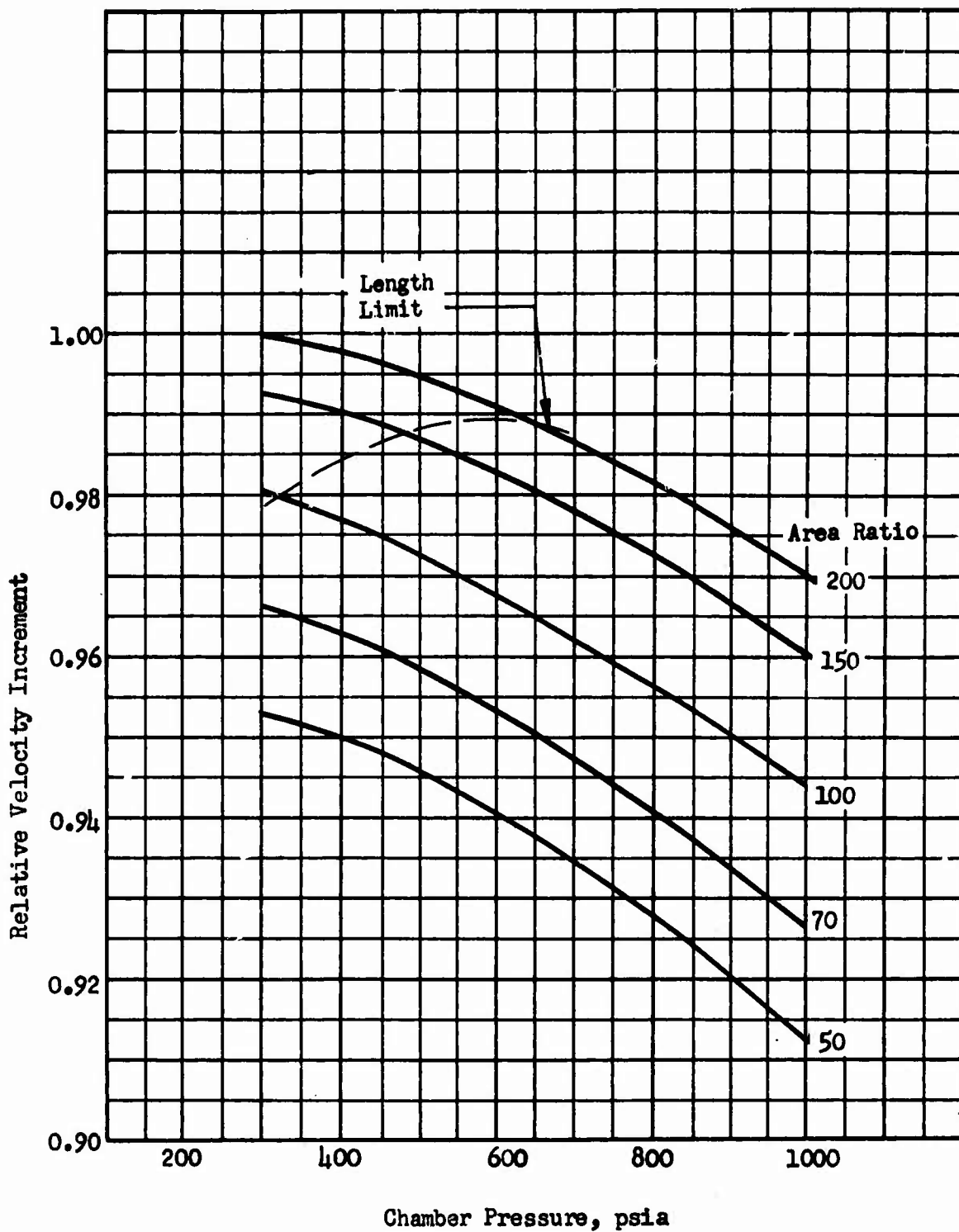


Figure 37. Chamber Pressure - Expansion Area Ratio Optimization for Oxygen-Hydrogen 7500 lbf Bell Engine

CONFIDENTIAL

**CONFIDENTIAL**

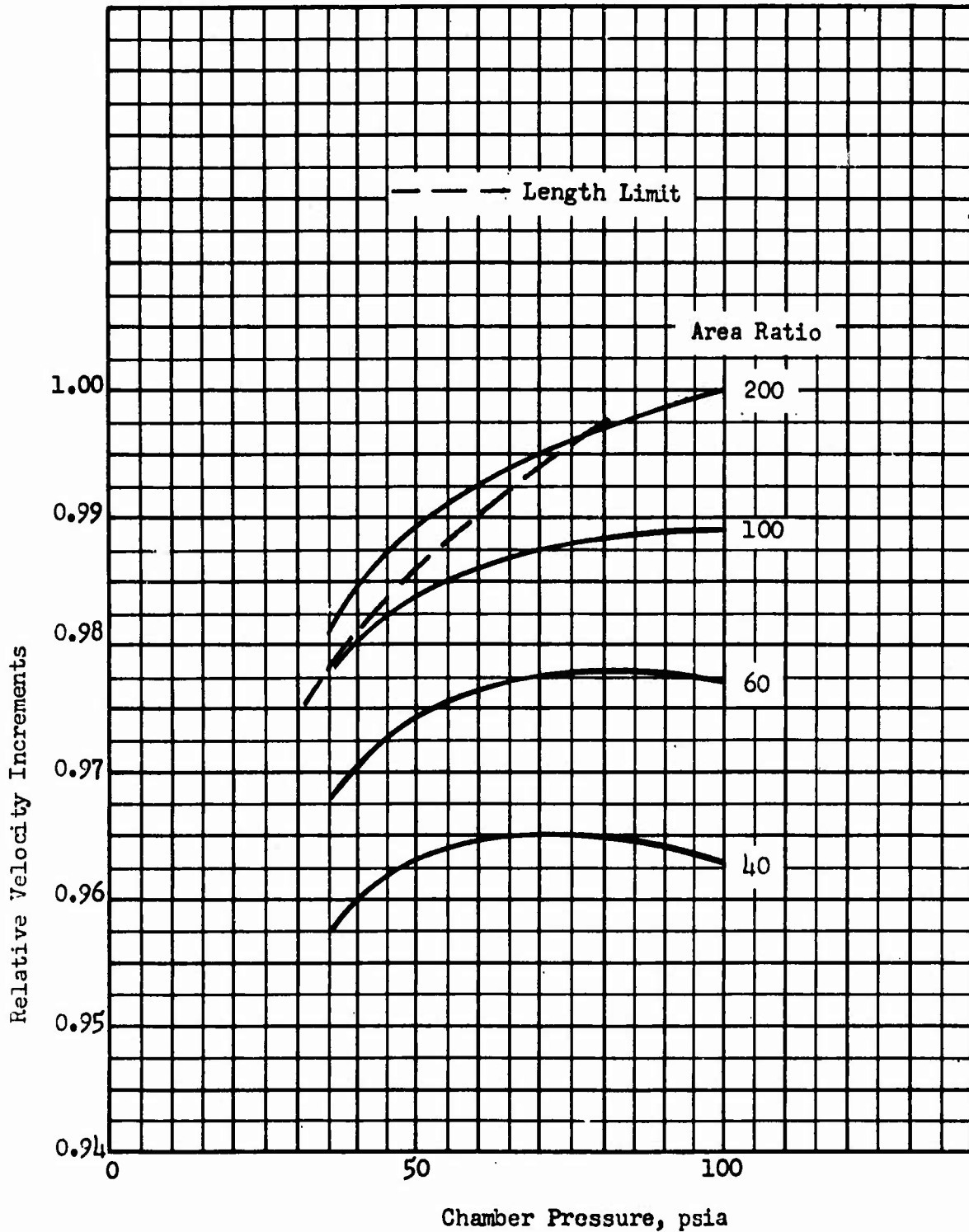


Figure 38. Throttling Effects on Chamber Pressure - Expansion Area Ratio Optimization for Liquid Oxygen - Hydrogen 3,300 lbf Bell Engine

**CONFIDENTIAL**

- (U) The thrust duty cycle or mission effects were examined by selecting chamber pressure and area ratio values in a region bracketed by the full-thrust and minimum-thrust optimum values. The Maneuvering Space Propulsion System's  $\Delta V$  capabilities were compared for various divisions of full-thrust and throttled operation. These comparisons are shown in Fig. 39 where relative  $\Delta V$  is shown as a function of the percentage of the total  $\Delta V$  accomplished at full thrust. These results show that a relatively large range in the design values of chamber pressure and area ratio have only a minor effect on overall mission performance.
- (U) As in the case of the  $LF_2/LL_2$  systems the chamber cooling analysis results were used to specify the optimum chamber pressure for the large engines. In order to maintain the same simplicity of turbopump design for the small engines as with the  $LF_2/LL_2$  systems these turbopump performance analysis results were used to specify the chamber pressures for the small engines. The selected design parameters are shown in Table XXI.

TABLE XXI

DESIGN PARAMETER SELECTION FOR  
 $LO_2/LH_2$  PROPULSION SYSTEMS\*

Engine	Design Thrust, pounds	Chamber Pressure, psia	Area Ratio
Aerodynamic Spike	30,000 to 50,000	800	100
Bell Nozzle	3300	500	100
Bell Nozzle	5000	625	200
Bell Nozzle	7500	740	200

\*Mixture ratio = 6:1

4.  $N_2O_4/N_2H_4$ -UDMH (50-50) SYSTEMS

a. Engine Configuration Selection

- (U) A detailed configuration selection study was conducted for the  $N_2O_4/N_2H_4$ -UDMH (50-50) systems. This configuration selection study represents an extension of a brief analysis conducted for the alternate mission propulsion system of Ref. 4 and includes the effect of throttling capability on the system configuration selection. The propellant combination of  $N_2O_4/N_2H_4$ -UDMH (50-50) is grossly different from the previous all-cryogenic systems. Therefore, rather than extend the previous engine configuration selection studies a complete new configuration selection study was conducted. As in the fluorine/hydrogen and oxygen/hydrogen studies, multiple engine configurations were evaluated to achieve the required throttling ratios. Both annular and bell nozzle configurations were considered. A variety of cooling methods was included.

**CONFIDENTIAL**

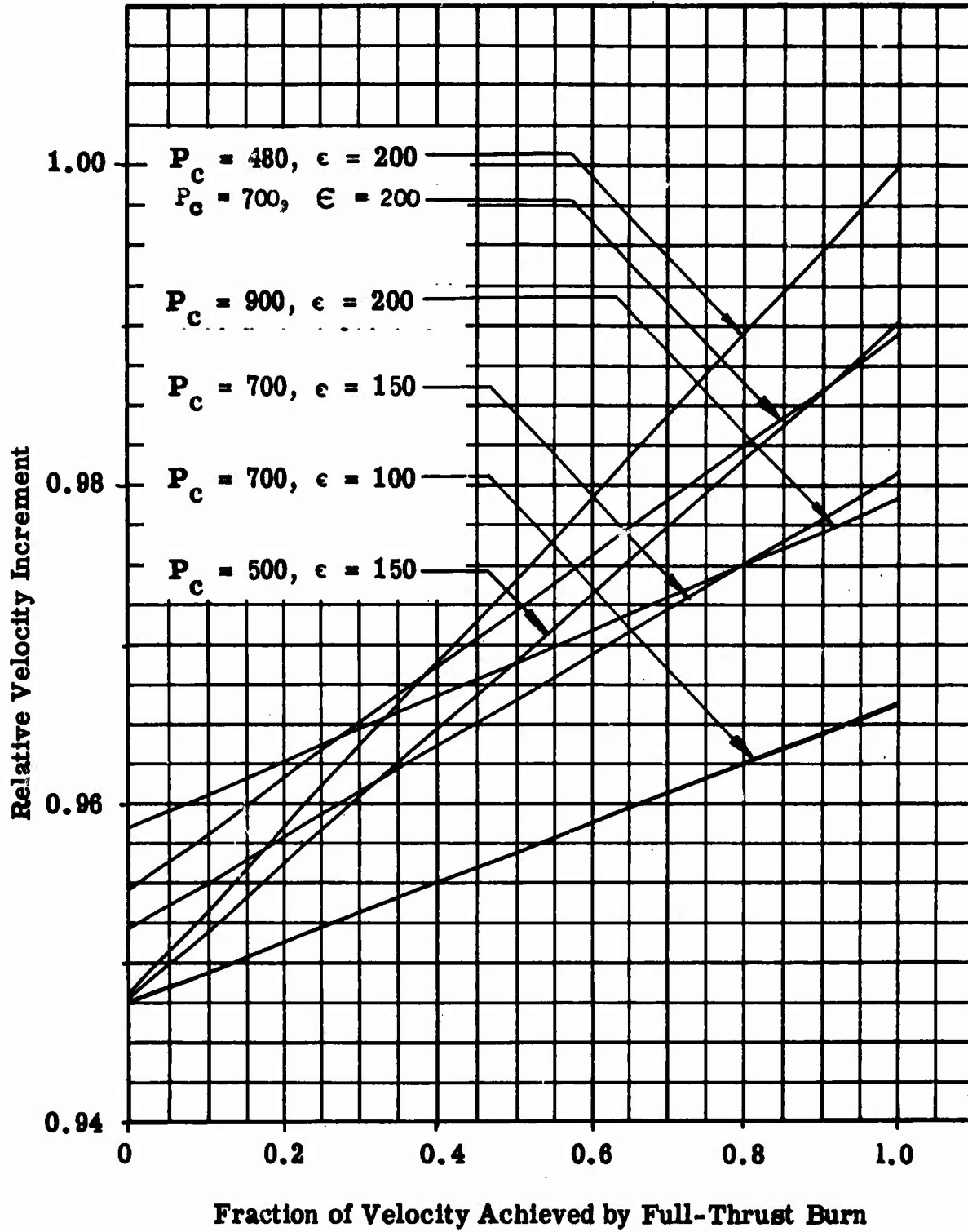


**Figure 39. Duty Cycle Influence on Design Parameter Selection for 3300-Pound-Thrust  $O_2/H_2$  Bell Engine**

**CONFIDENTIAL**

# CONFIDENTIAL

- (U) The regenerative cooling capability of this propellant combination was investigated first. The bulk temperature of the  $N_2H_4$ -UDMH (50-50) propellant limits regenerative cooling for this particular propellant combination. For relatively low-thrust propulsion systems, this limit can be restrictive, particularly for throttling engine systems.
- (U) A review of regenerative cooling/heat transfer studies (Ref. 5) conducted for annular combustors using both  $N_2O_4$  and  $N_2H_4$ -UDMH (50-50) as the regenerative coolant, has provided the regenerative-cooling feasibility limits for these type engine configurations. Regenerative cooling with  $N_2O_4$  was shown to be applicable for high operating chamber pressures (above 1400 psia) only. Because of the throttling requirement, low operating chamber pressures are unavoidable in the MSPS. This requirement then limited the regenerative coolant to  $N_2H_4$ -UDMH (50-50).
- (C) Regenerative cooling analysis conducted for the annular type combustion chambers indicated that for throttling systems of the relatively low thrust levels of interest (30,000 to 75,000 pounds), the  $P_c - \epsilon$  parameter combinations are limited to relatively low values. This of course is undesirable from the standpoint of achieving maximum performance. Other cooling methods for the annular type combustors, such as ablative designs, were also considered; however, because of the mission duty cycle requirements, the weight penalties would be excessive. Based on these considerations, therefore, the annular type engines were not considered further for  $N_2O_4/N_2H_4$ -UDMH (50-50) systems.
- (1) (U) Bell Nozzle Engine Configurations. The conventional bell nozzle thrust chamber evaluation was initiated with a brief analysis to determine the thrust chamber cooling requirements and capabilities over the range of design thrust levels and throttling ratios that might be required. Because of the depth of throttling required, it was recognized that multiengine propulsion systems would offer a definite advantage. Therefore, design thrust levels selected for the thrust chamber cooling analysis were chosen to represent the range of design thrust levels that would be used in the typical multiengine propulsion systems. The purpose of the thrust chamber cooling analysis was to determine any design or operating restrictions that must be considered in the comparison of the candidate systems. These restrictions could be in terms of maximum chamber pressure, mixture ratio, firing duration, and throttling ratio.
- (U) The methods of thrust chamber cooling considered for this comparison include regenerative, film, and ablative cooling. The operating conditions assumed for the cooling analysis were selected based upon the results of previous system optimization studies.
- (a) (C) Regenerative-Radiation Cooling Analysis. The regenerative-cooling analysis was conducted for conventional bell nozzle thrust chambers with design thrust levels between 5000 and 65,000 pounds and chamber pressures of 200 to 1000 psia. It was assumed that a radiation-cooled nozzle skirt would be used whenever possible to minimize the heat load to the coolant.

## CONFIDENTIAL

- (U) Combustion chamber heat transfer rates were calculated using the gas-side film coefficient determined from the Mayor equation.
- (U) The radiation equilibrium temperature profile is determined by a simple balance of the convective heat input and the radiative heat rejection along the length of the nozzle. This profile was combined with a specified maximum allowable skirt temperature to determine the attach point area ratio.
- (U) The results of the radiation-cooling analysis are summarized in Fig. 40 where the minimum area ratio attach point is given as a function of chamber pressure and thrust level. The specified temperature at the attach point is 2400 F, which is typical of a refractory material. A material emittance of 0.8 was assumed in conjunction with a nozzle view factor of unity to 0-degree Rankine space. It is seen in Fig. 40 that the chamber pressure has a significant effect upon the attach point. For example, at a chamber pressure of 200 psia, it is necessary to cool regeneratively only to an area ratio of approximately 15. At a chamber pressure of 1000 psia, it is necessary to continue regenerative cooling to an area ratio of almost 90.
- (C) The results of the radiation-cooling study were utilized in the regenerative-cooling chamber designs. Five discrete chamber operational points were studied. These points consisted of thrust levels of 5000, 25,000 and 65,000 pounds at a chamber pressure of 500 psia and additional chamber pressures of 200 and 1000 psia at the 5000-pound thrust level. To minimize the total heat input to the thrust chambers, high contraction ratio designs were used. The use of high contraction ratios for a fixed characteristic length results in a lower average heat flux level.
- (U) The basic nozzle geometry was the same for all cases consisting of a 100:1 area ratio, 80-percent-length bell contour. Regenerative cooling was limited to only a portion of this basic contour, as discussed above.
- (U) The nominal (full-thrust) cases of interest were analyzed by performing a heat balance along the chamber wall contour and determining the local regenerative-coolant tube shape necessary for adequate cooling. The incremental pressure drop and bulk temperature rise were calculated and summed to determine total jacket pressure drop and coolant temperature rise.
- (U) The results of the regenerative-cooling analysis for the nominal design points are presented in Fig. 41 where the coolant jacket pressure drops are shown as a function of chamber pressure and thrust level. It is seen that in all cases considered, the jacket pressure drop is less than one-half of the chamber pressure, and the designs appear to be feasible for nominal (full-thrust) operation. These results indicate considerably lower pressure drops than reported previously (Ref. 7). The primary differences between this study and the earlier one are the use herein of higher chamber contraction ratios with a more favorable (i.e., lower heat flux level) combustion-side convective film coefficient relation.

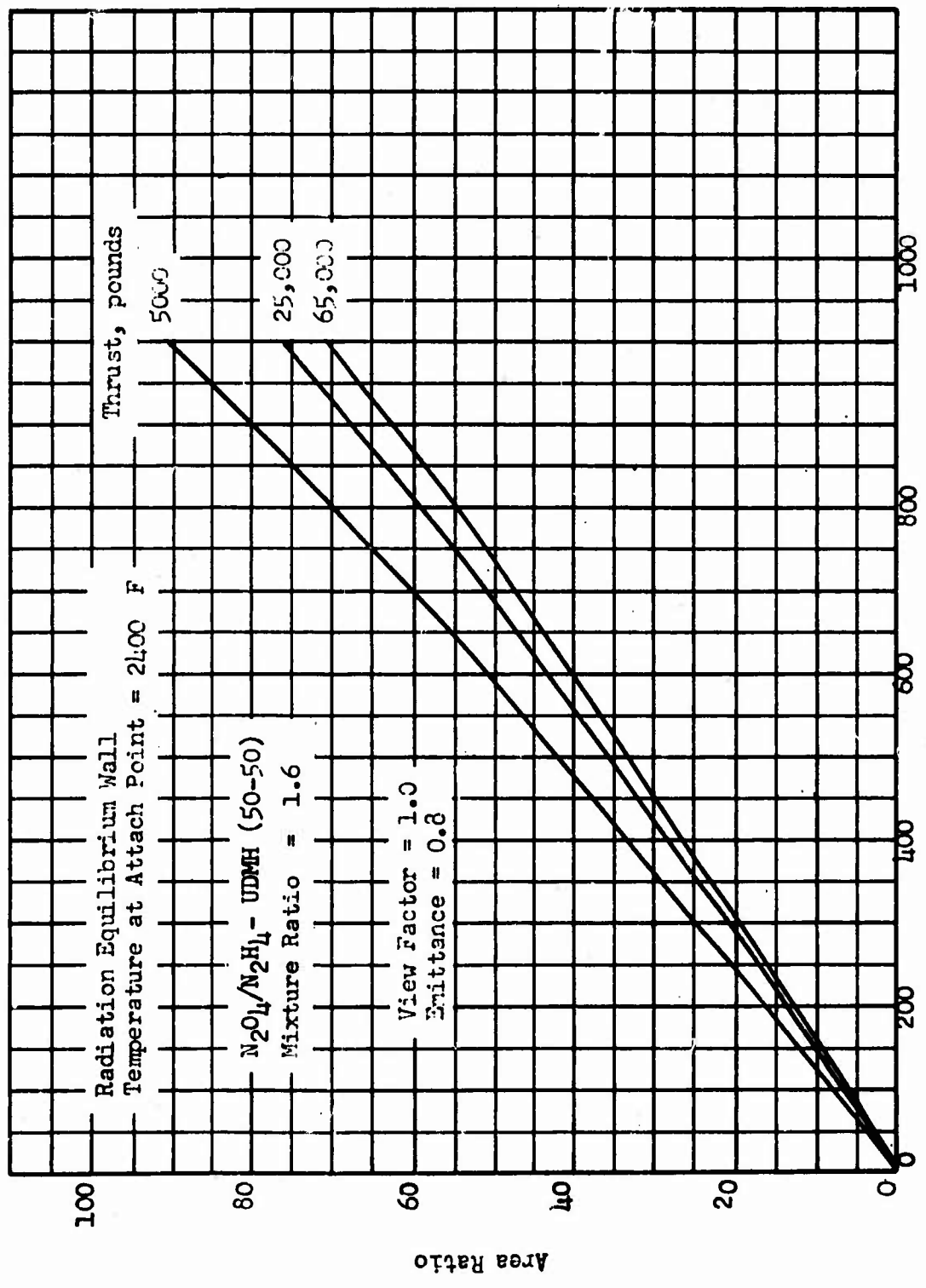


Figure 40. Minimum Area Ratio for Attaching a Radiation Cooled Nozzle.

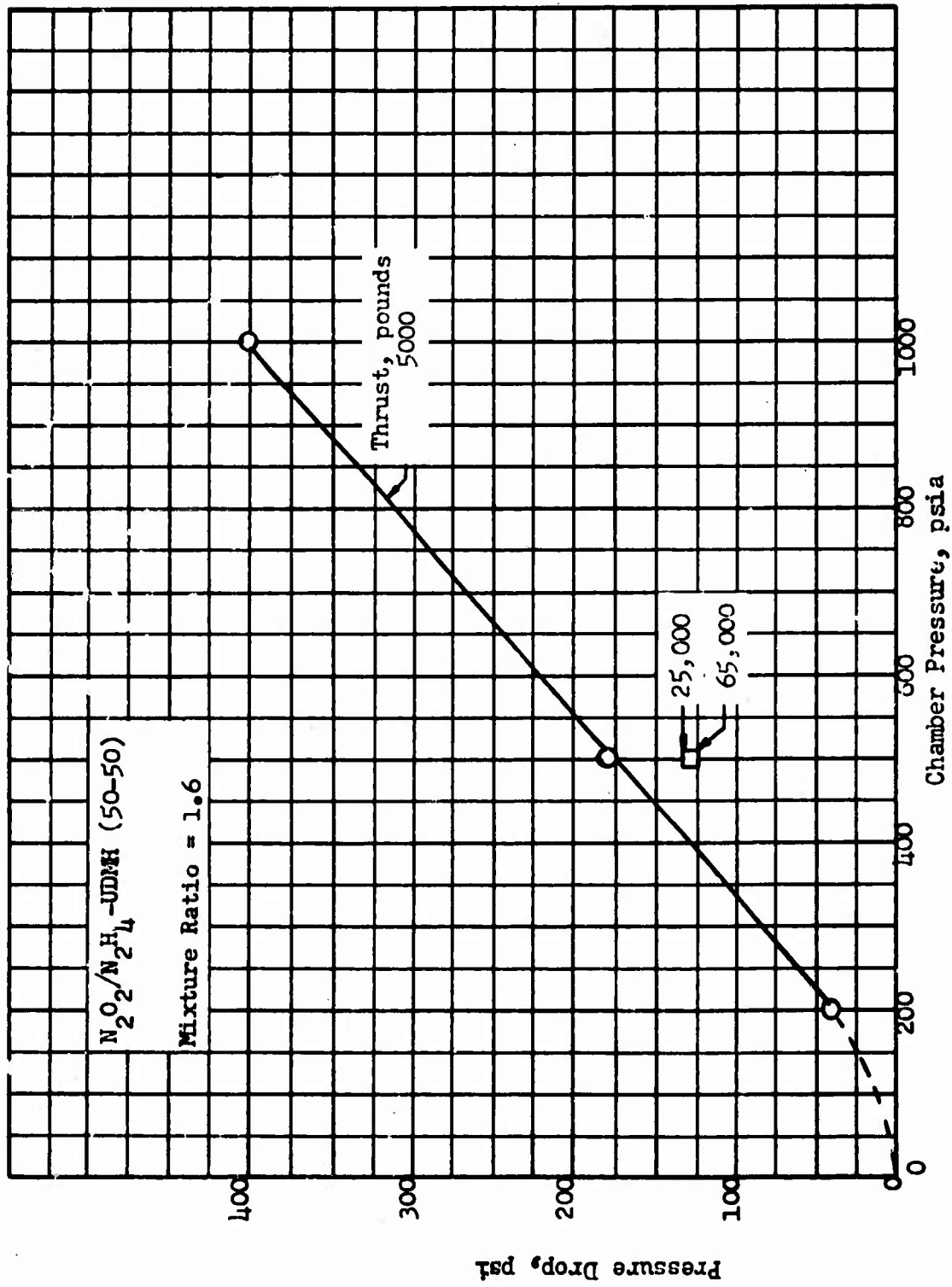


Figure 41. Regenerative Coolant Jacket Pressure Drops

## CONFIDENTIAL

- (U) In addition to the full-thrust operation, throttling operation was considered and the limit of throttling was described for each of these chamber designs. As the thrust chamber is throttled, two important changes occur in the coolant condition. One change is caused by the coolant flowrate decreasing faster than the heat flux level, thereby resulting in an effective increase in the bulk temperature rise of the coolant. The other change is a decrease in the local saturation temperature of the coolant caused by the decreasing coolant pressure at throttled conditions.
- (U) The absolute limit for throttling occurs when the coolant bulk temperature and saturation temperature are equal, resulting in a bulk boiling condition. Such a condition would result in a tube burnout caused by the very high thermal resistance of the coolant vapor film along the tube wall.
- (U) To determine the throttling limits based upon the above bulk boiling criteria, it was necessary to estimate the coolant exit saturation temperature and bulk temperature as a function of throttle ratio. It was assumed that the coolant pressure at the tube bundle exit was approximately 15 percent higher than chamber pressure. Using this assumption and the vapor pressure vs temperature curve for the  $N_2H_4$ -UDMH (50-50) fuel (Ref. 8) the coolant saturation temperature was determined as a function of throttle ratio.
- (U) The results of the throttling portion of this study are presented in Fig. 42 through 46 where the saturation temperature and bulk temperature are plotted as a function of throttle ratio. The point of intersection of the saturation temperature curve and the bulk temperature curves represent the maximum throttling because this point indicates a bulk boiling condition. In actuality, the throttling limit would be somewhat lower since film boiling is likely to occur somewhat before.
- (C) The results are summarized in Fig. 47 where it can be seen that high thrust (65,000 pounds) and low mixture ratio (1.6) tend to allow for deeper throttling, with the possibility of throttle ratios of approximately 6. Low thrust (5000 pounds) and/or high mixture ratio (2.0) limit the throttling ratio to approximately 4 or less. The effect of chamber pressure upon throttle ratio was found to be of secondary importance in this study.
- (C) The above throttling limits are based upon the assumption that the coolant jacket pressure decreases somewhat proportionally to chamber pressure (throttle ratio). This is the expected occurrence when the throttling occurs upstream of the coolant jacket by means of a reduced pump discharge or tank pressure. It would be desirable to maintain the coolant jacket pressure at a high level during throttling, thereby raising the saturation temperature of the coolant. This would shift the point of intersection of the saturation and bulk temperature lines to the right in Fig. 42 through 46, indicating the possibility of deeper throttling (approximate throttling ratios greater than 10). A graphical representation of this effect is shown in Fig. 45. Essentially, this approach requires that throttling occur downstream of the regenerative-cooling jacket. The primary difficulty with this method is that it requires a pump that will provide a decreasing flow while maintaining a relatively high discharge pressure. In pressure-fed design, of course, this problem is not encountered.

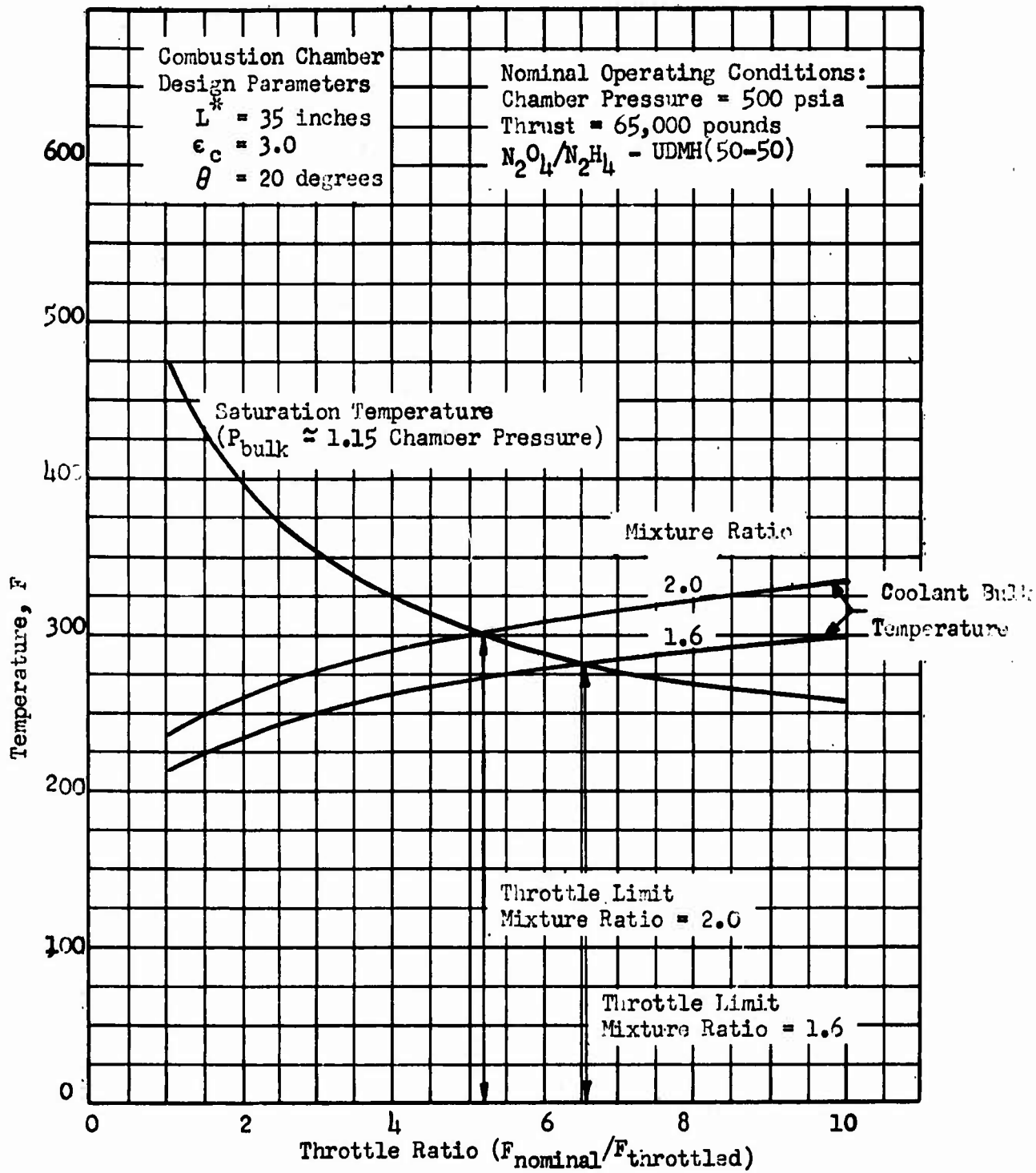


Figure 42. Throttling Limits for a Regeneratively Cooled Storable Propellant Thrust Chamber

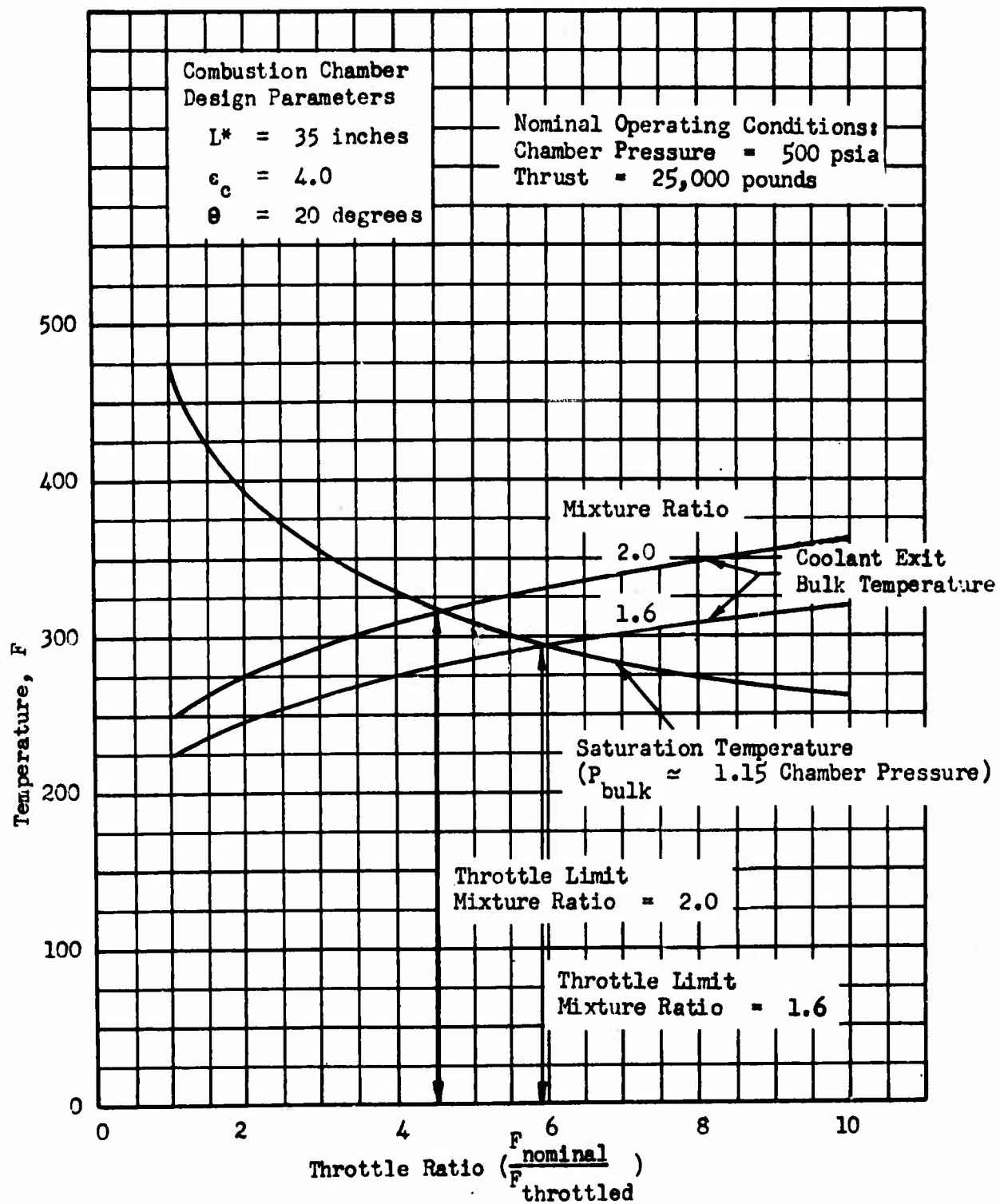


Figure 43. Throttling Limits for a Regeneratively Cooled, 25,000-Pound-Thrust  $N_2O_4/N_2H_4$ -UDMH(50-50) Propellant Thrust Chamber

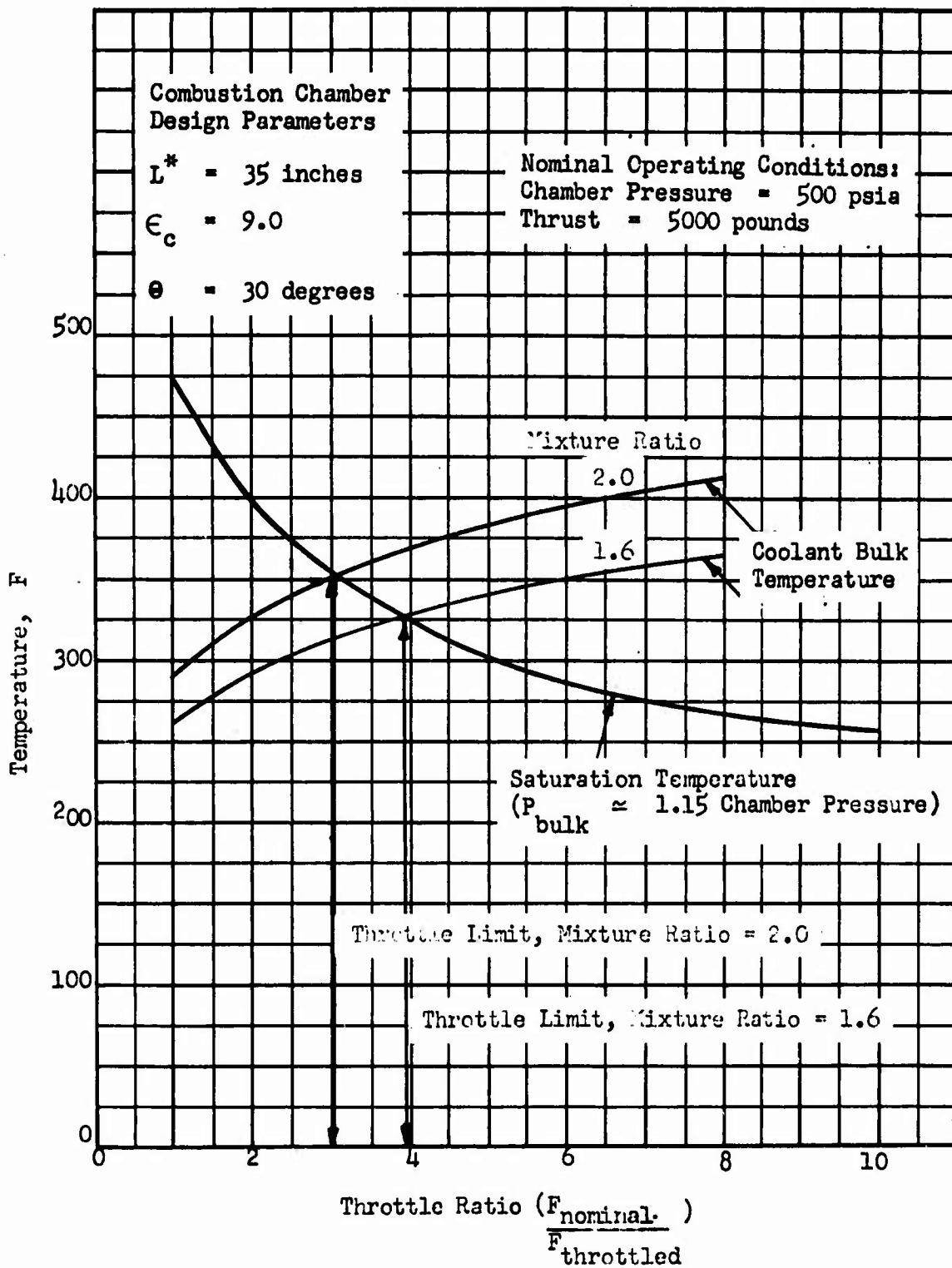


Figure 44. Throttling Limits for a Regenerative Cooled  $N_2O_4/N_2H_4$ -UDMH(50-50) 5000-Pound-Thrust Propellant Thrust Chamber

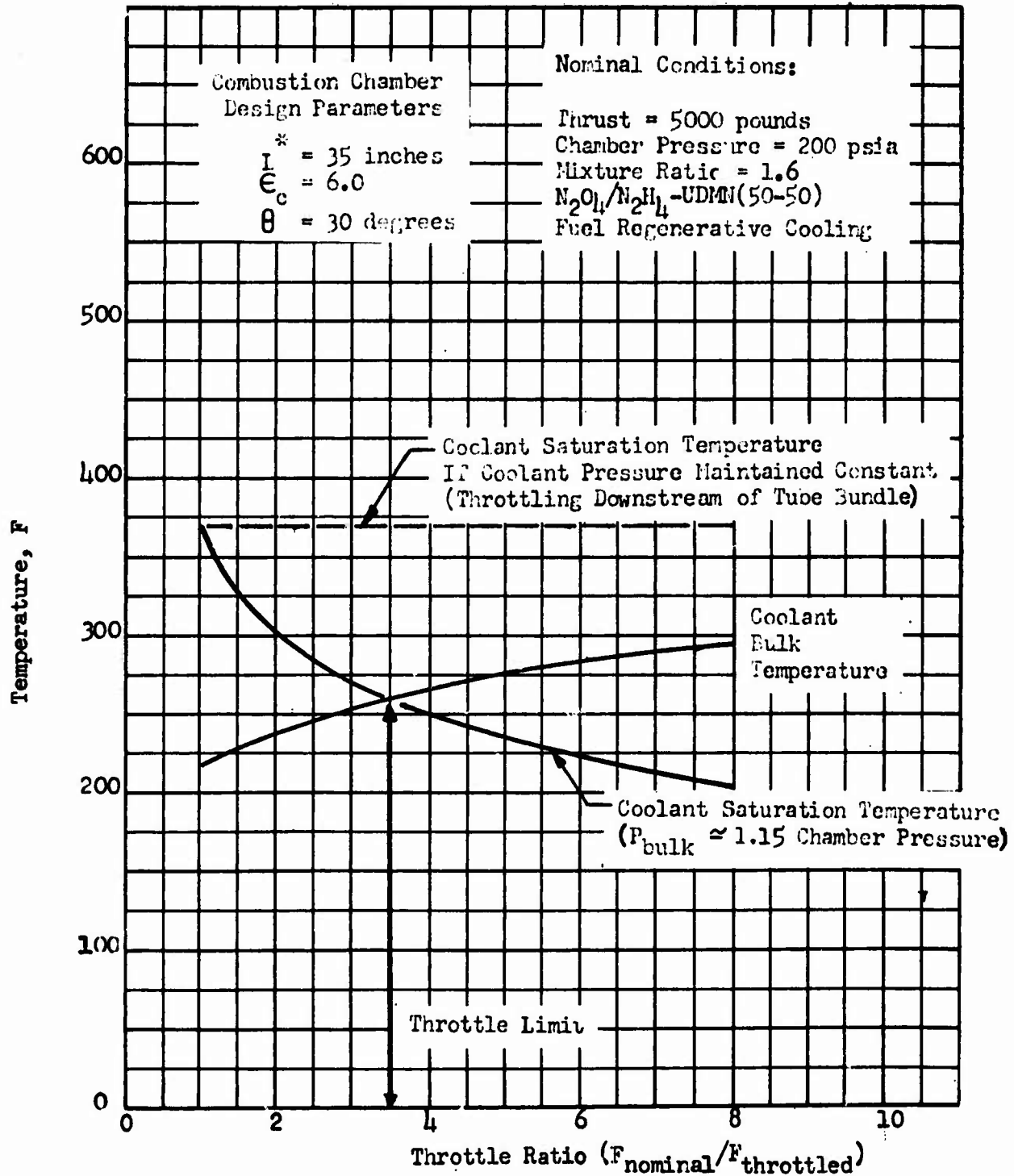


Figure 45. Throttling Limits for a Regeneratively Cooled  $N_2O_4/N_2H_4$ -UDMH (50-50) Propellant Thrust Chamber

Combustion Chamber  
Design Parameters

$L^*$  = 35 inches

$\epsilon_c$  = 12

$\theta$  = 30 degrees

Nominal Operating Conditions:  
Chamber Pressure = 1000 psia  
Thrust = 5000 pounds

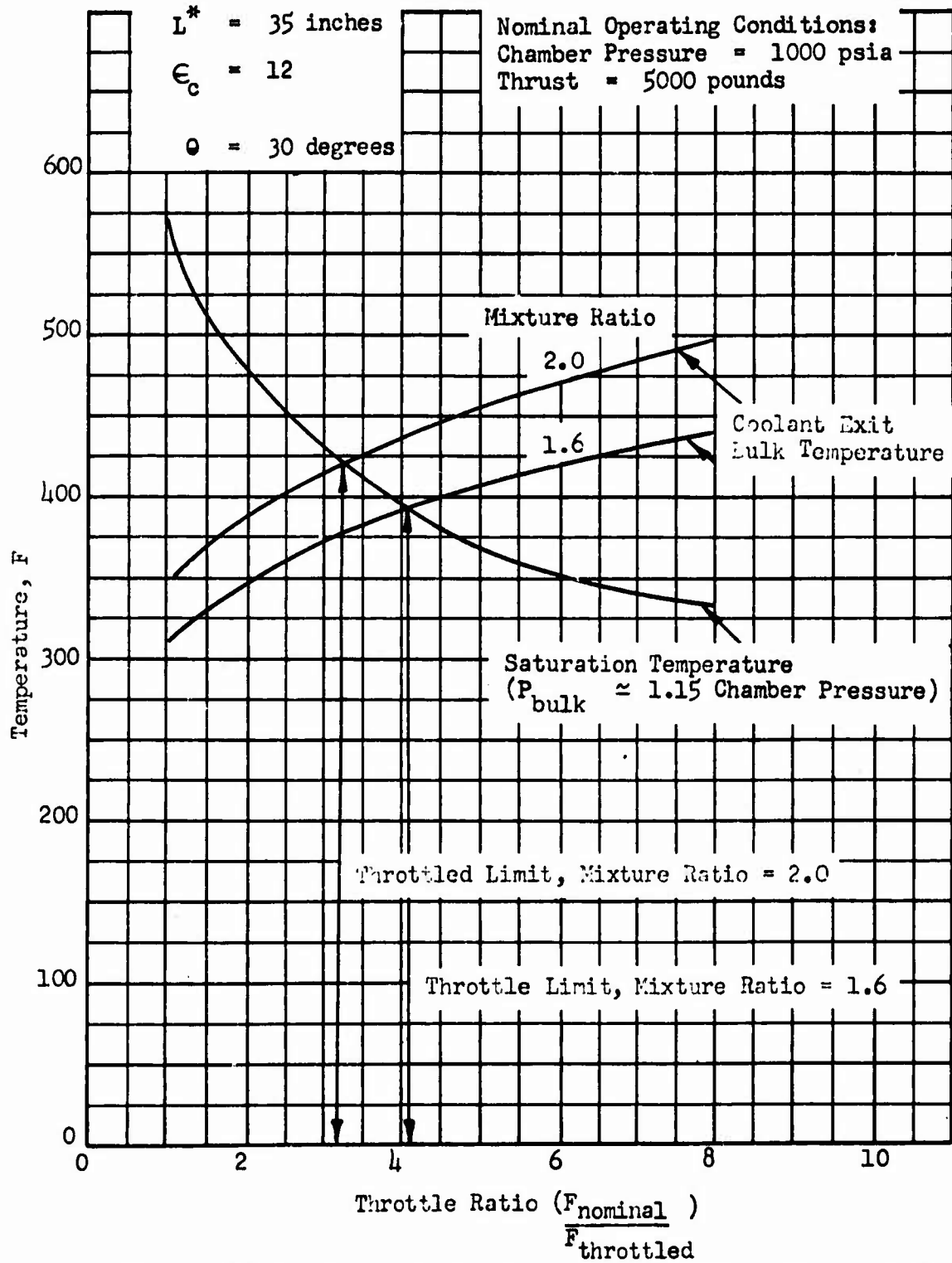


Figure 46. Throttling Limits for a Regenerative Cooled  $N_2O_4/N_2H_4$ -UDMH(50-50) Propellant Thrust Chamber

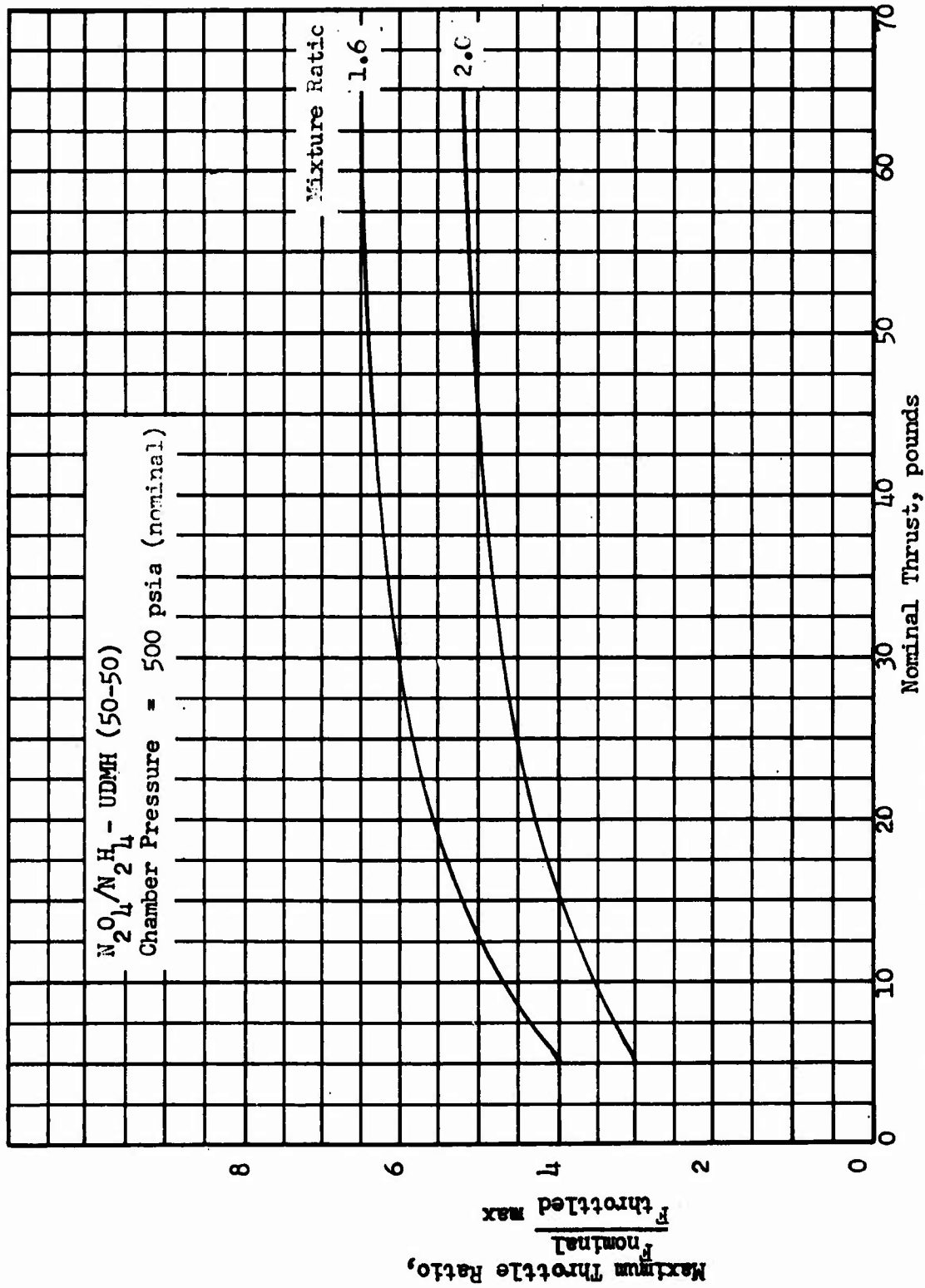


Figure 47. Effect of Nominal Thrust Level on Maximum Feasible Throttle Ratio

## CONFIDENTIAL

- (U) An alternate approach for deep throttling a pump-fed chamber is to over-design the pump discharge pressure at nominal conditions so that, at throttled conditions, the jacket coolant pressure is sufficiently high to prevent bulk boiling.
- (C) It is concluded on the basis of the foregoing analysis that it is feasible to regeneratively cool the throttlable low-thrust ( $\geq 5000$  pounds) moderate-to-high pressure ( $200 \leq P_c \leq 1000$  psia), storable-propellant, bell thrust chambers of interest in this study. The nominal chamber designs, however, require use of radiation skirts and high-combustion-zone contraction ratios to minimize the total heat load to the coolant. The throttling of these engines is limited somewhat using normal upstream (of the coolant jacket) throttling techniques because of the occurrence of bulk boiling of the coolant. Maximum-throttle-ratio limits in this case are in the range of 4 to 6. If a downstream throttling method is used so that the coolant jacket pressure is maintained at a relatively high level (thereby maintaining a high saturation temperature), the throttling ratio may be extended to a value of 10:1 or greater.
- (b) (U) Film and Ablative Cooling. Because of the limitations of cooling engines regeneratively during throttling with  $N_2O_4-N_2H_4$ -UDMH (50-50) propellants in the thrust range being considered, ablative and film cooling methods were also briefly considered. These methods are similar in that both form a protective layer between the wall and the hot gas. Film cooling is achieved by introducing a thin film of coolant (liquid  $N_2H_4$ -UDMH (50-50) was used in the present study) through slots in the wall, into the boundary layer on the hot-gas-side wall surface.
- (U) The approach used to evaluate film-cooling requirements neglected the effects of angle spacing and orifice or slot size. The heat transfer rate to the coolant injected into the hot-gas stream was calculated. The film coolant heat capacity, heat of vaporization, and an efficiency factor which accounts for losses of the film coolant to the mainstream flow without any beneficial effect were used to determine the temperature of the film coolant as it travels along the walls. More film coolant is injected when the temperature of the coolant at the wall approaches the maximum specified wall temperature.
- (U) The results of this analysis are shown in Fig. 48 for three specified maximum wall temperatures corresponding to nickel, stainless steel, and a refractory material. The effect of chamber pressure on the film-cooling requirement was found to be negligible for a wide range of chamber pressures because the added density which occurs when increasing chamber pressure was compensated for by the reduced nozzle area. Since the nozzles considered were assumed to be radiation cooled beyond an area ratio of 30, increased chamber pressure could affect the film-cooling requirements if the chamber pressure were raised to such an extent that radiation cooling was not possible beyond an area ratio of 30. However, for the purposes of this study, chamber pressure was assumed to have no effect. The film-cooling requirements given in Fig. 48 are for fully film-cooled engines (to an area ratio of 30). The film-cooling requirements would decrease significantly if the engines were partly regeneratively cooled.

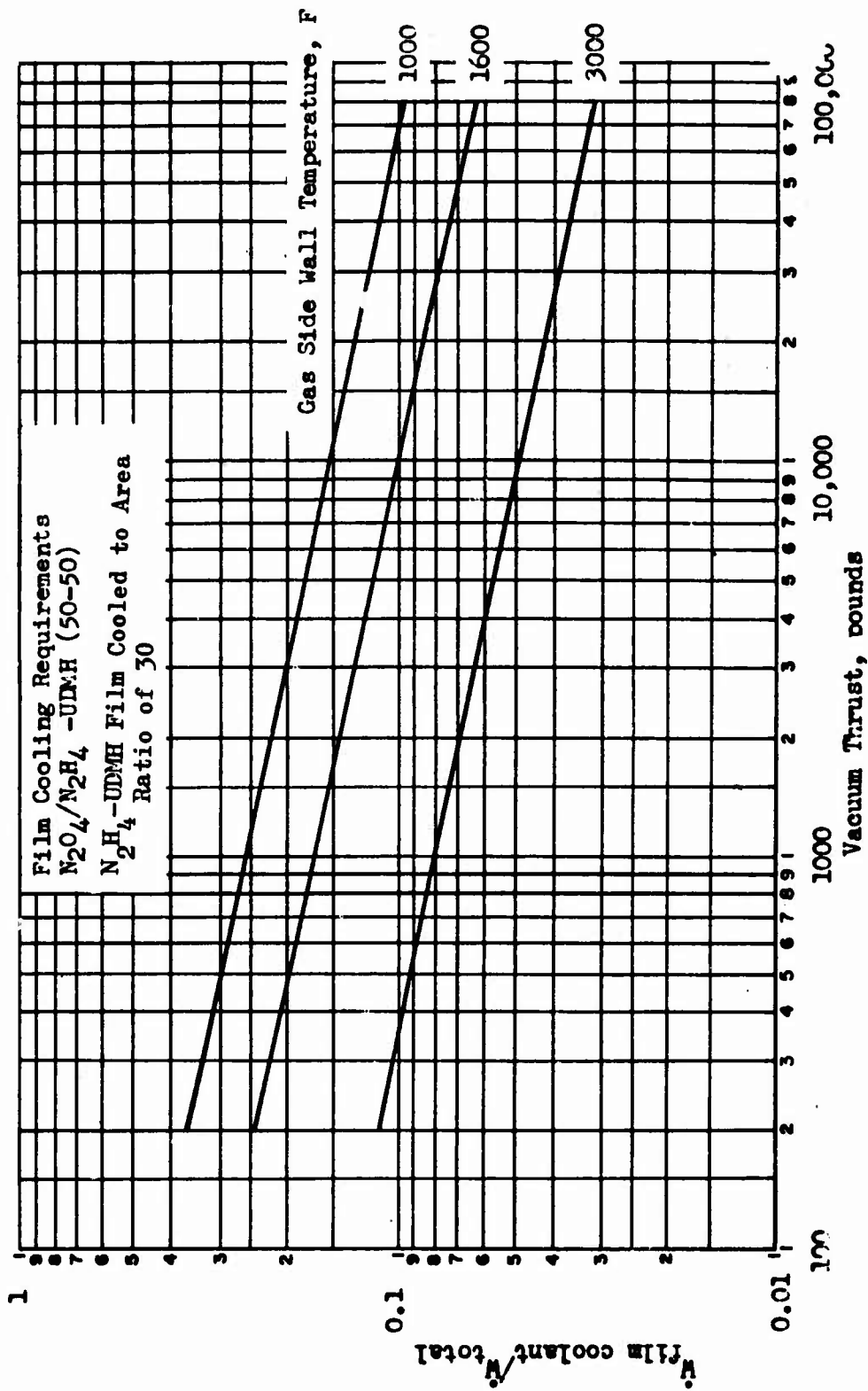


Figure 48. Film Cooling Requirements for Conventional Bell Nozzle Thrust Chamber.

## CONFIDENTIAL

- (U) For ablative cooling the required ablative thickness (shown in Fig. 49) was obtained using the LEM descent engine design as a reference. The LEM descent engine utilizes the same propellants, and approximate thrust and chamber pressure as the lower range thrust engines required for the application considered in this study. The only parameter which affects the required thickness significantly (Ref. 9) is the firing duration.
- (U) The required char depth thickness is approximately proportional to the square root of the firing duration. Since the required firing duration is not a fixed value for the MSPS application, a curve of required thickness vs time is shown in Fig. 49 based upon the LEM firing duration of 770 seconds and the  $\sqrt{T}$  variation. This required thickness would have to be increased, and possibly some erosion would take place, as a result of long-period shutdowns and numerous restarts. When shutdown occurs, the heat stored up in the char layer continues to release more pyrolysis gases, increasing the char layer depth.
- (3) (C) Selection of Candidate Propulsion Systems. The results of the thrust chamber-cooling studies for the bell nozzle engines provided the guidelines for the formulation of candidate propulsion system using the  $N_2O_4/N_2H_4$ -UDMH (50-50) propellant combination. In general, regenerative cooling was incorporated whenever feasible. Film cooling was found to require excessively high coolant flowrates and therefore was not considered as a primary method of thrust chamber cooling, but it may be considered as a means of augmenting the regenerative cooling for situations where operating conditions exceed the regenerative-cooling capabilities. For those design thrust levels and throttling ratios where regenerative cooling is feasible only by maintaining high coolant jacket pressures, ablative liners were considered as an alternate cooling method.
- (C) The list of candidate propulsion systems selected for evaluation is presented in Table XXII for the three values of system design thrusts (30,000, 50,000, and 75,000 pounds). System A consists of a single thrust chamber and therefore must be capable of operation over the entire indicated throttling ratios. In view of the inability of a regenerative-cooling system to function over the required range, this engine was assumed to be ablatively cooled. In the following comparison, all of the ablative chambers are assumed to have a 2.0-inch thickness which provides a burn duration of approximately 2000 seconds. This burn duration is below that which would result if all propellants were burned at minimum thrust. However, in the case of the multiengine systems, the operating time can be divided between two or more engines, thus significantly increasing the maximum burn durations for the system at reduced operating thrust levels.
- (U) Systems B and L are four equal-thrust engines with regeneratively and ablatively cooled chambers, respectively. Since relatively high throttling ratios are required for the individual engines, a high pump discharge pressure and cooling jacket pressure must be maintained over the throttling range to provide adequate regenerative-cooling capabilities. The ablative chamber provides a method whereby this operating penalty may be avoided.

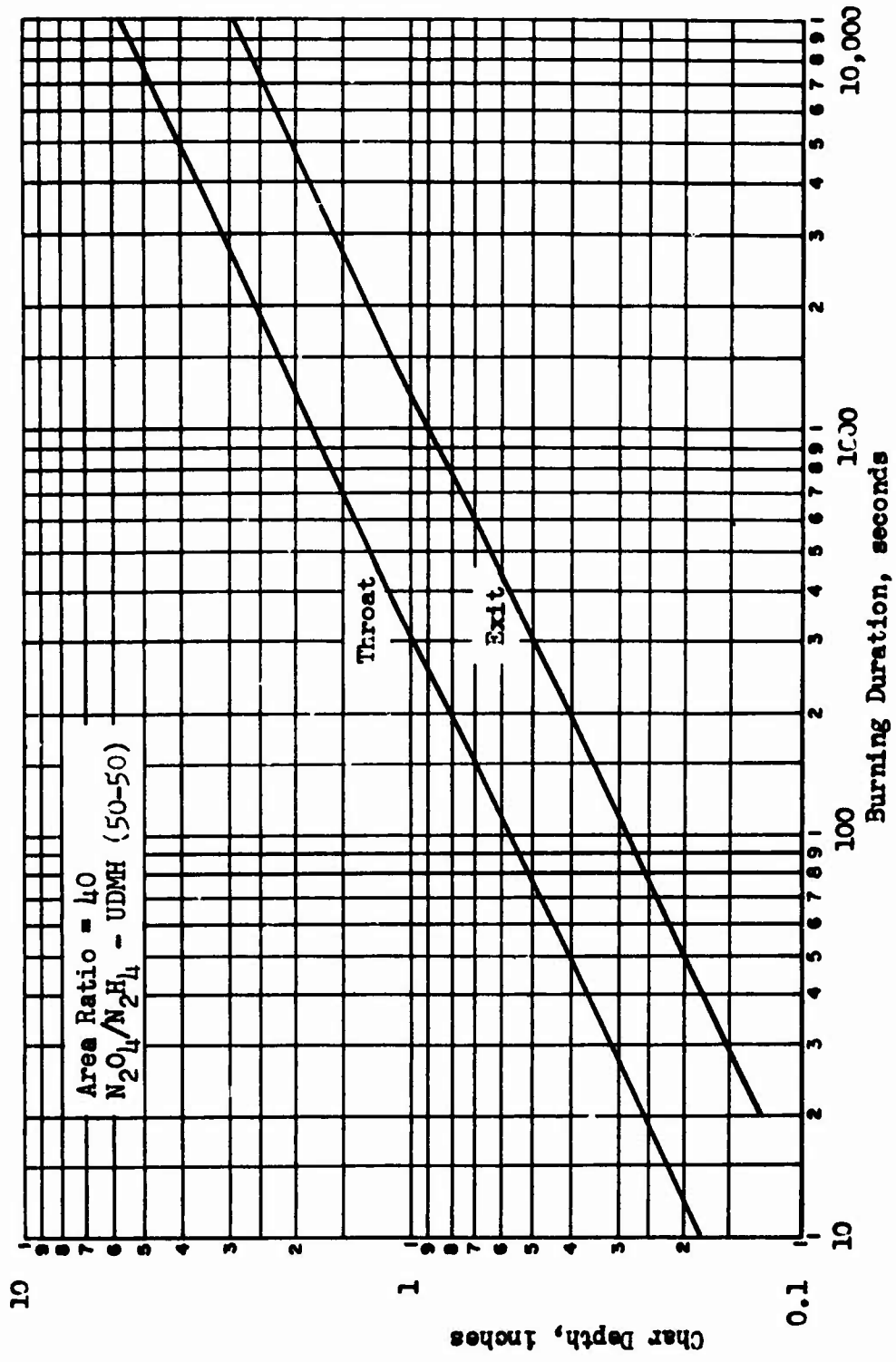


Figure 49. Ablative Material Thickness vs Burning Duration

CONFIDENTIAL

TABLE XXII

CANDIDATE PROPULSION SYSTEMS SELECTED FOR EVALUATION

System	Level	No. of Engines	Thrust Level, pounds x 10 <sup>-3</sup>	Throttling Ratio	Thrust Level pounds x 10 <sup>-3</sup>	Throttling Ratio	power
A		1	30	70	50	82	
$\frac{B}{L}$		4	7.5	17.5	12.5	20.5	
$\frac{C}{H}$	High Thrust	1	25.71	6	42.86	6	
	Low Thrust	2	2.14	4.98	3.57	5.85	
$\frac{G}{M}$	High Thrust	1	25.71	6	42.86	6	
	Low Thrust	3	1.43	3.4	2.38	3.9	
$\frac{D}{I}$	High Thrust	1	25.71	6	42.86	6	
	Low Thrust	4	1.07	2.5	1.79	2.9	
$\frac{E}{J}$	High Thrust	2	13.85	6	23.08	6	
	Low Thrust	2	1.15	2.7	1.92	3.1	
$\frac{F}{K}$	High Thrust	2	13.85	6	23.08	6	
	Low Thrust	4	0.577	2	0.962	2	

1

TABLE XXII

PULSION SYSTEMS SELECTED  
FOR EVALUATION

st l 10 <sup>-3</sup>	Throttling Ratio	Thrust Level pounds x 10 <sup>-3</sup>	Throttling Ratios	Method of Cooling	Feed System Type
	82	75	90	Ablative	Turbopump
	20.5	18.75	22.5	<u>Regenerative</u> Ablative	Turbopump
	6	64.29	6	Regenerative	Turbopump
	5.85	5.36	6.42	<u>Regenerative</u> Ablative	Turbopump
	6	64.29	6	Regenerative	Turbopump
	3.9	3.57	4.2	<u>Regenerative</u> Ablative	Turbopump
	6	64.29	6	Regenerative	Turbopump
	2.9	2.68	3.2	<u>Regenerative</u> Ablative	Turbopump
	6	34.62	6	Regenerative	Turbopump
	3.1	2.88	3.5	<u>Regenerative</u> Ablative	Turbopump
	6	34.62	6	Regenerative	Turbopump
	2	1.442	2	<u>Regenerative</u> Ablative	Turbopump

2

# CONFIDENTIAL

- (C) It was shown previously that regeneratively cooled engines with design thrust levels from 25,000 to 75,000 pounds thrust could be throttled through a range of approximately 6:1 without compromising the overall system. With this restriction in mind, several multiengine systems were formulated in an effort to reduce the required throttling ratio for the individual thrust chambers. Systems C and H consist of a primary high-thrust engine which is throttled 6:1 and two low-thrust engines which provide the remainder of the required throttling range. The throttling ratios of the low-thrust engines are still above that which can be accomplished without some system compromise. Therefore, ablative chambers are also considered as an alternate cooling method for the low-thrust engines.
- (U) The remaining systems (D through M) illustrate possible variations of the multiengine propulsion systems. By increasing the number of engines at either the high- or low-thrust level, the required throttling ratio for the individual engines is reduced.
- (U) All systems selected for comparison are pump fed. Each thrust chamber is provided with an individual turbopump set.
- (U) In establishing these candidate propulsion system configuration for comparison consideration was given to pressure-fed systems. The primary advantage of the pressure-fed system for this application is in connection with the regenerative-cooling requirements. It was shown that greater throttling depth could be achieved with a regenerative-cooling system if the cooling jacket pressure could be maintained at or near a constant value over the throttling range. For a pump-fed system, this places rather severe operational requirements on the turbomachinery and results in a system performance penalty at the throttled operating conditions. The pressure-fed systems permit the use of a throttling valve downstream of the coolant jacket, thereby maintaining a high coolant jacket pressure without a performance degradation.
- (C) A comparison of pump- vs pressure-fed systems for an  $LF_2/H_2$  maneuvering satellite system was presented in Ref. 3 for single and multiengine systems. It was shown that the increased tank pressure requirements resulted in a severe stage weight penalty and the lower operating chamber pressures, typical of the pressure-fed systems, caused a significant reduction in engine performance when compared with pump-fed systems. The final comparison presented in Ref. 3 indicated an approximate  $\Delta V$  advantage of 3000 ft/sec for the 20,000-pound gross weight pump-fed systems. It is expected that a similar but possibly less-pronounced result would be obtained for the  $N_2O_4/N_2H_4$ -UDMH (50-50) propellants. Other system characteristics not illustrated in this comparison are significant in the feed system selection. The low operating chamber pressures require large engine dimensions to achieve the specified thrust levels. This requirement results in increased engine weights and propulsion system envelope requirements exceeding the 10-foot-diameter limit established by the booster vehicle diameter. Also, the low design chamber pressures will probably result in a limitation on the depth of throttling than can be achieved because of stability problems at the very low operating chamber pressures.

b. Propulsion System Criteria

(U) The candidate propulsion system configurations selected for a comparative evaluation were presented in Table XXII. Selection criteria were established and are shown in Table XXIII. The relative importance of each item is also shown. These criteria are largely based upon criteria established for the selection analysis presented in Ref. 3.

TABLE XXIII  
ENGINE SELECTION CRITERIA

	<u>Percent</u>
Performance	
$\Delta V$ Capability	45
Operational Suitability	40
Throttling (15)	
Depth	
Regenerative Cooling Limits	
Firing Time Limitation (5)	
Engine Length (5)	
Transient Losses (5)	
Number of Throttling Control Operations (10)	
Complexity and Reliability	15
Number of Major Components	

(1) (U) Rating Method. The selection criteria were chosen to provide a relative comparison of the most important characteristics of the candidate systems. It was established that performance was the most important criterion for the MSPS vehicle: therefore, the performance was given major emphasis in the comparison. System operating characteristics other than performance that differed among the candidate systems were compared on the basis of the items listed under operational suitability. Complexity, reliability, and development considerations are all compared on the basis of the number of major components contained in the system and the number of different components to be developed.

(U) Each item was given a weighting which reflected its importance to overall propulsion system selection. The actual rating number was obtained by assigning the maximum value achievable to the most desirable system for the particular criterion being considered. The least-desirable system then received exactly one-half the maximum value. Intermediate systems received their rating based upon a linear interpolation between the two end points.

# CONFIDENTIAL

- (C) The propulsion system performance comparison was based upon the system  $\Delta V$  capability at the full-thrust operating condition of the candidate propulsion systems. All of the systems considered in this comparison are pump fed, and the individual thrust chambers would be expected to optimize at approximately the same chamber pressure and area ratio. The optional thrust chamber-cooling methods considered for the smaller thrust chambers may result in small variations in the optimum design parameters. However, for this preliminary comparison, all of the individual thrust chambers were assumed to have the same design values of chamber pressure and area ratio. Values of 650 psia and 100:1 for the chamber pressure and area ratio, respectively, were selected based upon the results of previous optimization studies and the regenerative-cooling studies. After the system configuration selection had been made, an optimization analysis was conducted to determine the maximum performance design parameters for the selected system. An optimization for each candidate system would involve a much more extensive effort and is unwarranted for this preliminary comparison.
- (U) Since all of the individual thrust chambers of the candidate propulsion systems have the same design chamber pressure and area ratio, the full-thrust specific impulse will be approximately the same for all systems. This assumption neglects the relatively minor variations in nozzle drag, kinetic performance, and turbopump energy requirements within the range of design thrust levels required for these propulsion system configurations.
- (U) The system performance or  $\Delta V$  comparison then reflects only the difference in engine weights for each candidate system. Parametric engine weight data were generated for a range of design thrust levels typical of those required in the various propulsion system assemblies. These weight estimates were made based upon a computerized analysis that provides a component-by-component weight evaluation of the thrust chamber and accessories. The analytical methods used in determining the component weights are derived from a large range of design and manufacturing experience. Ablative chamber weights were based upon a 2.0-inch ablative material thickness.
- (C) The full-thrust  $\Delta V$  capability was obtained for a constant system gross weight of 20,000 pounds and a payload of 2000 pounds. Composite engine system weights varied by as much as 135 pounds, which resulted in a variation in the system  $\Delta V$  capability of approximately 300 ft/sec. The candidate systems were then rated on a relative basis by assigning the highest  $\Delta V$  system the maximum rating points (45) and the lowest  $\Delta V$  system 22.5 rating points. Intermediate systems were rated on the basis of a linear interpolation. The individual system performance ratings are shown in Table XXIV.
- (C) The items listed under operational suitability were evaluated individually according to the distribution shown in Table XIV. A criterion was established to indicate the relative ease in obtaining the required throttling depth for each system. This included the depth of throttling required for the main engine or engines and for the secondary engines. The single-engine configuration would have to accomplish the entire overall throttling requirement and therefore was assigned the minimum rating for the main

**CONFIDENTIAL**

TABLE XXIV

ENGINE SELECTION EVALUATION

		A. Single Bell (Ablative)	B. $\frac{1}{4}$ Bell (Regenerative)	C. Bell/2 Bell (Regenerative)	D. Bell/4 Bell (Regenerative)	E. 2 Bell/2 Bell (Regenerative)	F. 2 Bell/4 Bell (Regenerative)	G. 1 Bell/3 Bell (Regenerative)
Performance $\Delta V$ at Full Thrust	(45)	32.5	40	45	31	40	29	37.5
Operational Suitability	(40)							
Throttling								
Main Engine	5							
Secondary Engine	5	2.5	4.5	9.0	10.0	10.0	10.0	10.0
Regenerative-Cooling Limitation	5	5.0	2.5	2.5	5.0	5.0	5.0	2.5
Firing Time Limitations	5	2.5	5	5	5	5	5	5
Engine Length	5	5.0	2.5	4.5	4.5	3.5	3.5	4.5
Transient Losses	5	5.0	3.3	3.7	3.0	3.3	2.5	3.3
Number of Throttling Control Operations	10	10.0	8.0	8.5	7.0	7.0	5.0	7.5
Complexity and Reliability	(15)							
Number of Major Components		15	10.5	12	9.0	10.5	7.5	10.5
Total:		77.5	76.3	90.2	74.5	84.3	67.5	80.8
Relative Rank:		7	8	1	9	3	11	4

1

ON EVALUATION

	D: Bell/4 Bell (Regenerative)	E: 2 Bell/2 Bell (Regenerative)	F: 2 Bell/4 Bell (Regenerative)	G: 1 Bell/3 Bell (Regenerative)	H: 4 Bell (Ablative)	I: 1 Bell/2 Bell (Regenerative/Ablative)	J: 1 Bell/4 Bell (Regenerative/Ablative)	K: 2 Bell/2 Bell (Regenerative/Ablative)	L: 2 Bell/4 Bell (Regenerative/Ablative)	M: 1 Bell/3 Bell (Regenerative/Ablative)
	40	29	37.5	28.5	41.5	27	36.0	22.5	35	
0.0	10.0	10.0	10.0	4.5	9.0	10.0	10.0	10.0	10.0	
5.0	5.0	5.0	2.5	5.0	5.0	5.0	5.0	5.0	5.0	
5	5	5	5	2.5	2.5	2.5	2.5	2.5	2.5	
4.5	3.5	3.5	4.5	2.5	4.5	4.5	3.5	3.5	4.5	
6.0	3.3	2.5	3.3	3.3	3.7	3.0	3.3	2.5	3.3	
7.0	7.0	5.0	7.5	8.0	8.5	7.0	7.0	5.0	7.5	
7.0	10.5	7.5	10.5	10.5	12	9.0	10.5	7.5	10.5	
5	84.3	67.5	80.8	64.8	86.7	68.0	77.8	58.5	78.3	
	3	11	4	12	2	10	6	13	5	

2

engines. The four bell nozzle engine systems required the next greatest throttling depths and were rated accordingly. The remaining systems consist of main engines with a 6:1 throttling capability, and the remainder of the throttling requirement is accomplished with the smaller-secondary engines. Therefore, the throttling depth rating for the main engines are rated according to their throttling depth requirement. Those secondary engines with throttling depths of 3:1 or less received the maximum rating points.

- (U) The regenerative-cooling restrictions are the major limitation on throttling capability. Certain systems will require system compromises (increased pump discharge pressures, film cooling, etc.) to achieve the required throttling depths and provide adequate cooling capabilities over the operating thrust range. The use of ablatively cooled thrust chambers for the secondary engines eliminates this problem. The systems in which the nominal regenerative-cooling/throttling capabilities are exceeded received the minimum rating. The systems not requiring some system compromise received the maximum number of rating points.
- (U) The firing-time limitation rating reflects the fact that the ablatively cooled thrust chambers are limited to approximately 2000 seconds of firing duration. With some duty cycles, it is possible that this burn duration would be exceeded. In the multiengine configurations, alternate engines could be used to increase this limiting burn duration. However, this results in added complexity. In theory, the regeneratively cooled thrust chambers are not limited in firing duration.
- (U) Engine length ratings were obtained by assigning the maximum of 5.0 points to the shortest overall engine system length and 2.5 points to the longest engine system, with a linear interpolation for the intermediate systems.
- (U) A simplified relative accounting of the transient losses experienced by each system was obtained by summing the number of engine startup and shutdown operations required in traversing the required system throttling depth. The system with the minimum total transients losses received the maximum rating.
- (U) Because of the possible variations in the mission thrust level duty cycle requirements, the throttling control comparison was made by counting the number of control operations necessary in throttling the system from maximum to minimum thrust (initial start and final shutdown included). A throttling control operation is defined as an engine start or shutdown and each separate throttling operation. The system with the smallest number of control operations received the highest rating.
- (U) System complexity, reliability, and development ease were rated solely on the basis of the number of major components contained within a candidate propulsion system. For the purpose of this comparison, major components were assumed to be individual thrust chambers, turbopump sets, and the number of engine control sets. The system containing the smallest number of major components received the maximum rating (15 points), while the system with the largest number received 7.5 points.

# CONFIDENTIAL

- (U) The evaluation and rating summary is shown in Table XXIV. The overall system comparison was obtained by summing the rating points assigned to each of the 13 systems. The relative standing is indicated by the number immediately below the total rating points.
- (U) Based upon this comparison, system C, consisting of a single primary engine and two secondary engines, was selected for the optimization analysis and further evaluation. All three thrust chambers are regeneratively cooled and pump fed. The second highest ranking system was this same configuration, but with ablatively cooled secondary engines. The third ranking system consists of two primary and two secondary engines. Thus, it can be seen that there are significant advantages to the multiengine systems using primary and secondary thrust chambers.

## c. Engine System Optimization

- (C) An optimization analysis was conducted for the selected  $N_2O_4/N_2H_4$ -UDMH (50-50) engine systems to define the maximum performance design parameters for each engine utilized in the multiengine propulsion systems. System thrust levels of 30,000, 50,000, and 75,000 pounds were investigated to correspond with the range of selected MSPS gross weights of primary interest to this study. Each system consists of three bell nozzle engines, one primary engine flanked by two secondary engines of lower thrust. Design thrust levels of individual thrust chambers and the required throttling ratios are shown below.

System Thrust*	Primary Engine		Secondary Engines	
	Thrust	Throttling Ratio	Thrust	Throttling Ratio
30	25.7	6:1	2.15	5:1
50	42.8	6:1	3.6	5.9:1
75	64.3	6:1	5.35	6.4:1

\*Thrust levels are expressed in thousands of pounds force

Each engine is pump fed and the thrust chambers are regeneratively cooled.

Optimizations were conducted for each of the primary engines and for the 5350-pound-thrust secondary engine. Since there is a small difference in the thrust levels of the secondary engines, an optimization of each of these engines is unnecessary. Past experience indicates that this variation in design thrust would have an insignificant effect upon the selection of the maximum performance design parameters.

The optimizations for each engine were conducted for continuous operation at both full and minimum thrust.

# CONFIDENTIAL

- (1) (U) Engine Performance. Performance estimates for the  $N_2O_4/N_2H_4$ -UDMH (50-50) engines were based upon the equilibrium propellant performance model. An engine mixture ratio of 1.6:1 was selected based upon the results of the regenerative-cooling studies and mixture ratio optimization analyses such as that presented in Ref. 6. Kinetic efficiencies were calculated for the large engines at the full-thrust and throttled operating conditions using a one-dimensional analysis assuming a divergence half-angle of 34 degrees. This angle approximates a bell nozzle contour just downstream of the throat in a region where the chemical reactions are expected to freeze. A similar analysis was performed on the small engine, but a divergence angle of 15 degrees was used, approximating a bell nozzle with a controlled-expansion throat region.
- (U) Nozzle divergence losses and viscous drag losses were obtained from parametric data presented in Ref. 6. Some additional analysis was conducted to obtain drag-loss data for the required range of operating thrust levels.
- (U) Combustion efficiencies ( $c^*$ , shifting) of 99 percent at full thrust and 98 percent at minimum thrust were assumed for the performance analysis.
- (U) Each engine uses two propellant pumps powered by a single turbine. The turbines are driven by gases tapped from the combustion chamber. Tapoff gas properties, turbine and pump efficiencies, and system operating characteristics are presented in Table XXV. Pump discharge pressures were estimated based upon the methods used for the  $LF_2H_2$  and  $LO_2/H_2$  systems.
- (U) An engine balance analysis was conducted for each engine to provide parametric engine specific impulse information to be used in the optimization.
- (2) (U) System Weights. Parametric engine weight information was generated for each engine thrust level. These weights were obtained with the aid of a computer program which estimates the weights of individual engine components as a function of operating characteristics. Nozzle weights and performance were based upon 80-percent-length contours.
- (U) Stage inert weights, including main propellant tanks, pressurization system, structure, and attitude control system, were obtained from the studies conducted for the alternate mission vehicles reported in Ref. 2.
- (C) Engine Optimization Results. Optimizations for the 25,750-, 42,800-, and 64,300-pound-thrust engines were conducted with constant gross weights of 20,000, 33,300, and 50,000 pounds, respectively. The relative  $\Delta V$  capabilities vs chamber pressure for each of these systems are shown in Fig. 50 through 55. The 5350-pound-thrust engine optimization used a constant stage gross weight of 50,000 pounds. The full-thrust and throttled optimization results are shown in Fig. 56 and 57.

# CONFIDENTIAL

TABLE XXV

$N_2O_4/N_2H_4$ -UDMH (50-50) BELL NOZZLE ENGINES  
SYSTEM OPERATING CHARACTERISTICS

	Full Thrust	Throttled
Engine Mixture Ratio	1.6	1.6
Combustion Efficiency	0.99	0.98
Tapoff System Mixture Ratio	0.1	0.1
Tapoff Gas Temperature, R	2060	2060
Tapoff Gas, $\gamma$	1.281	1.281
Tapoff Gas, $C_p$	0.686	0.686
Oxidizer Pump Efficiency	0.65	0.6
Full Pump Efficiency	0.65	0.6
Turbine Efficiency	0.41	0.112

CONFIDENTIAL

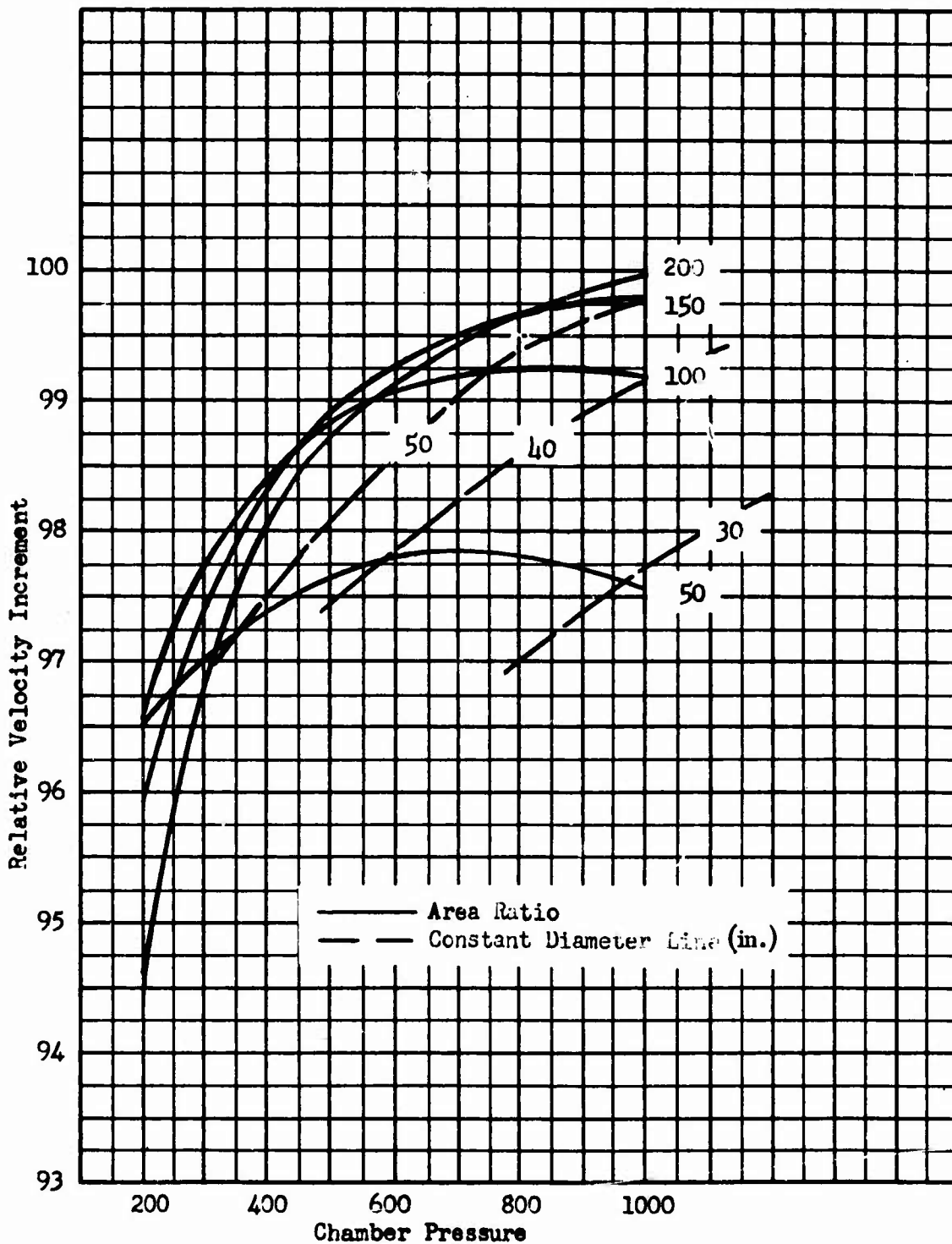


Figure 50. Chamber Pressure - Expansion Area Ratio Optimization for  $N_2O_4/N_2H_4$ -UDMH (50-50) 25,700-Pound Thrust Bell Engine at Full Thrust

CONFIDENTIAL

CONFIDENTIAL

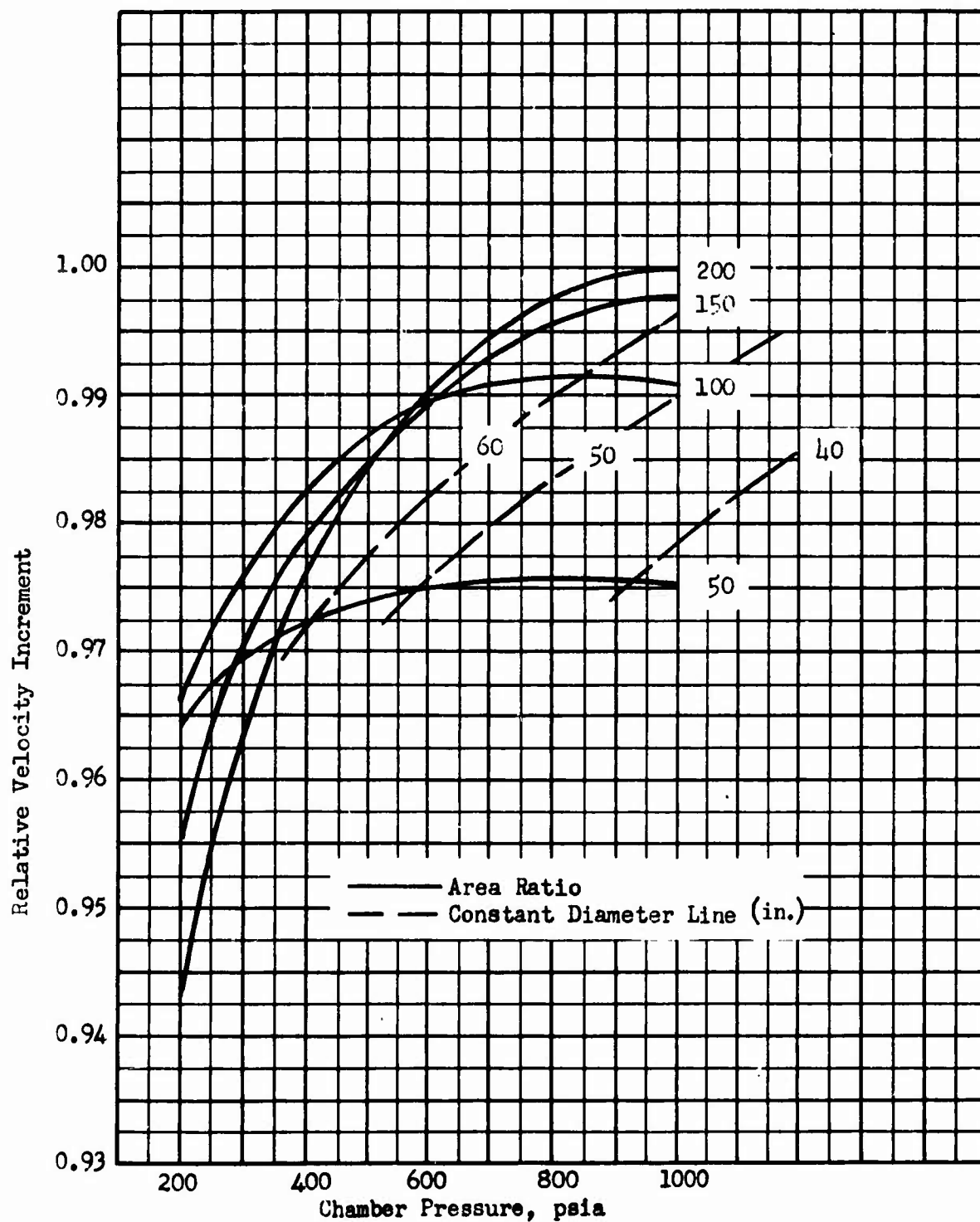


Figure 51. Chamber Pressure - Expansion Area Ratio Optimization for  $N_2O_4/N_2H_4$ -UDMH (50-50), 42,900-Pound Thrust Bell Engine at Full Thrust

CONFIDENTIAL

CONFIDENTIAL

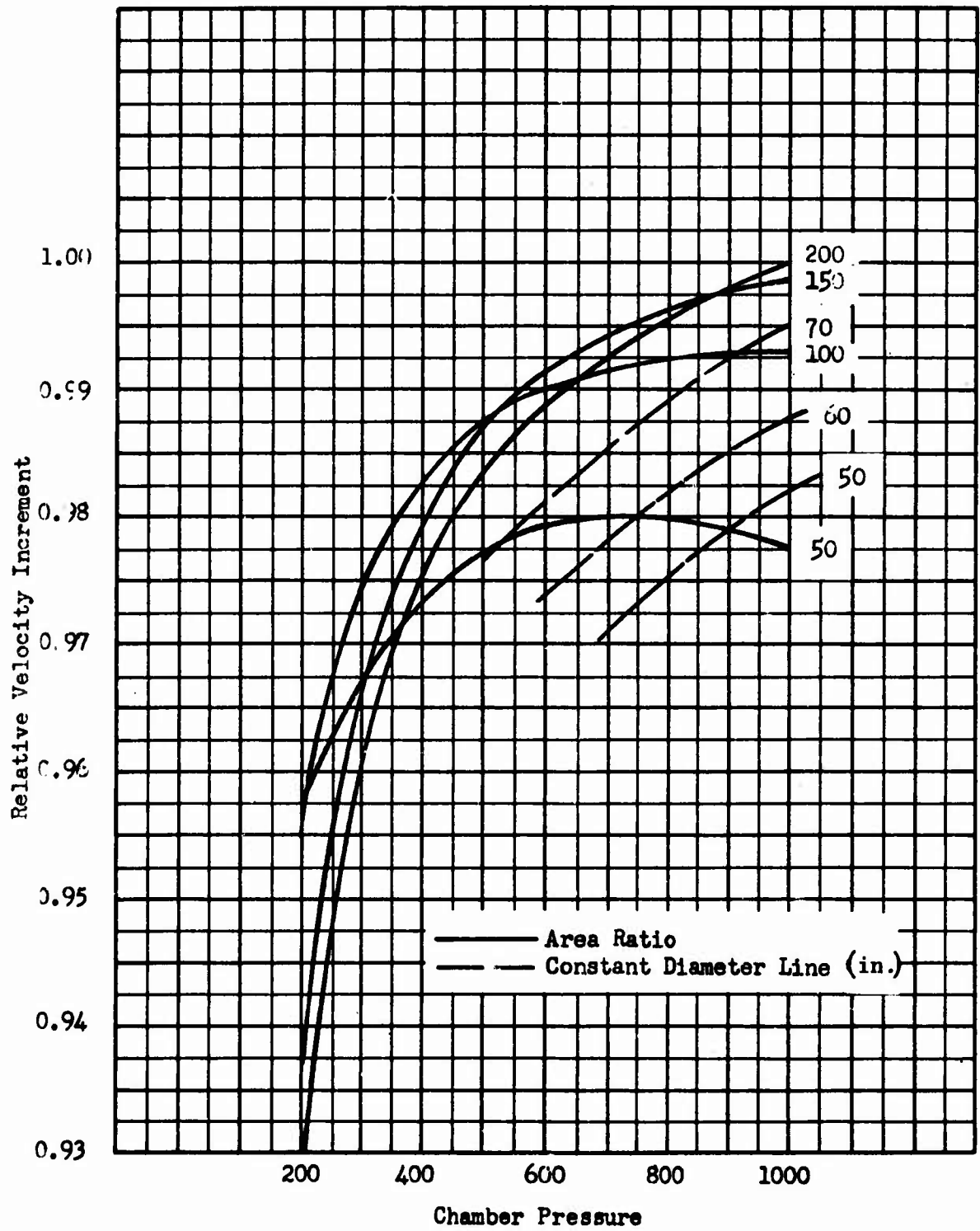


Figure 52. Chamber Pressure - Expansion Area Ratio Optimization for  $N_2O_4/N_2H_4$ -UDMH (50-50) 64,300-Pound Thrust Bell Engine at Full Thrust

CONFIDENTIAL

CONFIDENTIAL

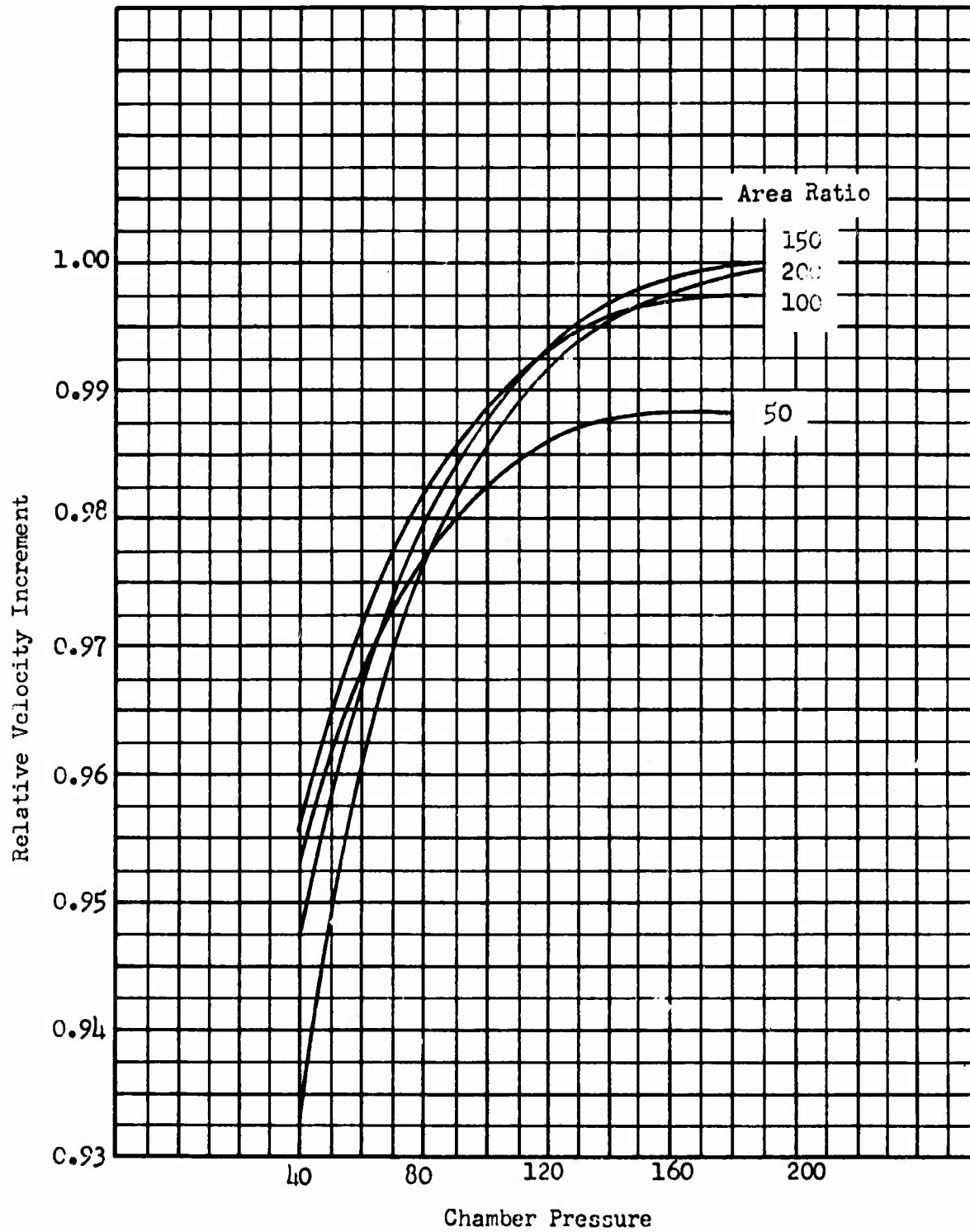


Figure 53. Chamber Pressure-Expansion Area Ratio Optimization for  $N_2O_4/N_2H_4$  - UDMH (50-50) 25,700-Pound Thrust Bell Engine. Throttled 6:1

CONFIDENTIAL

CONFIDENTIAL

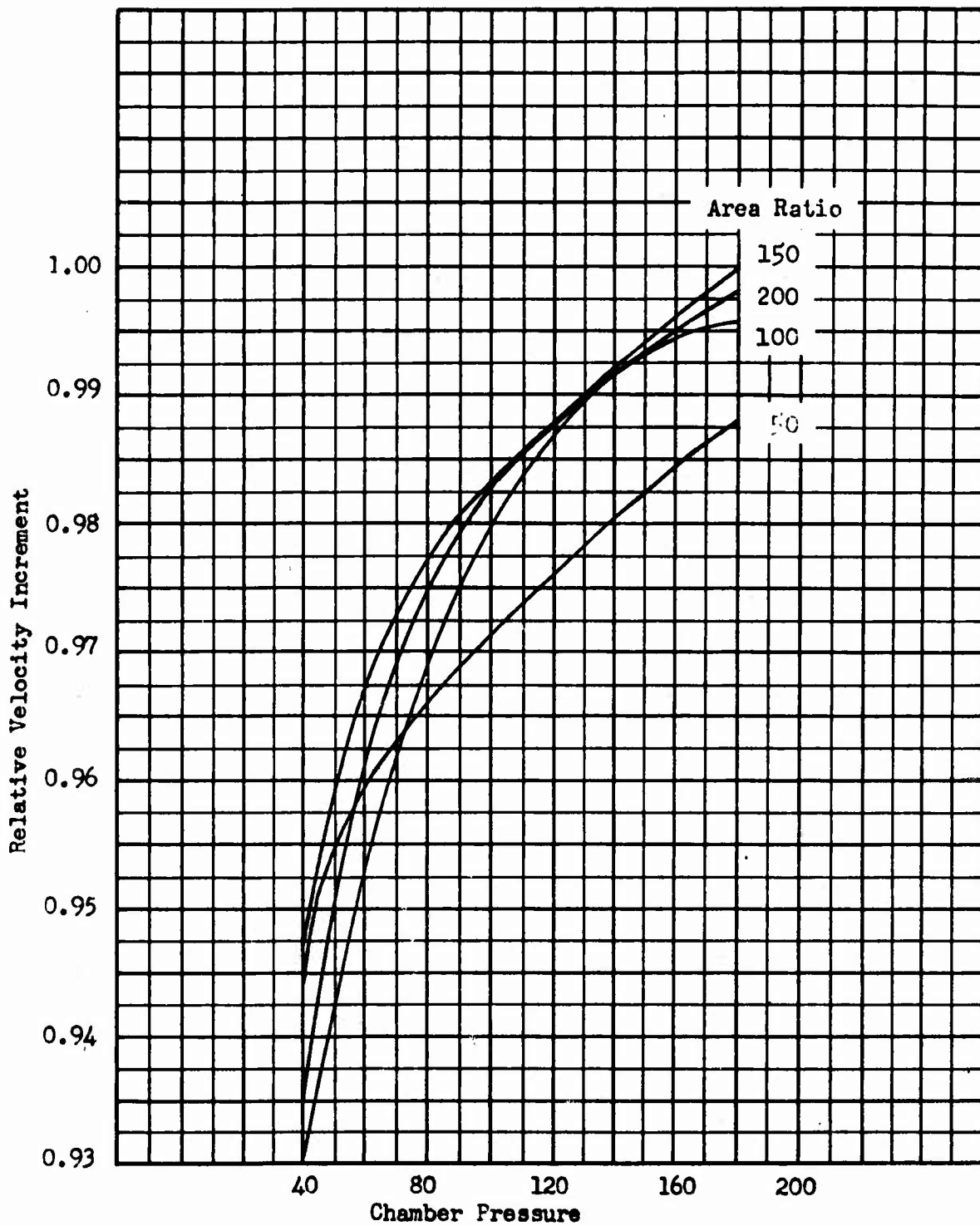


Figure 54. Chamber Pressure-Expansion Area Ratio Optimization for  $N_2O_4/N_2H_4$  - UDMH (50-50) 42,900-Pound Thrust Bell Engine. Throttled 6:1

CONFIDENTIAL

CONFIDENTIAL

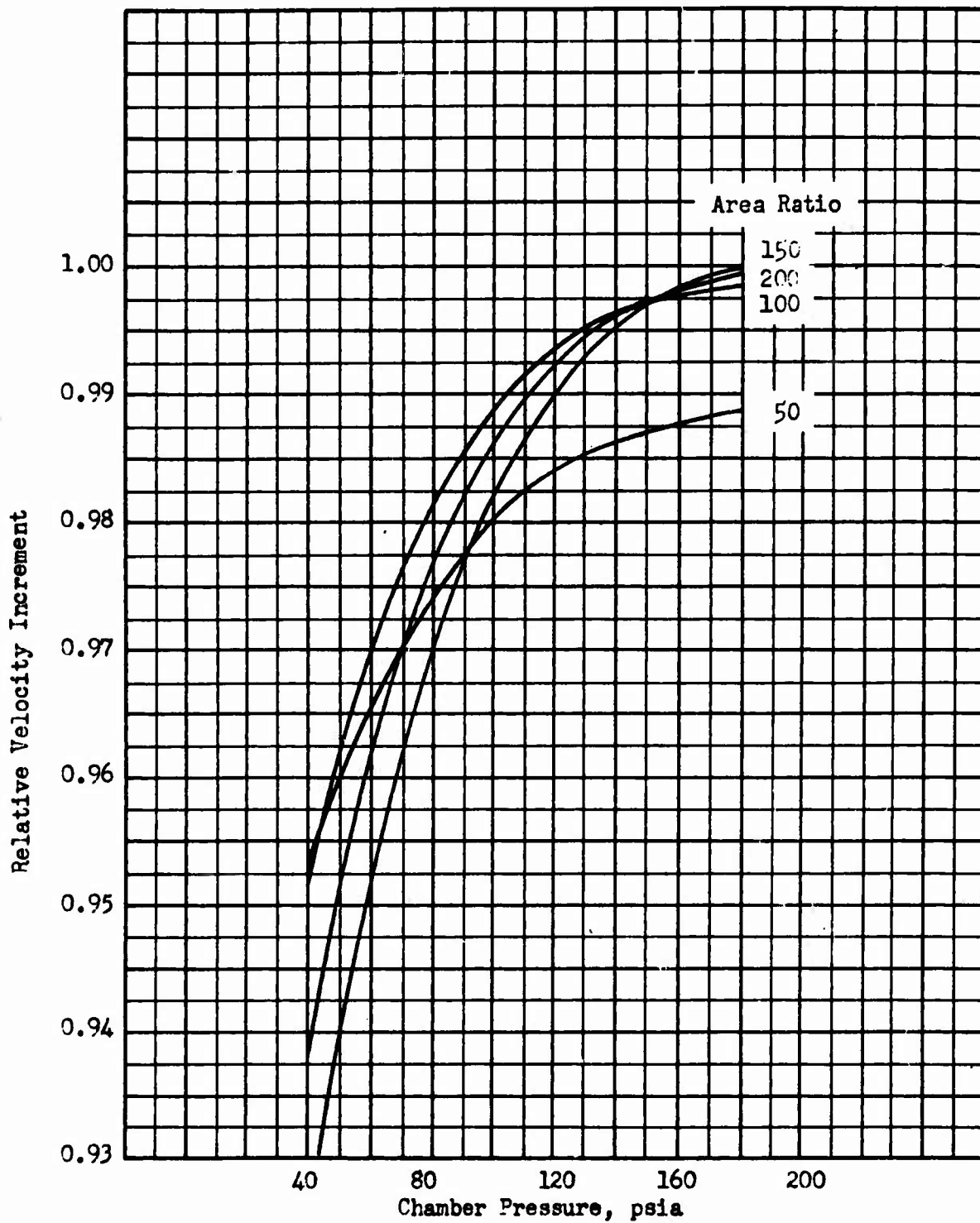


Figure 55. Chamber Pressure-Expansion Area Ratio Optimization for  $N_2O_4/N_2H_4$  - UDMH (50-50) 64,300-Pound Thrust Bell Engine. Throttled 6:1

CONFIDENTIAL

CONFIDENTIAL

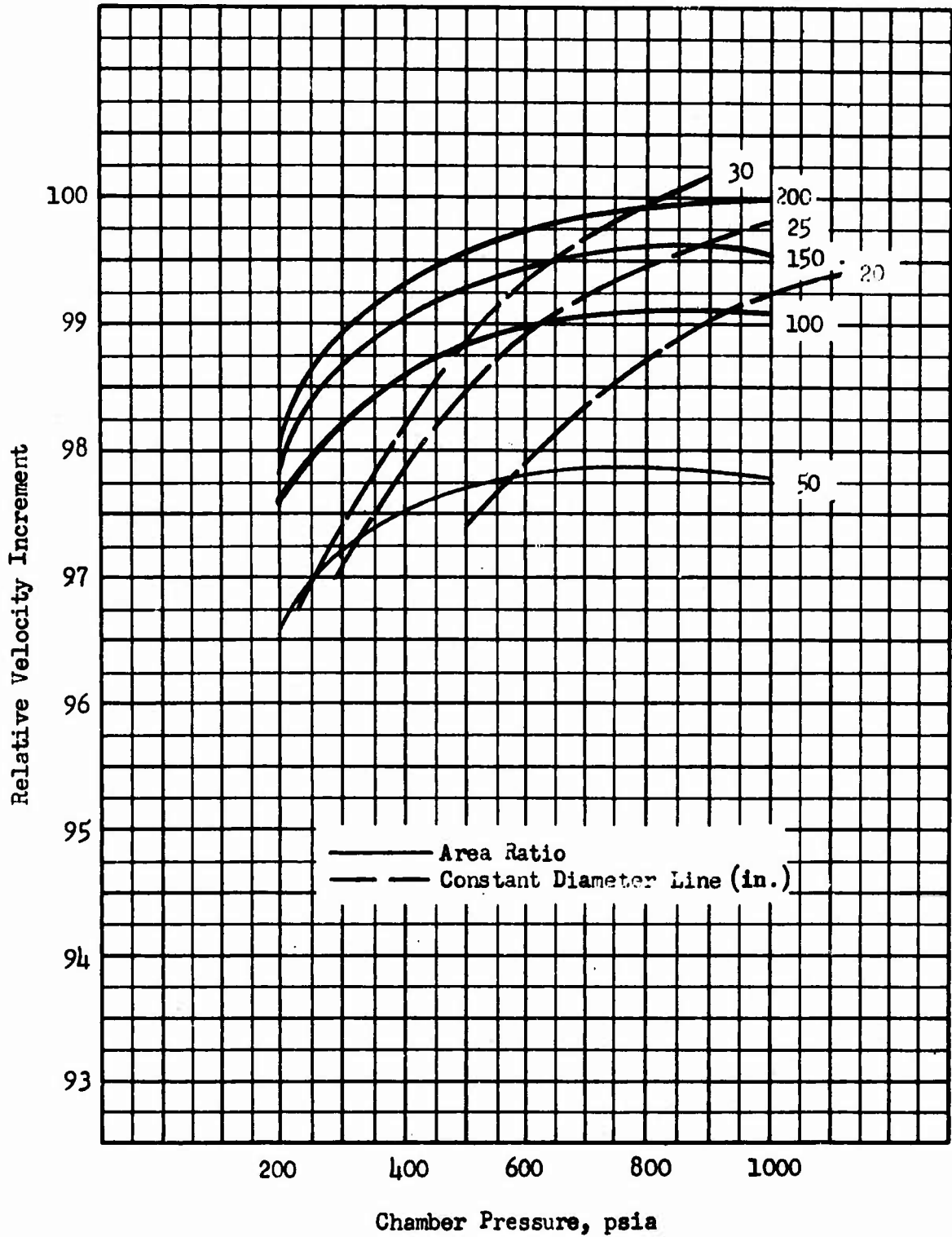


Figure 56. Chamber Pressure-Expansion Area Ratio Optimization for  $N_2O_4/N_2H_4$  - UDMH (50-50) 5,370-Pound Thrust Bell Engine at Full Thrust

CONFIDENTIAL

**CONFIDENTIAL**

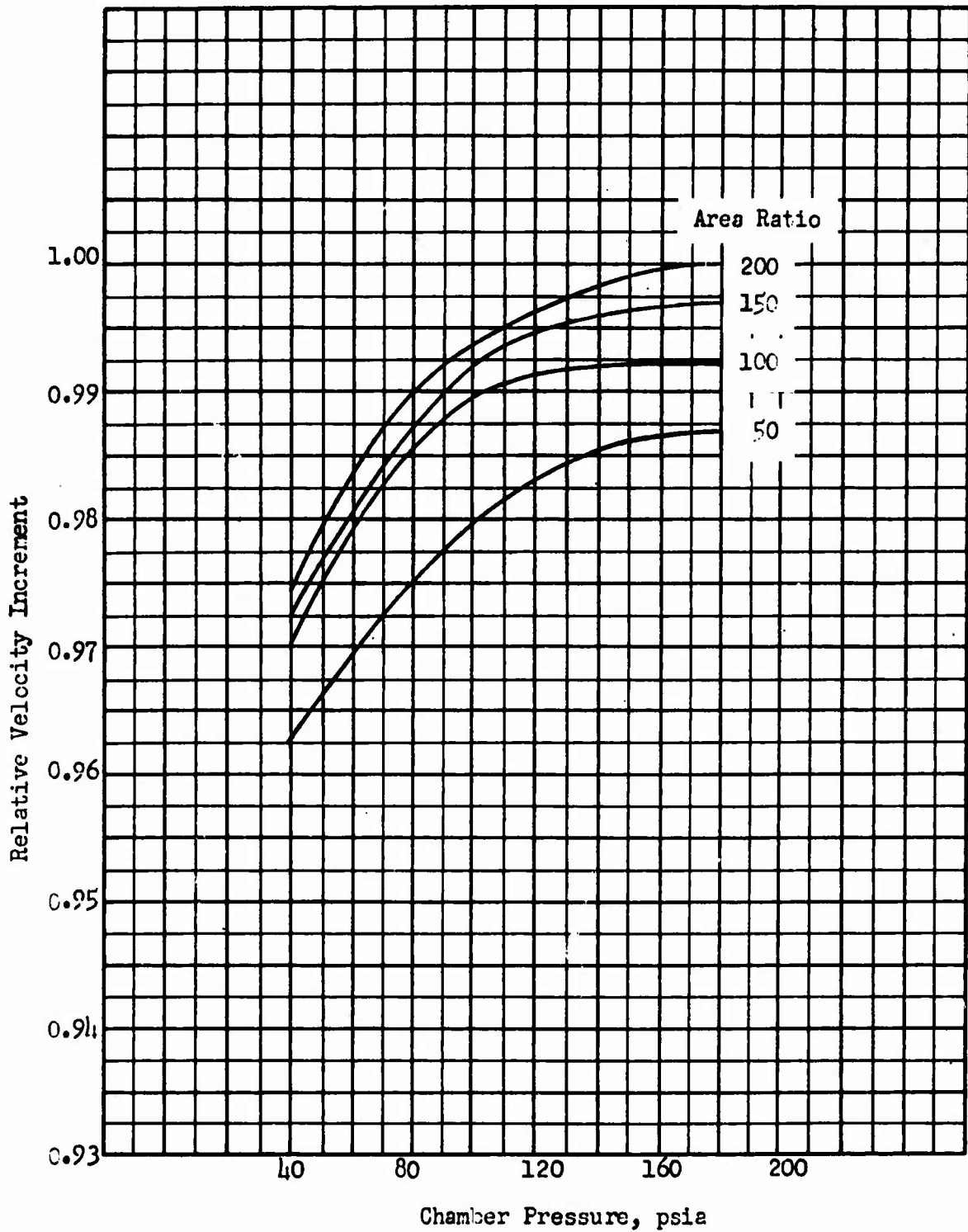


Figure 57. Chamber Pressure-Expansion Area Ratio Optimization for  $N_2O_4/N_2H_4$  - UDMH (50-50) 5,370-Pound Thrust Bell Engine. Throttled 6:1

**CONFIDENTIAL**

# CONFIDENTIAL

- (C) Over the range of parameters investigated, the optimization results indicated that maximum system performance is attained with a full-thrust design chamber pressure of approximately 1000 psia and a nozzle area ratio of 200.
- (4) (U) Operating Parameter Selection. Selection of operating and design parameters for each engine was based upon results of the optimization analysis combined with physical limitations imposed by envelope restrictions and engine grouping. A maximum propulsion system diameter of 10 feet was assumed throughout this study based upon the diameter of the Titan launch vehicle. To provide clearance for stage structure and engine gimbaling, the sum of the individual diameters of the three engines was limited to 9.0 feet. Lines of constant engine exit diameter are indicated on the optimization curves of Fig. 50 through 57 to aid in selecting the maximum performance design parameters within the diameter limitation.
- (U) The relative length of the primary and secondary engine is an additional consideration that will influence selection of design parameters. It is important that exits of each engine be in the same plane to avoid impingement of the exhaust gases on the adjacent engine. If the primary and secondary engine are of greatly different lengths, a very long and heavy thrust structure must be designed to mount the secondary engine to the stage structure. Since these engines must be gimballed, the design of the thrust structure becomes increasingly more complex. This is a difficult factor to include in a parametric optimization analysis because detailed design studies are required to determine the thrust structure weight involved. However, results of the present optimization analysis provide a means of selecting design parameters that result in near-equal primary and secondary engine lengths with a minimum loss in overall mission performance.
- (U) If the engines are maintained nearly equal in length, the thrust structure and gimbaling system design is greatly simplified. Engine length is approximately inversely proportional to the square root of chamber pressure and directly proportional to the square root of expansion area ratio. Therefore, by selecting high chamber pressures and low expansion area ratios for the primary engines and the reverse for the secondary engines, the respective engine lengths can be adjusted to be nearly equal. An area ratio of 200 was considered to be a maximum from design considerations.
- (U) With these physical limitations, the results of the optimization analysis were reviewed and the engine design parameters were selected for each system. A summary of the selected parameters is presented in Table XXVI along with the percentage of  $\Delta V$  that could be obtained with the optimum design parameters. The maximum loss resulting from the physical limitations is seen to be 2.4 percent. These losses would be reduced and perhaps even negated by the inclusion of thrust structure weight variations with engine length difference.

## 5. PROPULSION SYSTEM COMPARISON

- (U) In this analysis, the results of the launch vehicle payload capability analysis and the engine configuration selection and optimization analysis is

CONFIDENTIAL

TABLE XXVI

$N_2O_4/N_2H_4$ -UDMH (50-50) ENGINE PARAMETER SELECTION\*

System Maximum Thrust, pounds	Primary Engine			Secondary Engine				
	Thrust, pounds	Chamber Pressure, psia	€	Percent Maximum $\Delta V$ Full Thrust/Throttled	Thrust, pounds	Chamber Pressure, psia	€	Percent Maximum $\Delta V$ Full Thrust/Throttled
30,000	25,700	1000	50	97.7/99.0	2,150	500	200	99.6/99.0
50,000	42,800	1000	50	97.6/98.9	3,600	500	200	99.6/99.0
75,000	64,300	1000	50	97.8/98.9	5,350	800	200	100/99.8

\*Based Upon System  $\Delta V$ , Engine Envelope, and Thrust Structure Requirements

CONFIDENTIAL

## CONFIDENTIAL

are combined. The purpose is to provide a comparison of the stage configuration, engine performance, and mission performance capabilities of the MSPS using the three propellant combinations considered in this study ( $\text{LF}_2/\text{LH}_2$ ,  $\text{LO}_2/\text{LH}_2$ , and  $\text{N}_2\text{O}_4/\text{N}_2\text{H}_4$ -UDMH (50-50)).

- (C) Previous system comparison studies presented in Ref. 3 were for a 20,000-pound gross weight MSPS. Based upon the results of the launch vehicle studies presented in Section III of this report, a gross weight of 36,000 pounds was selected for this comparison. This is not to be considered a recommended MSPS gross weight but merely a typical increased gross weight version. A gross weight of 36,000 pounds was shown to provide near-maximum mission performance for the 2000-pound payload  $\text{LF}_2/\text{LH}_2$  MSPS used in conjunction with any of the candidate launch vehicles.
- (C) A maximum thrust level of 50,000 pounds was also selected for this gross weight. For most launch vehicle applications, suborbital firing of the MSPS is required for a 36,000-pound gross weight. This results in an initial thrust-to-weight ratio in orbit of approximately 1.5.
- (C) A design thrust level of 50,000 pounds was also investigated in the optimization analysis for each of the selected propulsion systems. Therefore, the results of the optimization analysis are directly applicable to this comparison to provide the maximum performance design parameters for each propulsion system.
- (U) A more complete system definition was then established for each propellant combination based upon the selected MSPS gross weight, design thrust level, propulsion system configuration, and operating parameters. A detailed engine system balance was conducted for each engine to define the specific impulse over the throttling range and other system operating characteristics. Stage inert weight and engine weight calculations were made based upon parametric data generated for the optimization analysis. Inboard profile drawings were completed for each system to illustrate relative size and component arrangement.
- (C) System weights and engine performance were then used to determine mission performance capability of the three systems. The  $\Delta V$  capabilities were calculated for continuous operation at full thrust, at minimum thrust, and for a series of nonevasive target satellite intercept maneuvers. A computer model of the intercept maneuvers was developed and described in detail in Ref. 3. This model performs a simulated intercept mission by commanding the engine operations in the same manner as would be performed in an actual mission. The program monitors propellant expenditures during the maneuvers and records the velocity increments accumulated during each mission phase. The nonevasive intercept maneuver is typical of intercept maneuvers with a 5-degree plane change maneuver between each intercept. The  $\Delta V$  capability at full-thrust and throttled operated conditions provides the maximum and minimum system capabilities. The maximum and minimum thrust  $\Delta V$  capabilities were calculated with the two extreme variations in the accounting of the ACS propellants. In one case, the ACS propellants were subtracted from both the gross weight and the burnout

# CONFIDENTIAL

weight which corresponds to the situation where all of the ACS propellants are used prior to the propulsive maneuver. The alternate method was to include the ACS propellant weight in the burnout weight which infers that the ACS propellants are used after the main propulsion maneuvers. These two methods bracket the probable actual ACS use schedule.

## a. MSPS Description

- (1) (C) LF<sub>2</sub>/LH<sub>2</sub> Systems. The LF<sub>2</sub>/LH<sub>2</sub> MSPS consists of a concentric aerospike/bell nozzle propulsion system. The aerodynamic spike engine provides a maximum thrust of 50,000 pounds and is continuously throttleable to 5000 pounds. The bell engine which is mounted in the center of the aerodynamic spike engine provides a maximum thrust of 5000 pounds. The engines are fired sequentially and, when throttled to their lower limit, provide an overall thrust variation of 100:1. Both engines are pump fed and regeneratively cooled. The engine component design and operational features are identical with the selected LF<sub>2</sub>/LH<sub>2</sub> system described in Ref. 4. The engine operating characteristics are summarized in Table XXVII. The delivered specific impulse vs operating thrust level is shown in Fig. 58.
  
- (C) An inboard profile drawing of the 36,000-pound LF<sub>2</sub>/LH<sub>2</sub> MSPS is shown in Fig. 59. The stage design is consistent with the original 20,000-pound system. The propellant tanks are enclosed within the shell structure, constructed of corrugated aluminum sheet retained in a circular shape by aluminum frames. The LF<sub>2</sub> tank is spherical and the LH<sub>2</sub> tank has hemispherical ends with a short cylindrical section. To maintain the 10-foot stage diameter limit with the increased propellant weight, it was necessary to incorporate the cylindrical section in the LH<sub>2</sub> tank. The propellant-orientation device, consisting of a fine mesh screen, is included in each tank. Both propellant tanks are supported with tubular fiberglass heat blocks which attach to the shell structure. The pressurization system for the main propellant tanks consists of two separate systems. The prepressurization system consists of a tridyne heat source which uses a nonflammable mixture of H<sub>2</sub>, O<sub>2</sub>, and He gases from a high-pressure storage bottle. The mixture flows through a catalytic reactor which provides high-temperature gases for fluorine tank prepressurization. Prior to being used as pressurant gases, these hot gases are run through a heat exchanger to heat the helium gases used for hydrogen tank prepressurization. This helium is stored in the hydrogen tank at liquid hydrogen temperatures.
  
- (C) The main expulsion pressurization system consists of helium taken from the cryogenic storage and ducted through heat exchangers in the engine. This heated helium pressurizes the fluorine tank during the engine firing. The hydrogen tank is pressurized by bleeding warm hydrogen gas from the engine injector manifold.
  
- (U) The propellant tanks and lines are covered with an NRC-2-type superinsulation.
  
- (C) The ACS consists of 16 thrusters mounted in groups of 4 on the exterior of the vehicle shell at a station near the vehicle center of gravity. A helium pressurization bottle, isolation valve, filter, control valve, and pressure

# CONFIDENTIAL

TABLE XXVII

50,000-POUND-THRUST  $LF_2/LH_2$  MSPS ENGINE  
OPERATING CHARACTERISTICS

	Aerodynamic Spike		Bell	
	Maximum Thrust	Throttled	Maximum Thrust	Throttled
Thrust, pounds	50,000	5000	5000	500
Chamber Pressure, psia	700	70	625	62.5
Expansion Area Ratio	100	100	200	200
Nozzle, Percent Length	20	20	80	80
Engine Mixture Ratio	13	13	13	13
Thrust Chamber Mixture Ratio	14.6	13.3	15.1	13.1
Total Engine Flowrate, lb/sec	107.1	11.23	10.90	1.166
Thrust Chamber Fuel Flowrate, lb/sec	6.7	0.78	0.66	0.08
Thrust Chamber Oxidizer Flowrate, lb/sec	98.3	10.40	9.98	1.08
Turbine Weight Flowrate, percent	0.0191	0.0044	0.0243	0.0013
Throttling Ratio	10:1	10:1	10:1	10:1
Fuel Pump Discharge Pressure, psia	1880	186	1360	134
Oxidizer Pump Discharge Pressure, psia	1280	144	1265	127
Turbine Mixture Ratio	1.21	1.21	1.21	1.21
Turbine Inlet Temperature, R	1960	1960	1960	1960

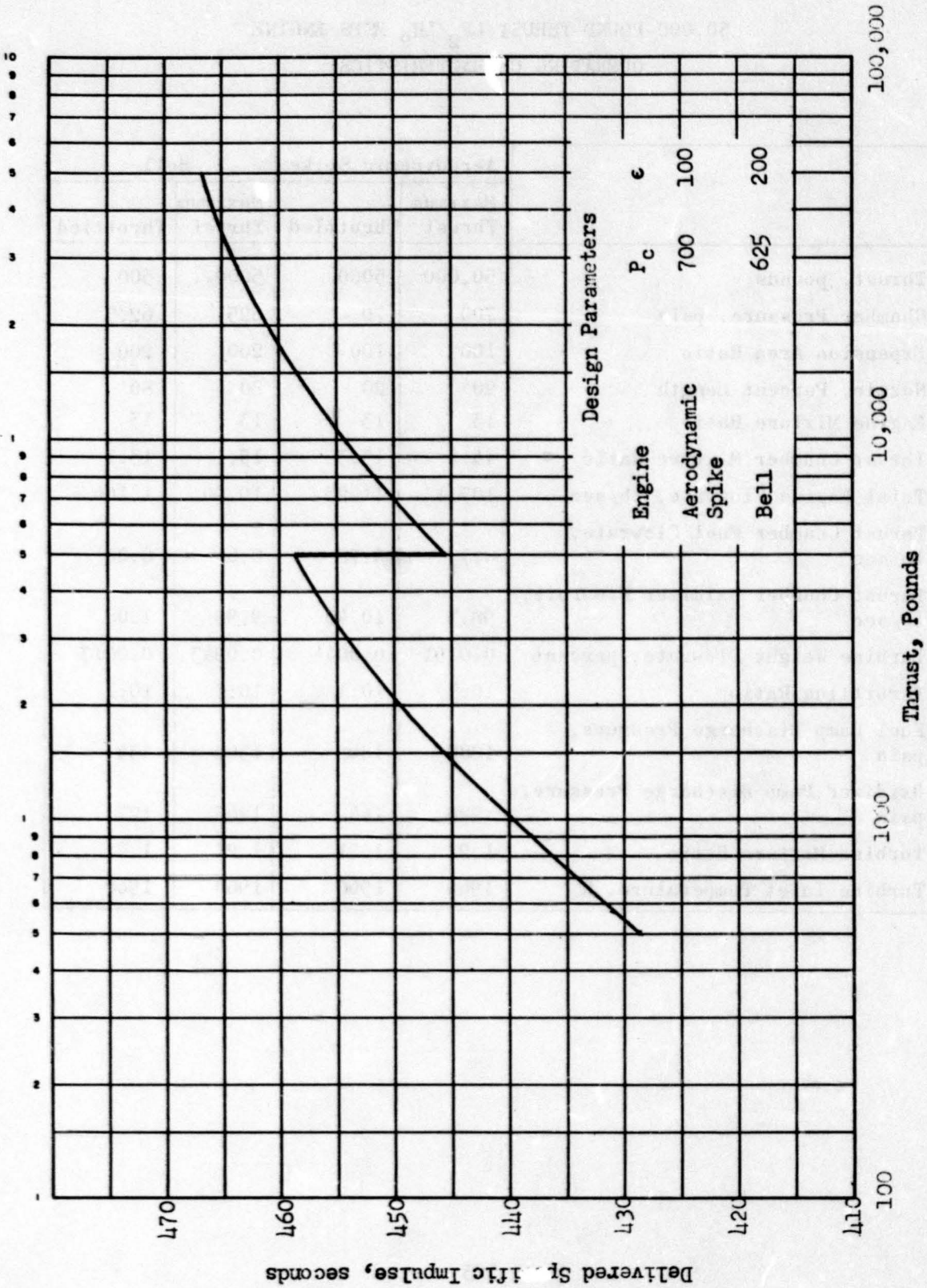
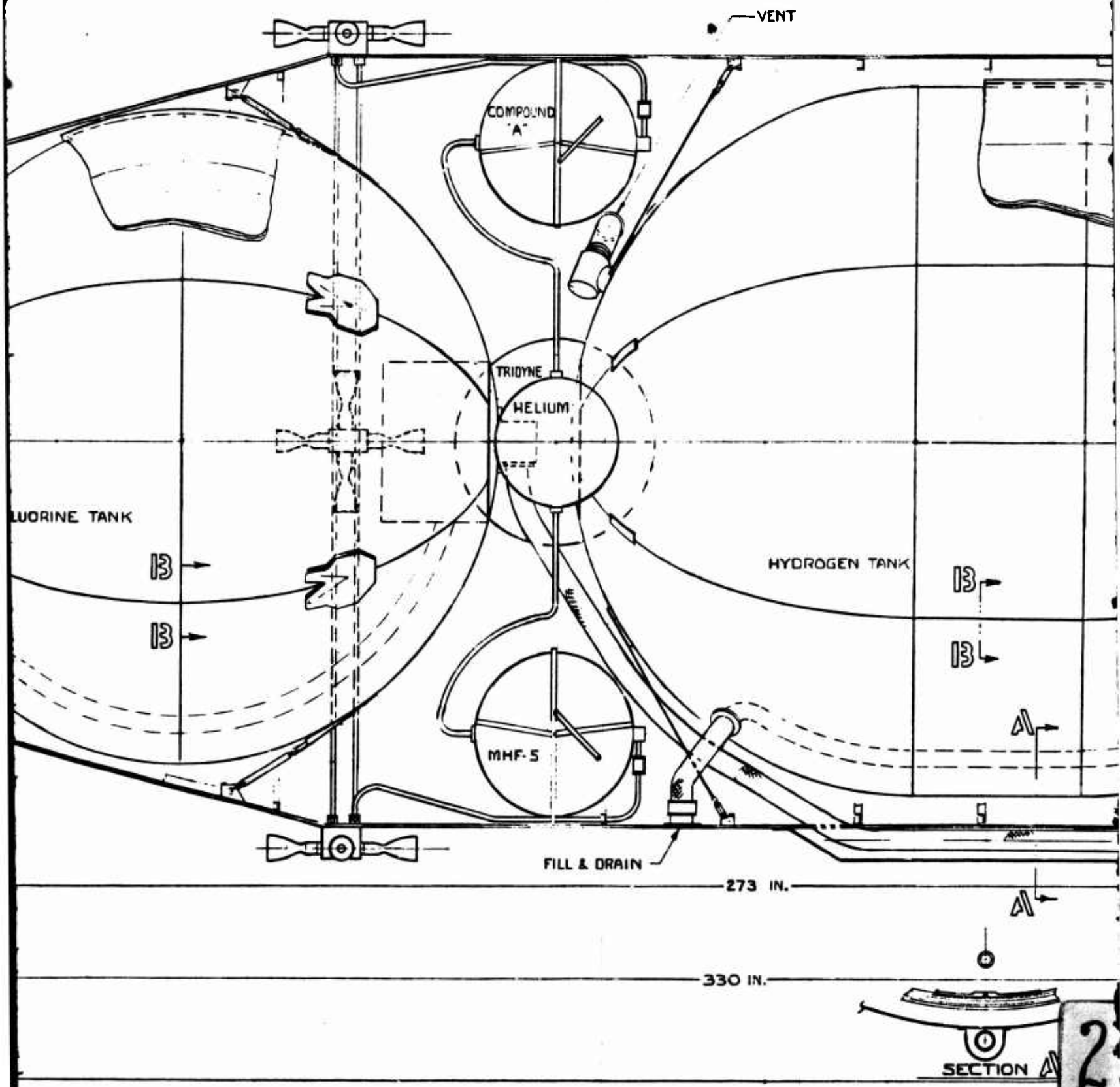


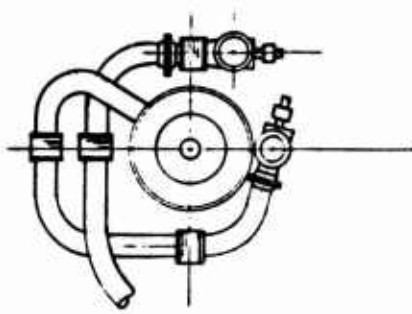
Figure 58. 50,000-Pound -Thrust  $LF_2/LH_2$  MSPS Engine Performance

Delivered Specific Impulse, seconds

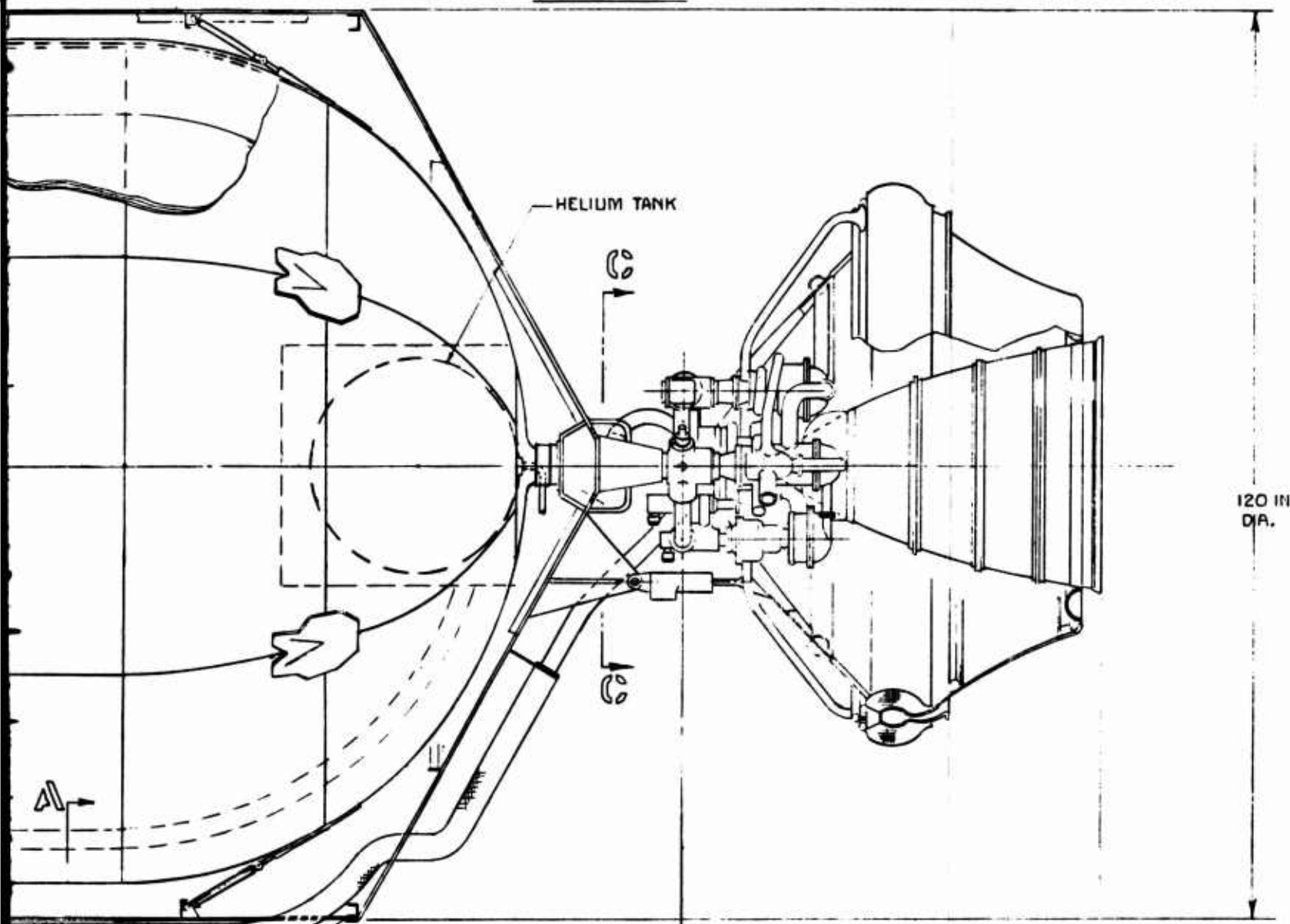




2



VIEW C-C



120 IN  
DIA.

Figure 59.  $LH_2/LH_2$   
Pound  
50,000

125/126

3

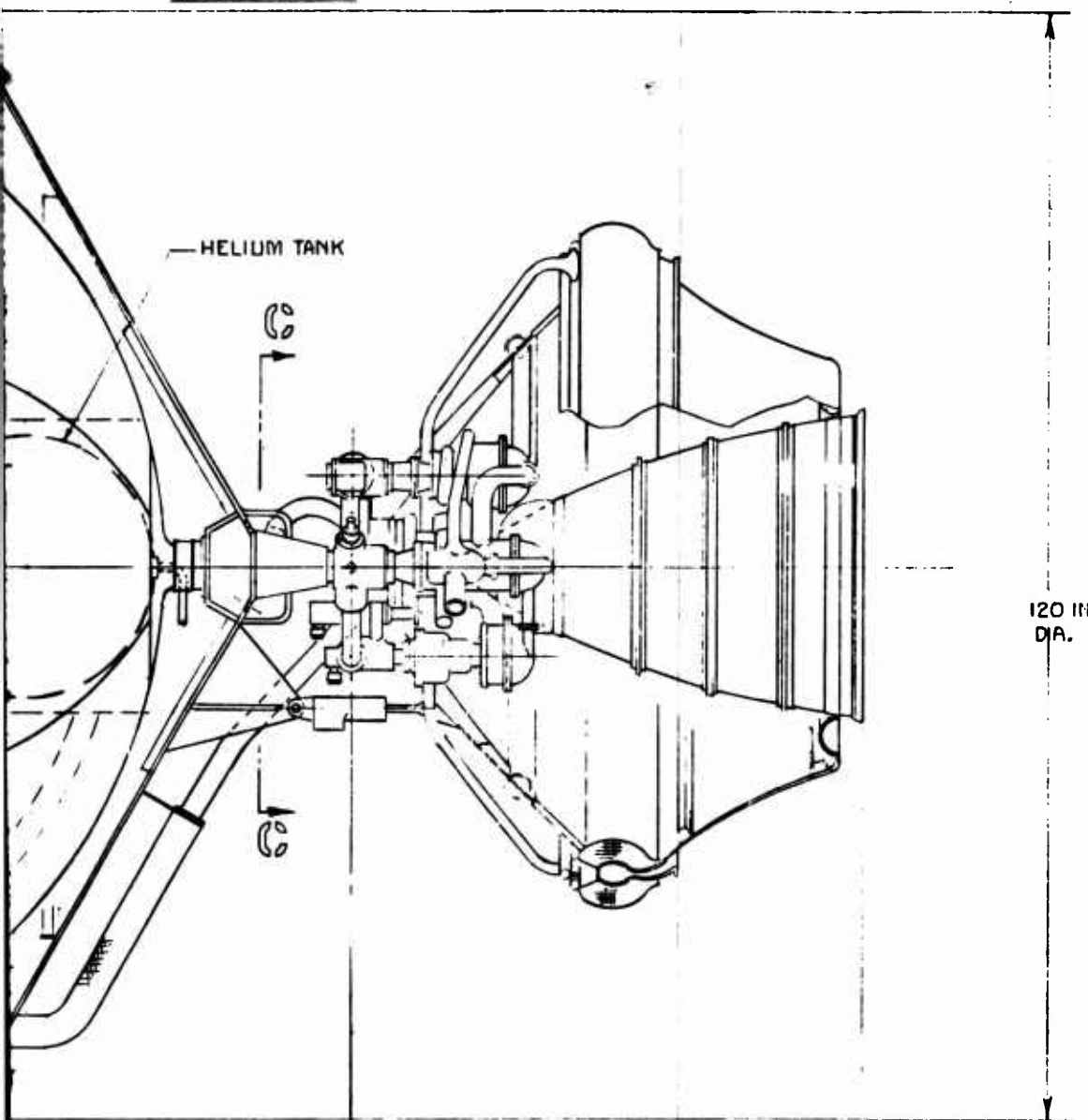
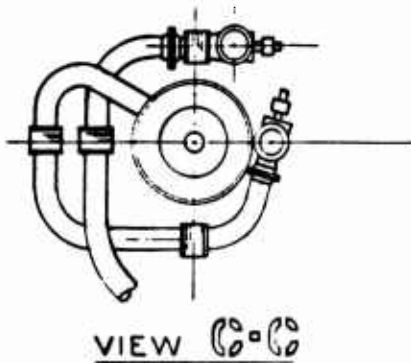


Figure 59.  $LH_2/LF_2$  MSPS, 36,000-Pound  $LH_2$  Gross Weight, 50,000-Pound Thrust

4

# CONFIDENTIAL

regulator provide pressurant flow to the propellant tanks. These tanks contain the Compound A oxidizer and the MHF-5 fuel. Each tank has a screen tension propellant-orientation device.

- (U) A summary weight breakdown of the 36,000-pound-thrust  $LF_2/LH_2$  MSPS is presented in Table XXVIII. The ACS propellant weights were calculated on the basis of detailed studies presented in Ref. 4. The ACS is identical with that described in Ref. 4. The ACS propellant weight requirements were calculated to account for the increase in stage weight and size and also the increased  $\Delta V$  capability of the system.

TABLE XXVIII

$LF_2/LH_2$  MSPS VEHICLE WEIGHT SUMMARY\*

Gross Weight	36,000
Payload Weight	2,000
ACS Propellant Weight	740
Usable Propellant Weight	30,300
Step Burnout Weight	3,700
Propellant Fraction	0.89

\*Weights are in pounds

- (C) The mission velocity capabilities for the 36,000-pound-thrust  $LF_2/LH_2$  MSPS are summarized in Table XXIX for each candidate launch vehicle and for MSPS payloads of 2000 and 5000 pounds. The difference in MSPS  $\Delta V$  capabilities for the various launch vehicle occurs because of the sub-orbital firing  $\Delta V$  requirements; only the in orbit  $\Delta V$  capabilities are shown. The  $\Delta V$  capabilities are shown for continuous operation at full and minimum thrust. The effect of the use of the ACS propellants is also shown. The nonevasive rendezvous maneuver capabilities are also shown.
- (2) (C)  $LO_2/LH_2$  System. As a result of the engine configuration section and optimization study, the concentric aerodynamic spike-bell nozzle engine system was also selected for this propellant combination. However, slightly different engine design parameters were recommended. The engine design philosophy and operational procedure are identical with the  $LF_2/LH_2$  system. The 50,000-pound-thrust  $LO_2/LH_2$  MSPS engine design and operating characteristics obtained from the optimization analysis are presented in Table XXX. The delivered engine specific is shown in Fig. 60 for the selected system. The performance shown, represents that achievable for an engine of this thrust level with relatively deep throttling capability. Change of the basic requirements such as thrust level, throttling ratio, etc. can result in an optimized configuration of greater delivered performance.

**CONFIDENTIAL**

TABLE XXIX

MISSION PERFORMANCE CAPABILITIES FOR D

	2000-Pound Payload						
	$\Delta V$ -ft/sec				Rendezvous $\Delta V$ , No Evasion	$\Delta V$	
	$F_{max}$ (1)	$F_{max}$ (2)	$F_{min}$ (1)	$F_{min}$ (2)		$F_{max}$ (1)	$F_{max}$ (2)
Nominal Titan III-C	25,600	23,910	23,515	21,960	23,640	18,480	17,500
Titan III With Seven Segments, 120-Inch Solids	28,360	26,590	26,050	24,430	26,050	21,260	20,200
Titan III With Three Segments, 156-Inch Solids	29,460	27,690	27,060	25,430	27,200	22,360	22,000
Nominal Saturn Saturn I-B	28,360	26,590	26,050	24,430	26,050	21,260	20,200
Saturn I-B With Minuteman Strap-ons	29,460	27,690	27,060	25,430	27,200	22,360	22,000

\* Gross weight = 36,000 pounds; payload = 2000 and 5000 pounds

(1) ACS propellant used before rendezvous maneuvers

(2) ACS propellant included in burnout weight

1

TABLE XXIX

PERFORMANCE CAPABILITIES FOR LF<sub>2</sub>/LH<sub>2</sub> MSPS\*

Rendezvous $\Delta V$ , ft/sec	5000-Pound Payload				
	$\Delta V$ -ft/sec				Rendezvous $\Delta V$ No Evasion
	F <sub>max</sub> (1)	F <sub>max</sub> (2)	F <sub>min</sub> (1)	F <sub>min</sub> (2)	
17,640	18,480	17,550	16,970	16,120	17,240
19,050	21,260	20,250	19,530	18,600	19,770
20,200	22,360	22,040	20,530	20,240	20,930
21,050	21,260	20,250	19,530	18,600	19,770
22,200	22,360	22,040	20,530	20,240	20,930

nds

2

# CONFIDENTIAL

TABLE XXX

50,000-POUND-THRUST  $LO_2/LH_2$  MSPS ENGINE  
OPERATING CHARACTERISTICS

	Aerodynamic Spike		Bell	
	Maximum Thrust	Throttled	Maximum Thrust	Throttled
Thrust, pounds	50,000	5000	5000	5000
Chamber Pressure, psia	800	80	625	62.5
Expansion Area Ratio	100	100	200	200
Nozzle Percent Length	20	20	80	80
Engine Mixture Ratio	6	6	6	6
Thrust Chamber Mixture Ratio	6.58	6.12	6.80	6.16
Total Engine Flowrate, lb/sec	112.6	11.67	11.43	1.10
Thrust Chamber Fuel Flowrate, lb/sec	14.4	1.63	1.40	0.153
Thrust Chamber Oxidizer Flowrate, lb/sec	94.5	9.96	9.54	0.941
Turbine Weight Flowrate, percent	0.0332	0.0071	0.0447	0.0097
Throttling Ratio	10	10	10	10
Fuel Pump Discharge Pressure, psia	1750	172	1325	131
Oxidizer Pump Discharge Pressure, psia	1450	152	1265	127
Turbine Mixture Ratio	1.12	1.12	1.12	1.12
Turbine Inlet Temperature, R	1960	1960	1960	1960

CONFIDENTIAL

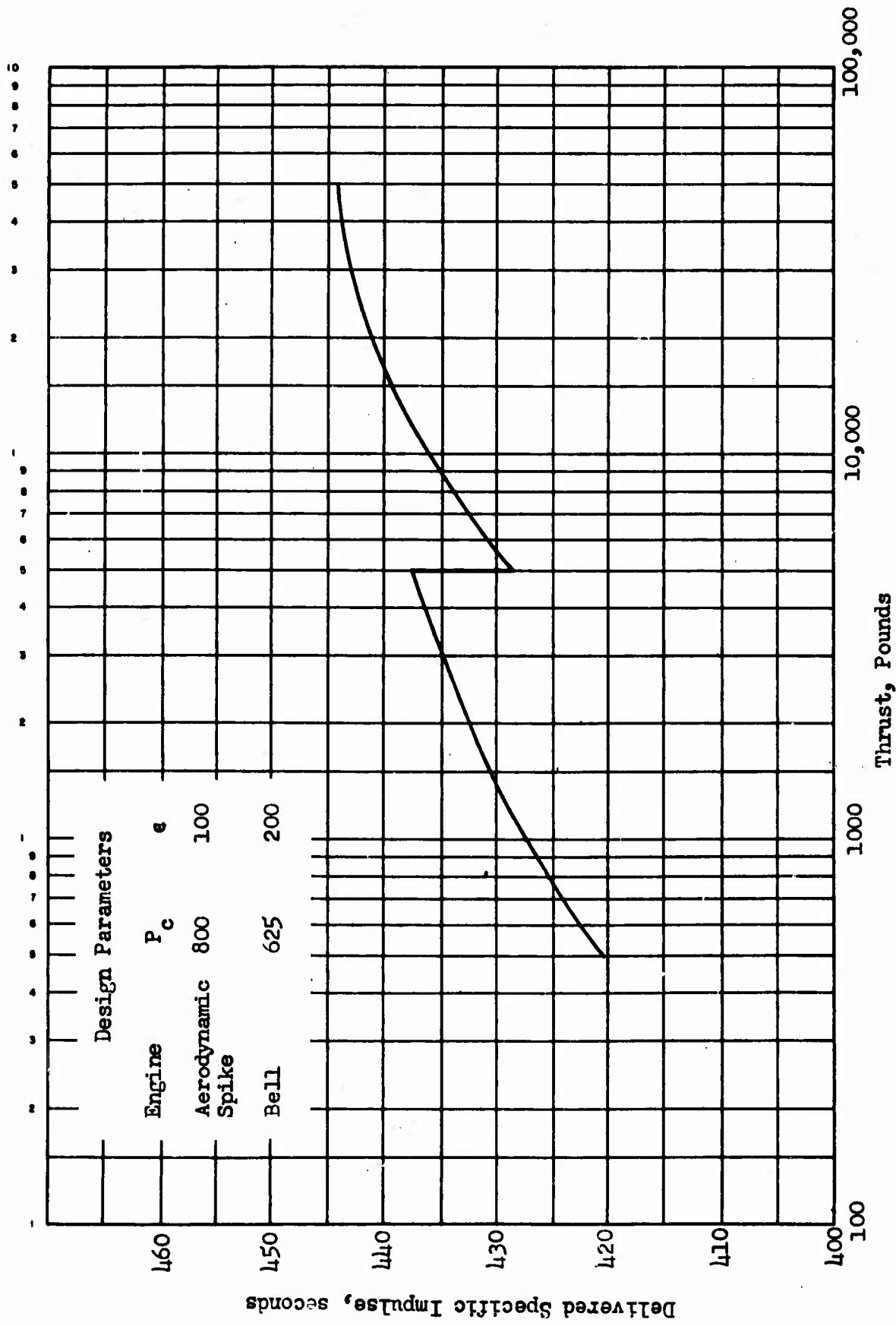


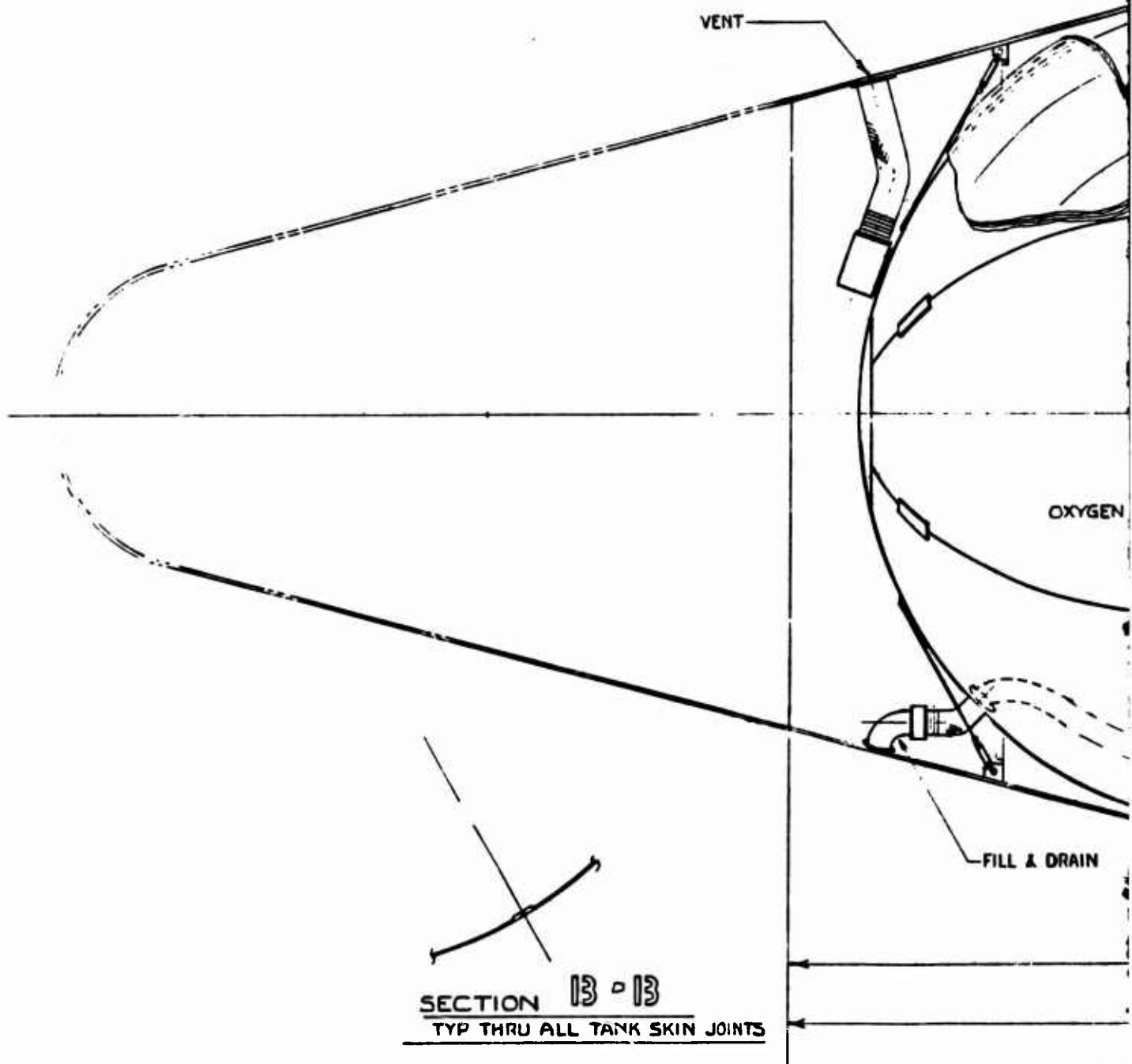
Figure 60. 50,000-Pound-Thrust  $L_0LH_2$  MSFS Performance

CONFIDENTIAL

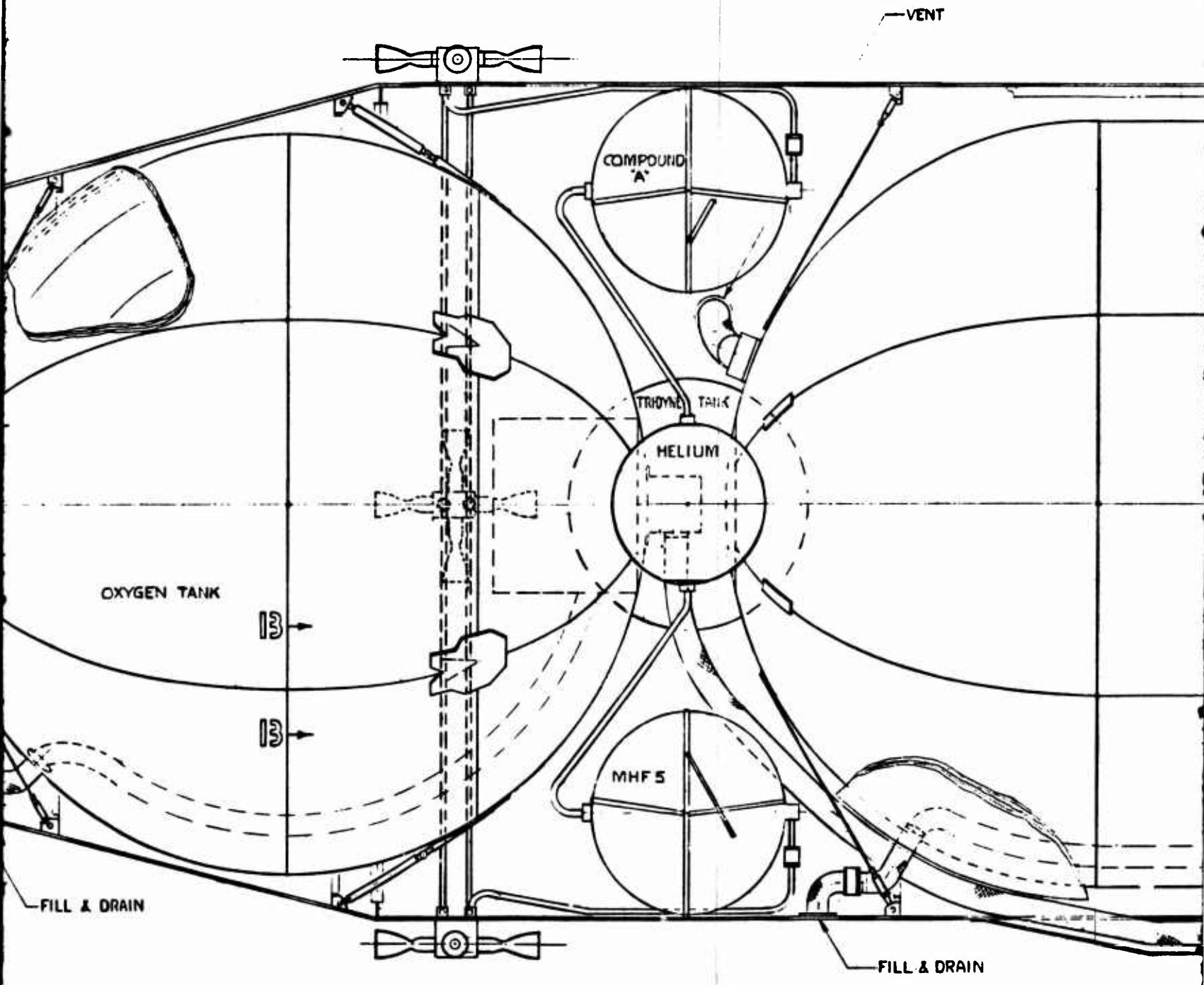
# CONFIDENTIAL

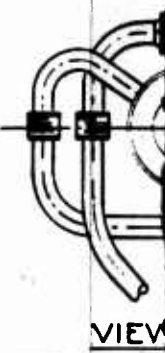
- (C) The vehicle stage design concept is identical with the  $LF_2/LH_2$  system, with the exception of the propellant tank volumes and overall stage length. An inboard profile drawing of the selected 36,000-pound-thrust  $LO_2/LH_2$  MSPS with a 2000-pound payload is shown in Fig. 61. A much longer cylindrical section was required in the  $LH_2$  tank because of the lower mixture ratio and greatly increased  $LH_2$  weight. The stage structure, materials, pressurization system, and ACS are identical with the  $LF_2/LH_2$  MSPS. The ACS propellant weights for the  $LO_2/LH_2$  system were calculated to account for the difference in stage size. A stage weight summary is presented in Table XXXI.
- (C) The mission velocity capabilities are shown in Table XXXII for the 2000- and 5000-pound-payload  $LO_2/LH_2$  MSPS used in conjunction with each candidate launch vehicles. Only the in-orbit  $\Delta V$  capabilities are shown. The  $\Delta V$  expended for suborbital firing is not included. In general, the  $LO_2/LH_2$  MSPS achieves approximately 15 to 18 percent less in-orbit  $\Delta V$  than the equivalent  $LF_2/LH_2$  MSPS.
- (3) (C)  $N_2O_4/N_2H_4$ -UDMH (50-50) Systems. The selected propulsion system for the storable MSPS consists of a 42,900-pound-thrust primary engine and two 3570-pound-thrust secondary engines. The primary engine throttles 6:1, and the two secondary engines each throttle 5.9:1. This provides an overall throttling ratio of 85:1. The primary engine is rigidly mounted. The secondary engines are canted 6 degrees to the vehicle axis and have a gimbal capability of  $\pm 6.0$  degrees for thrust vector control. The engine operating characteristics and the design parameters selected in the optimization analysis are presented in Table XXXIII for the 50,000-pound-thrust system. The estimated delivered specific impulse over the system throttling range is shown in Fig. 62. These performance predictions include combustion efficiency, nozzle divergence and drag losses, chemical kinetic reaction losses, and turbine power requirements. A cant angle correction is also included for the secondary engines. At the full-thrust or 50,000-pound-thrust level, all engines are firing. Overall system throttling is then accomplished by throttling the primary engine to its minimum thrust level. Further throttling is achieved by throttling the two secondary engines to their minimum thrust level. At this point, the primary engine is shut down and the two secondary engines are brought up to full thrust. Further throttling is obtained by throttling the two secondary engines to the point where their total thrust is equal to the design thrust of a single secondary engine. At this point, one of the secondary engines is shut down and the remaining throttling is accomplished by the last secondary engine. When only one secondary engine is firing, the vehicle assumes a canted attitude with its thrust vector through the center of gravity, and the cant angle correction to the thrust and specific impulse does not apply.
- (C) An inboard profile drawing of the  $N_2O_4/N_2H_4$ -UDMH (50-50) MSPS is shown in Fig. 63 for a gross weight of 36,000 pounds and a payload weight of 2000 pounds. The vehicle design concept is consistent with the storable

**CONFIDENTIAL**

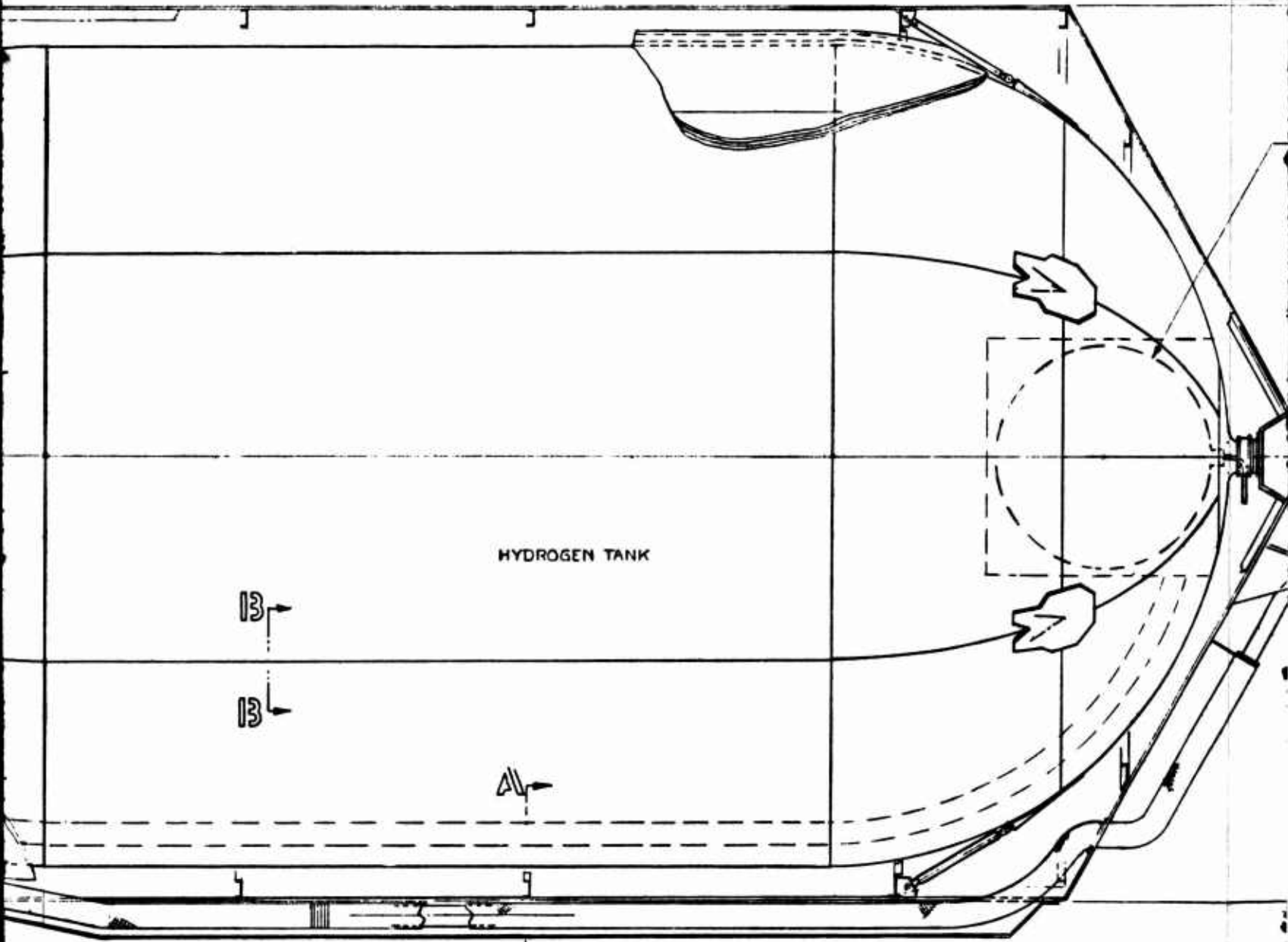


13





VIEW



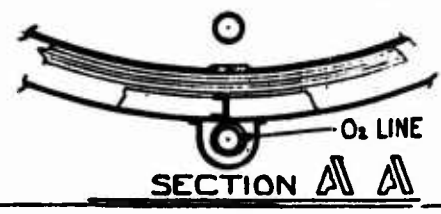
HYDROGEN TANK

B-B  
B-B

A-A  
A-A

367 IN.

424 IN



O<sub>2</sub> LINE  
SECTION A-A

3

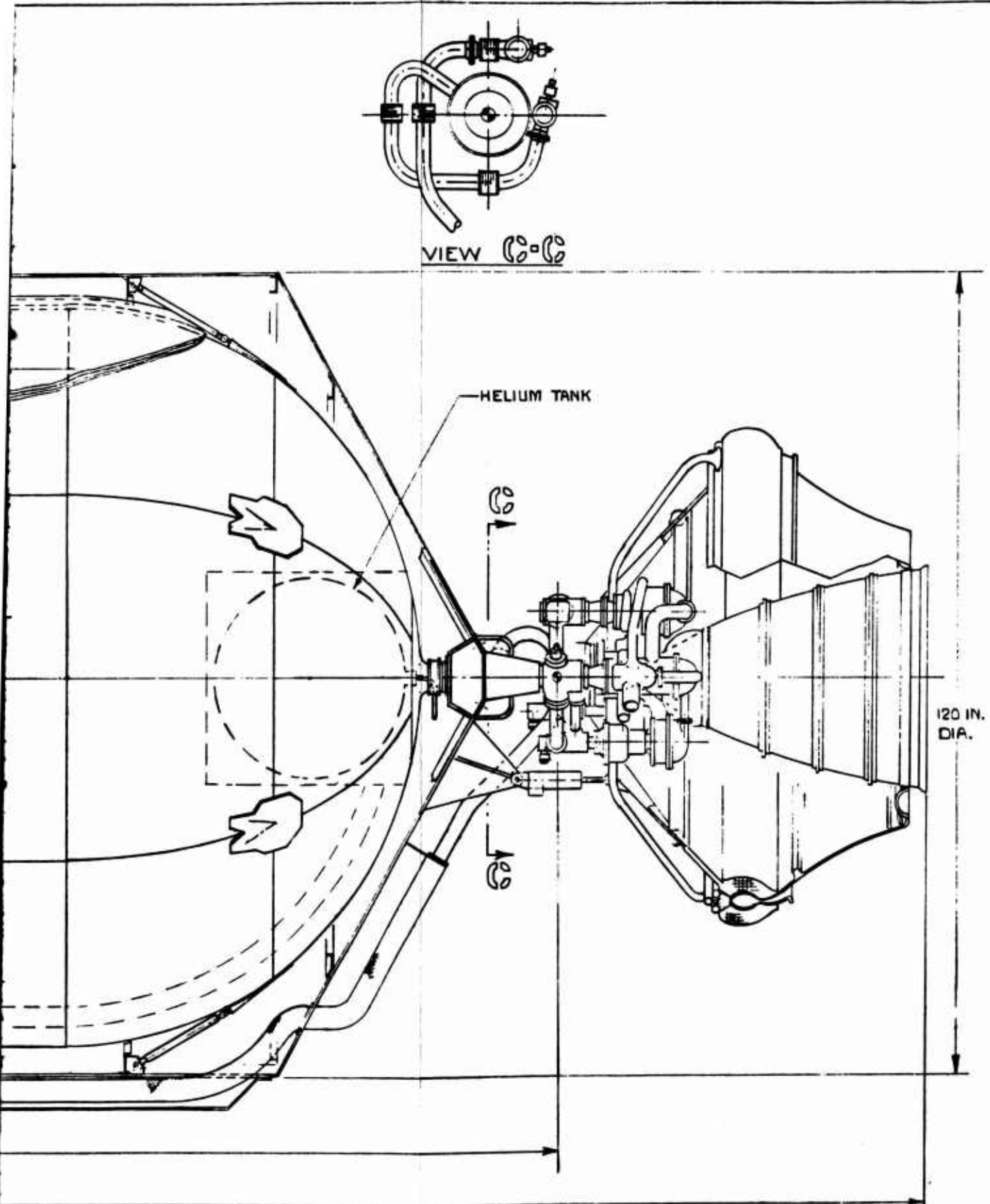


Figure 61.  $LO_2/LH_2$  MSPS 36,000-Pound Gross Weight, 50,000-Pound-Thrust

135/136

**CONFIDENTIAL**

O<sub>2</sub> LINE



4

# CONFIDENTIAL

TABLE XXXI

## LO<sub>2</sub>/LH<sub>2</sub> MSPS WEIGHT SUMMARY\*

Gross Weight	36,000
Payload Weight	2,000
ACS Propellant Weight	1,135
Usable Propellant Weight	28,834
Step Burnout Weight	5,166
Propellant Fraction	0.85

\*Weights are in pounds

**CONFIDENTIAL**

**TABLE XXXII**

**MISSION PERFORMANCE CAPABILITIES FOR LO<sub>2</sub>**

	2000-Pound Payload					Rendezvous $\Delta V$ , No Evasion	$F_{max}$ (1)
	$F_{max}$ (1)	$F_{max}$ (2)	$F_{min}$ (1)	$F_{min}$ (2)			
Nominal Titan III-C	20,760	18,920	19,660	17,910	19,160	14,990	
Titan III With Seven Segments, 120-Inch Solids	24,020	22,050	22,750	20,880	22,040	18,250	
Titan III With Three Segments, 156-Inch Solids	25,080	23,080	23,750	21,850	23,130	18,250	
Nominal Saturn I-B	24,240	22,260	22,950	21,080	22,040	18,450	
Saturn I-B With Minuteman Strap-ons	25,080	23,080	23,750	21,850	23,130	18,250	

\*Gross weight = 36,000 pounds; payload = 2000 and 5000 pounds

- (1) ACS Propellant Used Before Rendezvous Maneuvers
- (2) ACS Propellant Included in Burnout Weight

1

TABLE XXXII

PERFORMANCE CAPABILITIES FOR LO<sub>2</sub>/LH<sub>2</sub> MSFS\*

Payload	5000-Pound Payload				Rendezvous Δ V, No Evasion
	F <sub>max</sub> (1)	F <sub>max</sub> (2)	F <sub>min</sub> (1)	F <sub>min</sub> (2)	
19,160	14,990	13,910	14,190	13,170	14,360
22,040	18,250	17,050	17,280	16,140	17,070
23,130	18,250	18,080	18,290	17,120	18,100
22,040	18,450	17,260	17,470	16,340	17,280
23,130	18,250	18,080	18,290	17,120	18,100

2

# CONFIDENTIAL

TABLE XXXIII

50,000-POUND-THRUST  $N_2O_4/N_2H_4$ -UDMH (50-50) MSPS  
ENGINE OPERATING CHARACTERISTICS

	Primary Engine		Secondary Engine	
	Maximum Thrust	Throttled	Maximum Thrust	Throttled
Thrust, pounds	42,900	6890	3570	590
Chamber Pressure, psia	1000	167	500	85
Expansion Area Ratio	50	50	200	200
Nozzle Percent Length	80	80	80	80
Engine Mixture Ratio	1.6	1.6	1.6	1.6
Thrust Chamber Mixture Ratio	1.71	1.63	1.65	1.61
Total Engine Flowrate, lb/sec	134.1	22.15	11.11	1.89
Thrust Chamber Fuel Flowrate, lb/sec	48.15	8.34	4.13	0.72
Thrust Chamber Oxidizer Flowrate, lb/sec	82.18	13.6	6.82	1.16
Turbine Weight Flow, percent	0.0289	0.0098	0.0142	0.0026
Throttling Ratio	6	6	5.9	5.9
Fuel Pump Discharge Pressure, psia	2230	233	1140	113
Oxidizer Pump Discharge Pressure, psia	1640	216	843	105
Turbine Mixture Ratio	0.1	0.1	0.1	0.1
Turbine Inlet Temperature, R	2060	2060	2060	2060

CONFIDENTIAL

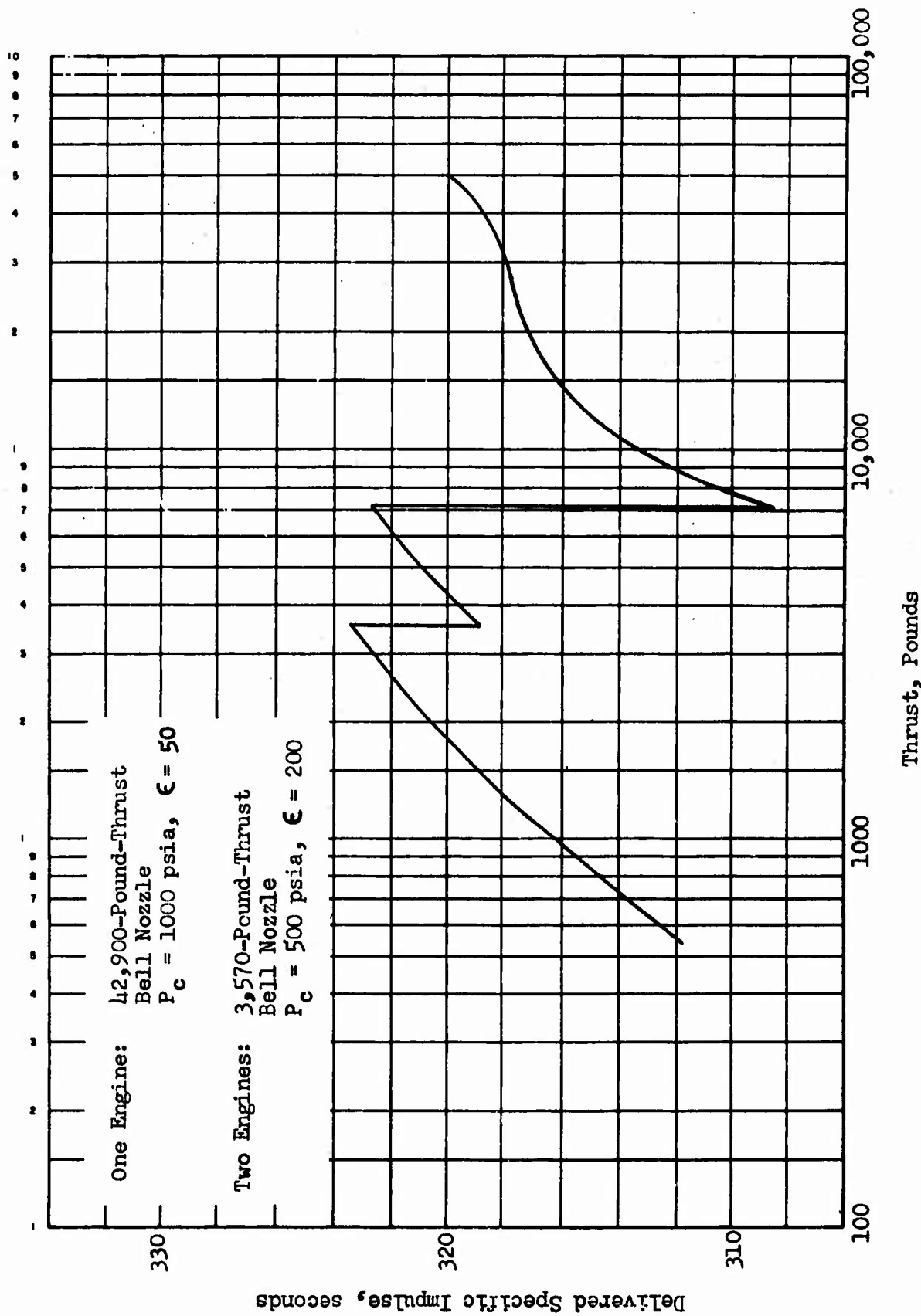
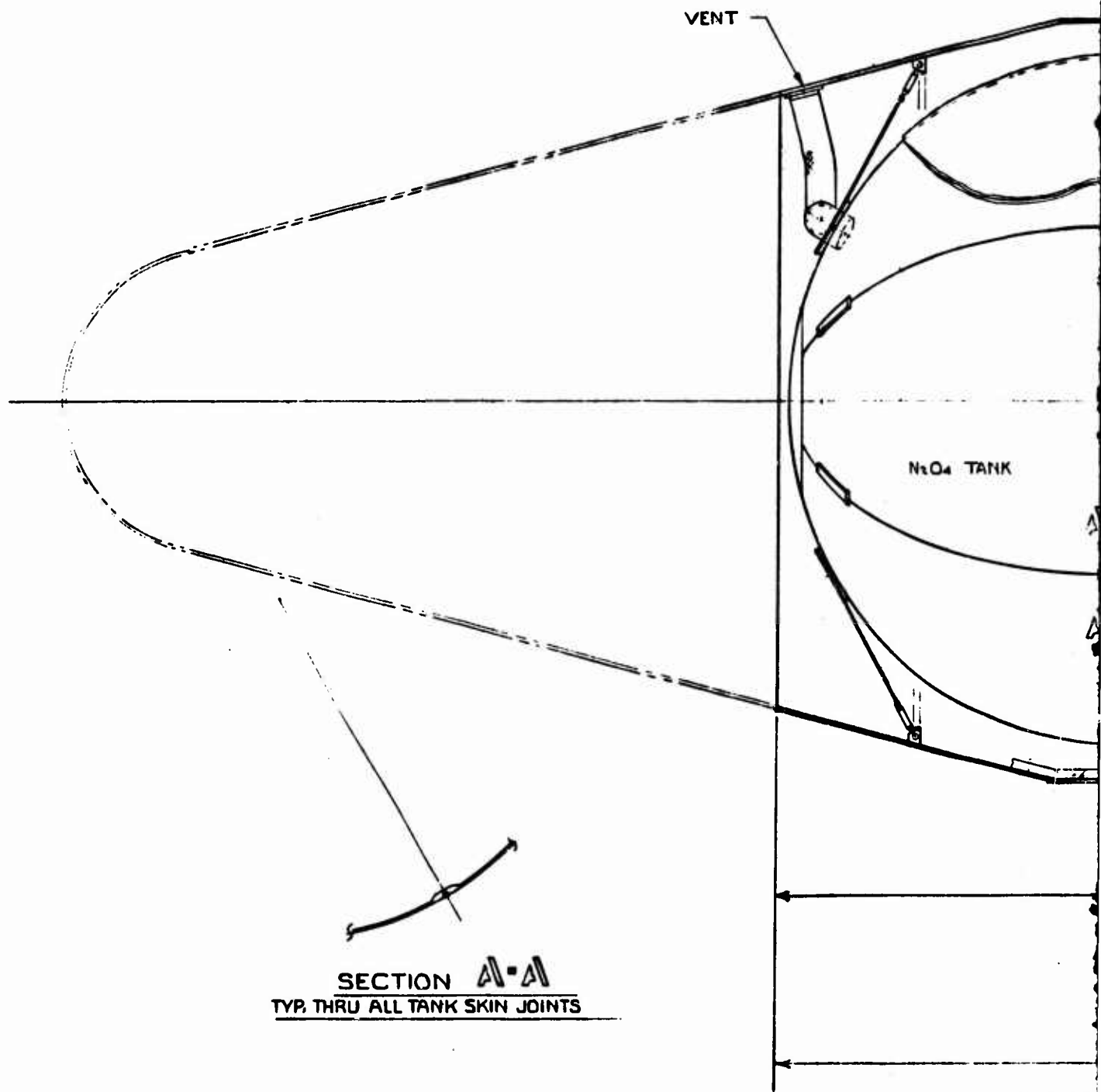


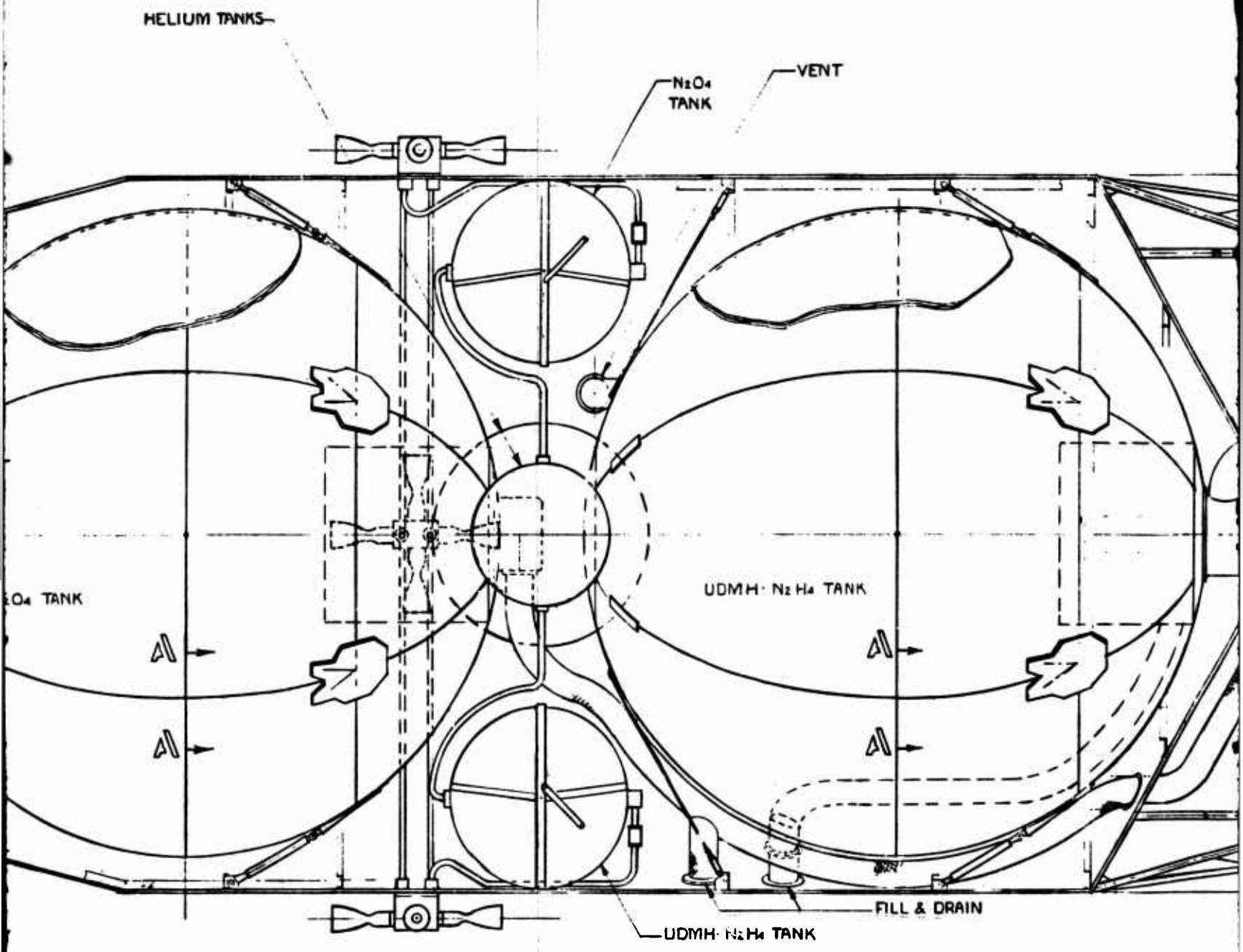
Figure 62. 50,000-Pound-Thrust  $N_2O_4/N_2H_4$  - UDMH (50-50) MSPS Performance

CONFIDENTIAL

**CONFIDENTIAL**



1



211 IN.

268 IN.

2

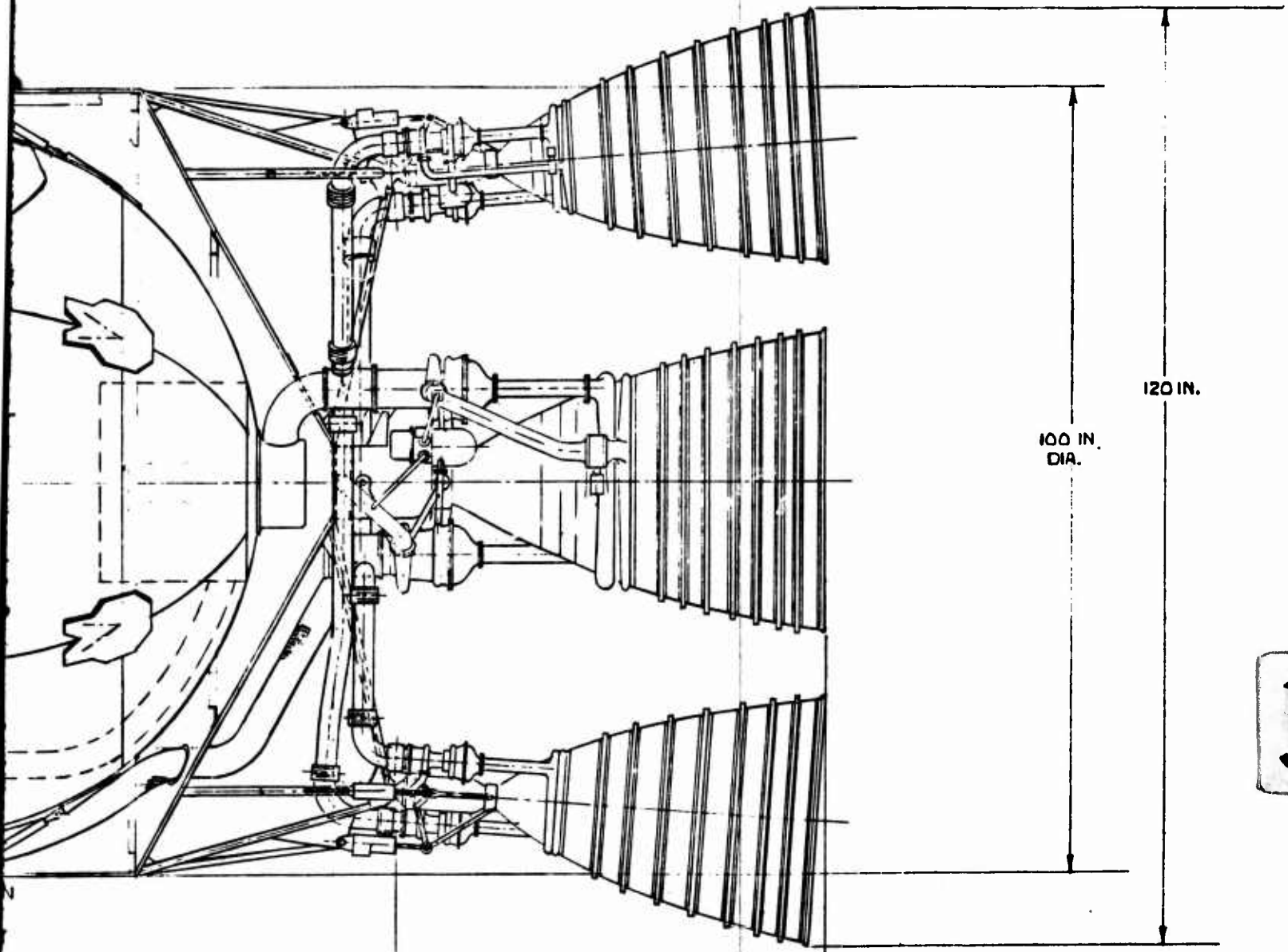


Figure 63.  $N_2O_4/N_2H_4$ -UDMH  
(50-50) Engine  
MSPS, 36,000-Pound  
Gross Weight,  
50,000-Pound-Thrust

143/144

**CONFIDENTIAL**

3.

# CONFIDENTIAL

alternate mission vehicle configuration. Basically, the concept consists of spherical aluminum tanks mounted within the vehicle structure, constructed of corrugated aluminum with stiffening rings. The tank supports and lines are designed for maximum thermal isolation of the propellant tanks to permit long-term propellant storage while subject to a wide range of thermal environments. The ACS system consists of 16 thrusters arranged in a manner similar to the  $\text{LO}_2/\text{LH}_2$  and  $\text{LF}_2/\text{LH}_2$  systems which are in groups of four on the periphery of the vehicle at a station approximating the center of gravity. The major difference is that  $\text{N}_2\text{O}_4/\text{N}_2\text{H}_4$ -UDMH (50-50) is also used for the ACS propellants on the storable propulsion system. This provides thermal compatibility, high performance, and redundancy or high reliability in that propellants can be transferred between the main tanks and the ACS tanks. A positive-expulsion device is used in the ACS tanks. Ambient helium is used for main tank expulsion. The high density of the storable propellants resulted in nearly equal-volume spherical tanks that could be contained within a 100-inch-diameter stage. The overall diameter of the engine system was allowed to extend to the maximum stage diameter of 120 inches. A weight summary of the 36,000-pound-thrust  $\text{N}_2\text{O}_4/\text{N}_2\text{H}_4$ -UDMH (50-50) MSPS is presented in Table XXXIV for the 2000-pound-payload system.

- (C) The mission performance capabilities of the 36,000-pound-thrust  $\text{N}_2\text{O}_4/\text{N}_2\text{H}_4$ -UDMH (50-50) MSPS are summarized in Table XXXV. The  $\Delta V$  capabilities are shown for those extreme cases where maximum and minimum thrust are required for one continuous firing. The effect of the ACS propellant use schedule is indicated by the two extreme situations. In one case, the ACS propellants are used prior to the propulsive maneuver and results are also shown where the entire ACS propellant load is carried through the propulsive maneuver. The  $\Delta V$  capabilities are also shown for a series of rendezvous maneuvers. These results are presented for 2000- and 5000-pound-thrust payload systems used in conjunction with each of the candidate launch vehicles. A general comparison indicates that the storable MSPS provides approximately 30 to 33 percent less in-orbit  $\Delta V$  capability than the equivalent  $\text{LF}_2/\text{LH}_2$  MSPS.

# CONFIDENTIAL

TABLE XXXIV

$N_2O_4/N_2H_4$ -UDMH (50-50) MSPS  
VEHICLE WEIGHT SUMMARY\*

Gross Weight	36,000
Payload Weight	2,000
ACS Propellant	706
Usable Propellant	30,337
Step Burnout Weight	3,663
Propellant Fraction	0.89

---

\*Weights are in pounds

**CONFIDENTIAL**

TABLE XXXV

MISSION PERFORMANCE CAPABILITIES FOR  $N_2O_4/N_2H_4$

	2000-Pound Payload				Rendezvous $\Delta V$ , No Evasion	$F_{max}$ (1)
	$F_{max}$ (1)	$F_{max}$ (2)	$F_{min}$ (1)	$F_{min}$ (2)		
Nominal Titan III-C	17,180	16,090	16,750	15,680	16,150	12,310
Titan III With Seven Segments, 120-Inch Solids	19,180	18,020	18,690	17,570	18,030	14,300
Titan III With Three Segments, 156-Inch Solids	20,220	19,040	19,710	18,560	19,060	15,340
Nominal Saturn I-B	19,180	18,020	18,690	17,570	18,030	14,300
Saturn I-B With Minuteman Strap-ons	20,220	19,040	19,710	18,560	19,060	15,340

\*Gross weight = 36,000 pounds; payload = 2000 and 5000 pounds

(1) ACS Propellant Used Before Rendezvous Maneuvers

(2) ACS Propellant Included in Burnout Weight

14

TABLE XXXV

PERFORMANCES FOR  $N_2O_4/N_2H_4$ -UDMH (50-50) MSPS\*

Payload	5000-Pound Payload				Rendezvous $\Delta V$ , No Evasion
	$F_{max}$ (1)	$F_{max}$ (2)	$F_{min}$ (1)	$F_{min}$ (2)	
16,150	12,310	11,710	12,000	11,420	11,740
18,030	14,300	13,650	13,940	13,300	13,660
19,060	15,340	14,670	14,950	14,300	14,680
18,030	14,300	13,650	13,940	13,300	13,660
19,060	15,340	14,670	14,950	14,300	14,680

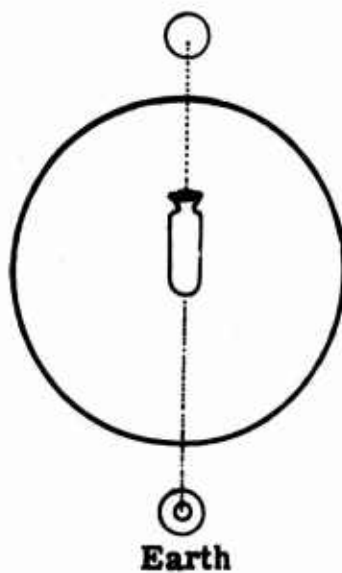
2

# CONFIDENTIAL

## SECTION V

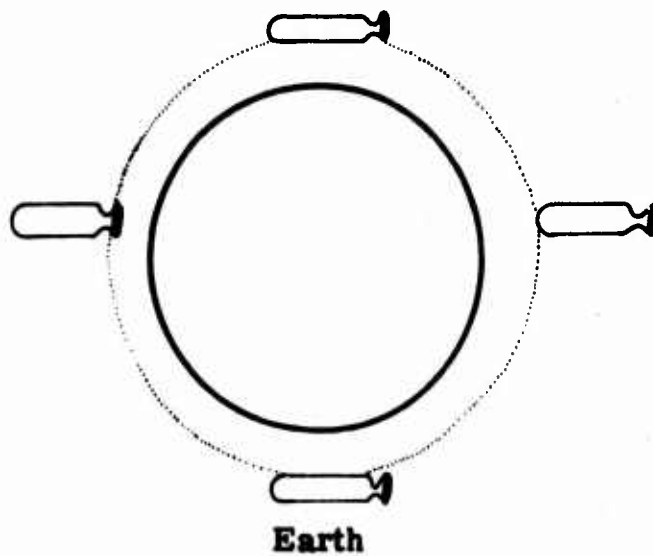
### MANEUVERING SPACE PROPULSION SYSTEM ORBITAL LIFE INVESTIGATION

- (U) The effect of the Maneuvering Space Propulsion System (MSPS) mission environment on the propellant storage capabilities of the  $\text{LF}_2/\text{LH}_2$ ,  $\text{LO}_2/\text{LH}_2$ , and  $\text{N}_2\text{O}_4/\text{N}_2\text{H}_4$ -UDMH (50-50) systems was investigated to determine the relative mission performance capabilities of these systems for extended earth orbit periods. To evaluate the ease with which a propellant combination could be stored, models of each spacecraft stage based upon realistic design assumptions were formulated. Then, with the definition of the thermal environment and the pertinent characteristics of the propellants, a thermal analysis was performed to determine the storage system requirements in terms of insulation thickness, vehicle characteristics, tank ullage volumes, tank pressure and propellant losses. This approach permitted investigation of the various design parameters most influential to the storage capabilities. The results of these parametric analyses provide a means of selecting the most efficient storage system designs for each propellant combination. These system requirements were then converted into stage inert weight penalties and usable propellant losses and the system velocity capability determined as a function of storage time.
- (U) The analytical methods and system characteristics required in the evaluation of the cryogenic systems are greatly different from those of the earth-storable propellant combinations. Therefore, the thermal analyses of the  $\text{LO}_2/\text{LH}_2$  and  $\text{LF}_2/\text{LH}_2$  systems are discussed together. The thermal analysis of the  $\text{N}_2\text{O}_4/\text{N}_2\text{H}_4$ -UDMH (50-50) system is then discussed in a separate section. The results of the detailed parametric thermal analyses are then used to define the final propellant-storage system characteristics for each of the propellant combinations, and the system  $\Delta V$  capabilities are compared as a function of orbital storage time.
1. GROUND RULES
- (U) Certain ground rules were established to provide a guide for the analysis of the storage capability of the three propellant combinations. Some of these ground rules were based on the previous studies of Ref. 2, 3, and 4 and others were selected to provide a common realistic basis for the analysis.
- (C) The 20,000-pound gross weight vehicles selected for the alternate mission propulsion systems in Ref. 2 were specified as the thermal models to be used in the analysis of the respective propellant combinations. The orbital storage life of these systems was specified as the subject for comparison. The Titan III-C launch trajectory was used as the basis for the boost phase heating calculations. An orbit altitude of 100 n mi was specified and two orbital inclination angles and vehicle orientations are considered to determine the extremes in the orbital thermal environment. These two extremes, which are illustrated in Fig. 64, establish the critical conditions for the cryogenic and storable propellant systems. A



Earth

(a) polar orbit sidewall toward sun



Earth

(b) equatorial orbit nose toward sun

Figure 64. Orbital Orientations

## CONFIDENTIAL

"polar" orbit where the vehicle is continuously in "view" of the sun with the vehicle sidewall maintained constantly toward the sun, describes the severest external heating condition. Therefore, this is the critical external heating condition for the cryogenic propellants and if the storage system can be designed to provide adequate thermal protection under these conditions, it is sufficient for all orbital heating conditions.

- (U) The other extreme in the orbital thermal environment results from the "equatorial" orbit where the orbit plane contains the earth and sun and the vehicle travels into the earth's shadow for nearly one half of the orbit. A vehicle orientation where the payload is pointed toward the sun combined with this orbit inclination describes the minimum heating thermal environment. This vehicle orientation where the payload is pointed toward the sun during the entire orbit provides maximum shading to the propellant tanks and results in the minimum vehicle equilibrium temperatures. This orbital thermal environment would actually benefit the storage capabilities of the cryogenic propellants, but would also result in the eventual freezing of the earth storable propellants. In an actual military application it is uncertain if specified favorable vehicle orientations could be maintained for long periods. The cryogenic propellant storage systems are designed for the most severe or highest temperature orbital environment. The  $N_2O_4/N_2H_4$ -UDMH (50-50) storage system must be designed to provide thermal protection for both of the limiting orbital environments to prevent either over-heating or freezing of the propellants.
- (U) Two mission duty cycles were specified to be investigated in the storage analysis. These two duty cycles also offer two extremes in the propellant storage requirements. In essence the duty cycle describes the amount of propellant in the tanks for the orbital storage duration. One of the mission duty cycles that is considered is where all of the propellant is consumed in a single firing at the end of the storage period. Therefore the storage analysis is based on essentially full propellant tanks and thus the largest heat capacity for external heating. However, this duty cycle is critical in selecting the required tank ullage volume to accommodate the expansion of the propellants with a heat input.
- (U) The other propellant use schedule is specified as the 90/10 mission duty cycle. An amount of propellant is consumed as soon as the vehicle achieves orbit such that 10 percent of the propellant remains after the pressurant gas and liquid propellant come to equilibrium following this initial firing. This means that at the beginning of the orbital coast period, only 10 percent of the initial propellant load remains in the tank. Pre-orbital heating and pressurant gas heating are also included in the analysis of this duty cycle.
- (U) A set of propellant condition limits based on the system design characteristics was also established. First, the propellant temperatures were allowed to fall no lower than 5 degrees above their freezing points to ensure the absence of solid particles of propellant. Second, the pressure in the tank was not permitted to exceed the run pressure of 70 psia. Third, the system was always required to be able to supply the required NPSP (net

# CONFIDENTIAL

positive suction pressure) to the pumps. This requirement was translated into a maximum vapor pressure through inclusion of the tank run pressure and line pressure drop. For the hydrogen tanks, which are pressurized with gaseous hydrogen, the NPSP was always the limiting condition. For the propellants pressurized with helium the tank pressure on occasion was the limiting condition. A fourth limiting condition was applied to the full tank cases to account for thermal expansion of the propellants.

In addition to the ullage required for pressurization, the ullage volume of each tank was sized to allow propellant expansion.

## 2. VEHICLE DESCRIPTION

- (U) For the analysis, nominal MSPS vehicles were defined based on the alternate mission vehicles of Ref. 2. The storage evaluation was performed based on these vehicle configurations. The configurations were then perturbed and the effect on storage described.
- (C) The nominal vehicles had a gross weight of 20,000 pounds and a payload of 2000 pounds. The configurations consist of spherical propellant tanks enclosed by an outer structural shell and differ only slightly in propellant weight from the MSPS vehicles described previously. Propellant tanks are supported by low thermal conduction supports. The outer structure also supports the payload.
- (U) Vehicle characteristics are described in Table XXXVI. These characteristics are based on the designs of Ref. 2. The cryogenic systems use heated helium as the run pressurant for the oxidizer tank and heated hydrogen for the fuel tank. As recommended in Ref. 4, the temperature of the hydrogen pressurant was varied and its effect on the system was further investigated. The  $N_2O_4/N_2H_4$ -UDMH (50-50) vehicle uses a helium pressurization system for both tanks. A propellant line heat exchanger was used to provide a minimum temperature of 500 R. The required NPSP for pump operation is shown and in conjunction with the tank pressure and line pressure drop define the maximum propellant vapor pressure at which the system can operate.

## 3. THERMAL ANALYSIS

- (U) The thermal analysis of the maneuvering propulsion vehicle was performed by considering steady-state radiation, convection, and conduction. The heat transferred to the propellant tanks by each of the methods was calculated separately and the individual contributions were summed to give the total heat input rate from sources external to the propellant tanks. The analysis determining the effects of the external conditions including ground hold heating, aerodynamic heating and orbital heating is described below. The analysis concerning the effects of the heat input on the thermal condition of the propellants is then described for the vented and nonvented storage systems in Appendix III. The major portion of the analysis was based on bulk heating of the propellant. In certain specified cases temperature distribution in the tanks was considered.

TABLE XXXVI  
VEHICLE CHARACTERISTICS

Vehicle	LF <sub>2</sub> /IH <sub>2</sub>		IO <sub>2</sub> /IH <sub>2</sub>		N <sub>2</sub> O/N <sub>2</sub> H <sub>4</sub> -UDMH(50-50)	
Wall Material	Aluminum		Aluminum		Aluminum	
Tank	LF <sub>2</sub>	IH <sub>2</sub>	IO <sub>2</sub>	IH <sub>2</sub>	N <sub>2</sub> O	N <sub>2</sub> H <sub>4</sub> -UDMH(50-50)
Run Pressure, psia	70	70	70	70	70	70
Pressurant, psia	He	H <sub>2</sub>	He	H <sub>2</sub>	He	He
Pressurant Temperature, R	500	Variable	500	Variable	500	500
NPSP, psia	31.5	1.5	31.5	1.5	31.5	31.5
Tank Burst Pressure, psia	90	90	90	90	90	90
Line Pressure Drop, psi	15	10	15	10	15	15
Maximum Propellant Vapor Pressure, psi	23	58	23	58	23	23
Ullage, max., percent	2	15	3	15	2	2
Ullage, min., percent	2	5	3	5	2	2

a. Analysis of Thermal Environment

- (U) The thermal environment that the MSPS experiences in a normal mission consists of a period of prelaunch hold on the launch pad, a boost phase, and an orbital phase. Each phase can be analyzed separately and each has a different effect upon the propellant storage.
- (1) (U) Prelaunch Environment. The prelaunch environment was analyzed by assuming a vehicle outer-wall temperature and calculating the heat transferred from the wall to the tanks through all wall-to-tank connections and through the gas surrounding the tanks. This gas may be air or an inert purge gas depending upon the insulation concept and the temperature of the propellants. The heat transfer from the gas to the tank wall takes place almost entirely by conduction because the purge gas flowrate would be relatively low and the connection heat transfer is negligible. For this analysis the outer wall was assumed to be at 560 R. In these ground hold periods the propellant tanks were considered to be closed. A range of prelaunch ground hold durations were considered and the effects described. For the system comparisons, ground hold times based on current vehicle launch procedures were used.
- (2) (U) Boost Phase Environment. The boost phase heat input was found by calculating the temperature history of the vehicle outer wall and by assuming that the interior conditions are the same as those during prelaunch hold. This temperature history was based on a Titan III-C boost trajectory. Heat input was calculated based on the temperature history of three points on the vehicle (Fig. 65). The skin temperature histories at points adjacent to the tanks were used to compute heat fluxes into the respective tanks. The maximum heating curve is shown for reference only. The heat transfer was calculated by taking a series of steady-state conditions at many time increments in the boost trajectory. The steady-state heat input rate was calculated at each increment and multiplied by the increment. The sum of these incremental heat inputs over the whole boost phase was then calculated. The heat remaining in the vehicle structure after attainment of orbit was also considered.
- (3) (U) Orbit Environment. Three external sources of radiant energy control the thermal environment of an orbiting vehicle: direct solar radiation, reflected solar radiation from the earth surface (albedo), and radiation emitted by the earth. The largest of these sources is the solar radiation which, for purposes of this analysis, was assumed to be in the form of parallel rays. The planetary sources, reflected and emitted, are also controlled by the solar radiation. The radiation reflected by the planet is

aI

(a is the albedo and I is the intensity of solar radiation at the earth.) The radiation emitted by the earth can be found by assuming that the planetary surface is uniform and at a constant temperature. An energy balance between absorbed, emitted (E), and reflected radiation then gives:

$$(1 - a) I \pi R^2 = 4 \pi R^2 E$$

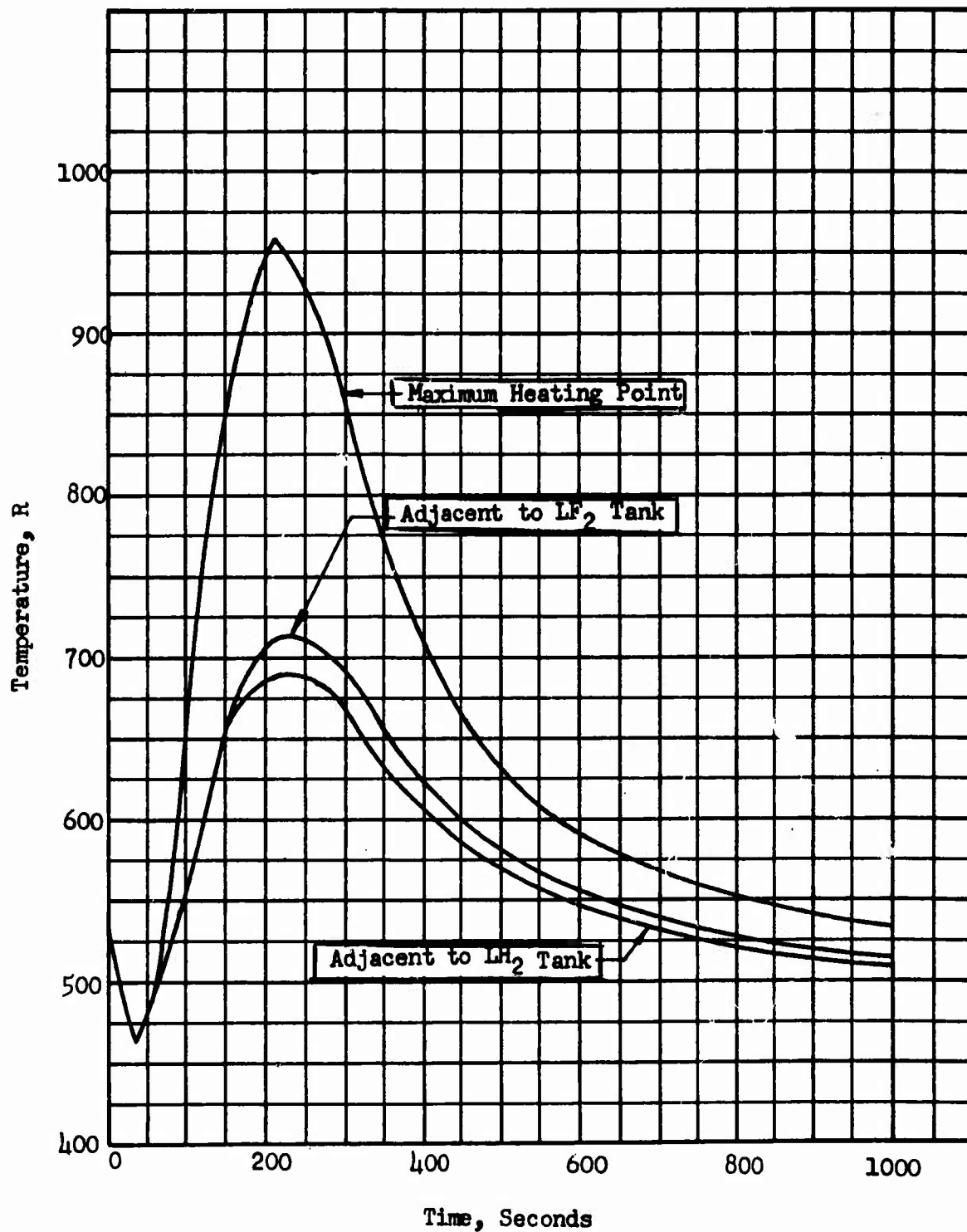


Figure 65. Temperature History During Boost Phase for Nominal Vehicle Launched by Titan III-C From WTR

# CONFIDENTIAL

and

$$E = \frac{(1 - a)}{4} I$$

- (U) Previously developed analytical techniques, incorporating radiation view factors from the earth to the orbiting vehicle, were used to determine the radiation incident on the vehicle. Assuming that, at each stage of its orbit, the vehicle was in thermal equilibrium, an energy balance between absorbed and emitted radiation was performed upon the vehicle to give an equilibrium outer wall temperature. This energy balance was based upon the exact vehicle configuration and included all radiation and conduction from the vehicle shell to the propellant tanks.
- (U) The extreme cases of orbital thermal environment were considered and are illustrated in Fig. 64. Case (a) represents the maximum heat input case and was the basis of design for the cryogenic systems. The  $N_2O_4/N_2H_4$ -UDMH (50-50) systems were analyzed both for the maximum heating case (a) and the minimum heating case (b) since propellant freezing must also be considered for these propellants.
- (4) (U) Pressurant Heat Input. During the expulsion phase all propellants are pressurized with heated pressurant, either  $GH_2$  or He. During expulsion, heat and mass exchange between the hot pressurant and the propellant results in propellant vaporization and a reduction in pressurant temperature. This is accounted for in the pressurization calculations described in Ref. 4. The vaporized propellant is considered to be unusable and is treated as residual fluid.
- (U) Following the expulsion of a portion of the propellant, the system is shut down and coasts until additional propellant is used. Upon shutdown the hot pressurant in the tank and the liquid propellant come to equilibrium resulting in additional propellant vaporization and a reduction in the useable (liquid) propellant.
- (U) These pressurant heat loads were considered only for the cryogenic propellant since the  $N_2O_4/N_2H_4$ -UDMH (50-50) pressurant is always at or near the liquid temperature because of the propellant line heat exchangers. As indicated the temperature of the hydrogen pressurant was varied and its effect on storage described.

## 4. CRYOGENIC SYSTEMS

### a. Vehicle Model

- (c) The 20,000-pound gross weight alternate mission vehicles described in Ref. 2 were specified as the basic configuration to be used in the propellant storage analysis. The vehicle design and tank configuration employed in the alternate mission vehicles are identical to the equivalent MSPS with only slight variations in the propellant weight and tank volumes. The design layout of the  $LF_2/LH_2$  alternate mission vehicle is shown in Fig. 66. The stage configuration for the  $LO_2/LH_2$  vehicle is similar

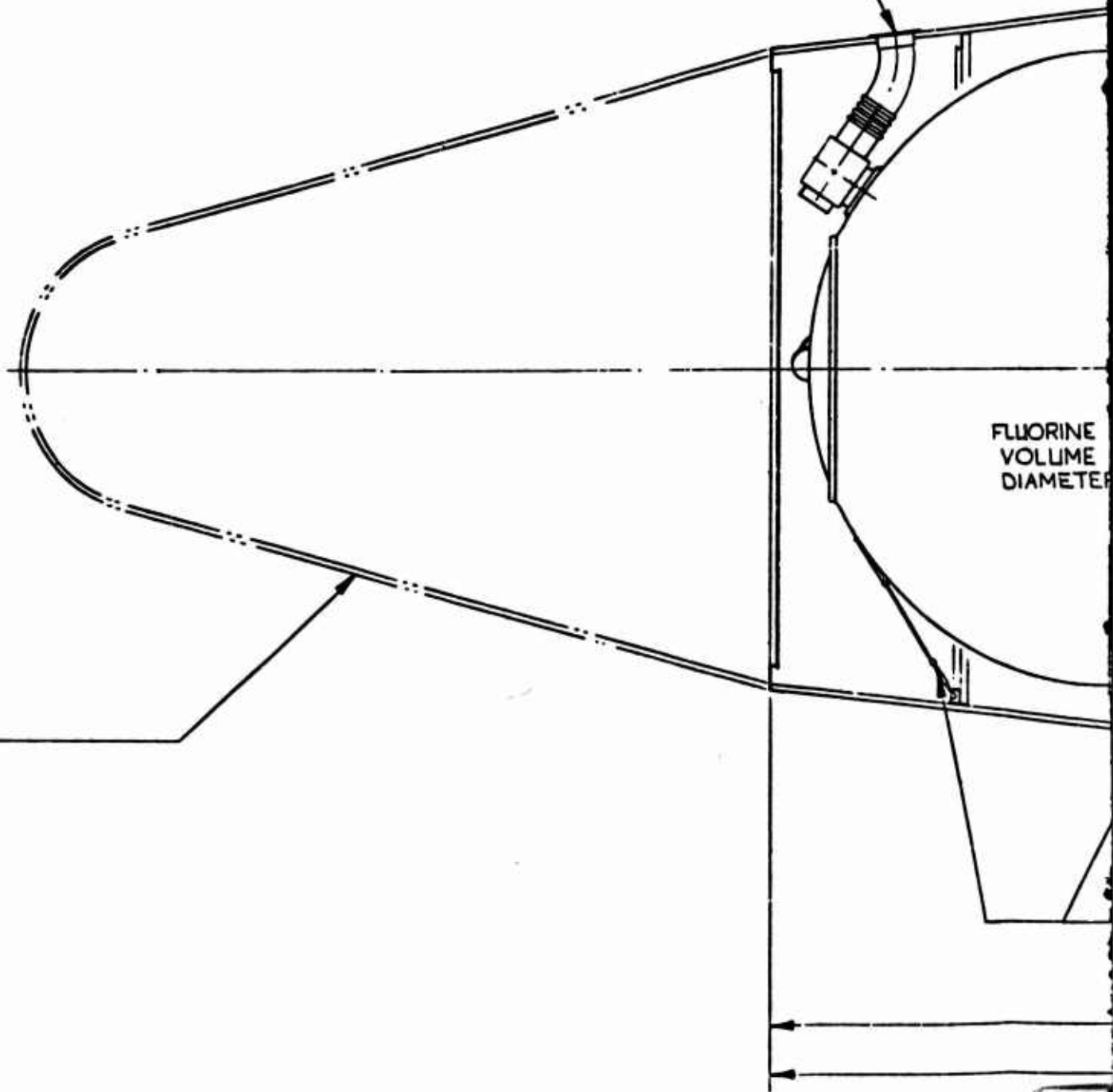
**CONFIDENTIAL**

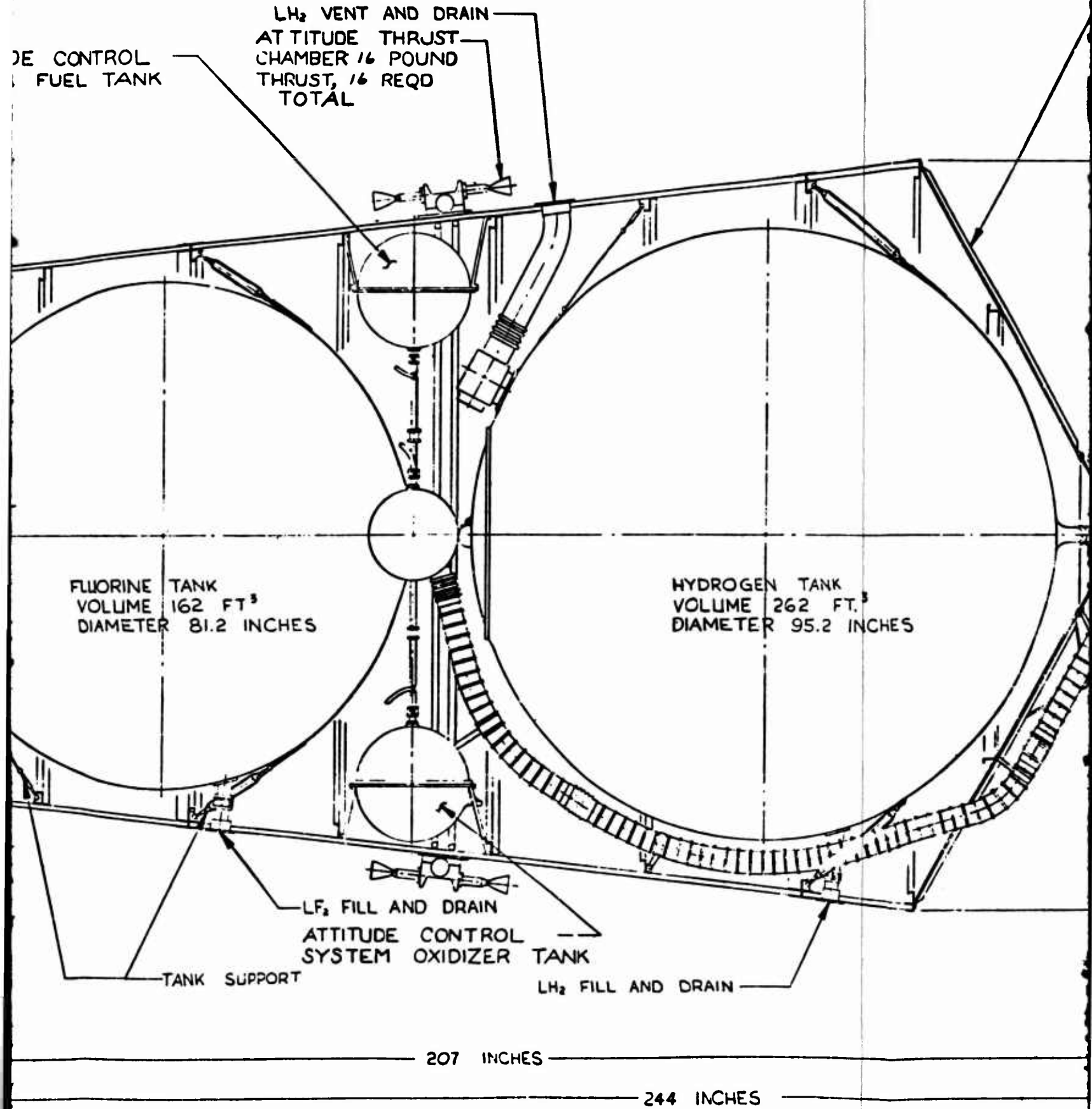
LF<sub>2</sub> VENT AND DRAIN

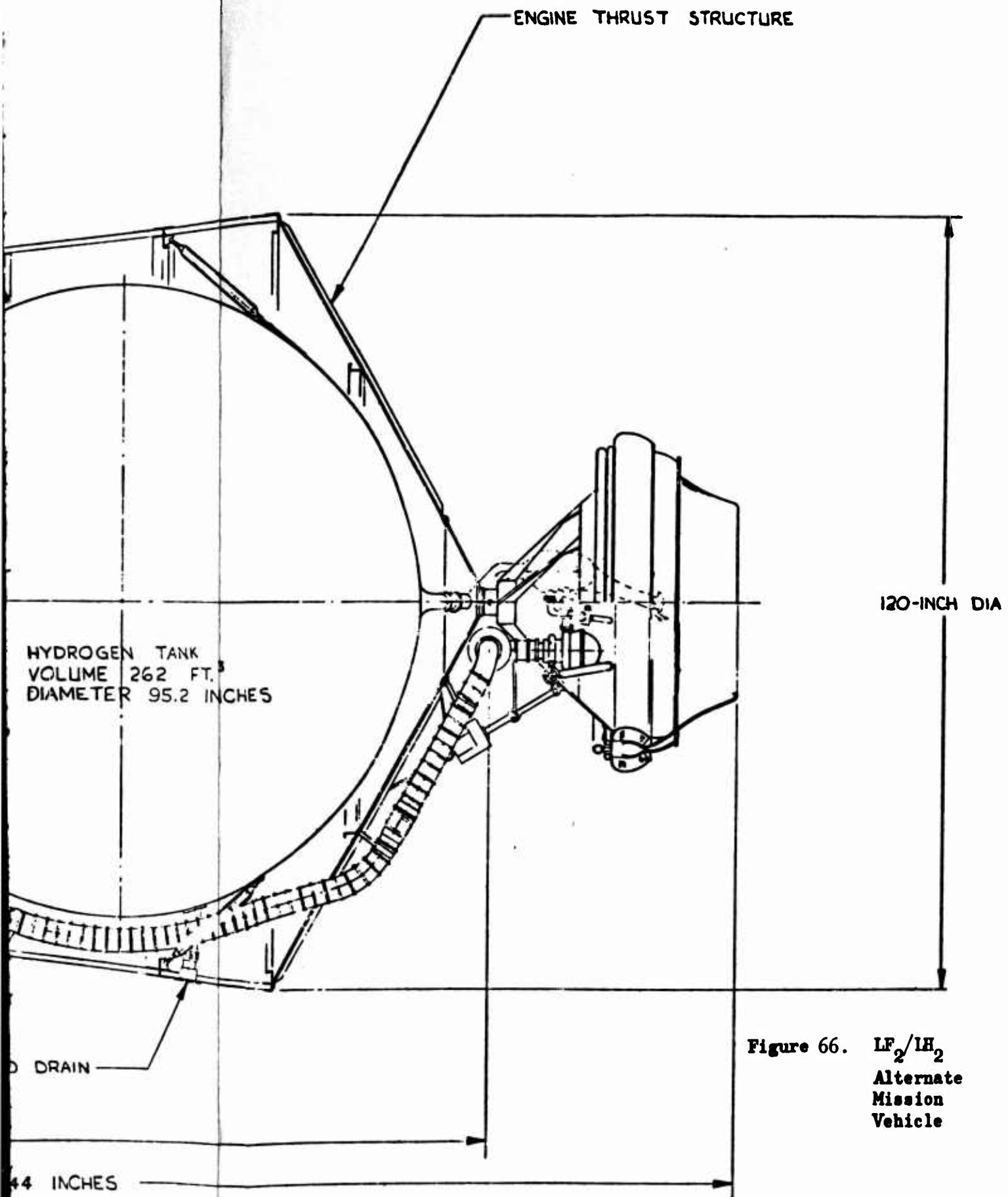
ATTITUDE CONTROL  
SYSTEM FUEL TANK

PAYLOAD

FLUORINE  
VOLUME  
DIAMETER







157/158

**CONFIDENTIAL**

3

# CONFIDENTIAL

except for the difference in tank volumes. The tanks are aluminum and are supported by hollow, fiberglass rods. The governing tank design criteria that are important to the propellant thermal analysis are presented in Table XXXVI.

- (C) The pressurization system of the nominal vehicle was chosen during the study reported in Ref. 4. The system uses tridyne ( $H_2-O_2-He$ ) for pre-pressurization of the fluorine tank and helium (heated by the reacted tridyne) to prepressurize the hydrogen tank. The nominal tank injection temperature of each is 500 R. The expulsion pressurant of the fluorine tank is helium which has been heated by an engine-mounted heat exchanger; the hydrogen tank pressurant is hot hydrogen tapped from the engine injector manifold. The helium is injected into the tank at a pressure of 70 psia and a temperature of 500 R; the hydrogen is injected at 70 psia and a range of temperatures depending upon thrust level.
- (U) The heat conduction paths from the vehicle wall to the propellant tanks are the feed, fill, and vent lines insulation attachments, and the tank supports. Many designs of these lines and supports have been described in the literature (Ref. 4). A review of several design possibilities was conducted and their effective thermal resistivity described (Appendix IV). The resistivity values ranged from 2.5 to 640 hr-R/Btu. For the nominal vehicle a value of 115 hr-R/Btu was selected and reflects a reasonable design with the fiberglass supports and heat blocks in the feed lines. The resistivity values were perturbed and the effect on the vehicle described.
- (U) A number of insulation schemes were reviewed. Based on the requirements of these cryogenic vehicles and the current level of technology, a system utilizing the superinsulations and a helium purge during ground hold (Appendix II) was selected. Laboratory testing indicates that this system has good outgassing characteristics and the helium purge prevents freezing air within the insulation.
- (U) A variety of superinsulations was considered (Appendix II). For purposes of this study, NRC-2 was chosen. The conductivity used for this insulation is  $2 \times 10^{-5}$  Btu/ft-R, (approximately 50 layers per inch) which is much higher than the conductivity of  $6 \times 10^{-6}$  Btu/ft-R used in Ref. 4 which was computed by theoretical methods. The value of  $2 \times 10^{-5}$  Btu/ft-R is more representative of the achievable, installed conductivity.

## b. Effects of Thermal Environment

- (U) The method of analysis describing the external thermal environment and the internal heating of the propellants was discussed previously. In the following discussions the results of the analysis and their effect on the selection of the propellant storage system design parameters are given. The preorbital heating rates are established and the basis for the selection of the insulation thickness, vehicle surface coatings, and heat short resistivities is presented.

- (1) (U) Prelaunch Environment. During prelaunch hold, the insulation on the maneuvering propulsion vehicle is purged with helium gas. There are two reasons for this choice of purge gas: (1) the helium outgasses from the superinsulation faster than other gases, and (2) the helium does not condense upon the tank walls. The vehicle outer wall is assumed to be frost free.
- (U) The overall heat transfer coefficients through the purge gas and tank wall to the liquids were found to be (Ref. 4) 0.282 Btu/hr-ft<sup>2</sup>-R for the LO<sub>2</sub> and LF<sub>2</sub> and 0.381 Btu/hr-ft<sup>2</sup>-R for the LH<sub>2</sub> tank. The conduction through wall-to-tank connections was also determined and makes up less than 1 percent of the input during ground hold. For hold conditions in which the wall temperature rises to 100 degrees (an extreme limit), the heat input rates for the F<sub>2</sub>/H<sub>2</sub> system are 16,500 Btu/hr for LF<sub>2</sub>, and 41,177 Btu/hr for LH<sub>2</sub>. The heat input rates for the O<sub>2</sub>/H<sub>2</sub> system are 17,800 Btu/hr for the LO<sub>2</sub> and 64,400 Btu/hr for the LH<sub>2</sub>.
- (2) (U) Boost Phase Environment. The integrated heat transfer during boost for the F<sub>2</sub>/H<sub>2</sub> system is 5240 Btu's for the LF<sub>2</sub> tank and 11,200 Btu's for the LH<sub>2</sub> tank. For the O<sub>2</sub>/H<sub>2</sub> system, the integrated heat transfer rates are 5400 Btu for the LO<sub>2</sub> tank and 17,500 Btu for the LH<sub>2</sub> tank. Nearly all the latent heat in the vehicle structure after attaining orbit will be radiated to space if the insulation outgassing is rapid and will not, therefore, impose any additional heat load upon the propellants. These values were also generated in Ref. 4.
- (U) During boost, the heat input to the tanks may not be evenly distributed throughout the tank or the ullage gas may not have time to come to equilibrium with the liquid. If all of the heat is assumed to be input to the ullage gas (the most conservative assumption), the maximum tank pressure will be exceeded in the hydrogen tank and the tank will have to vent during boost. If a fraction of the heat equal to the tank ullage surface area over the total tank surface area is assumed to be input to the ullage gas, the hydrogen vent pressure is still exceeded. These results are reasonable when compared with the flight results of the Centaur vehicle. Since the amount of ullage gas vented will be small and the tank will come to thermal equilibrium after orbit is achieved this effect can be ignored in the storage analysis. However, in the vehicle design it may be necessary to provide a vent system and a venting strut to keep the vented hydrogen away from the vehicle so that there is no possibility of fire in the vicinity of the vehicle.
- (3) (U) Orbital Environment. Based upon the two extreme orbit conditions, the possible extremes of outer wall temperature are shown in Fig. 67 as a function of wall absorptivity-to-emissivity ratio. Surface coating material limitations constrained the lowest temperature to 405 R. Heat transfer to the tanks was assumed to occur from this temperature continuously during the storage period. This temperature was assumed to be uniform over the outer wall of the vehicle.

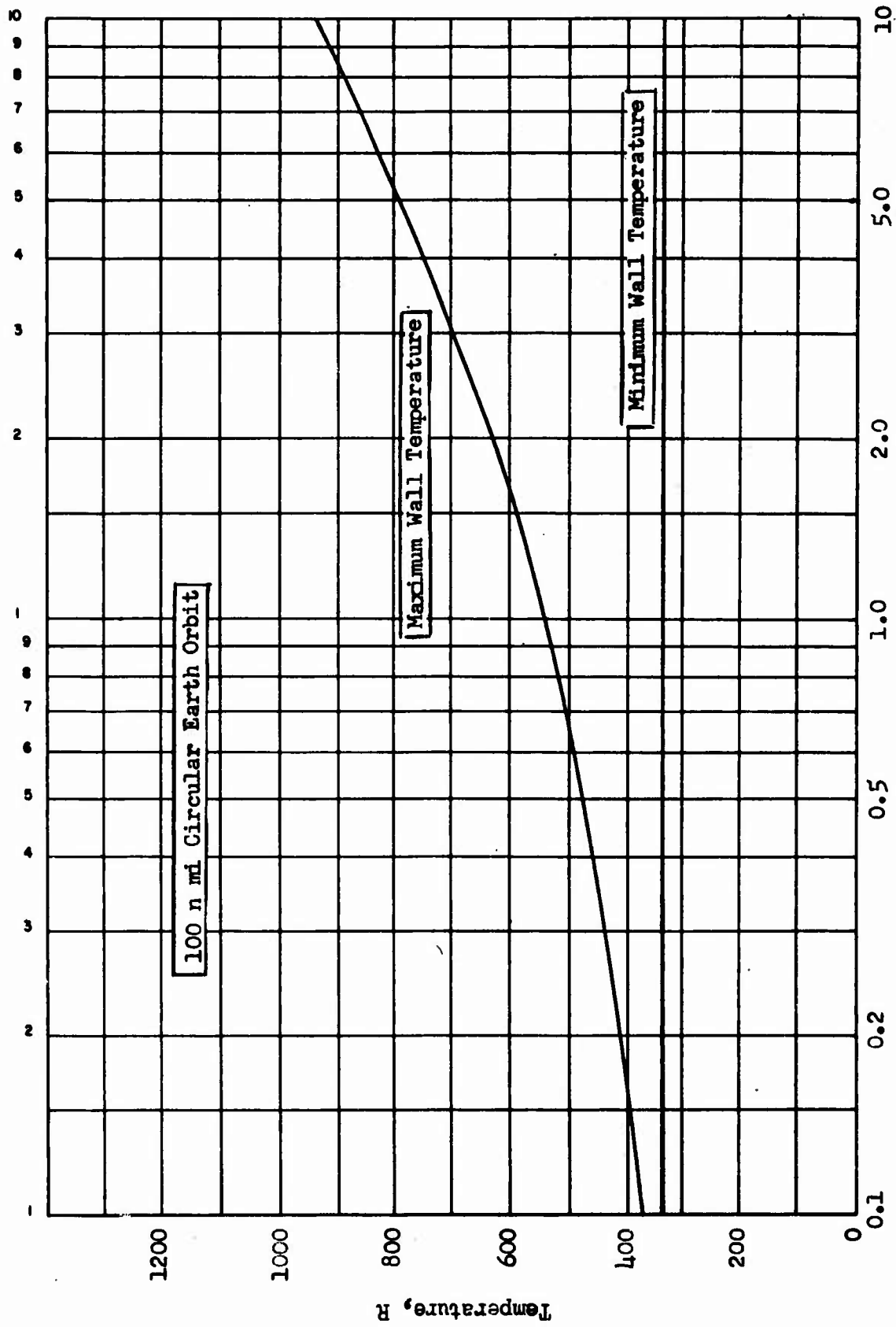


Figure 67. Ratio of Absorptivity to Emissivity,  $\alpha/\epsilon$   
 Maximum and Minimum Possible Outer Wall Temperatures for a Vehicle in any  
 100 n mi Circular Earth Orbit in the Limit of Negligible Heat Transfer to the  
 Propellants

- (U) The outer wall coating of zircon-potassium silicate was chosen to give an  $\alpha/\epsilon$  value of 0.185 with an emissivity of 0.91. This choice was made to give the lowest possible maximum wall temperature, 405 R. A review of available temperature control surface coatings is presented in Appendix V.

The ullage was sized to accommodate the expansion associated with the maximum pressure consistent with pump NPSH for full tanks. The variation of ullage requirement with allowable vapor pressure for fluorine, oxygen, and hydrogen is shown in Fig. 68.

- (U) The heat leak rate to the propellants through the superinsulation is shown as a function of thickness in Fig. 69 for the  $LF_2$  and  $LH_2$  tanks. The heating rate has been normalized to the tank volume and scales as  $V^{-1/3}$  for tanks of other sizes. Similar working curves were also generated for the  $LO_2/LH_2$  tank system. These predicted heat leak curves do not include conduction through lines and supports.

c. Parametric System Storage Analysis

- (U) A parametric investigation of the operating and design parameters of each of the storage systems was conducted for a nominal vehicle design. The effect of propellant-use schedule, ground hold times, propellant sub-cooling, variations in pressurant injection temperature and many other storage system design or operating characteristics were investigated. The final results are presented in the form of vapor pressure, total tank pressure and liquid remaining in the propellant tanks as a function of storage time. These final results are presented for the two limiting use schedules or duty cycles.

- (1) (U) Nominal Vehicle Design. A nominal vehicle model was formulated to provide the basis of the parametric system analysis. The design selections were based upon reasonable insulation and conduction path heat leaks as follows:

	<u>Hydrogen</u>	<u>Fluorine and Oxygen</u>
Insulation Thickness, inches	3	2
Conductive Thermal Resistivity (hr-R/Btu)	115	115

The nominal design point orbital heating rates for the  $LF_2/LH_2$  system are 205 Btu/day for the hydrogen tank and 140 Btu/day for the fluorine tank. The design point heating rates for the  $LO_2/LH_2$  system were 140 Btu/day for oxygen and 280 Btu/day for hydrogen. A 2.0-percent ullage was chosen for the fluorine tank and 1.0-percent for the oxygen tank based upon the 23 psia vapor pressure limit. A 15 percent ullage was assumed for the hydrogen tank to correspond with the maximum vapor pressure of 58 psia.

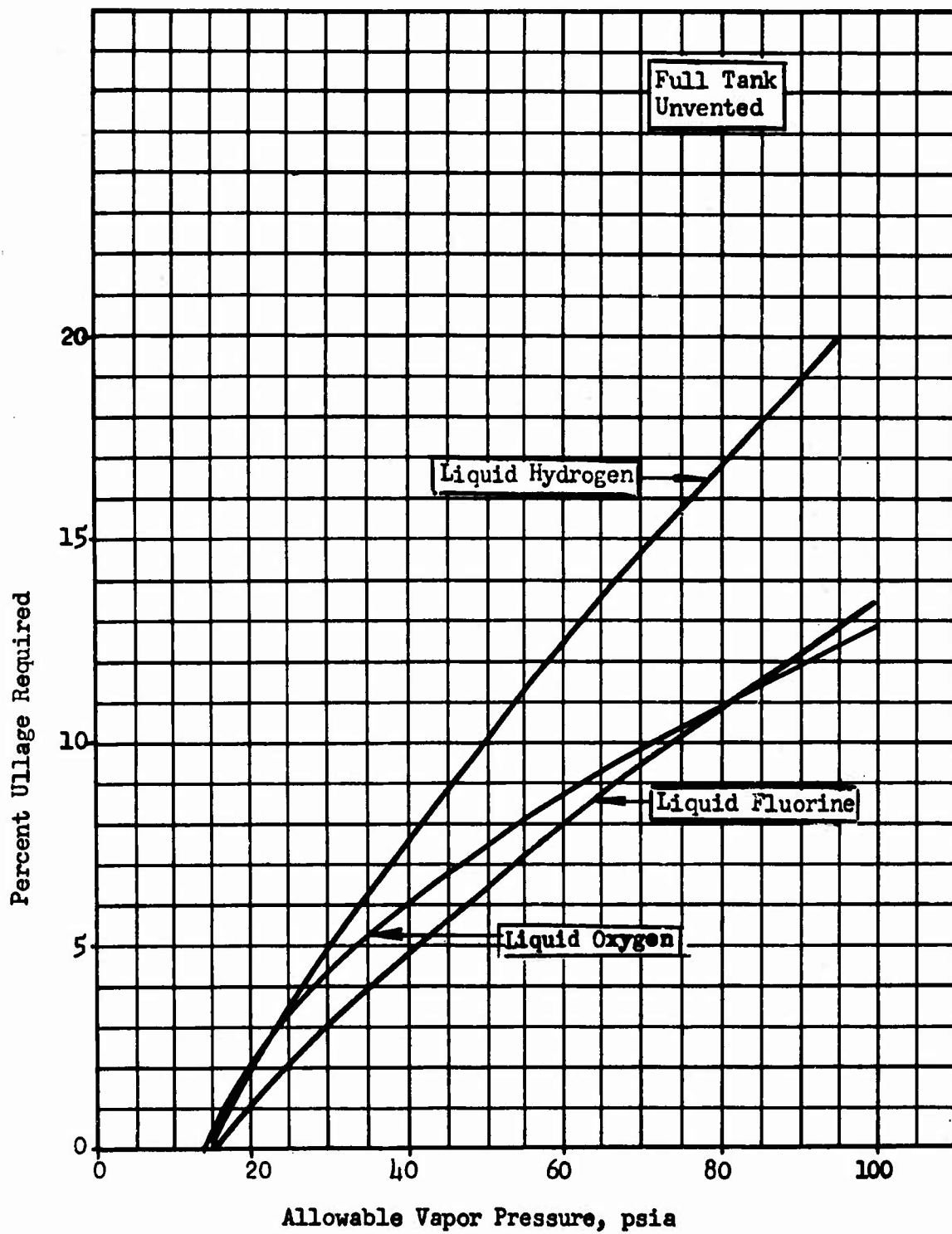


Figure 68. Ullage Requirement as a Function of Allowable Vapor Pressure for Liquid Hydrogen, Fluorine, and Oxygen

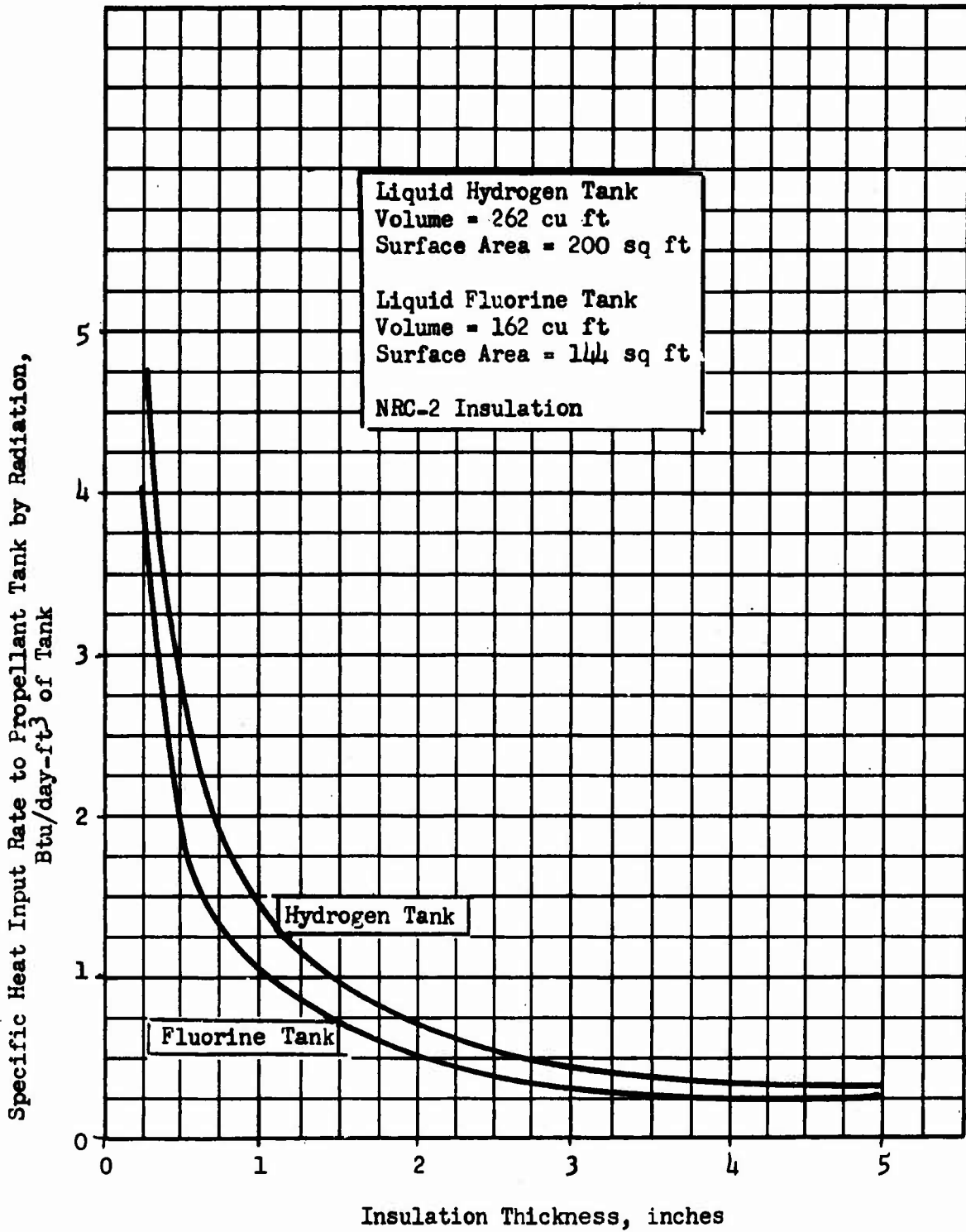
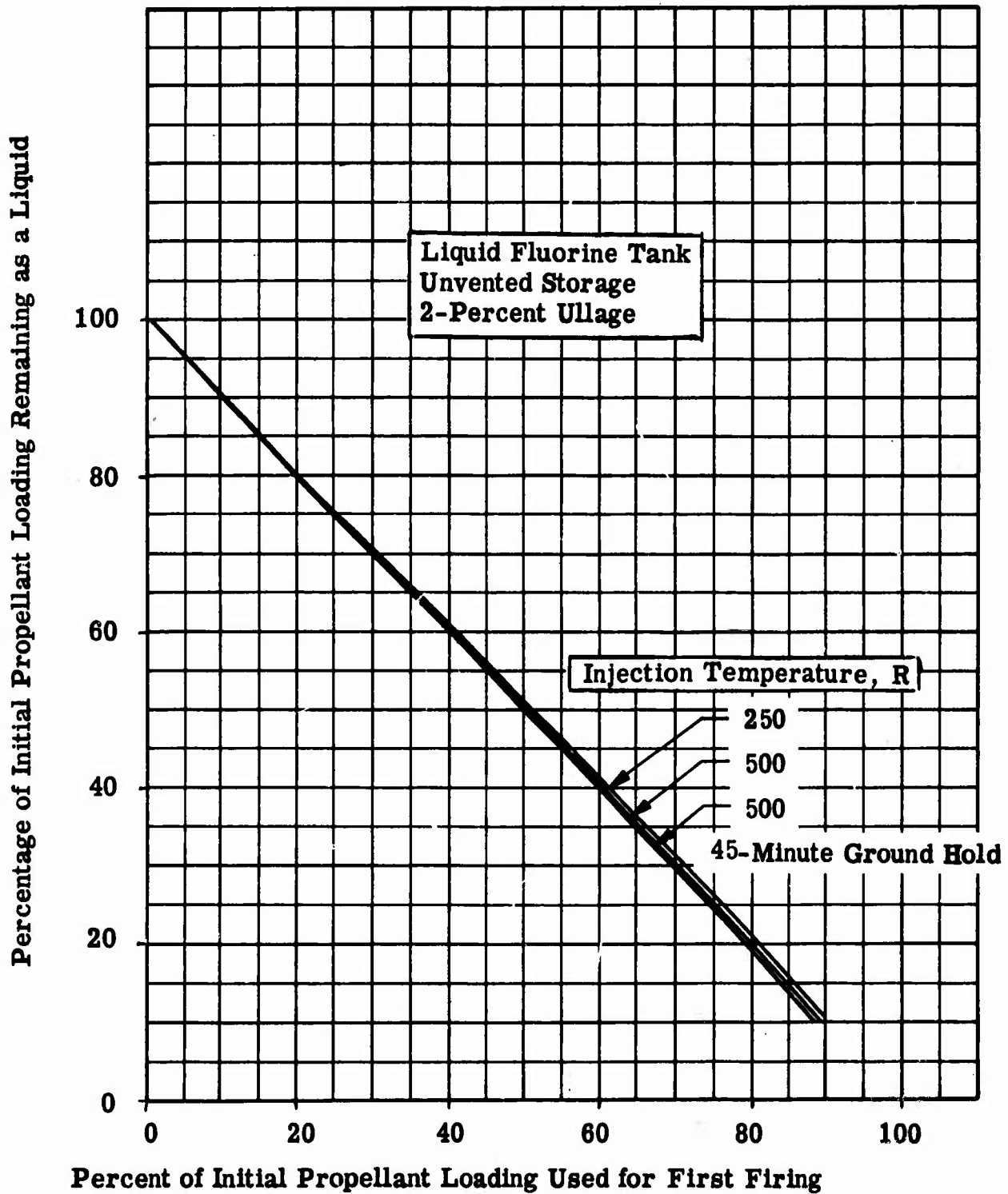


Figure 69. Specific Heat Input to Tank by Radiation as a Function of Insulation Thickness

(2) Fluorine/Hydrogen System (Fluorine Tank).

- a. (U) Unvented Storage. The initial conditions at the start or orbital coasting are shown in Fig. 70 and 71 as a function of the percentage of the initial fluorine loading used during the first firing (before coast). Three conditions were considered: no preorbital heating with 250 R helium pressurant; no preorbital heating with 500 R helium pressurant; and 45 minute ground heating with full aerodynamic heating and 500 R helium pressurant.
- (U) The percentage of fluorine liquid remaining after the tank has come to equilibrium (Fig. 70) shows that very little propellant is vaporized as a result of a firing. The vapor pressure increases to 22 psia maximum for 90/10 duty cycle.
- (U) The total fluorine tank pressure (Fig. 71) is high after a firing even though the vapor pressure is low. The lower helium injection temperature results in a higher final helium partial pressure following a firing. This occurs because the helium pressure drop from run pressure to equilibrium pressure is nearly proportional to the temperature drop. The smaller temperature drop results in a smaller pressure decay. The highest total pressure calculated for a 90/10 burn duty cycle was 74 psia, which is within maximum tank pressure tolerance since the vapor pressure is low.
- (U) The vapor pressure of the liquid fluorine in a full, unvented tank is shown in Fig. 72 as a function of orbital storage time for the design heat input rates. Seven preorbital conditions are considered, four having no prechill and three having a nitrogen prechill. For the unprechilled propellant, the storage times corresponding to orbital heating; orbital and aerodynamic heating; orbital, aerodynamic and 20-minute ground hold; and orbital, aerodynamic and 45-minute ground hold are shown. For the prechilled propellant all but the first preorbital heating conditions are shown.
- (U) The vapor pressure of the fluorine is well below the system limitations of 58 psia for all the preorbital conditions considered, and for the selected design orbital heat input rate for orbital coast times less than 100 days.
- (U) The percentage of liquid remaining and total fluorine tank pressure are shown in Fig. 73 and 74 for 10-percent full tanks. The preorbital conditions of no ground hold or aerodynamic heating and 45-minute ground hold with aerodynamic heating are shown. The nominal storage methods are adequate for periods of coasting of less than 20 days (Fig. 74). Coast times greater than this would require venting of helium pressurant after firing to lower the total tank pressure.
- (b) (U) Vented Storage. Calculations indicated that vented storage for the fluorine tank at times other than immediately following engine firing was undesirable. Therefore, no time history of the continuously vented fluorine tank was calculated. The fact that the total tank pressure



**Figure 70. Percentage of Liquid Fluorine Remaining as a Function of Percentage Used for First Firing for  $LF_2/LH_2$  Vehicle. (Helium Pressurant)**

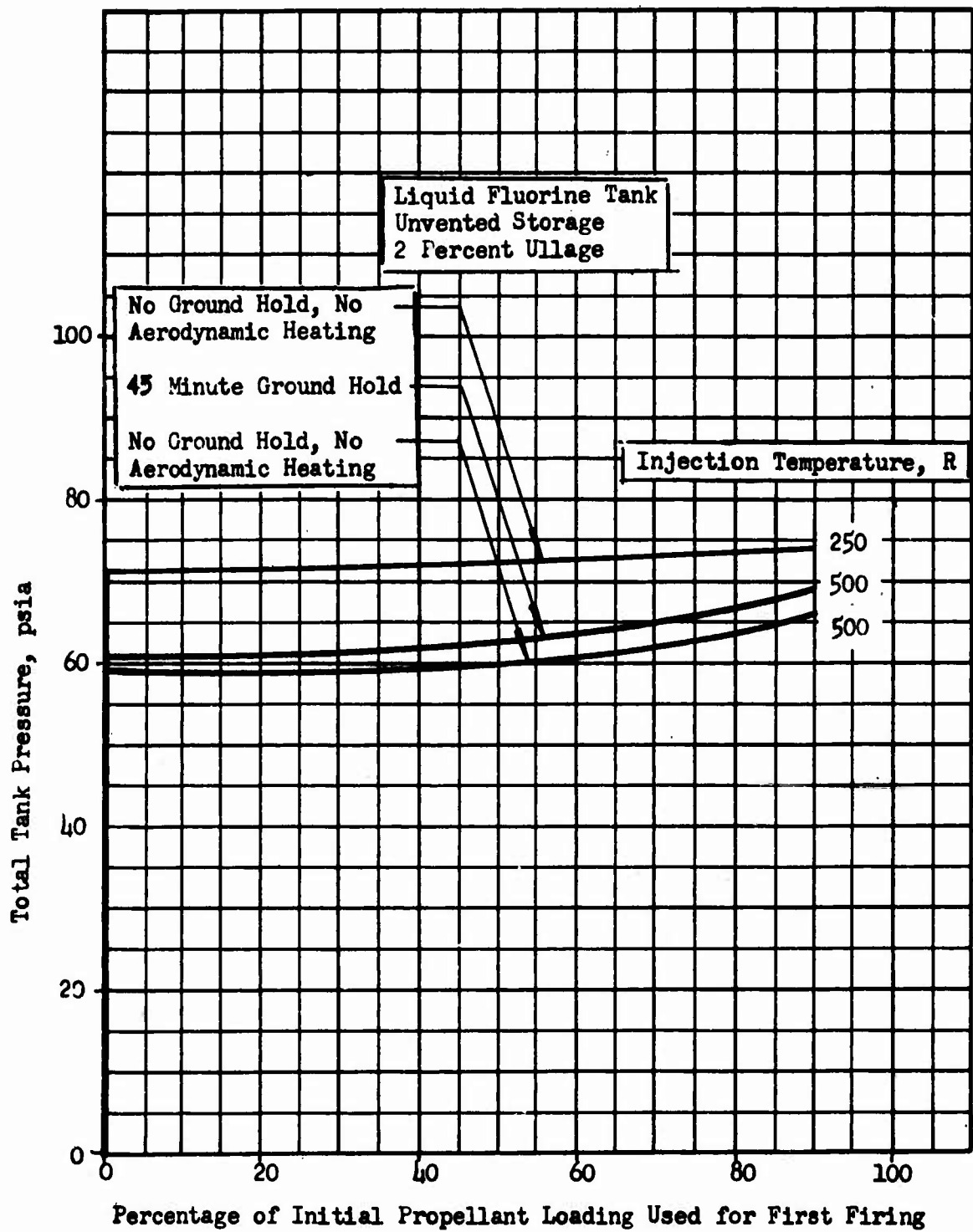


Figure 71. Total Fluorine Tank Pressure as a Function of Percentage of Initial Propellant Loading Used for First Firing for LF<sub>2</sub>/LH<sub>2</sub> Vehicle. Helium Pressurant

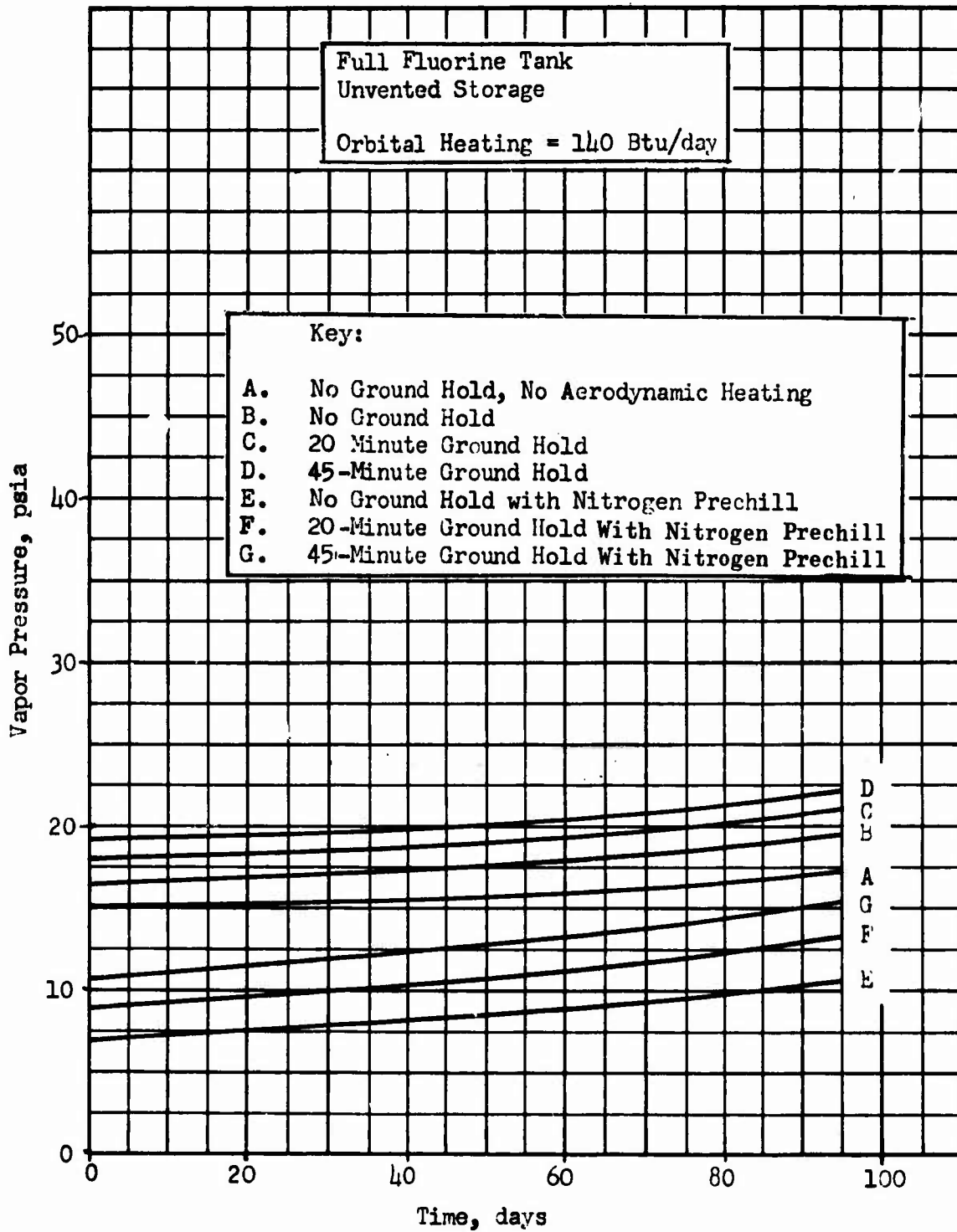


Figure 72. Fluorine Vapor Pressure as a Function of Time in Orbit for Various Preorbital Conditions

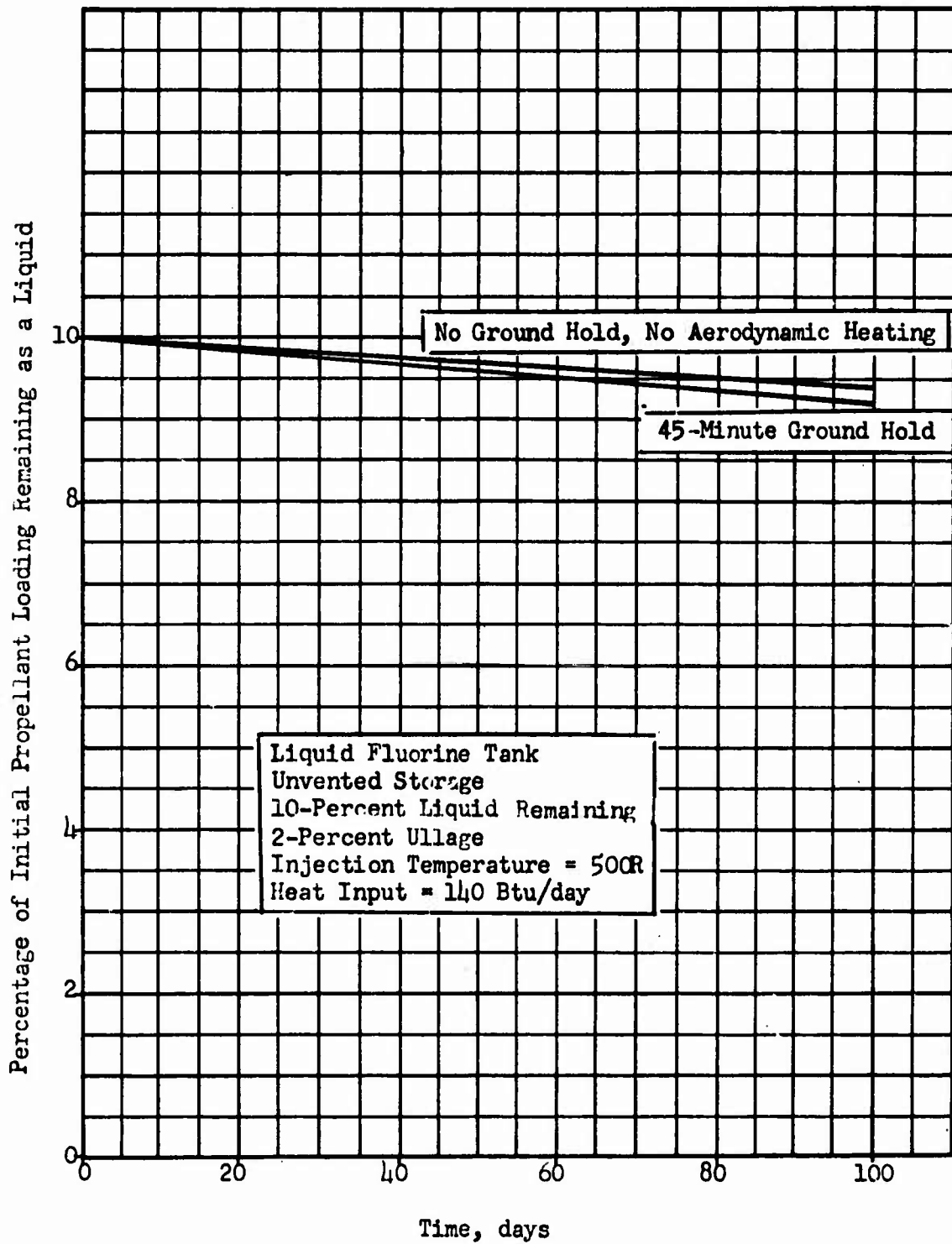


Figure 3. Percentage of Liquid Fluorine Remaining as a Function of Storage Time for 10-Percent Remaining on First Day for  $LF_2/LH_2$  Vehicle. Helium Pressurant.

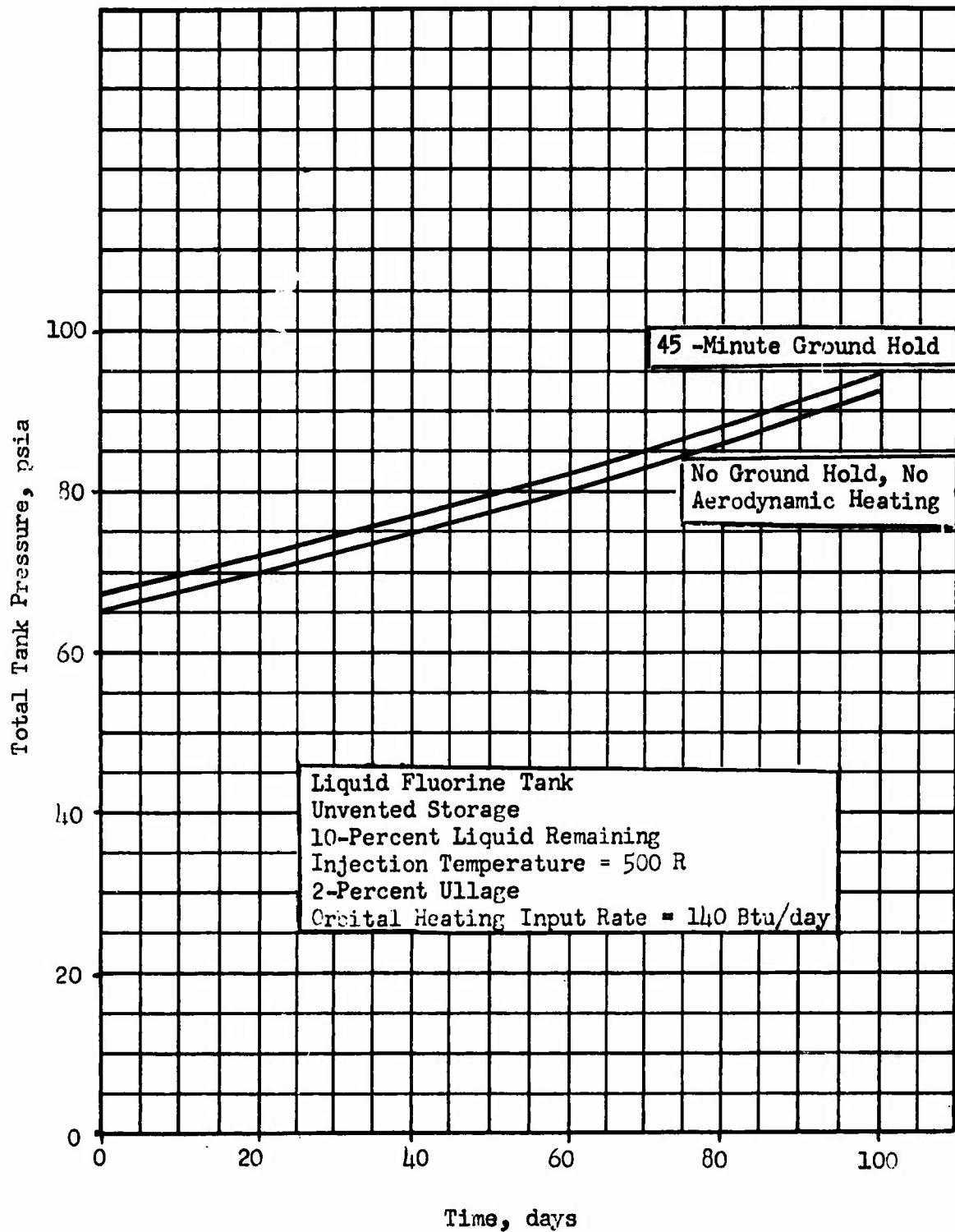


Figure 74. Total Fluorine Tank Pressure as a Function of Storage Time for 10-Percent of Original Propellant Loading Remaining as a Liquid on the First Day for  $LF_2/LH_2$  Vehicle. Helium Pressurant.

remains high could cause prepressurization difficulties and might require venting. The prepressurization scheme requires prepressurization gas flow to the fluorine tank in order to heat the hydrogen tank pressurant. If the fluorine tank pressure is high, there will be no flow.

(3) Fluorine/Hydrogen System (Hydrogen Tank).

- (a) (U) Unvented Storage. The initial conditions existing in the hydrogen tank before the start or orbital coasting after a firing on the first day are shown in Fig. 75 and 76 as a function of the percentage of the initial hydrogen loading used during the firing. The conditions considered are injection temperatures of 960 R, injection temperature with aerodynamic heating, and with 20-minute ground hold heating and aerodynamic heating.
- (U) A relatively large amount of hydrogen is vaporized by the hot pressurant. This high vaporization is caused by the high specific heat of hydrogen gas. For the nominal conditions in a firing in which 90 percent of the propellant was used, the remaining 10 percent liquid would all be vaporized as the tank came to equilibrium.
- (U) The hydrogen vapor pressure (Fig. 75), which is nearly equal to the total tank pressure, increases rapidly as more than 50 percent of the propellant is used for the first firing. When more than 85 percent of the propellant is used with the 960 R injection temperature, the equilibrium pressure in the tank exceeds the tank run pressure; however, no liquid is left so the pressure is irrelevant.
- (U) The hydrogen vapor pressure in a full propellant tank is shown in Fig. 77 as a function of orbital coast time for a number of preorbital conditions, including both prechill and no prechill. The tank pressure level is acceptable for the 14-day mission for all preorbital conditions to and including a 30-minute ground hold without prechill. Longer hold times will result in excessive tank pressure. The effect of prechill is to add an extra 30 minutes to the ground hold capability. However, prechilling liquid hydrogen is more difficult than prechilling liquid fluorine.
- (U) The percentage of liquid remaining for a 90/10 duty cycle in the hydrogen tank and the vapor pressure of the hydrogen are shown in Fig. 78 and 79. The liquid hydrogen has a higher vaporization rate than the liquid fluorine and its vapor pressure rises much faster. For all preorbital conditions, the vapor pressure limitation is exceeded for the nominal pressurant temperature.
- (b) (U) Vented Storage. The extremely poor propellant utilization caused by the vaporization of hydrogen liquid by the hot hydrogen pressurant suggests that a system in which the hot pressurant is vented after each firing might be desirable. Two vent pressures were evaluated, 50 and 15 psia. The results are shown in Fig. 80 and 81. The 50-psia venting condition is similar to the unvented condition (Fig. 77) but does have a small advantage in percentage of liquid hydrogen remaining. The 15-psia venting

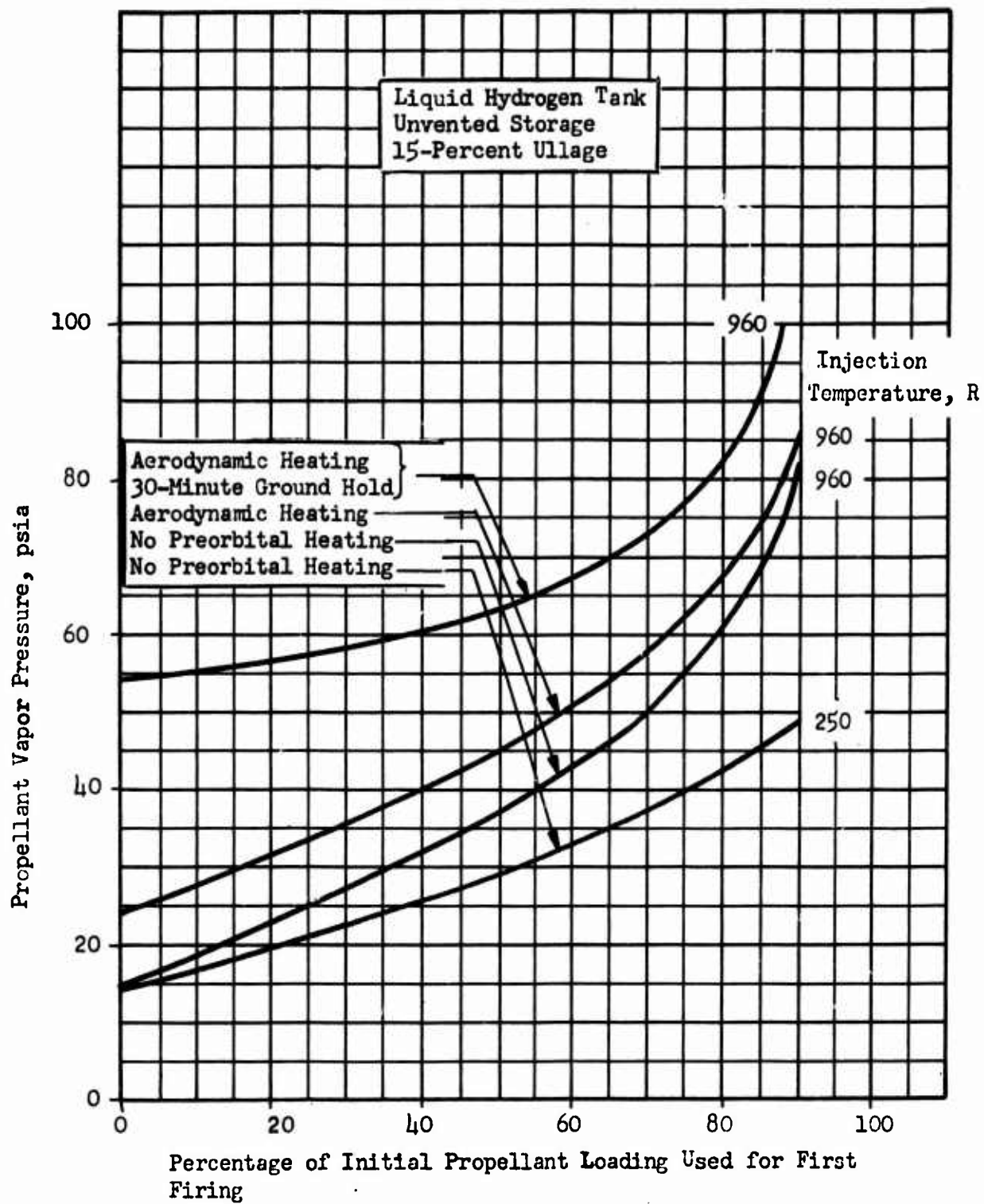


Figure 75. Hydrogen Vapor Pressure as a Function of Propellant Usage for First Firing for  $LF_2/LH_2$  Vehicle

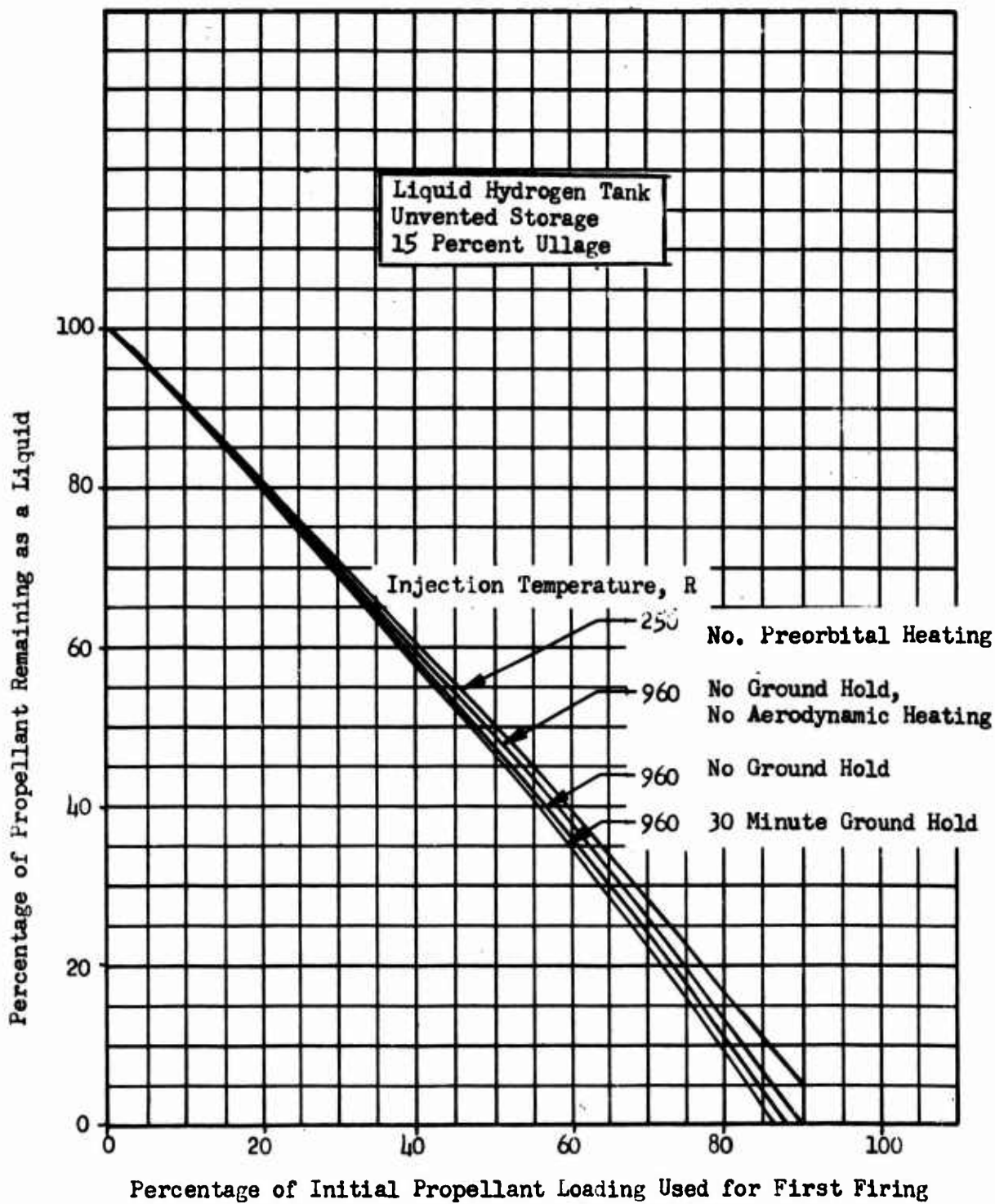


Figure 76. Percentage of Liquid Hydrogen Remaining as a Function of Percentage Used for First Firing for  $LF_2/LH_2$  Vehicle. Hydrogen Pressurant.

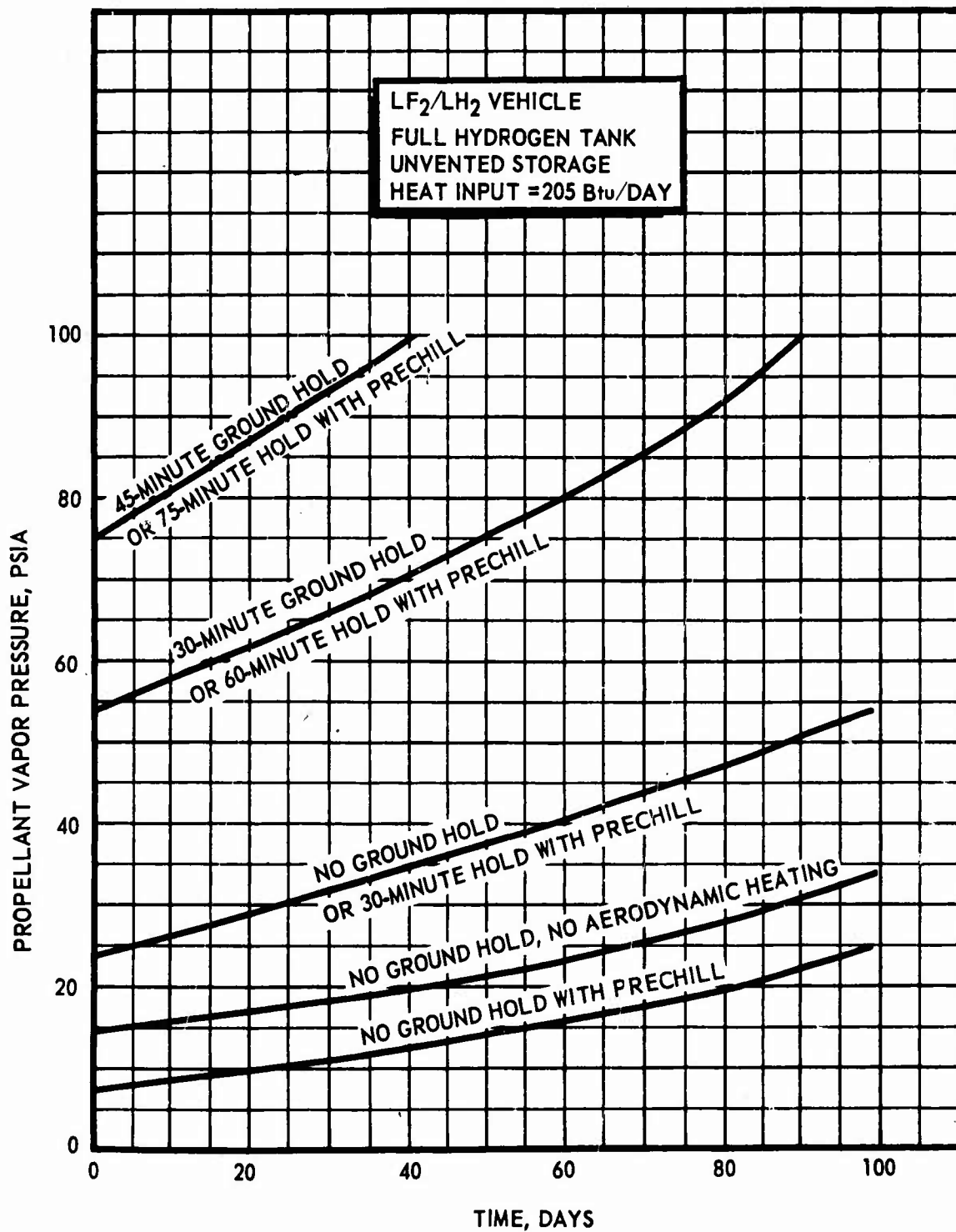


Figure 77. Hydrogen Vapor Pressure as a Function of Time for Various Pre-orbital Conditions

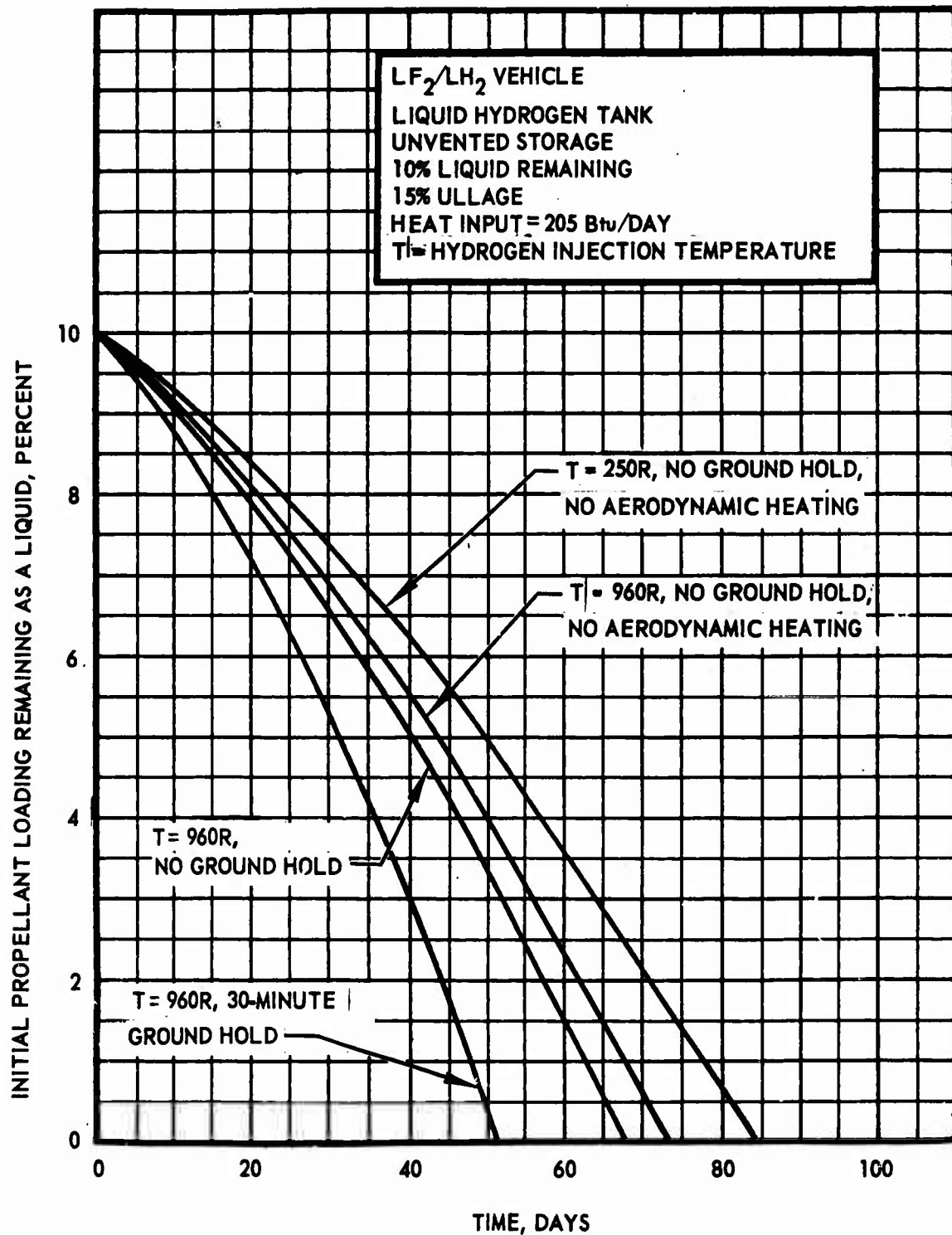


Figure 78. Percentage of Liquid Hydrogen Remaining as a Function of Orbital Storage Time and Hydrogen Pressurant Temperature

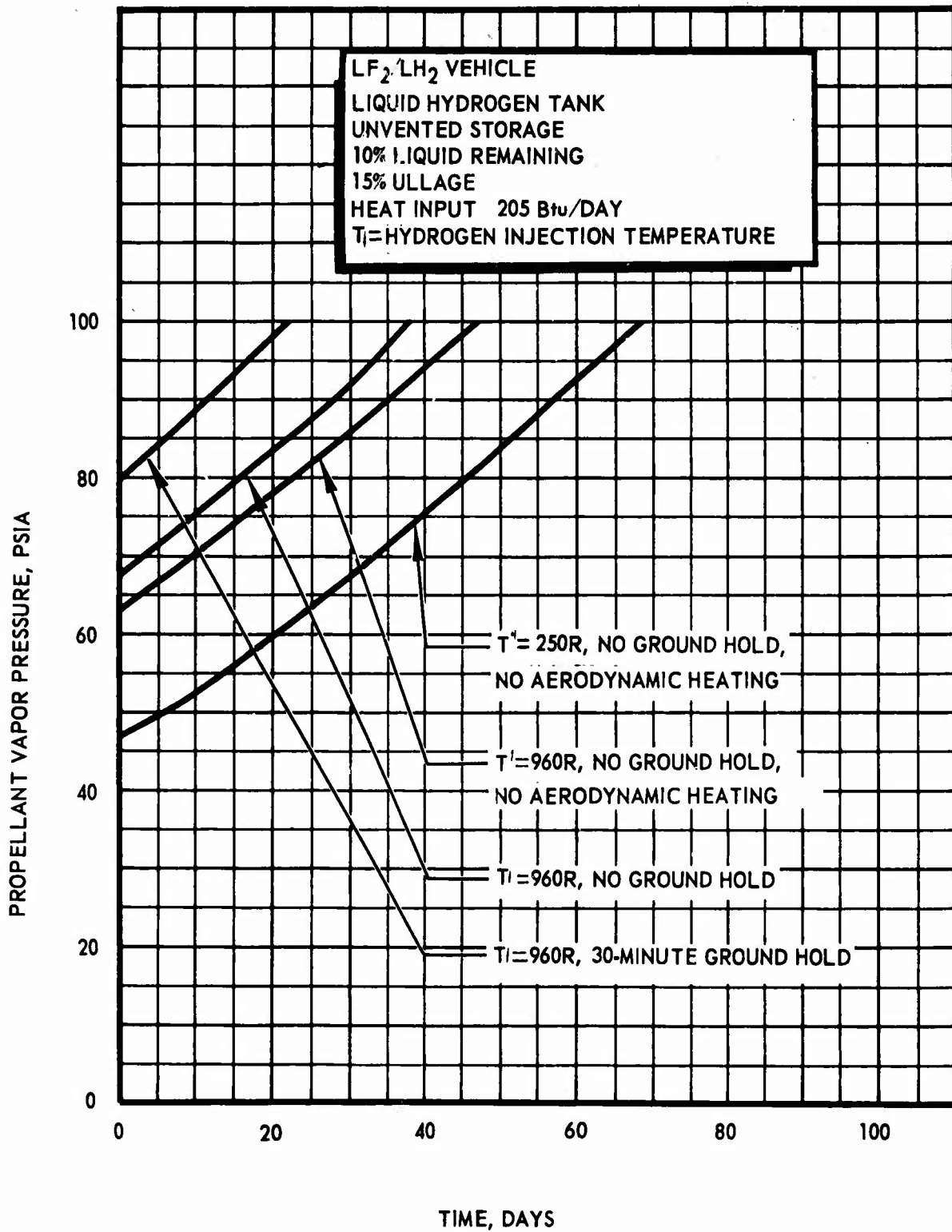


Figure 79. Hydrogen Vapor Pressure as a Function of Storage Time and Hydrogen Pressurant Temperature for 10 Percent of Hydrogen Remaining After the First day

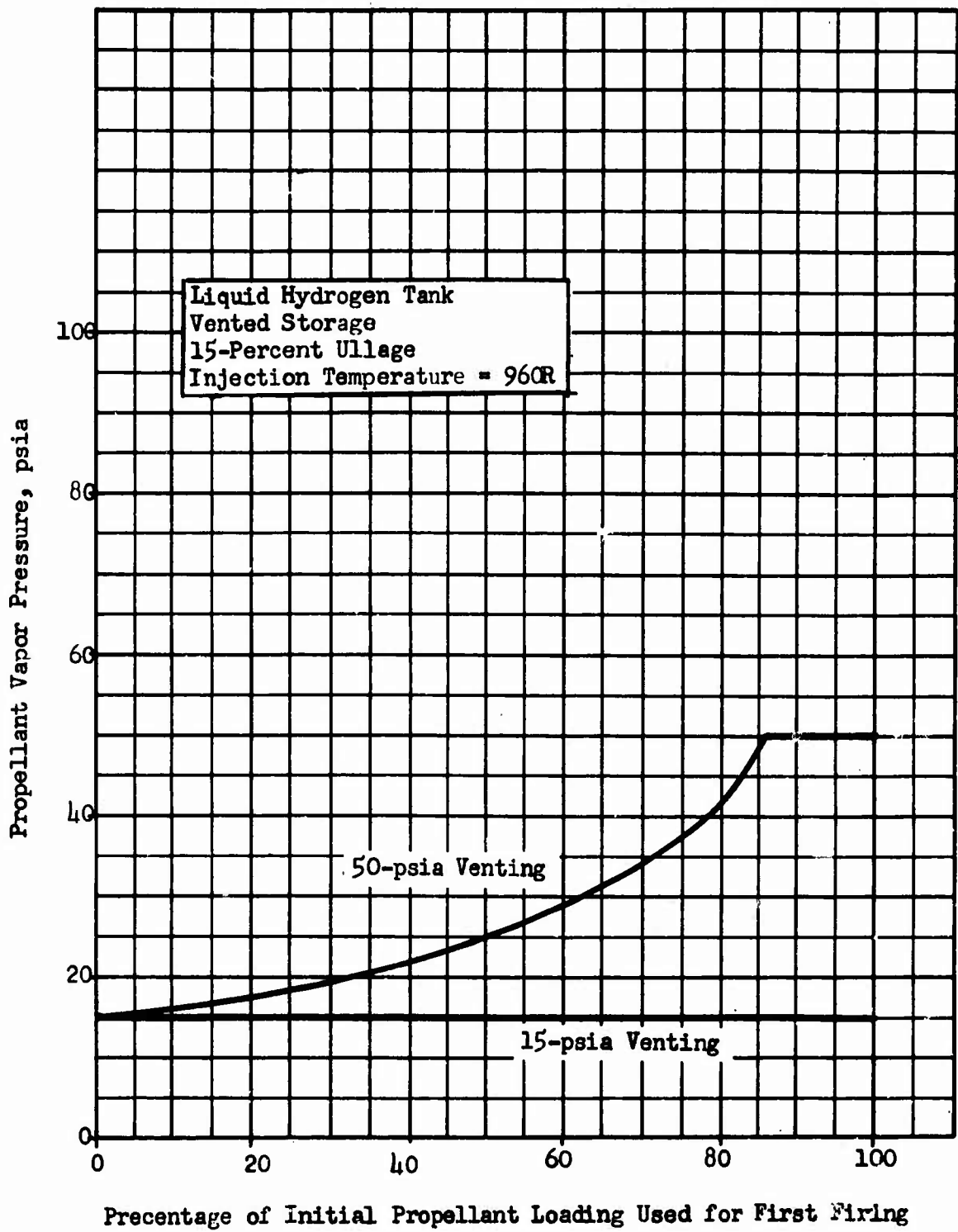


Figure 80. Hydrogen Vapor Pressure as a Function of Propellant Used for First Firing, No Preorbital Heating, Hydrogen Pressurant, for  $LP_2/LH_2$  Vehicle

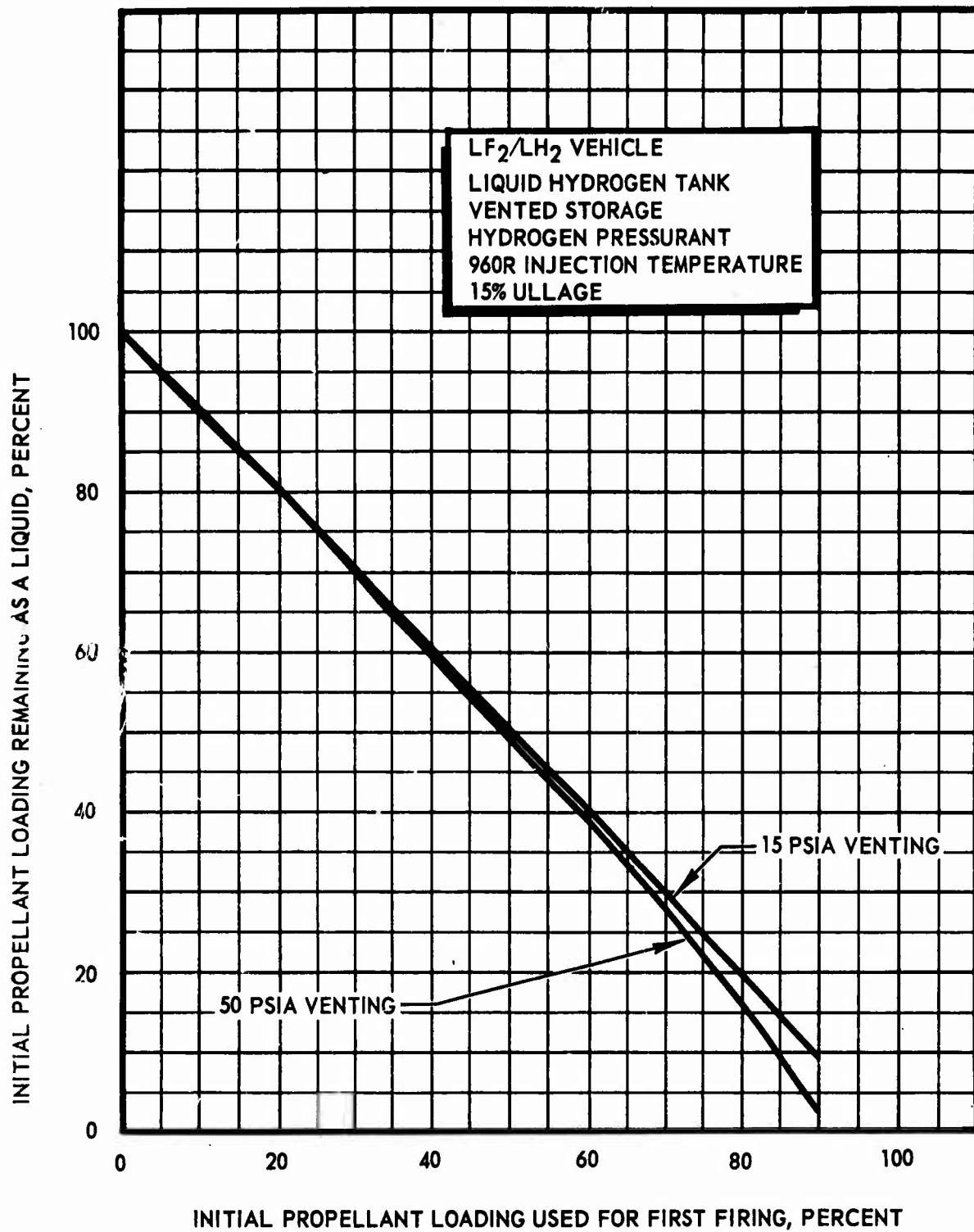


Figure 81. Percentage of Liquid Hydrogen Remaining as a Function of Initial Propellant Loading used for First Firing

condition gives the best propellant utilization. Since the pressurant gas is already lost as propellant, venting the pressurant does not penalize the system greatly and does prevent the vaporization of the remaining liquid; however, the pressurant requirements are increased.

- (U) The percentage of hydrogen vented from an initially full tank is shown in Fig. 82 as a function of storage time for a vent pressure of 50 psia. A variety of preorbital heating conditions are again considered. As in the case of the fluorine, the hydrogen loss is high enough to make continuous venting result in a major performance degradation.
- (U) The most critical storage condition is that of 10 percent propellant remaining at the start of orbital coast. For this condition, the hydrogen tank is the most critical because of the injection of hot hydrogen pressurant which vaporizes a large percentage of the liquid remaining immediately after a firing.
- (U) There are a number of possible solutions to this difficulty; lower pressurant temperatures, venting after firing, a combination of lower temperature and venting, or use of helium pressurant. The inherent disadvantage of venting is that the control system must sense whether a shutdown is a temporary one for vehicle reorientation or as part of a pulse operation mode or whether the shutdown is at the conclusion of an interception and precedes a period of coasting. If the tanks were vented routinely at each shutdown, prepressurant and pressurant requirements would be greatly increased. Restart times would also increase because prepressurization would be required before every firing rather than only at the start of each interception.

(4) Oxygen/Hydrogen System (Oxygen Tank).

- (a) (U) Unvented Storage. The percentage of liquid remaining and the total tank pressure immediately after a firing are shown in Fig. 83 and 84 as a function of the amount of propellant used for the firing. Two pressurant temperatures are considered, 250 R and 500 R. The preorbital heating of boost phase and a 45-minute ground hold are also shown for the 500 R pressurant temperature. The results are almost identical to those of the fluorine tank on the  $LF_2/LH_2$  vehicle. These results indicate that a fully loaded  $LO_2$  tank can be stored for very long periods of time.
- (U) The conditions in the oxygen tank with 10 percent liquid left are shown in Fig. 85 and 86 as functions of orbital storage time. Like the fluorine tank, the oxygen tank total pressure is too high. However, this problem can easily be corrected by venting the helium immediately after a firing. The oxygen vapor pressure increases more rapidly than the fluorine and could affect the relative performance of the  $LO_2/LH_2$  vehicle.

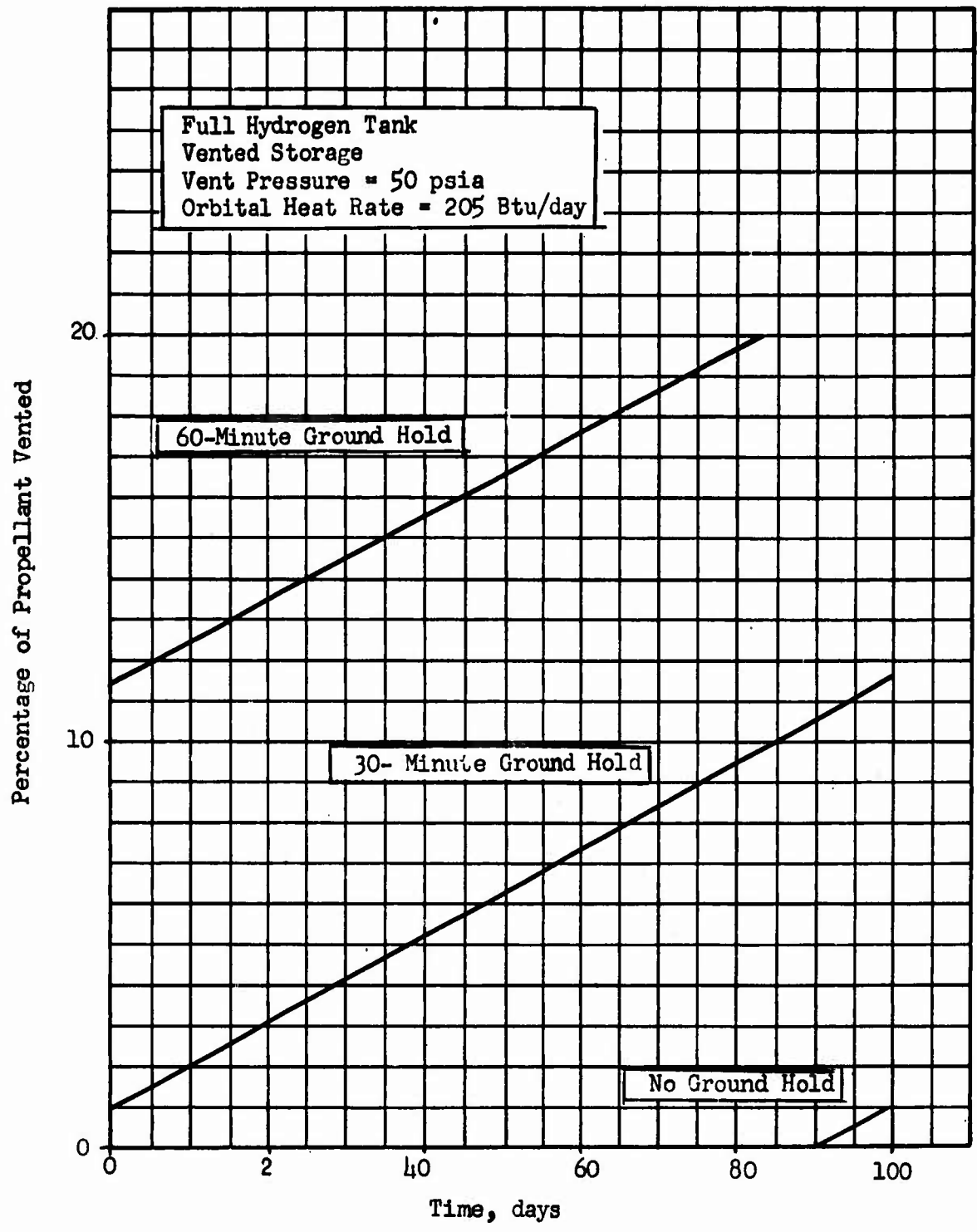


Figure 82. Percentage of Hydrogen Vented to Space as a Function of Orbital Storage Time for Various Preorbital Conditions for LF<sub>2</sub>/LH<sub>2</sub> Vehicle

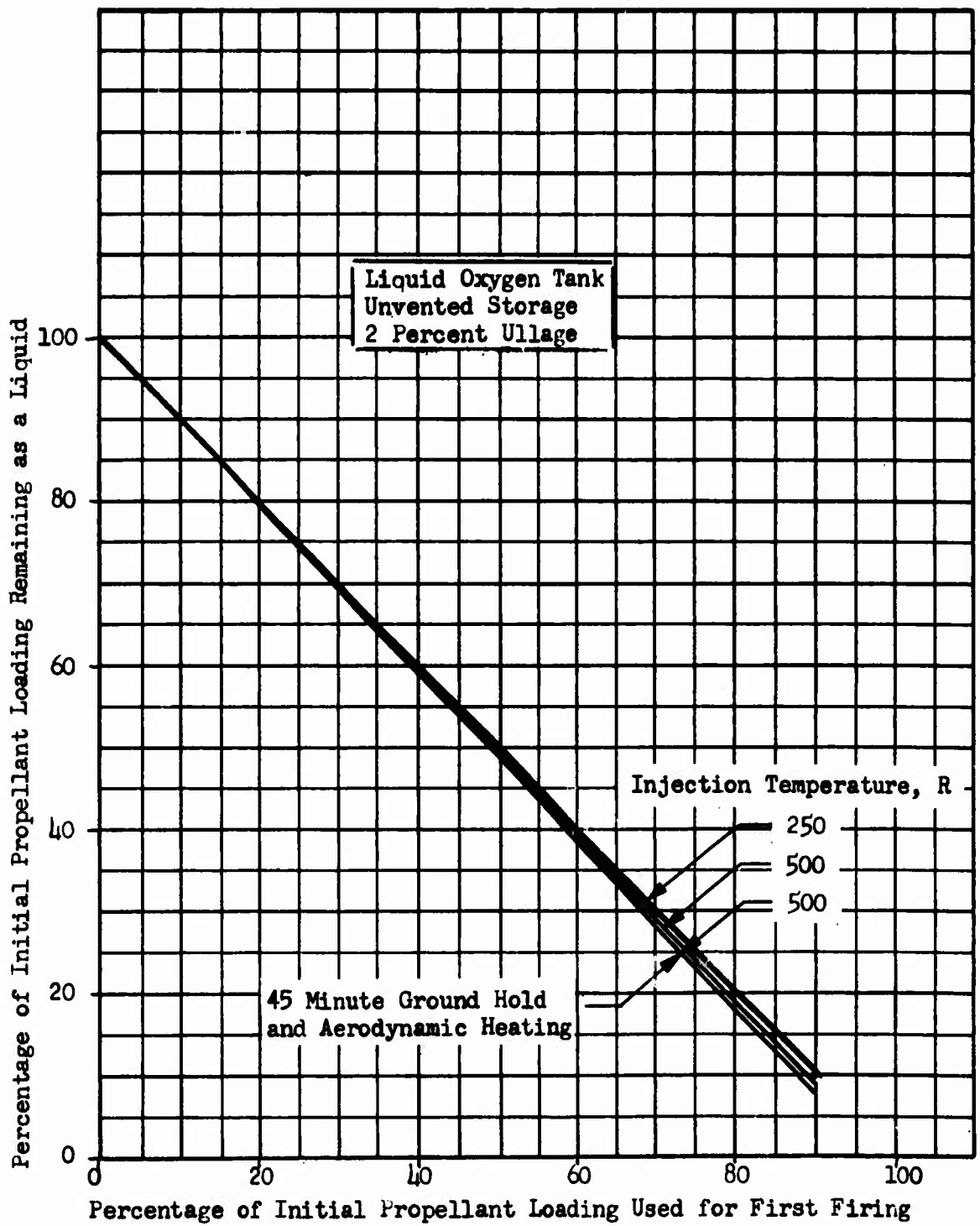


Figure 83. Percentage of Liquid Oxygen Remaining as a Function of Propellant Used for First Firing

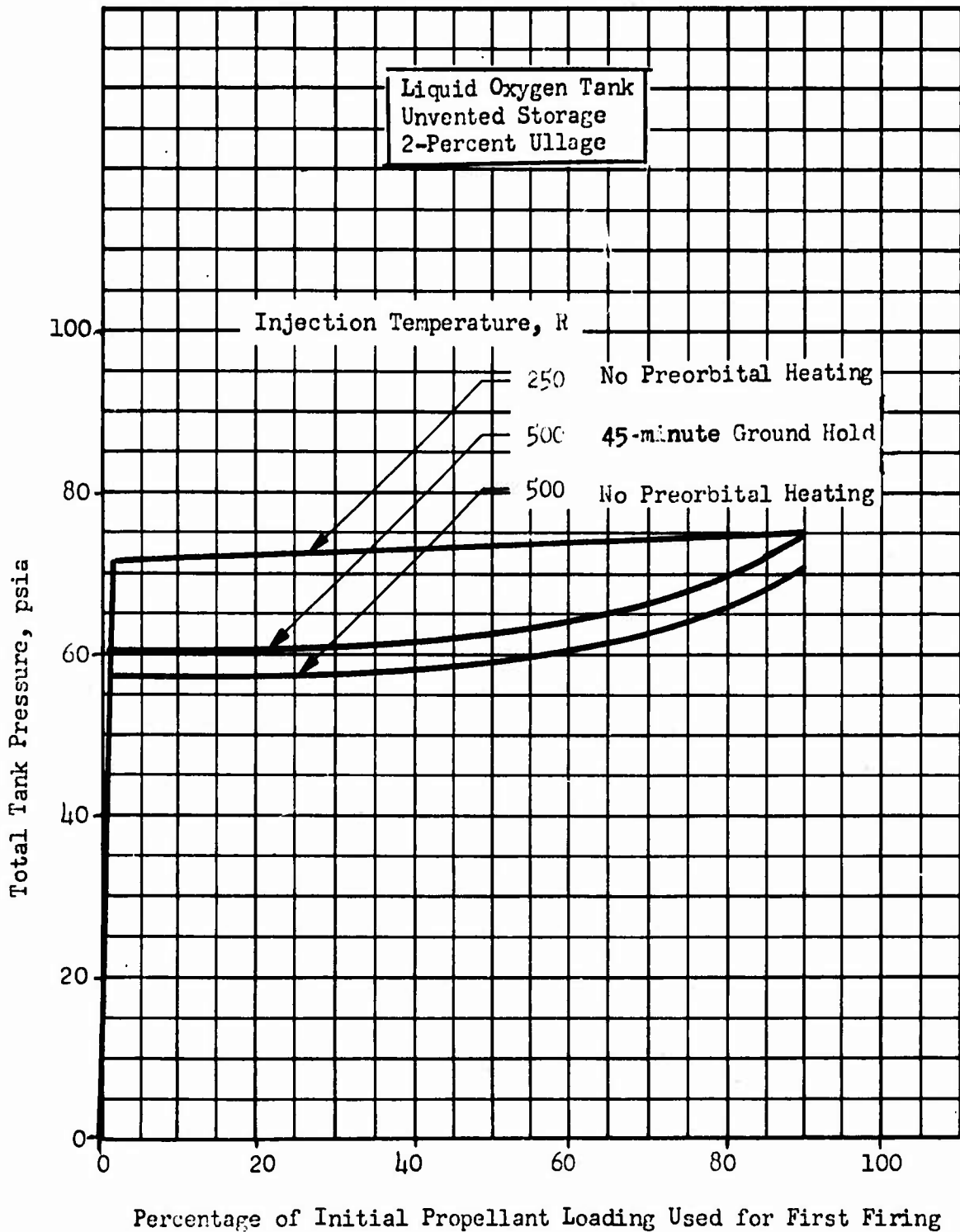


Figure 84. Total Oxygen Tank Pressure as a Function of Propellant Used for First Firing for  $LO_2/LH_2$  Vehicle. Helium Pressurant.

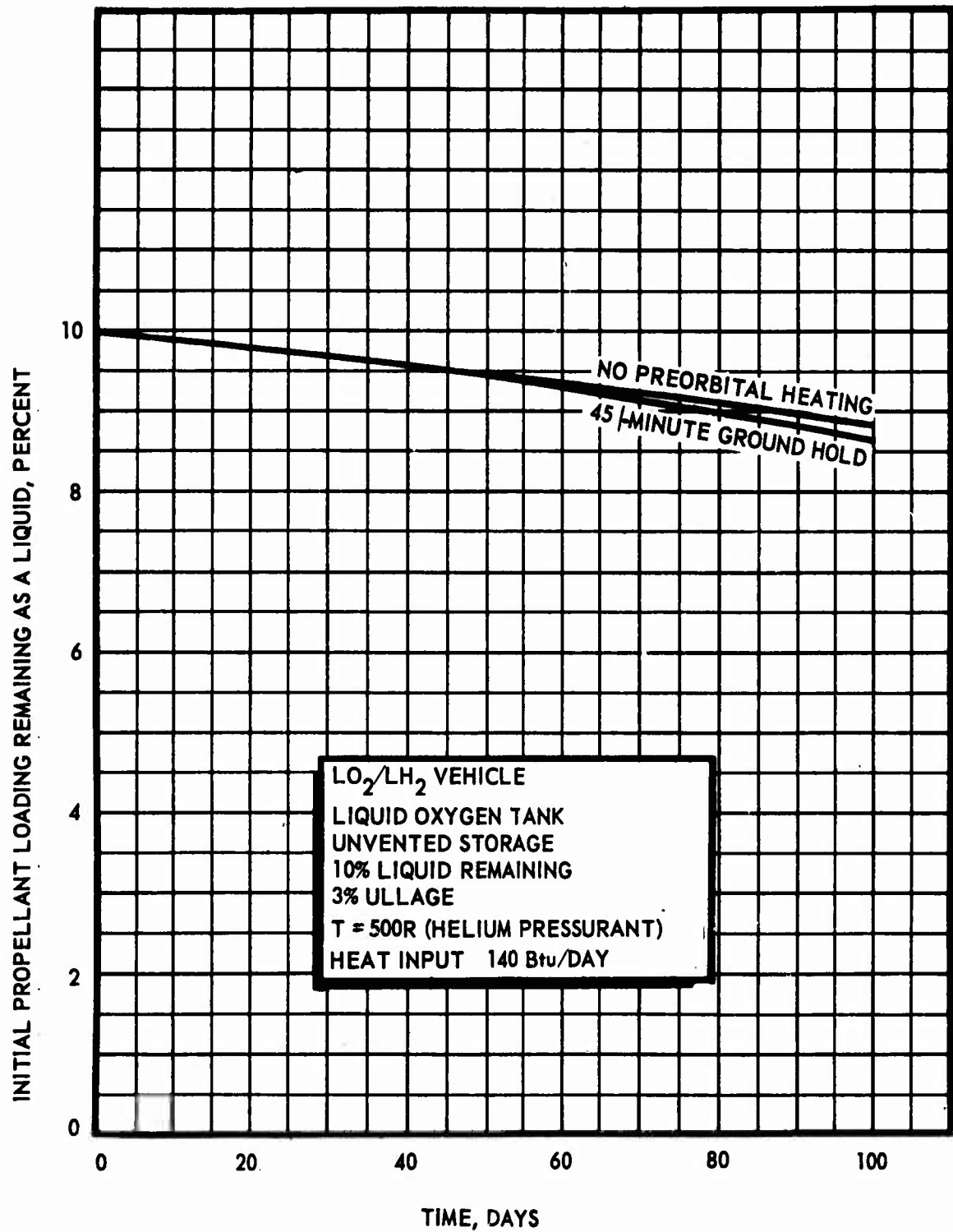


Figure 85.. Percentage of Liquid Oxygen Remaining as a Function of Storage Time, for 10 Percent Remaining on First Day, Helium Pressurant

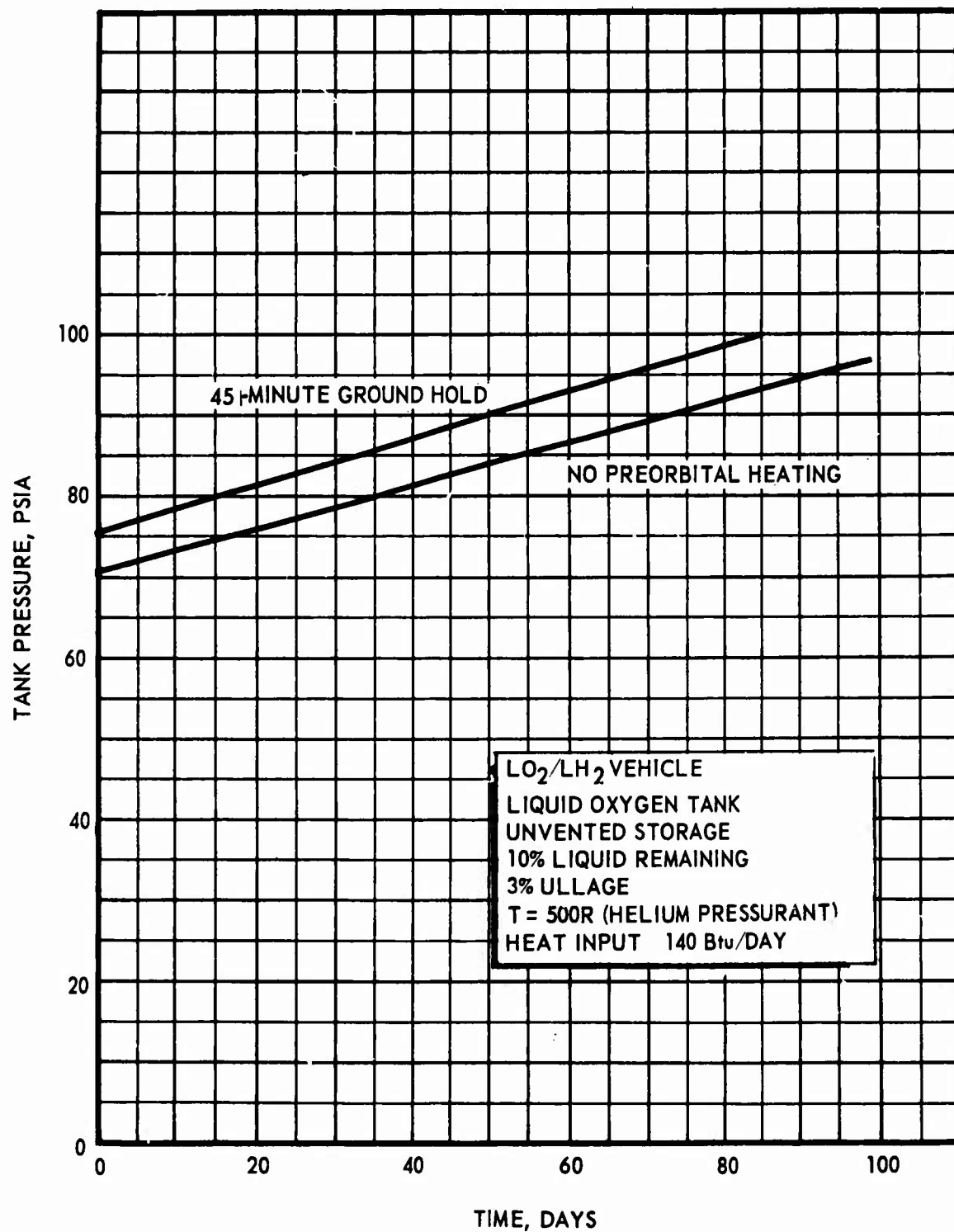


Figure 86. Total Oxygen Tank Pressure as a Function of Storage Time, for 10 Percent Remaining on First Day, Helium Pressurant

# CONFIDENTIAL

(5) Oxygen/Hydrogen System (Hydrogen Tank).

- (a) (U) Unvented Storage. The hydrogen tank conditions are identical to those found on the  $LF_2/LH_2$  vehicle for no preorbital heating. The effects of preorbital heating are smaller than for the  $LF_2/LH_2$  vehicle. The liquid remaining and the vapor pressure of the hydrogen after pressurant collapse are shown in Fig. 87 and 88. The hydrogen vapor pressure as a function of orbital storage time is shown in Fig. 89 for a variety of preorbital conditions for full tanks. The storage is better than that of the  $LF_2/LH_2$  hydrogen tank, but ground hold still creates difficulties in maintaining vapor pressure limitations for extended time periods.
- (U) The liquid remaining and the vapor pressure in the hydrogen tank are shown in Fig. 90 and 91 for 10 percent of the liquid remaining on the first day of orbital coasting.

5.  $N_2O_4/N_2H_4$ -UDMH (50-50) SYSTEMS

a. Vehicle Model

- (C) The 20,000-pound gross weight alternate mission vehicle of Ref. 2 (Fig. 92) was used in the propellant storage analysis. The vehicle configuration was two spherical propellant tanks within an outer structural shell. A helium pressurization system with heat exchangers was used. Tank supports were similar to those of the cryogenic vehicles. Since heat conduction paths would be similar to those of the cryogenic vehicles, the same nominal value of thermal resistivity (115 hr-R/Btu) was used. Where insulation was necessary, the NRC-2 super insulation was used. Since the freezing of air during ground hold was not a problem, a helium purge was not required.

System operating limits are listed in Table XXXVII

TABLE XXXVII  
SYSTEM OPERATING LIMITS

	<u><math>N_2O_4</math></u>	<u><math>N_2H_4</math>-UDMH (50-50)</u>
Tank Pressure Required Above Vapor Pressure to Provide NPSH, psia	46.5	46.5
Maximum Allowable Vapor Pressure, psia	23	23
Temperature for Maximum Vapor Pressure, R	580	660
Tank Run Pressure, psia	70	70
Tank Burst Pressure, psia	90	90
Freezing Point, R	472	479

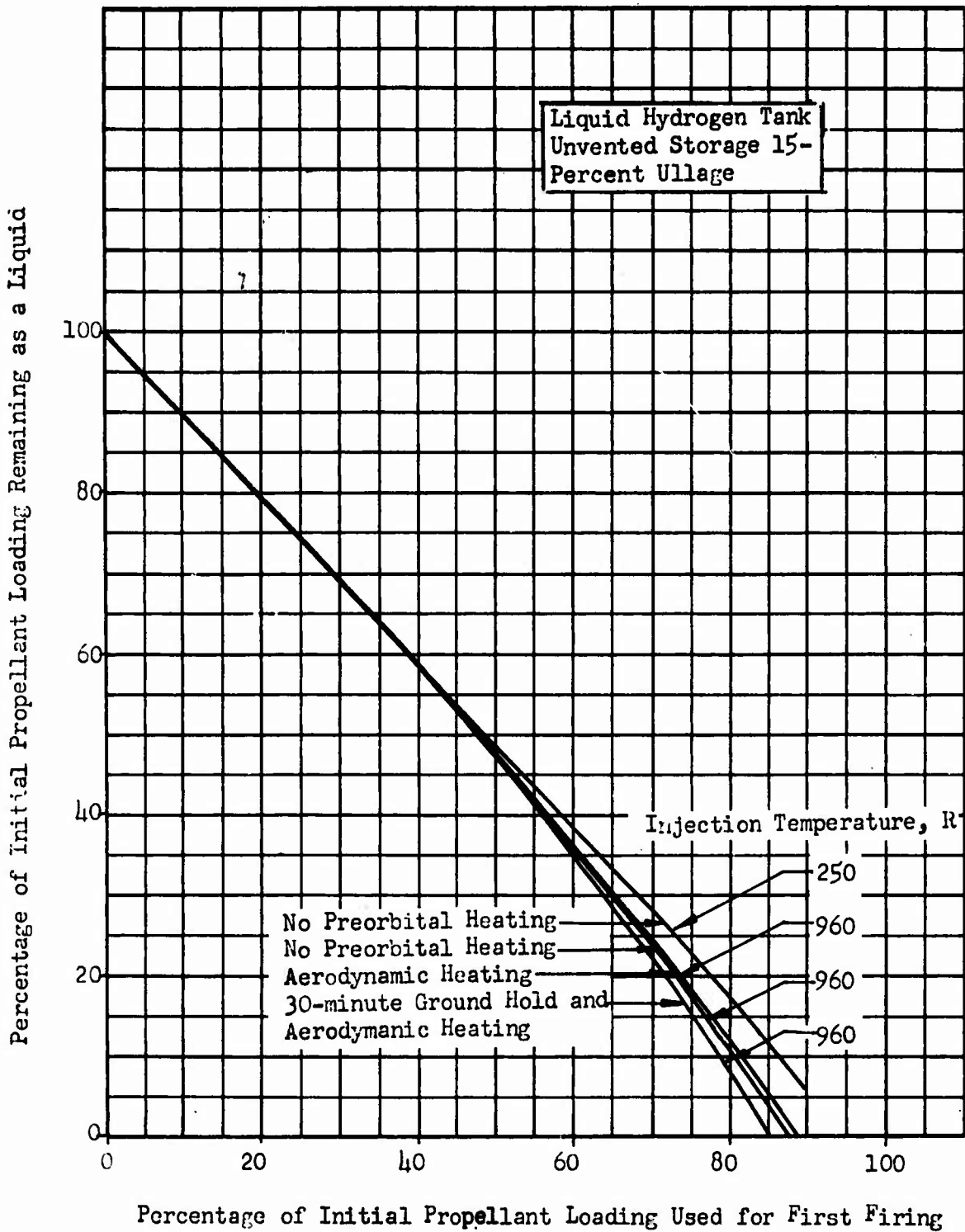


Figure 87. Percentage of Liquid Hydrogen Remaining as a Function of Percentage Used for First Firing for  $LO_2/LH_2$  Vehicle, Hydrogen Pressurant.

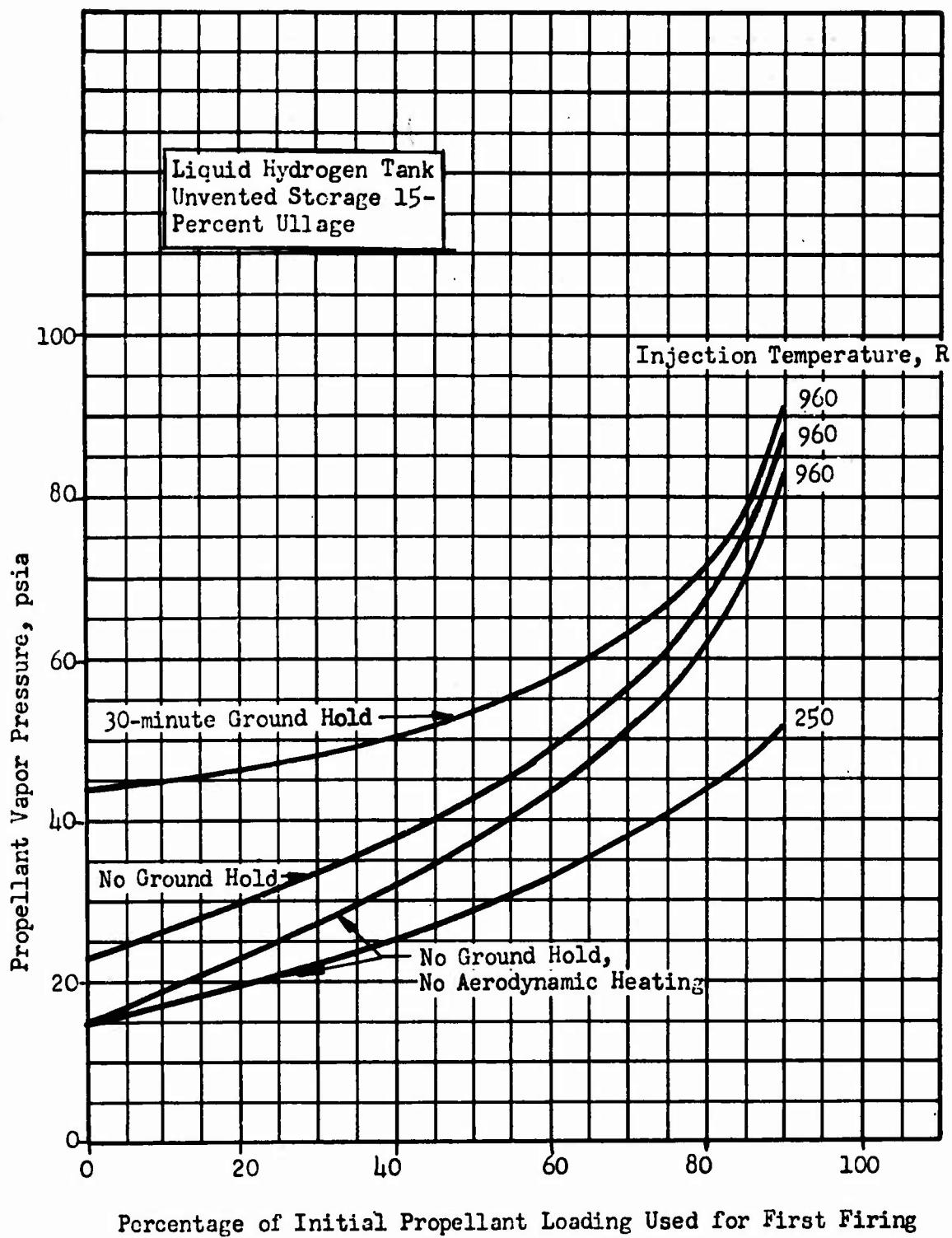


Figure 88. Hydrogen Vapor Pressure as a Function of Initial Propellant Loading Used for First Firing for  $LO_2/LH_2$  Vehicle.

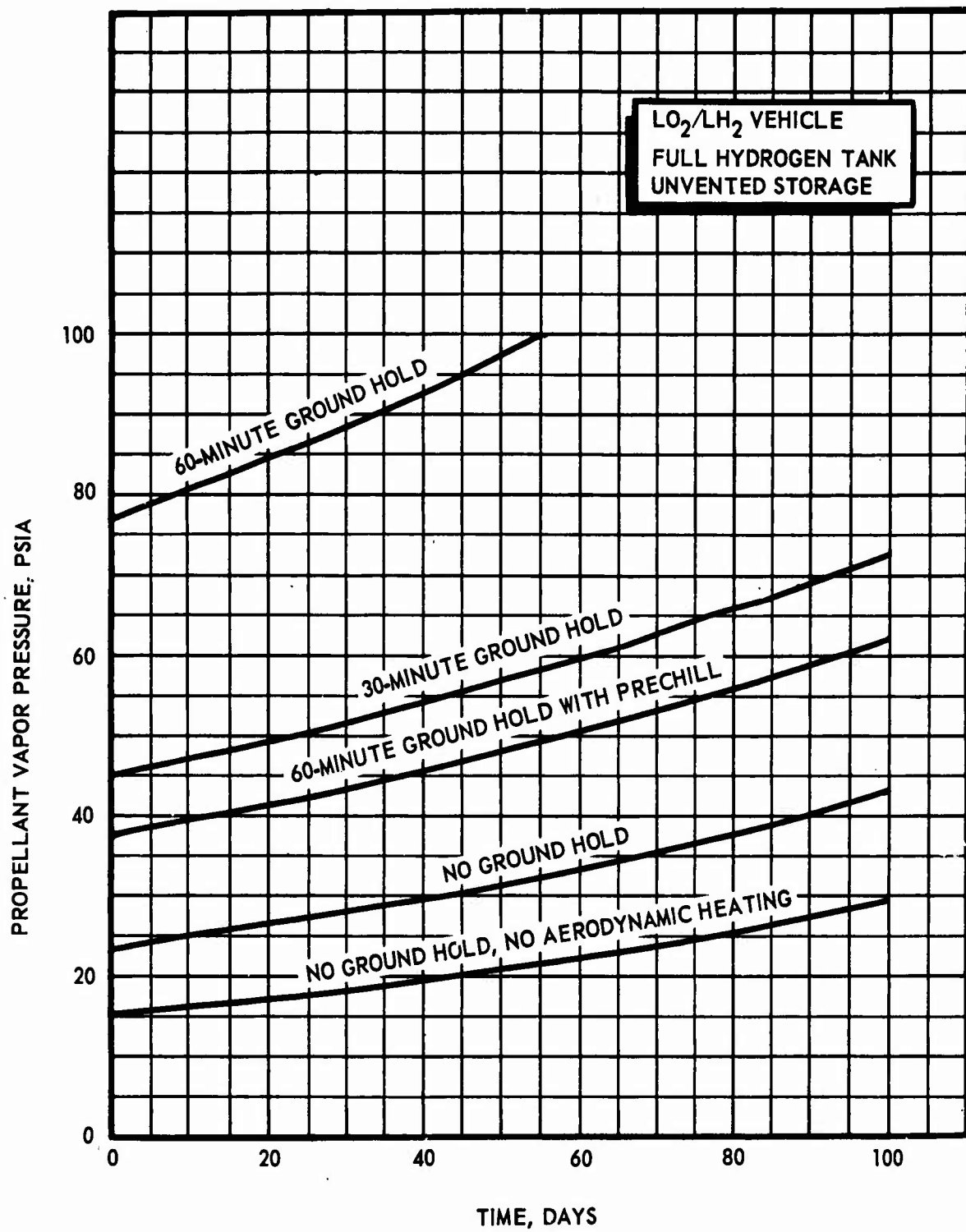


Figure 89. Hydrogen Vapor Pressure as a Function of Time in Orbit for Various Pre-Orbital Conditions.

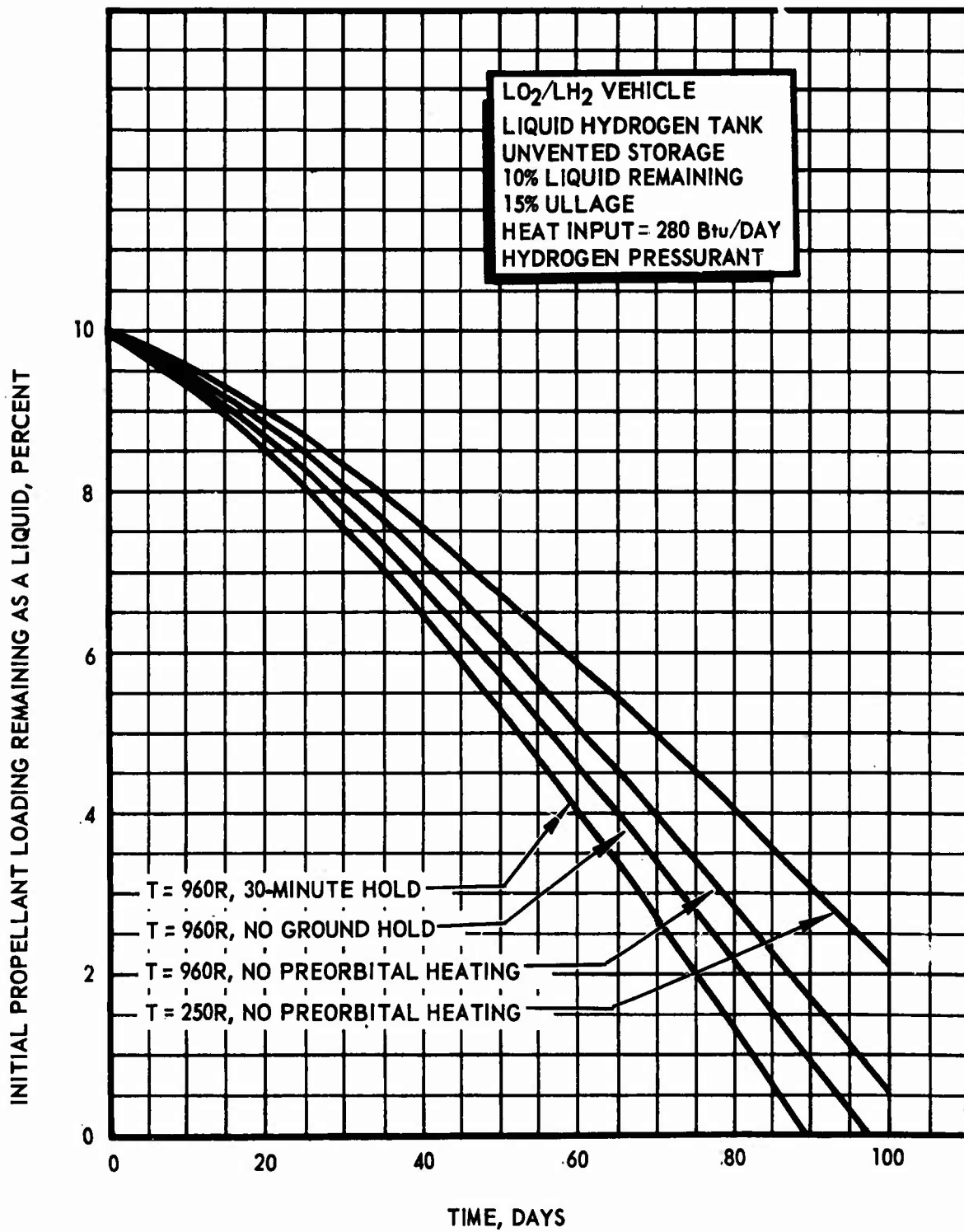


Figure 90. Percentage of Liquid Hydrogen Remaining as a Function of Orbital Storage Time, for 10 Percent Remaining on First Day, Hydrogen Pressurant

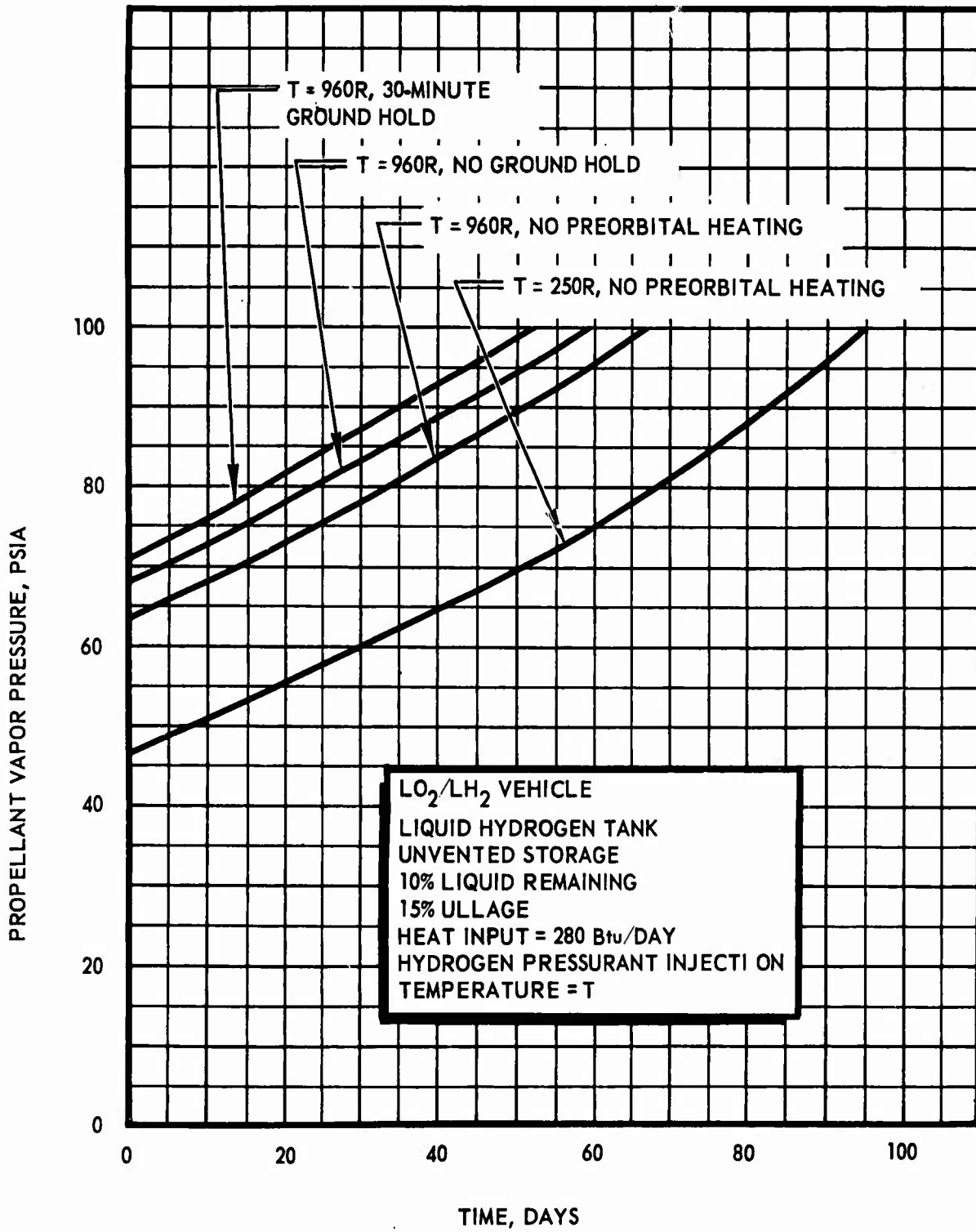
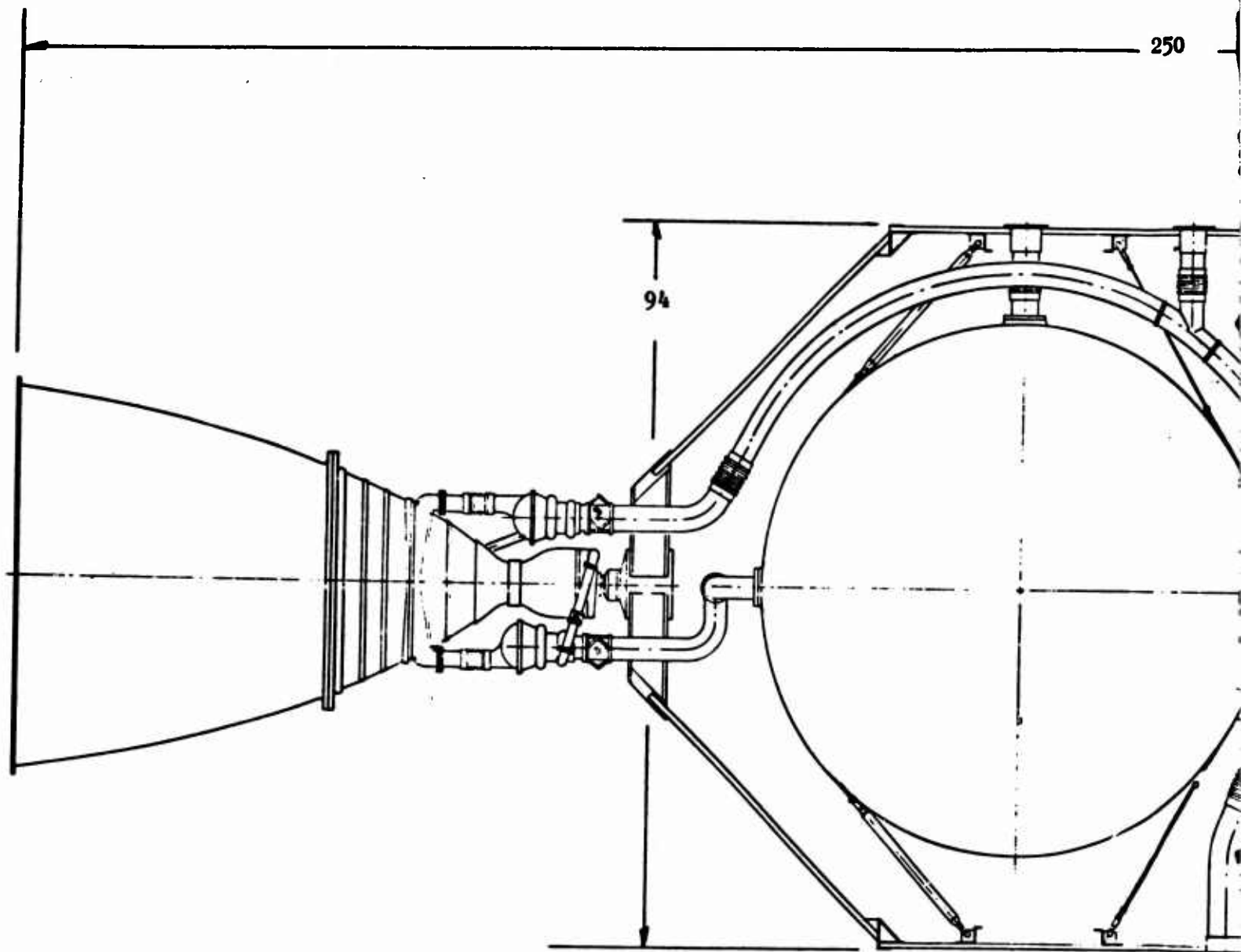


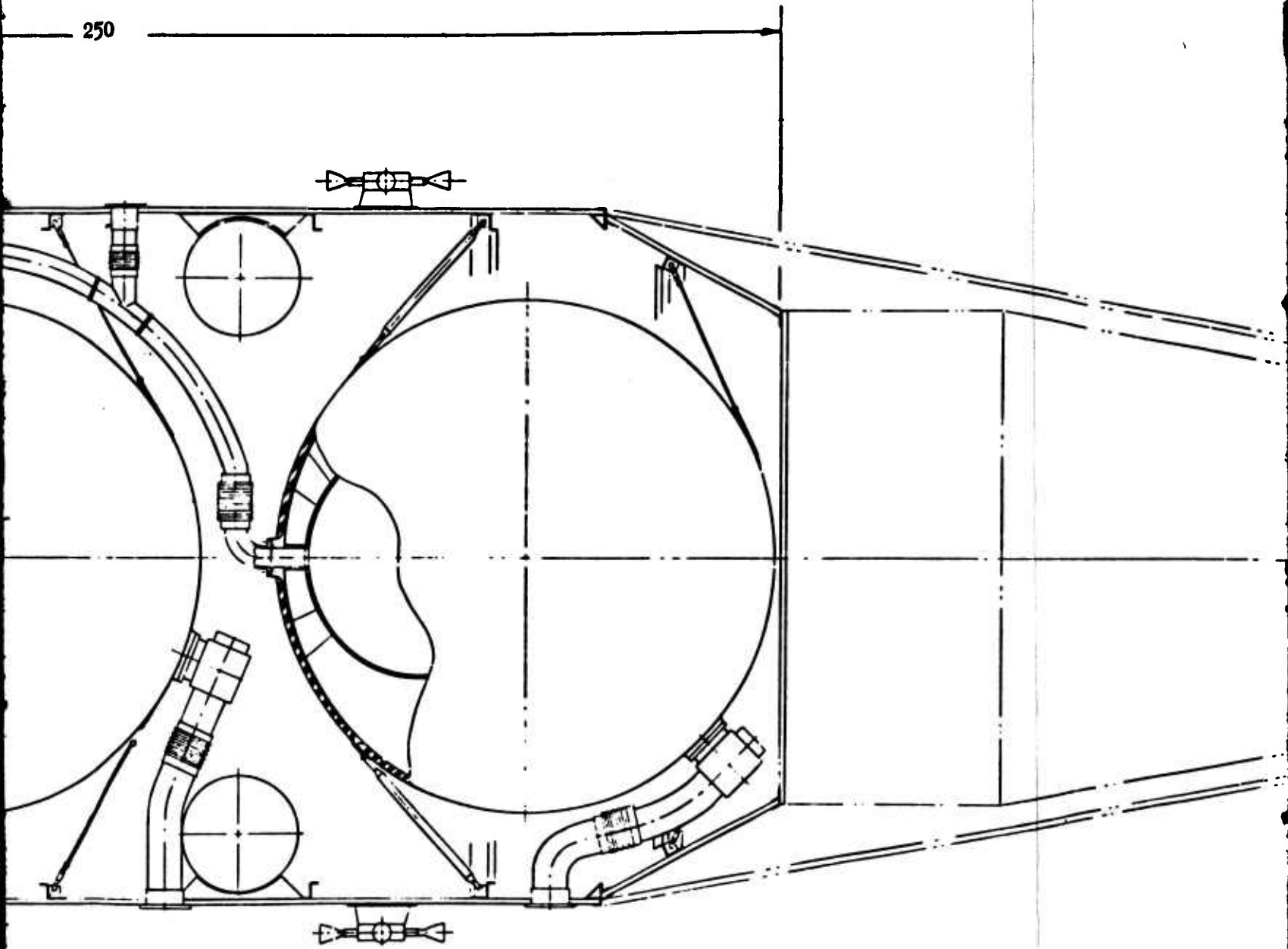
Figure 91. Hydrogen Vapor Pressure as a Function of Storage Time, For 10 Percent Remaining on First Day, Hydrogen Pressurant



**CONFIDENTIAL**

1

250



**CONFIDENTIAL**

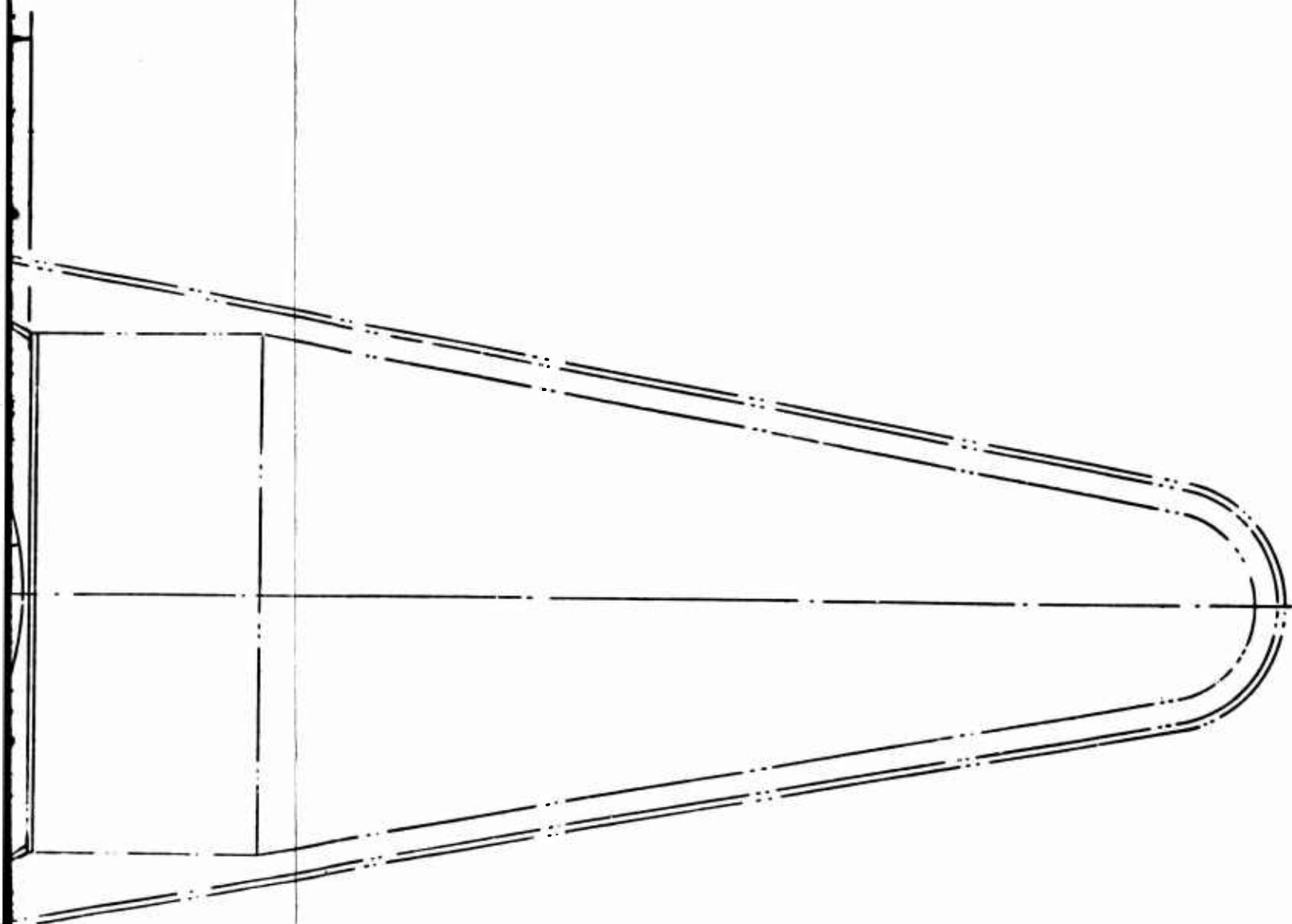


**Figure 92. Storable Propellant Alternate Mission Vehicle, 5000-Pound Payload**

191/192

3

# CONFIDENTIAL

## b. Propellant Heating

- (1) (C) Thermal Environment. The thermal environment of the  $N_2O_4/N_2H_4$ -UDMH (50-50) vehicle is qualitatively the same as that of the two cryogenic vehicles. However, for the storable propellant, vehicle temperature control in orbit is the most important factor in the performance of the vehicle. Ground hold and aerodynamic heating were negligible factors.
  - (a) (U) Prelaunch Phase. The maneuvering propulsion vehicle using storable propellants will have no performance degradation for any ground hold conditions in which its Titan III-C launch vehicle will operate.
  - (b) (U) Boost Phase. The boost phase has no significant effect upon the orbital storage of the  $N_2O_4/N_2H_4$ -UDMH (50-50) propellants since the temperatures experienced by the propellants during boost are within the allowable range for both propellants. Heating of the ullage space may create the need for venting during boost. However, the Titan-III Transtage does not have a venting requirement so that venting during boost is an unlikely requirement.
  - (c) (U) Orbital Phase. The orbital phase calculations were performed using the two limiting orbital orientations shown in Fig. 64. The polar orbit with side wall toward the sun is the maximum heating condition. The equatorial orbit with payload toward the sun is the minimum heating condition.
  - (d) (U) Internal Heating Effects. The analytical methods used in determining the internal heating effects on the storable propellants are identical to those used in the analysis of the cryogenic systems. Since the pressurization system of the  $N_2O_4/N_2H_4$ -UDMH (50-50) vehicle uses ambient helium (within the usable temperature range of the propellants), no energy balance is necessary and the pressurization gas and propellants are in continuous thermal equilibrium.
- (2) Storage System Analysis
  - (U) The primary result of the thermal analysis is that either insulation or a variable outer wall coating is necessary for storage of the  $N_2O_4/N_2H_4$ -UDMH (50-50) propellant combination for all possible orbital heating conditions. The vehicle can be designed to operate indefinitely in a given orbit and vehicle orientation without insulation; however, it cannot then operate under other orbital heating conditions for long periods of time.
  - (U) The possible propellant and wall temperatures of a vehicle in a 100 nautical mile orbit are shown in Fig. 93 as a function of the solar absorptivity-to-infrared emissivity ratio of the vehicle outer wall ( $\alpha/\epsilon$ ). Curve A is a representation of the possible wall temperatures for a polar orbit with the sidewall oriented toward the sun. This temperature does not vary with

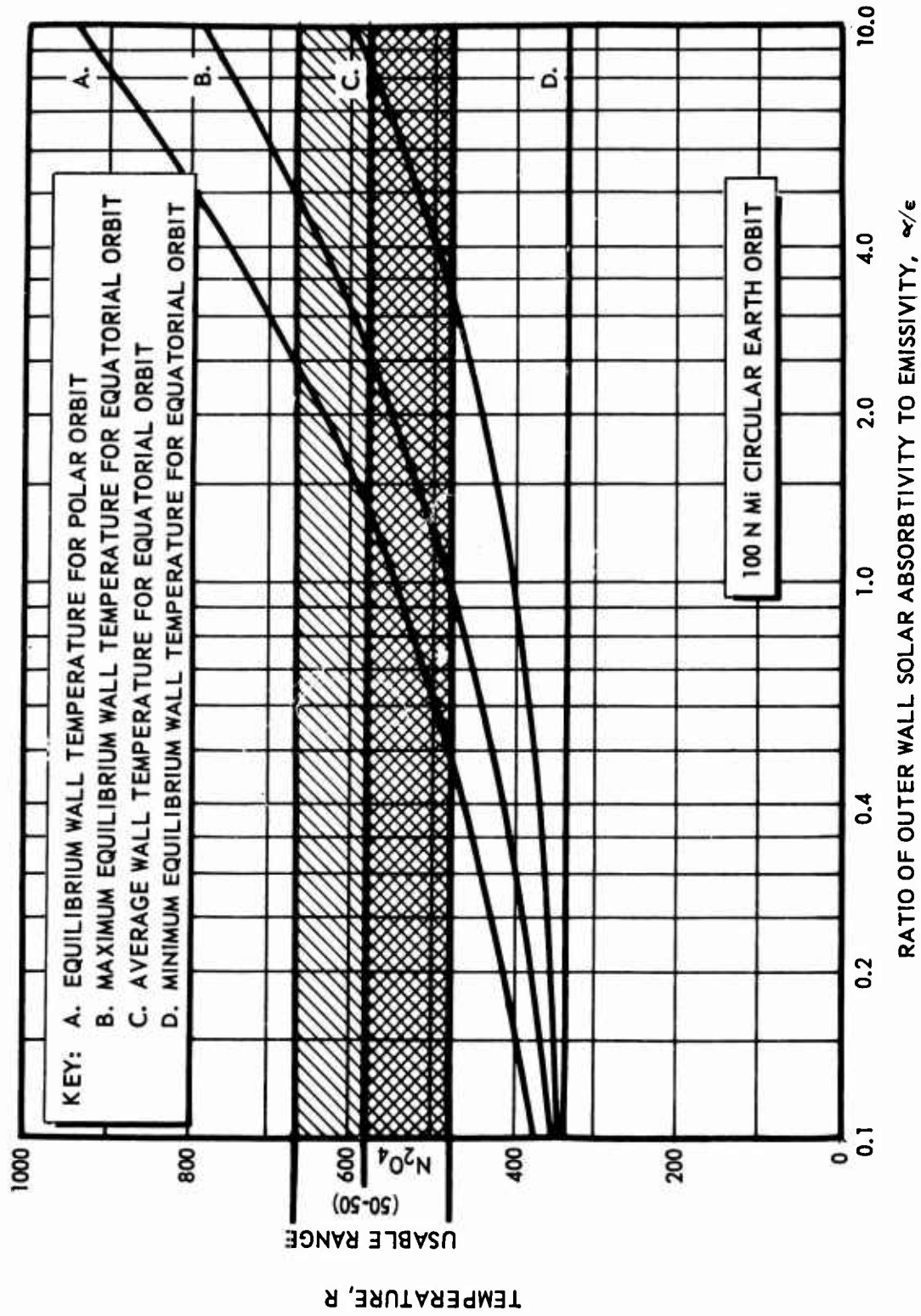


Figure 93. Wall Temperature Ranges for a Vehicle in 100 n mi Circular Earth Orbit

orbital position since the orientation of the vehicle with respect to the sun and earth does not change (Fig. 64). For very long storage times, the entire vehicle will reach this temperature.

- (U) Curves B, C and D of Fig. 93 are illustrations of the possible temperatures that could be experienced by a vehicle in an equatorial orbit with its payload toward the sun blocking all direct solar radiation. The range of temperatures of the outer wall of an insulated vehicle is shown in curves B and D. The change in temperature between these extremes is shown in Fig. 94 as a function of orbital position. With these temperatures a low wall heat capacity is assumed.
- (U) The average propellant temperature for a vehicle having very high wall-to-propellant conductivity is shown in Curve C. In this case, the wall temperature is almost equal to the propellant temperature. It was found that the propellant temperature varies from this average value by less than 1 degree during each orbit. The range of temperatures for which the storable propellants neither freeze nor require venting is shown shaded in Fig. 93 for each propellant. There is no single value of  $\alpha/\epsilon$  that will allow the propellants to stay in equilibrium in both a polar and equatorial orbit (one for which both curve A and C are in the allowable range). Therefore, either a variable wall configuration must be used so that the vehicle can adjust its  $\alpha/\epsilon$  to any orbit condition or one  $\alpha/\epsilon$  value must be chosen and insulation used to protect the propellants in other orbits for which this value does not attain an equilibrium temperature in the allowable range.
- (U) The only method of storing the  $N_2O_4/N_2H_4$ -UDMH (50-50) propellant combination indefinitely in any orbit that is not specified in advance is with a variable outer wall  $\alpha/\epsilon$ . This variation could be achieved by use of rotating panels in the outer wall. One side of each panel could have a very low value of  $\alpha/\epsilon$ , the other side a high value. By varying the combination of panels turned outward, a variety of average vehicle  $\alpha/\epsilon$  values could be obtained. An onboard sensing system would be necessary to control the vehicle temperature by using the rotating panels. The use of rotating panels has the advantage of being adaptable to higher orbits for which the temperature range during an orbit and from orbit to orbit becomes wider. If vehicle orientation could be used for the purpose of thermal control, panels of the exterior surface with different  $\alpha/\epsilon$  coatings could be used in conjunction with vehicle orientation to achieve the effect of a variable  $\alpha/\epsilon$  system.
- (U) If a variable  $\alpha/\epsilon$  system is not used, insulation will be necessary for the vehicle tanks. An insulation system similar to that used on the cryogenic vehicles with NRC-2 type insulation could be used. The choice of  $\alpha/\epsilon$  is dictated by the choice between venting and freezing of the propellants. Since the  $N_2H_4$ -UDMH (50-50) fuel can sustain higher temperatures than the  $N_2O_4$ , the choice of allowing the vehicle temperatures to go above the allowable for some orbits should result in less insulation (for the  $N_2H_4$ -UDMH (50-50) tank) than the choice of allowing the propellants to approach freezing temperatures. For this reason, an  $\alpha/\epsilon$  value of 3.5 was selected. This  $\alpha/\epsilon$  is easily obtainable as shown in Appendix V.

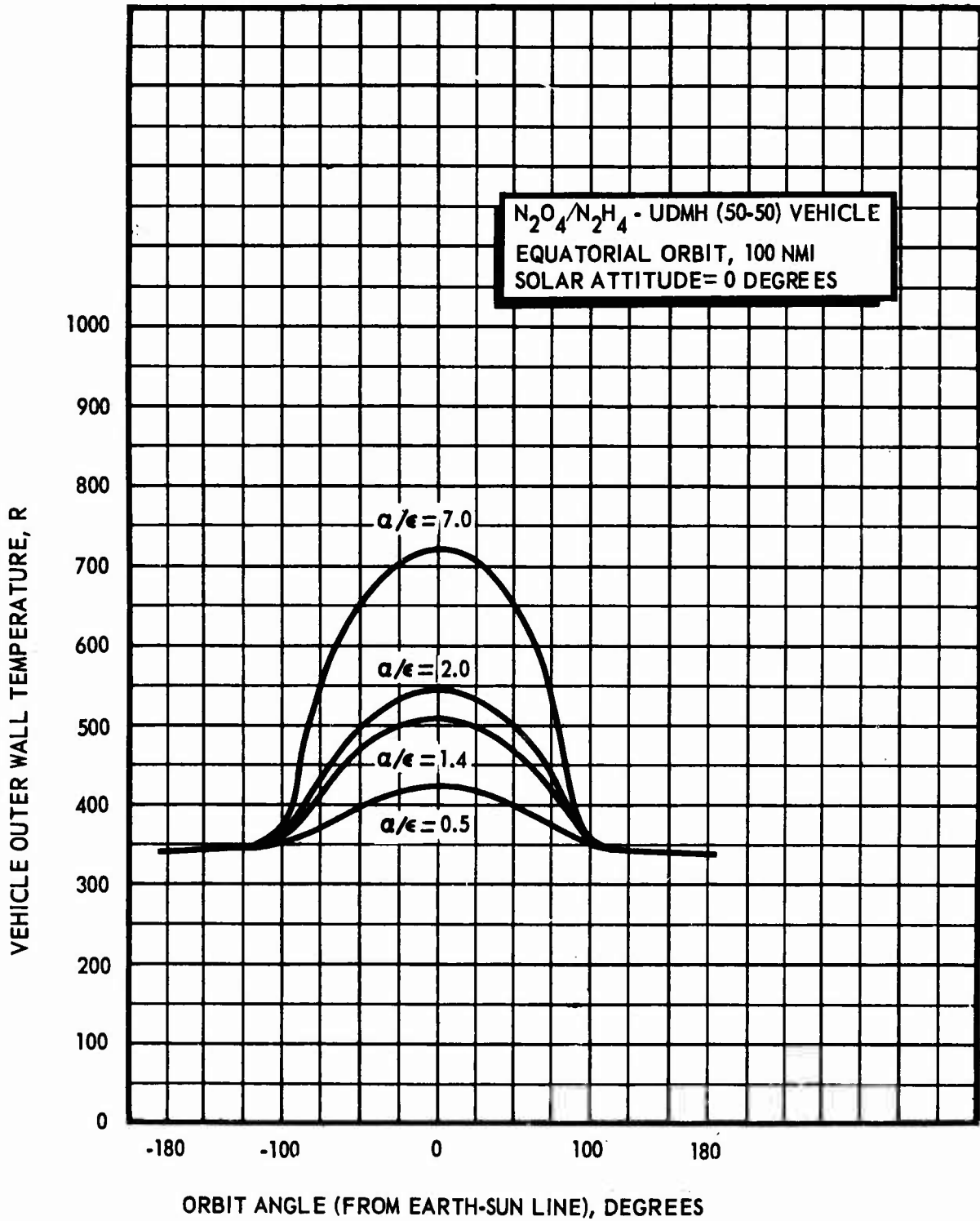


Figure 94. Vehicle Outer Wall Temperature as a Function of Orbital Position

- (U) Using the value of 3.5 for outer wall  $\alpha/\epsilon$ , the insulation thickness necessary to store the propellants a given length of time before venting is required, was calculated. The required insulation thickness is shown in Fig. 95 for a starting temperature of 530 R. This initial vehicle equilibrium temperature has been shown to be a reasonable estimate based on Agena vehicle flight results.
- (U) Although the propellant can be stored for long periods of time by the application of insulation, the pressurization system for partial burn duty cycles may be adversely affected. If the vehicle is in an orbit for which the equilibrium temperature is low, the pressurant temperature during a firing will be low. If the vehicle then transfers to an orbit for which the equilibrium temperature is high, the pressurant temperature and pressure will increase. Since the pressurant in the ullage was originally at the tank run pressure and there is no pressure collapse as there is with cryogenics, some pressurant must be vented to avoid exceeding the run pressure. For a vehicle going from a high-temperature orbit to a low-temperature orbit, additional pressurant is necessary to counter the pressure decrease in the tank. The only solution is to supply excess pressurant before the start of a mission and to provide some form of pressurant venting.
- (U) An MSPS using the  $N_2O_4/N_2H_4$ -UDMH (50-50) propellant combination can be designed to operate in space for long periods of time without major performance loss. However, design restrictions necessary to achieve this storage may impose slight weight penalties upon the vehicle. If a vehicle coating having a solar absorptivity-to-emissivity ratio of 3.5 is used and two inches of NRC-2 type insulation is applied to the propellant tanks, storage times of over 5 years can be obtained for any orbit and attitude with full tanks. Ten percent full tanks have significantly shorter storage times. Designs are possible that could give indefinite storage by using a variable  $\alpha/\epsilon$  shroud; however, the weight of such designs is probably greater than that of an insulated system.

## 6. STORAGE LIFE COMPARISON

- (U) The parametric storage system analyses previously discussed were used to define the most efficient thermal storage systems for each of the three propellant combinations. The relative performance capabilities vs storage time of the three systems were then compared based upon the most realistic mission thermal environment. Two limiting duty cycles were considered in the study. The first of these, extended orbital coast with full tanks, is critical in determining ullage requirements. The second, extended orbital coast with 10 percent of the propellant remaining is critical in determining pressurization system effects, heat input effects and insulation requirements.
- (U) The preorbital heating included in the comparison consists of the aerodynamic heating encountered during a Titan III-C launch trajectory. The effects of a short ground hold were also included based upon the launch procedure for current vehicles. The launch procedure time schedule shown

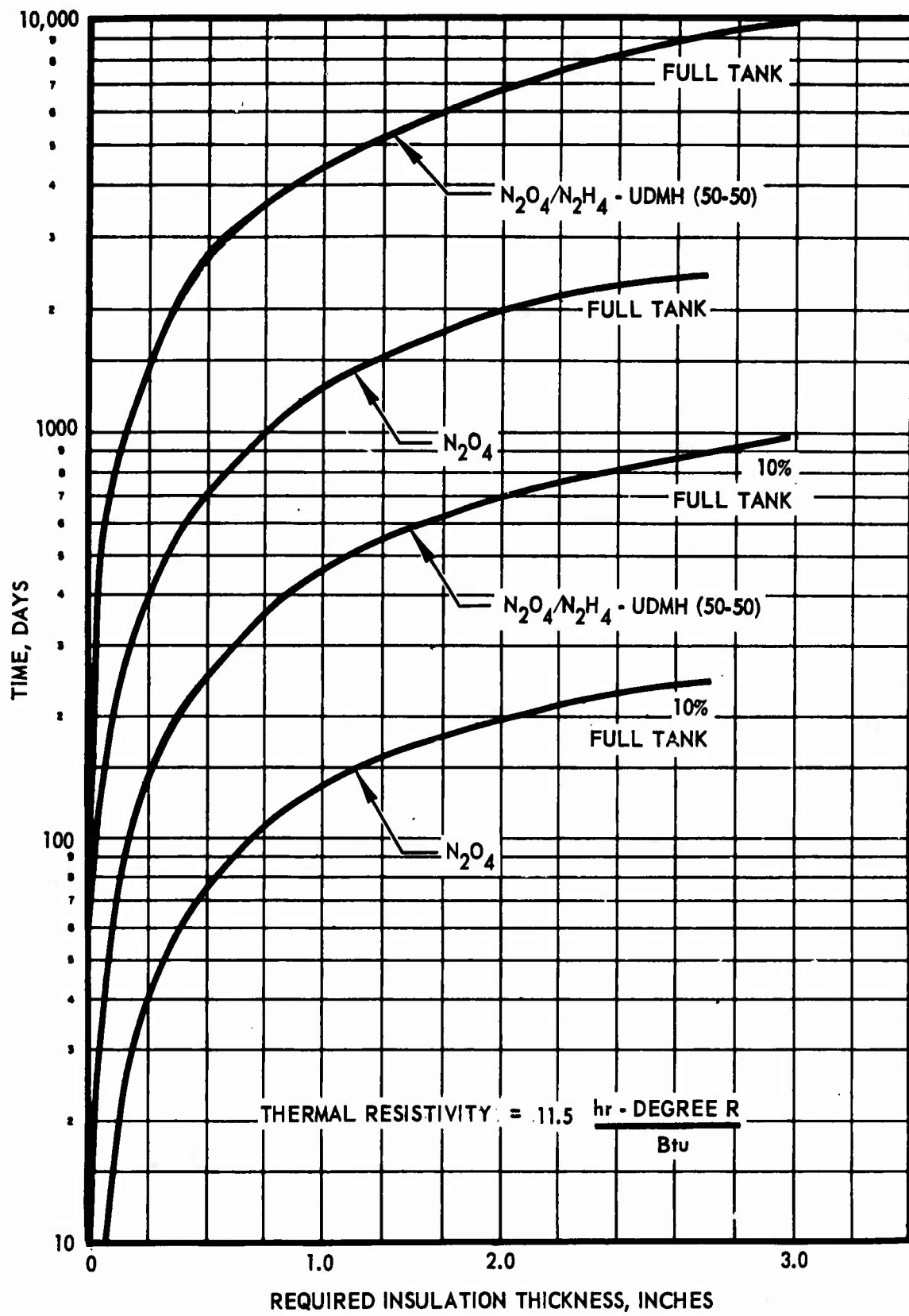


Figure 95. Required Insulation for NTO/50-50 Vehicle  
2% Ullage in Both Tanks

# CONFIDENTIAL

in Table XXXVIII for a Centaur vehicle, indicates that the LH<sub>2</sub> tank is closed approximately 7.0 seconds before launch and the tank can be topped off until this time. Similarly the LO<sub>2</sub> tank of the Atlas is closed less than 2 minutes prior to liftoff.

- (C) The mission performance or  $\Delta V$  comparison is presented for 20,000-pound gross weight MSPS with 2000-pound payloads. The effect of increased gross weights and/or increased payload will be shown in a later section. The  $\Delta V$  capability for each system was calculated for a series of individual design points dependent upon the storage time. The results are presented as normalized  $\Delta V$  for the three propellant combinations for full tanks and for 10-percent full tanks.

- a. Storage System Design Selection

- (U) The design requirements for the storage systems of each of the propellant combinations were found using the methods of thermal analysis described in the previous sections. Using the ullages and insulation thicknesses necessary to store the propellants a given number of days, the vehicle inert weights and  $\Delta V$  capabilities were determined. The vehicles were unvented by increasing the ullage volume and by applying insulation until the heat leak through the wall and tank connections became dominant and venting became unavoidable; i.e., a different vehicle thermal design for each storage period until venting occurs. The maximum insulation thickness used for the vehicles before venting became necessary was 6 inches. Vehicle size and insulation material limitations probably would make thicker insulations unattractive.
- (U) The point designs are not necessarily optimum designs since tradeoffs were not performed between ullage, insulation weight, pressurization-system weight, and venting methods for the various storage times. However, the variation in  $\Delta V$  capability from the optimum system would be very small. For example, venting the tanks sooner than the time chosen could result in an insulation weight saving that may result in a higher overall  $\Delta V$  for particular missions. However, since the mission cannot be specified in advance, the philosophy was adopted of storing as long as possible in the unvented mode. The same philosophy was applied in choosing tank ullages. By increasing the ullage volume, the full tanks can remain unvented longer than the 10-percent full tanks, but the additional ullage results in a slight penalty to the storage time of the 10-percent full tanks. Finally, the pressurant temperature of the hydrogen was reduced from 960 R to 250 R to improve the storage capabilities of the cryogenic vehicles without performing a temperature optimization. Recent studies conducted by Douglas Aircraft Company have indicated that a pressurant injection temperature of near 200 R is the optimum design for this application. A review of these results is presented in Appendix VI.
- (U) A summary of the present selection and alternate choices of the thermal protection concepts is presented in Table XXXIX; a summary of the vehicle design parameters is given in Table XL.

# CONFIDENTIAL

TABLE XXXVIII

CENTAUR LAUNCH COUNTDOWN  
ATLAS-CENTAUR NO.5, MARCH 1965 LAUNCH

	T Count Time		Clock Time	
	Minutes	Seconds	Minutes	Seconds
Start LO <sub>2</sub> Chillover	-66	30	0	
Start LO <sub>2</sub> Tanking	-60		6	30
Start H <sub>2</sub> Chill	-50		16	30
LO <sub>2</sub> System Secured at 60 Percent	-50		16	30
Start H <sub>2</sub> Tanking	-29	30	37	3
Start LO <sub>2</sub> Topping	-21	20	45	10
LO <sub>2</sub> Readout at 99.1 Percent Full Hold	-5		63	30
Centaur LO <sub>2</sub> Topping	-5		96	48
Automatic Countdown Phase		-13.05	106	34
LO <sub>2</sub> Tank Pressurized		-7.62	106	29
H <sub>2</sub> Vent is Closed		-7.35	106	29

TABLE XXXIX

MANEUVERING PROPULSION SYSTEM THERMAL  
PROTECTION DESIGN

Design Feature	Present Selection	Alternate Choices
	<b>Cryogenic Vehicles</b>	
Payload Shielding	Aluminum Foil	Superinsulation
High Resistivity Fill and Vent Lines	Stainless Steel Lines	Heat Blocks Detachable Lines
Low Conductivity Supports	Fiberglass Tubing and Fiberglass Straps	Stainless Steel Wires Stainless Steel Conic Section
Tank Insulation	NRC-2 Type with no Substrate, Tank Mounted	Dimplar Mylar and Paper Shroud Mounted Fiberglass Substrate
Wall Temperature Control	Zirconium Silicate in Potassium Silicate	Zinc Oxide in Potassium Silicate White Porcelain Enamel
Line Venting	Return to Tank Ullage	Used to Cool Heat Sources then Dumped
Pressurant Temperature Control	Propellant Feed Line Heat Exchanger for $\text{GH}_2$	Gas-Liquid Mixing Pressurant Venting
Tank Venting	$\text{LH}_2$ Vent Used to Cool Oxidizer Tank  Thermodynamic Vent Device	Vented to Space  $\text{LH}_2$ or Oxidizer Venting Used to Cool Shroud
High Resistivity Feed Lines	Stainless Steel Lines with Stainless Steel and Fiberglass Heat Blocks	Filament Wound Heat Blocks Filament Wound Lines

TABLE XXXIX  
(Concluded)

Design Feature	Present Selection	Alternate Choices
	$N_2O_4/N_2H_4$ -UDMH (50-50)	
Payload Shielding	None	Aluminum Foil Superinsulation
High Resistivity Fill and Vent Lines	Same as Cryogenics	
Low Conductivity Supports	Same as Cryogenics	
Tank Insulation	NRC-2 Type with no Substrate, Tank Mounted	Uninsulated Mylar Paper
Wall Temperature Control	Gold on Magnesium Sections of Black Kemacryl	Rotating Panels of Gold on Magnesium and Zirconium Silicate in Potassium Silicate
Pressurant Temperature Control	None Needed	
Tank Venting	None Needed	
High Resistivity Feed Lines	Same as Cryogenics	

TABLE XL

## PROPULSION SYSTEM DESCRIPTION

	System					
	LF <sub>2</sub> /LH <sub>2</sub>		LO <sub>2</sub> /LH <sub>2</sub>		N <sub>2</sub> O <sub>4</sub> /N <sub>2</sub> H <sub>4</sub> -UDMH (50-50)	
Propellant	LF <sub>2</sub>	LH <sub>2</sub>	LO <sub>2</sub>	LH <sub>2</sub>	N <sub>2</sub> O <sub>4</sub>	N <sub>2</sub> H <sub>4</sub> -UDMH (50-50)
Pressurant	He	H <sub>2</sub>	He	H <sub>2</sub>	He	He
Pressurant Temperature, R	500	250	500	250	500	500
Maximum Vapor Pressure, psi	23	58	23	58	23	23
Ullage, percent	2.0	15.0	3.0	15.0	2.0	2.0
Thermal Resistivity, hr-R/Btu	115	115	115	115	115	115
Outer Wall $\alpha/\epsilon$	0.185	0.185	0.185	0.185	3.5	3.5
Outer Wall Temperature (maximum), R	405	405	405	405	730	730
Ground Hold Time, seconds	360	60	360	60	-	-

- (U) A correlation of the calculated heating rates with experimental data is presented in Appendix VIII. These results compare the actual boiloff rates in an environment simulated test with the calculated values obtained in this study.
- (1) (U) LF<sub>2</sub>/LH<sub>2</sub> Vehicle Design Requirements. The ullage required for the liquid hydrogen tank is shown in Fig. 96 as a function of storage time. This ullage was chosen to keep the full tank from venting for the design point storage time.
- (U) A maximum ullage volume of 15 percent permits the liquid hydrogen to expand in the tank until a temperature is reached which corresponds to the maximum design hydrogen vapor pressure of 58 psia. Therefore, the full hydrogen tank must be vented after 167 days based upon the established heating rates. A 2-percent ullage was maintained for the fluorine tank as this corresponds to the density increase for the maximum vapor pressure limit.
- (U) The insulation thickness required on each of the tanks is shown in Fig. 97 as a function of time before venting is required. The limiting time is based upon the 10-percent full tanks. Ullage volume is increased from 5 to 15 percent as storage time is increased to delay the necessity of venting. The fluorine tank insulation thickness was chosen to keep the tank from venting until the hydrogen tank begins venting.
- (U) Both tanks were kept unvented as long as possible by increasing the ullage and adding insulation. However, a practical limit was set for insulation thickness, and, when this limit is reached, the fluorine tank must be maintained unvented by other methods. After the hydrogen tank begins to vent, the fluorine tank can be cooled with the hydrogen vapor. Therefore only enough insulation was used on the fluorine tank to keep it from venting until the hydrogen began venting.
- (U) The necessary thermal conditioning system would consist basically of an expansion unit which acts as a liquid vapor separator for the hydrogen tank, a heat exchanger unit for the fluorine tank, and associated control components. A mixer unit may also be required. The operation would be to expand the vented hydrogen and pass it through a heat exchanger to remove or intercept the heat entering the fluorine tank and then vent the heated vapor overboard. Several heat exchanger locations are possible: (1) on the fluorine tank surface; (2) in the fluorine tank bulk fluid; or (3) at maximum heat input points such as the tank supports and feed lines. For purposes of analysis, the complete unit was assumed to weigh 20 pounds.
- (2) (U) LO<sub>2</sub>/LH<sub>2</sub> Vehicle Design Requirements. The ullage requirement for the hydrogen tank is shown in Fig. 96 vs storage time. A constant ullage of 3.0 percent was maintained for the oxygen tank.

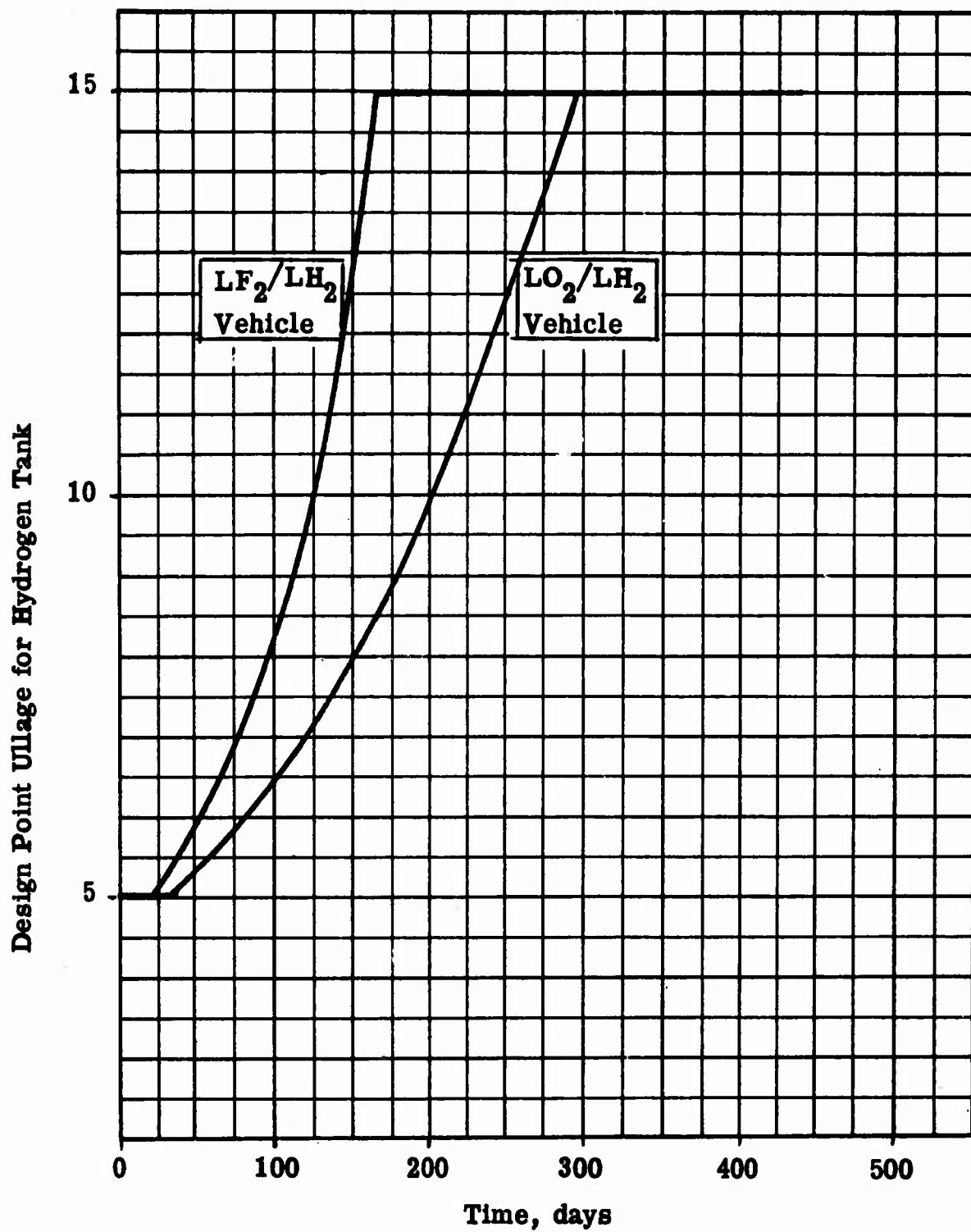


Figure 96. Design Point Ullage as a Function of Time for Performance Comparison

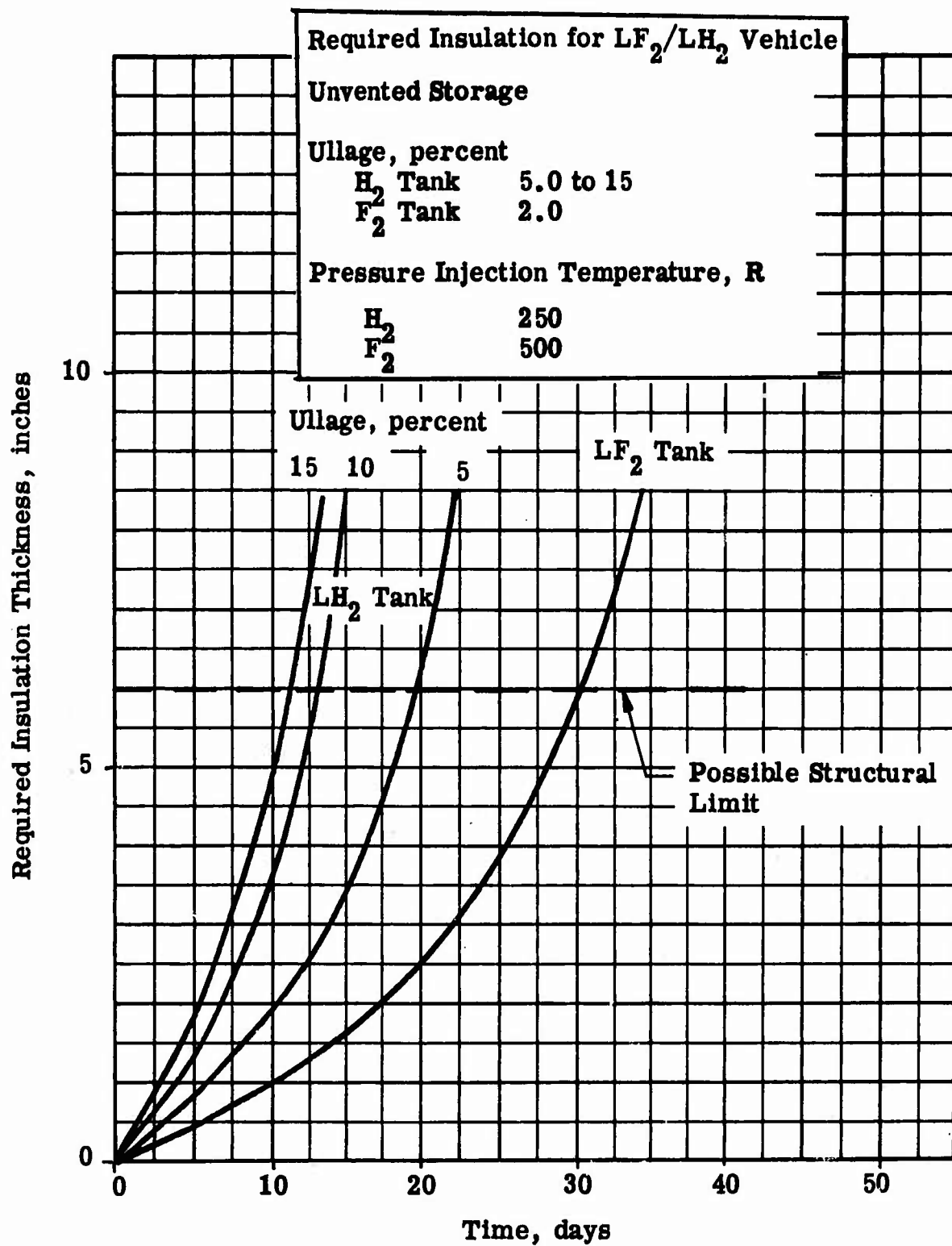


Figure 97. Point Design Insulation Thickness as a Function of Required Storage Time.

- (U) The insulation requirements of the  $LO_2/LH_2$  vehicle are shown in Fig. 98 as a function of storage time. The requirements for the hydrogen tank are similar to those for the  $LF_2/LH_2$  vehicle. The oxygen tank requires less insulation than the fluorine tank since the 10-percent full oxygen tank begins venting immediately independent of insulation thickness because of the high vapor pressure of the oxygen. The fluorine tank was insulated to prevent venting. The oxygen tank insulation was therefore chosen to prevent venting the full tank and to keep the venting loss rate from the 10-percent full tank low.
- (U) The hydrogen tank was maintained unvented until 6 inches of insulation were required. At this point, hydrogen venting cannot be avoided. Venting of the full oxygen tank is not required; however, continuous venting of the 10-percent full oxygen tank is necessary.
- (3) (U)  $N_2O_4/N_2H_4$ -UDMH (50-50) Vehicle Design Requirements. The only variable design requirement of the  $N_2O_4/N_2H_4$ -UDMH (50-50) is the insulation thickness. The 2-percent ullage for both tanks is the maximum required and the vehicle can be kept unvented for longer times than the cryogenic vehicles by adding insulation. The required insulation thickness are shown in Fig. 99 as a function of storage time.

b. Specification of Duty Cycle

- (U) The two duty cycles evaluated in the relative system performance capabilities are specified by the percentage of fuel remaining at the beginning of orbital coasting (the percentage of oxidizer is somewhat higher). The selected duty cycles were previously described as full propellant tanks and 10-percent full tanks. The system performance,  $\Delta V$ , is given for the condition where the final burn (or the only burn for the full tank case) is accomplished at the end of the specified duty cycle. The propellant storage system is designed to be capable of performing either duty cycle.
- (U) The tank pressure history experienced in the full tanks and the corresponding propellant vaporization is described in general in Fig. 100. From zero time to (1), the vapor pressure increases due to preorbital heating and subsequent propellant vaporization. The vapor pressure rise experienced during orbital coast is shown between (1) and (2) and the  $LH_2$  expands to nearly fill the tank at (2). At (2) the maximum hydrogen vapor pressure is reached and the hydrogen tank must be vented for longer storage durations and the vapor pressure remains constant. At (3), the tank is pressurized to (4) for propellant expulsion and engine firing.
- (U) A general description of the tank pressure history and propellant vaporization for the 90/10 duty cycle is presented in Fig. 101. The vaporization and pressure increase due to preorbital heating is shown between zero and (1). The vehicle fires immediately after achieving orbit and the tank is pressurized at (1). The tank then comes to equilibrium, vaporizing some propellant and leaving 10 percent as liquid (3). The vehicle then coasts until 58-psia vapor pressure is reached in the hydrogen tank by the

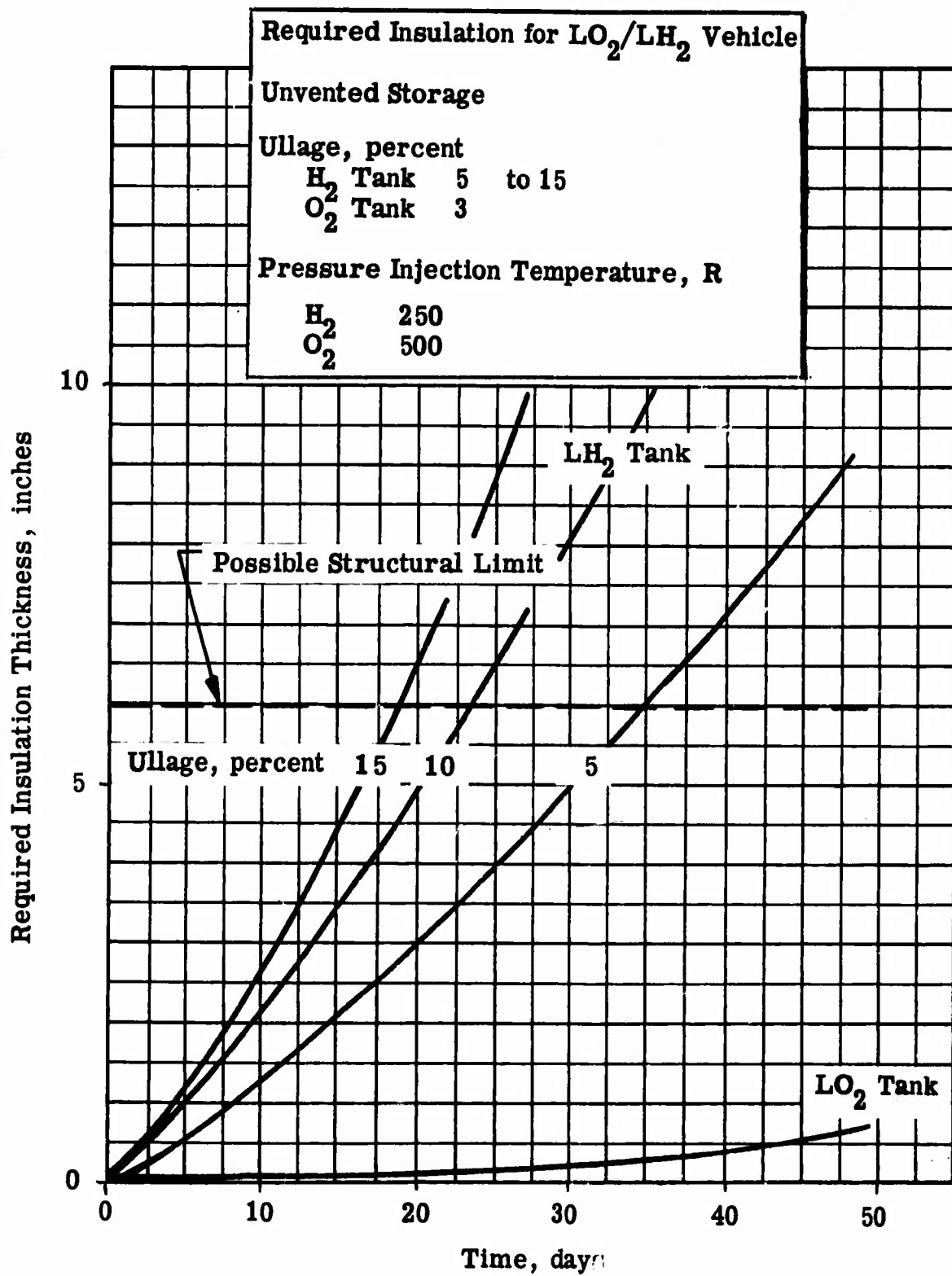


Figure 98. Point Design Insulation Thickness as a Function of Required Storage Time

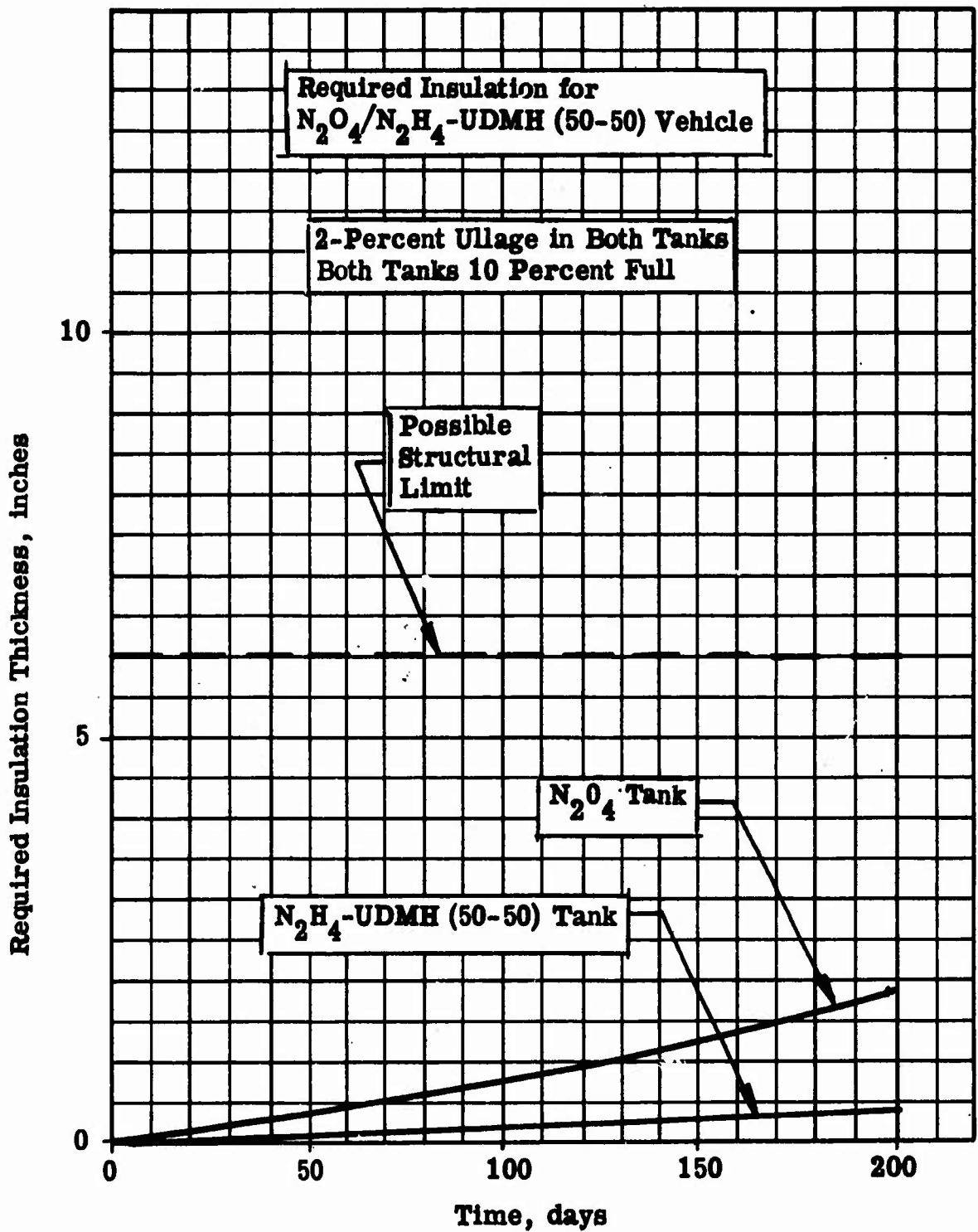


Figure 99. Point Design Insulation Thickness as a Function of Required Storage Time for the  $N_2O_4/N_2H_4$ -UDMH (50-50) Vehicle

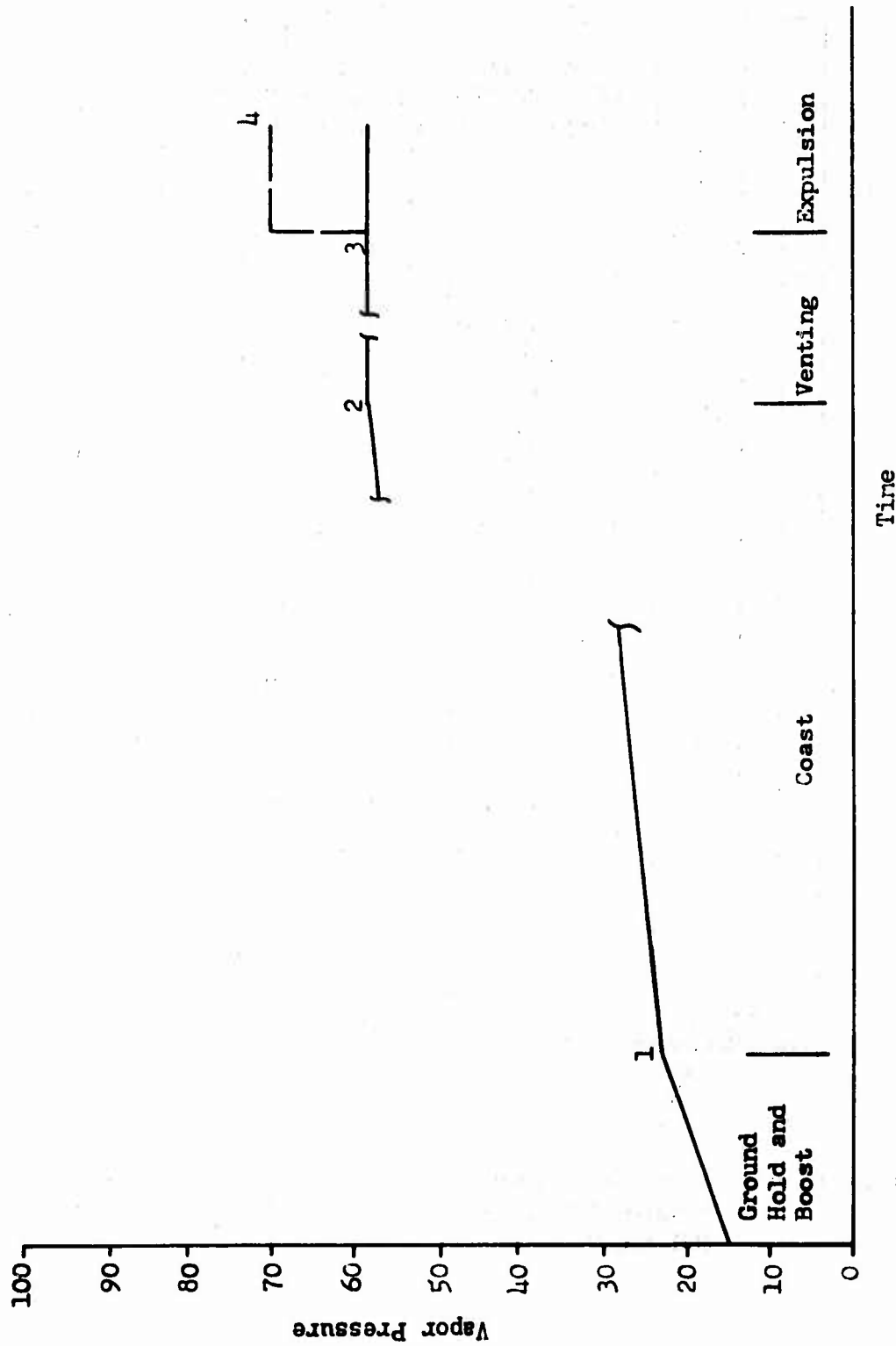


Figure 100 . Full Tank Cycle Pressure History (Hydrogen)

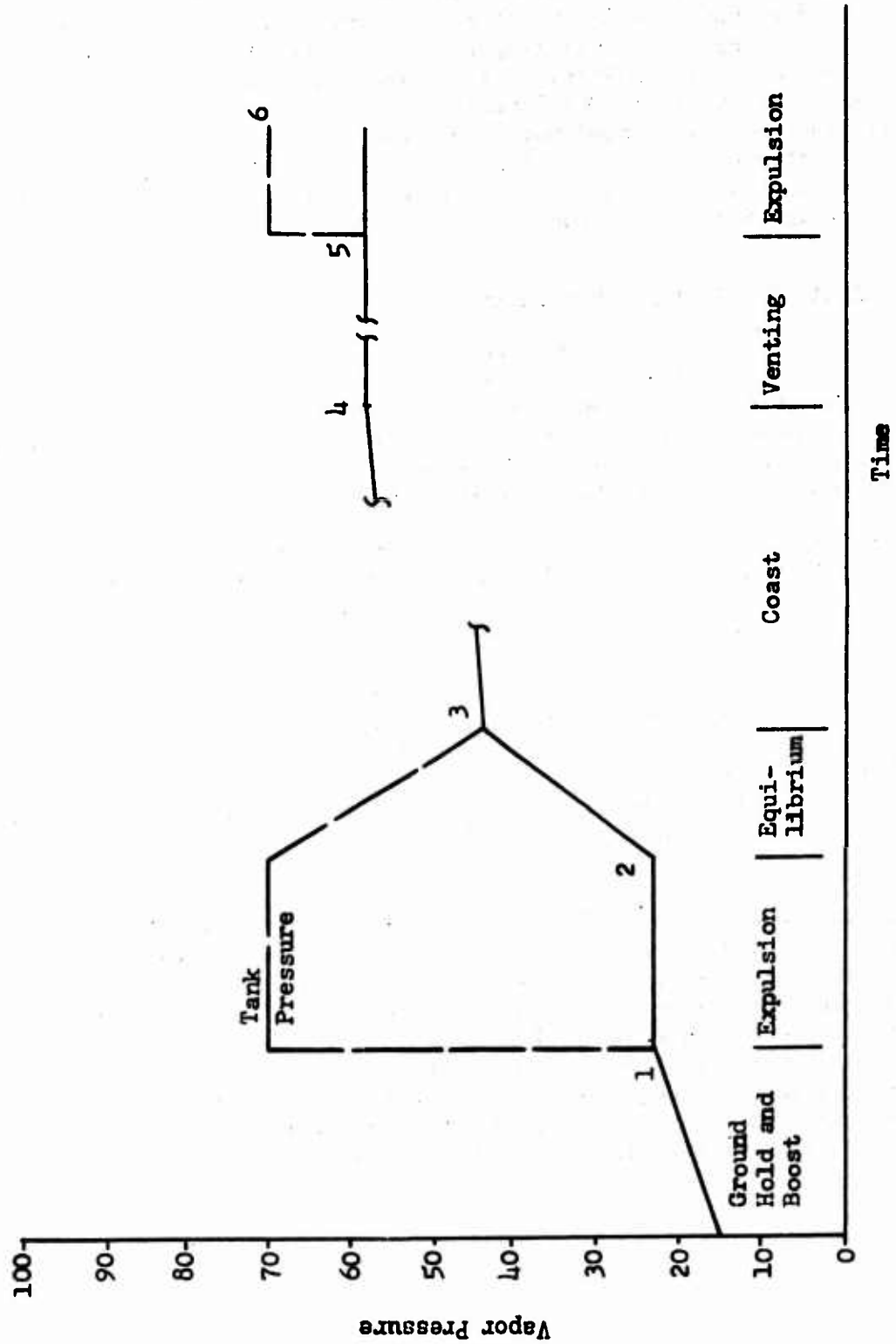


Figure 101. 90/10 Cycle Pressure History (Hydrogen)

# CONFIDENTIAL

continued vaporization of liquid (4). Additional vaporization (4) to (5) is then accommodated by venting. The tank is pressurized (5) to (6) for the final burn.

The time required to reach 58 psia and the venting rate are determined by the insulation thickness. A higher  $\Delta V$  is obtained if the vehicle is fired before the end of the specified storage period. The maximum vehicle  $\Delta V$  would be obtained if the engine were fired before the tank pressure has had a chance to decay after the first firing. As the pressurant cools by vaporizing the liquid propellant, the available  $\Delta V$  of the second burn decreases until equilibrium is reached. This occurs in a relatively short time. The available  $\Delta V$  decreases during coast as additional propellant is vaporized and vented until the time for the last firing is reached. The performance curves in the following discussion represent the locus of the end points of a set of  $\Delta V$  vs time curves for specific point designs of ullage and insulations.

## c. Mission Performance Capabilities

- (C) All the velocity increment calculations were based upon the 20,000-pound gross weight 2000-pound payload design. The effects of changing gross weight or payload weight will be discussed in a later section. The weight of a venting device was included in the inert weight of the vehicles after venting became necessary. The weight of the device was estimated to be 20 pounds, including the thermal conditioning system for the oxidizer tank.
- (U) The performance capabilities are shown in Fig. 102 for the three vehicles with full tanks. The performance is that obtained for complete expulsion on the last day of storage. All  $\Delta V$  values have been normalized to the 14-day value for the  $LF_2/LH_2$  vehicle reported in Ref. 2.
- (U) With full (fixed mixture ratio) propellant tanks, the  $LF_2/LH_2$  combination has better performance than the  $N_2O_4/N_2H_4$ -UDMH (50-50) for storage times less than 400 days and better performance than the  $LO_2/LH_2$  combination for storage times less than 290 days. If the initial tank mixture ratios are adjusted for the cryogenic systems, the propellant storage capabilities can be improved considerably.
- (U) The solid lines in Fig. 102 represent systems that have an initial tanked mixture ratio of 13:1 for  $LF_2/LH_2$  system, 6:1 for  $LO_2/LH_2$  system, and 1.8:1 for  $N_2O_4/N_2H_4$ -UDMH (50-50) system. These curves are characterized by the region where insulation is being added to each point design for storage times from zero to approximately 3 weeks for the cryogenic systems. In the next region where the  $\Delta V$  drops off more gradually with storage time, the initial tank ullage volume has been increased for each point design until an  $LH_2$  tank ullage volume of 15 percent is reached; for storage times beyond this point, hydrogen tank venting is required and the  $\Delta V$  capability is described by the solid lines.

CONFIDENTIAL

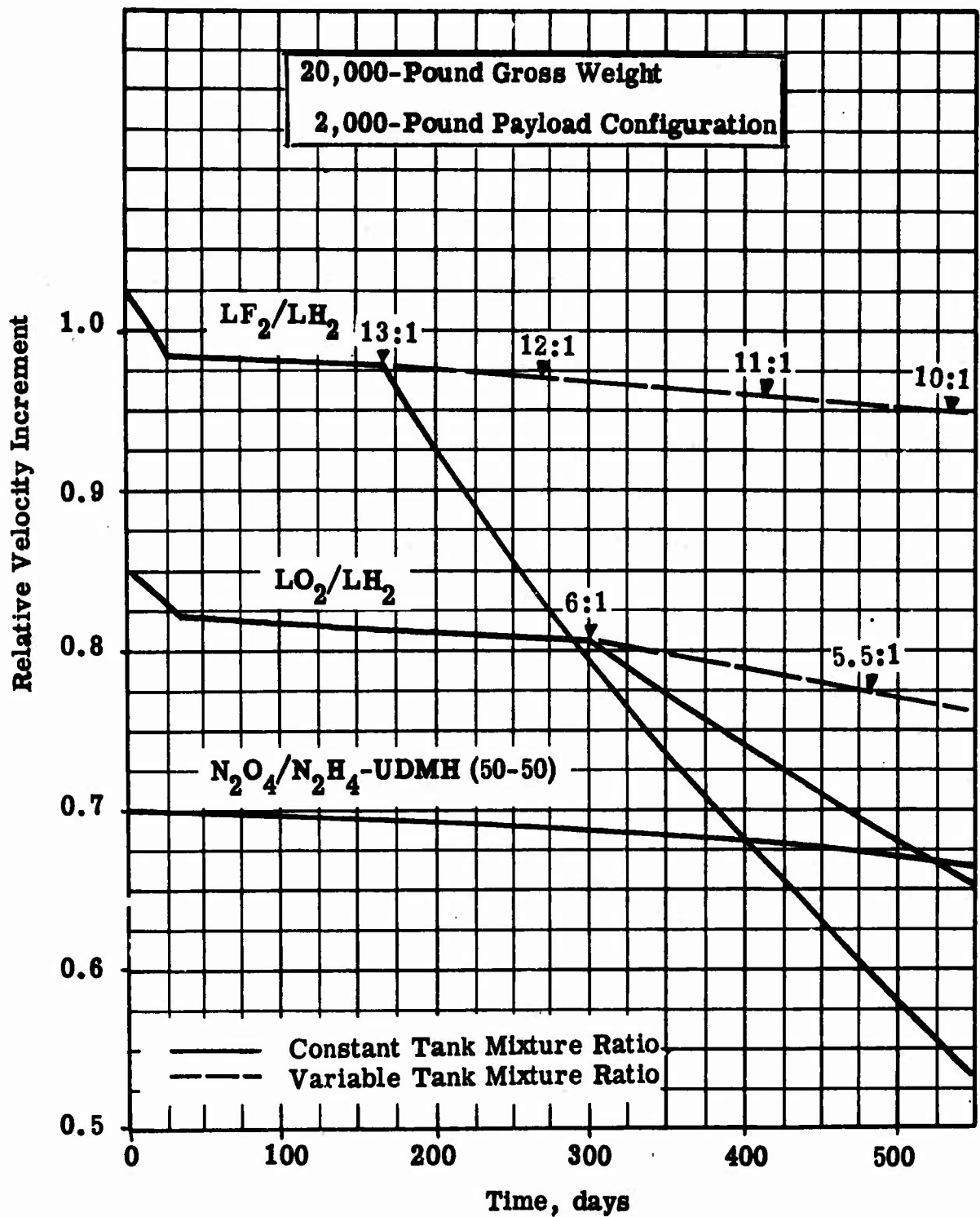


Figure 102. Vehicle Performance Comparison for Full Tank Complete Depletion Mission

CONFIDENTIAL

- (U) As an alternative to venting with a constant tank mixture ratio, the initial tanked propellant mixture ratio can be decreased such that the required hydrogen venting results in the design engine propellant mixture ratio being available at the end of the specified storage period. The  $\Delta V$  capabilities for the  $LF_2/LH_2$  and  $LO_2/LH_2$  systems under these conditions are represented by the dashed curves in Fig. 102.
- (U) In both cases, the engines operate at the design mixture ratios (13:1 for  $LF_2/LH_2$  and 6:1 for  $LO_2/LH_2$ ) for all storage times. There are two advantages to the variable initial tanked mixture ratio. The increased hydrogen weight improves the storage capabilities and there is no excess oxidizer remaining at the end of the storage period. In the constant tanked mixture ratio case represented by the solid line, the excess oxidizer is unavailable for propulsion and must be carried through the propulsive maneuver as inert weight.
- (U) These results indicate that very long storage times can be achieved with small  $\Delta V$  penalties for cryogenic systems by selection of proper tanked mixture ratio conditions. For this design philosophy the  $LF_2/LH_2$  system performance exceeds that of the  $LO_2/LH_2$  system for storage times of at least 2 years. The variable tanked mixture system performance is shown for storage times of just over 500 days; at this point the required tanked mixture ratios are approximately 5:1 for the  $LO_2/LH_2$  system and 10:1 for the  $LF_2/LH_2$  system.
- (U) The performance capabilities of the vehicles for the severe 90/10 duty cycle are shown in Fig. 103. The initial portion of the curve, to a storage time of approximately 20 days, is represented by vehicle point designs where the insulation thickness is progressively increased up to a maximum of 6.0 inches. At this point (or storage time) the hydrogen tank is vented. The point at which the curve breaks and becomes horizontal for the  $LF_2/LH_2$  system represents the storage time at which all of the remaining hydrogen has been vaporized, and the  $\Delta V$  capability shown is that achieved in the initial firing performed immediately after achieving orbit. The continued slight drop in the  $LO_2/LH_2$  system  $\Delta V$  is caused by the continued addition of insulation on the oxygen tank required for the full tank storage condition. The continuous increase in insulation thickness with storage time also explains the slight degradation in the performance of the  $N_2O_4/N_2H_4$ -UDMH (50-50) with time.
- (U) For the severe 90/10 duty cycle, the  $LF_2/LH_2$  vehicle has a higher total velocity increment than the  $N_2O_4/N_2H_4$ -UDMH (50-50) for storage times less than 115 days (Fig. 103) and higher than the  $LO_2/LH_2$  for all storage times. The  $LO_2/LH_2$  falls below the  $N_2O_4/N_2H_4$ -UDMH (50-50) after 35 days.

## 7. STORAGE SYSTEM SENSITIVITY ANALYSIS

- (U) In the preceding section nominal storage system design characteristics were selected and a mission performance comparison of the three propellant combinations was made to illustrate the effect of the propellant storage penalties on the overall mission performance as a function of

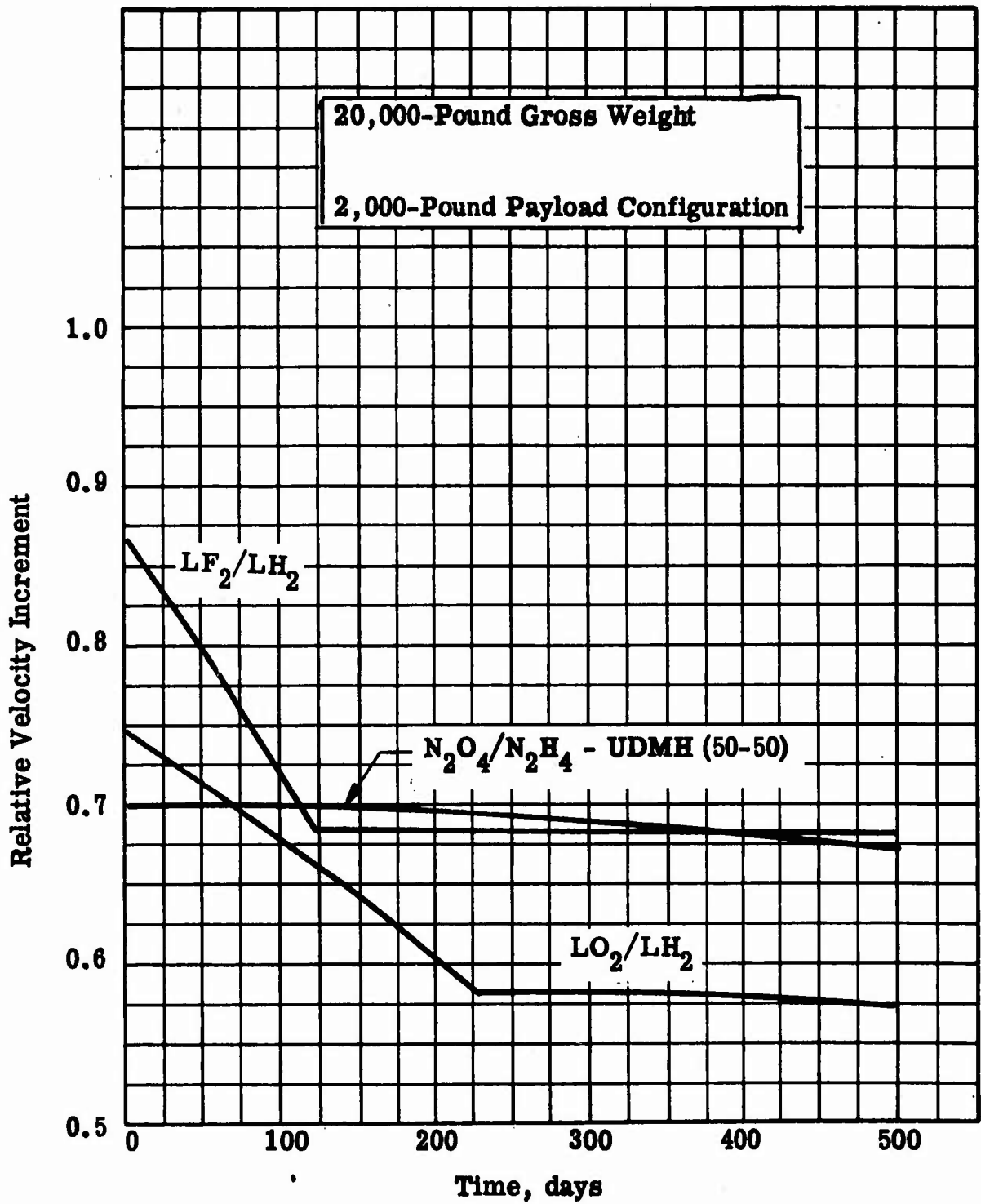


Figure 103. Vehicle Performance Comparison for 90/10 Duty Cycle Mission

storage time. The effects of alternate storage system design choices are presented in this section. The nominal storage system design that has been selected for each of the propellants represents sound compromises for the range of missions that the vehicle might be called upon to perform. However, more sophisticated designs or advanced concepts may improve the vehicle performance for specific mission applications. The results of the sensitivity analysis, which are presented in a parametric form, provide an indication of the areas where advanced design efforts may significantly benefit the storage capabilities of the MSPS.

- (U) Only the more important storage system design choices have been evaluated in the sensitivity analysis. These include heat conduction path resistivity, storage method, insulation, and external vehicle coatings. The effect of increased system gross weight and/or payload is also shown. Other system design variations may also benefit the storage capabilities and the effects may be derived from the parametric analysis presented in this report.

a. Effect of Thermal Resistivity of Wall-To-Tank Connections

- (U) Variations in the design of fill, vent, and feed lines and the tank supports can be illustrated by variation of the effective thermal resistivity. This resistivity can have a large range depending upon the designs and assumptions as was illustrated in the selection of the nominal system design. For purposes of analysis, a resistivity range of 10 to 500 hr-R/Btu was used (see Appendix IV). The thermal resistance affects the storage of the cryogenic vehicles in two ways: (1) it affects the insulation required to achieve a given storage time; and (2) it determines the maximum time allowable before the tank must be vented even with perfect insulation (no heat conducted through the insulation).
- (U) The insulation thicknesses required to perform a 14-day mission are shown in Fig. 104 for the three vehicles compared. The relatively low insulation requirements for the  $\text{LO}_2$  tank are discussed in item 6.a, (2). Changes in tank size, wall temperature and pressurant effects would, of course, change the insulation thicknesses for each resistivity, but the overall trend would be the same. The  $\Delta V$ 's achievable in the 14-day mission are shown in Fig. 105 as a function of resistivity for full propellant tanks.
- (U) The performance of the cryogenic vehicles is almost insensitive to thermal resistivity for resistivity values above 100. For resistivity values below 100, the required insulation thickness increases rapidly, and the  $\Delta V$  performance decreases. This illustrates the change from radiation-dominated to conduction-dominated heat transfer mode. For large values of resistivity, almost all heat transfer is by radiation. For small values of resistivity, radiation is much smaller than conduction. The performance of the  $\text{N}_2\text{O}_4/\text{N}_2\text{H}_4$ -UDMH (50-50) vehicle is completely insensitive to resistivity for moderate storage times since very little insulation is required even for small resistivities.

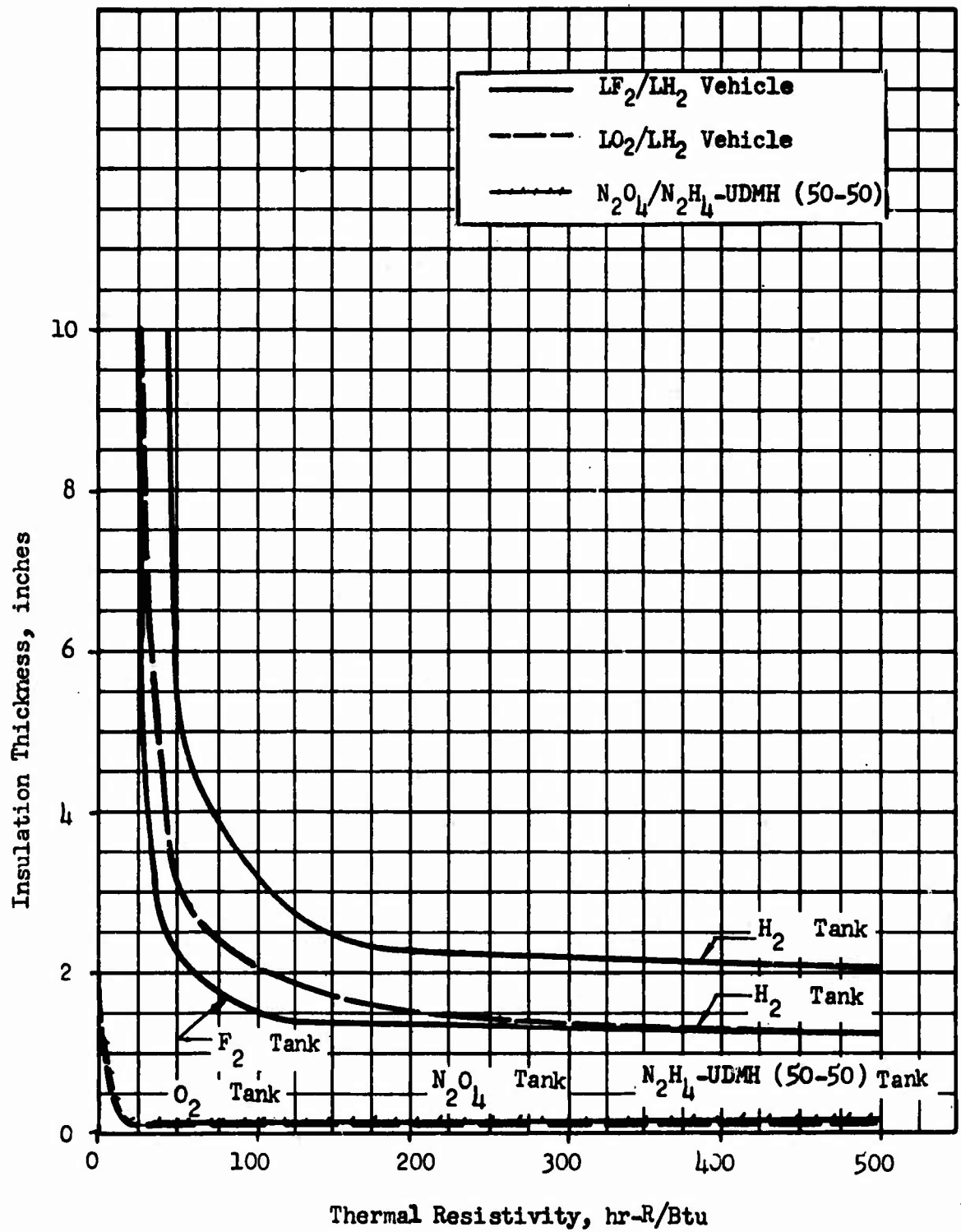


Figure 104. Insulation Thickness Required to Perform 14-Day Mission as a Function of Thermal Resistivity for an Unvented Vehicle

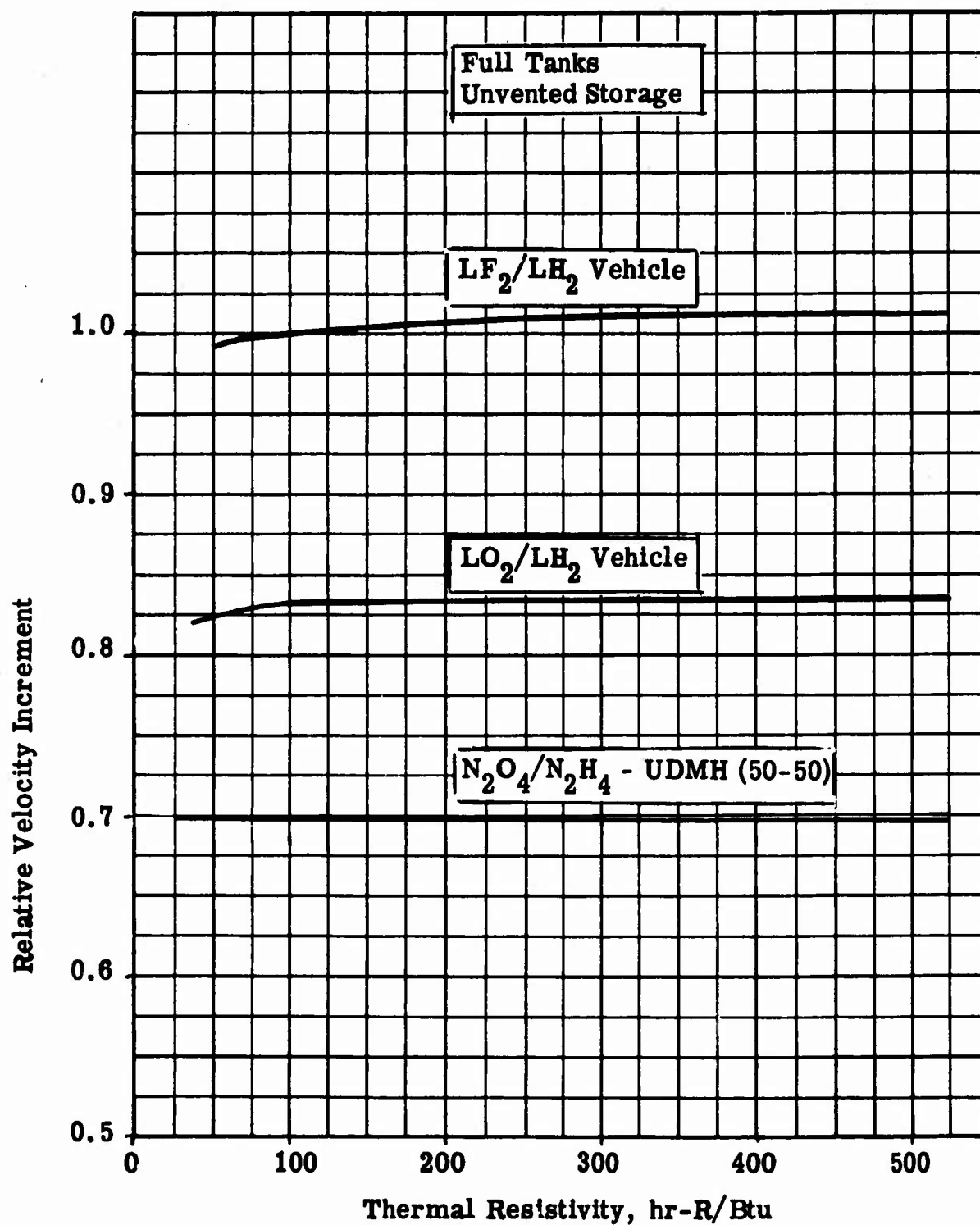


Figure 105. Relative Velocity Increment as a Function of Effective Thermal Resistivity of Wall-to-Tank Connections. 14-Day Mission

- (U) The maximum number of days that the propellants can be stored without venting is shown in Fig. 106 for 10-percent full tanks as a function of thermal resistivity for the three comparison vehicles. The maximum unvented storage time is linear with resistivity for a perfect insulation. Full tanks can be stored for an equal or longer time before venting is required depending upon the ullage. The maximum unvented storage time with 6 inches of insulation is also shown for the cryogenic vehicles.

b. Effect of Tank Insulation

- (U) Insulation changes can affect performance in two ways. First, a change in the density-conductivity product,  $\rho k$ , of the superinsulation will change the required insulation weight for a constant heating rate. Secondly, the addition of an insulation substrate to reduce preorbital heating (while the superinsulation is outgassing) would affect both the vehicle inert weight and the effect of preorbital heating.
- (U) The change in performance caused by a change in the  $\rho k$  product of the insulation is shown in Fig. 107 for the  $LF_2/LH_2$  vehicle with full tanks (this vehicle was chosen because it requires the largest amount of insulation and the effect is more pronounced) for a 14-day mission. The effect of the addition of a substrate is more complicated since the vehicle inert weight will be increased by the addition of the substrate. However, less vacuum insulation would be required to store the propellants for a given time, since the effect of the preorbital aerodynamic heating would be smaller.

c. Effect of Vehicle External Surface

The effect of vehicle surface coating material and changes in this material with time in a space environment occurs because of the equilibrium outer wall temperature associated with given material properties. The material properties that directly affect the wall temperature are the solar radiation absorptivity and the infrared emissivity. The effect of the absorptivity emissivity ratio ( $\alpha/\epsilon$ ) upon the required insulation thickness and vehicle performance is shown in Fig. 108 and 109 for the cryogenic vehicles for a 14-day mission. The effect of  $\alpha/\epsilon$  upon the storable propellants was discussed in the selection of the nominal system design.

- (U) These results are based upon a 100-nautical mile Polar Earth orbit environment with the vehicle sidewall toward the sun. Other orbit altitudes, inclinations, and vehicle orientations would show smaller variations.

d. Effect of Pressurant Temperatures

- (U) The effect of the hydrogen pressurant gas can be controlled in two ways; by reducing gas temperature, and by venting the gas to space immediately after each firing. The  $\Delta V$  performance for a 90/10 duty cycle mission is shown in Fig. 110 as a function of pressurant injection temperature for the  $LF_2/LH_2$  vehicle. The injection temperature affects this performance through insulation weight requirements and through propellant vaporization.

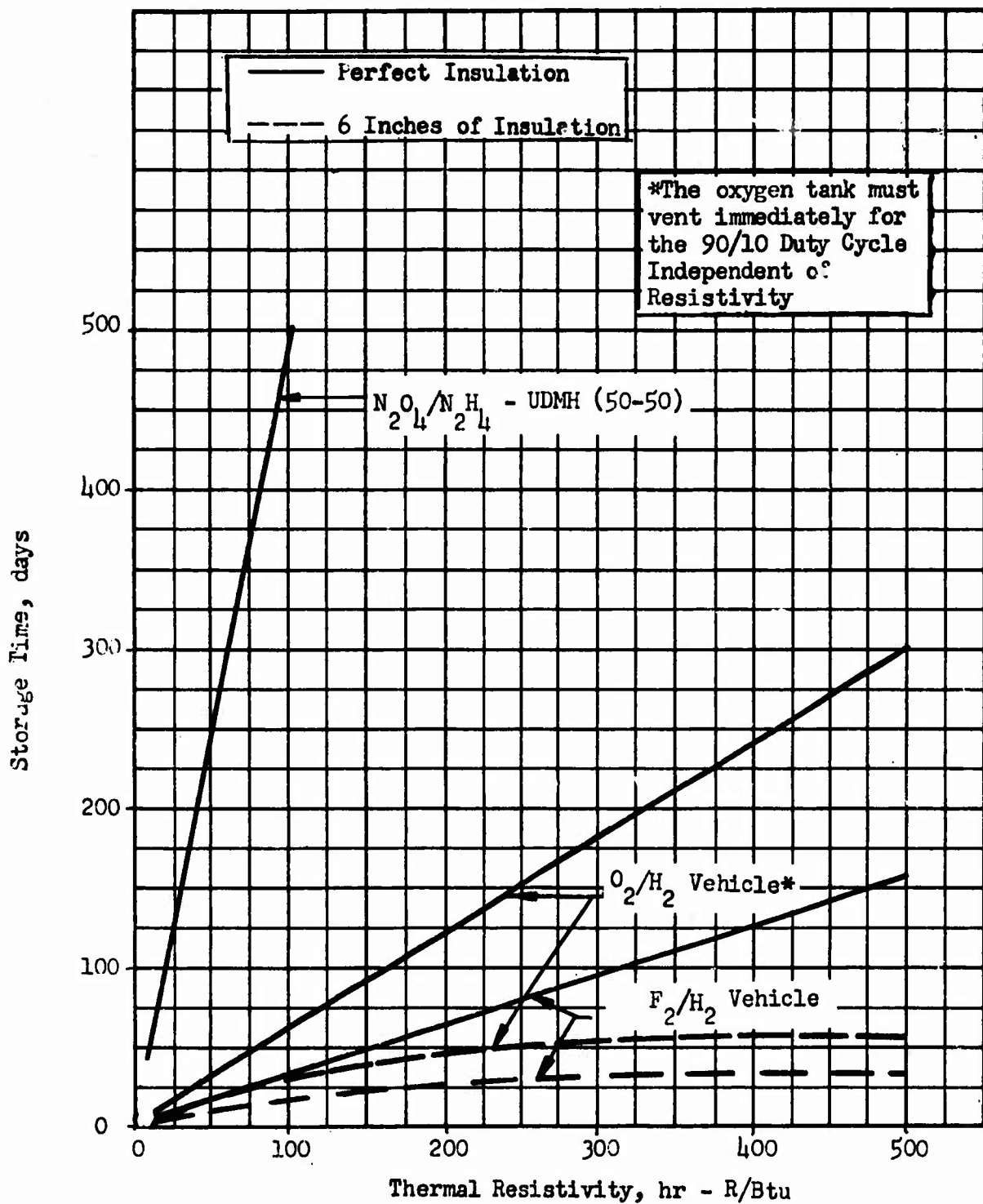
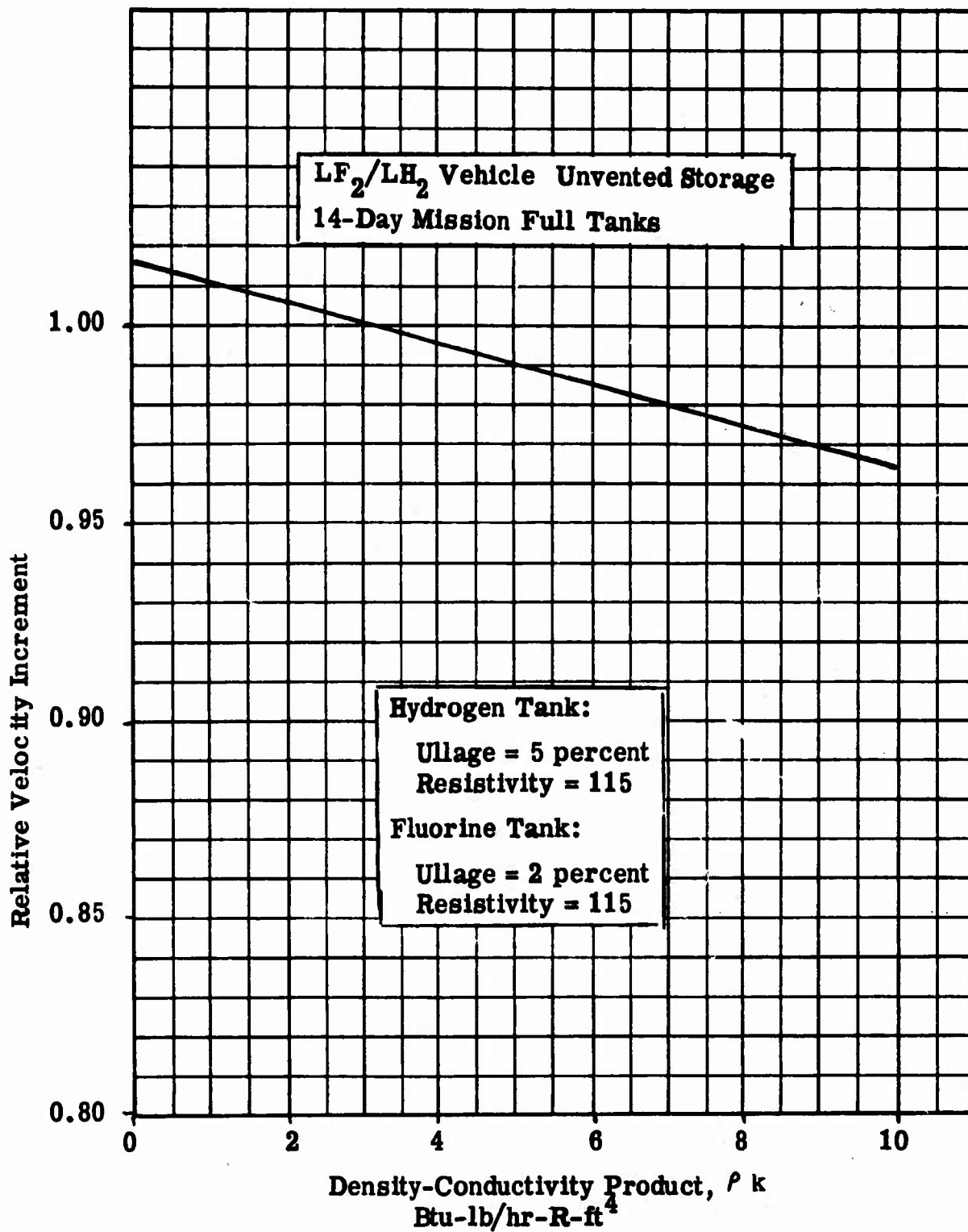


Figure 106 . Maximum Unvented Storage Time as a Function of Thermal Resistivity for Perfect Insulation and for Six Inches of Insulation



**Figure 107. Relative Velocity Increment as a Function of  $\rho k$  Product of Thermal Insulation for the LF<sub>2</sub>/LH<sub>2</sub> Vehicle on a 14-Day Mission**

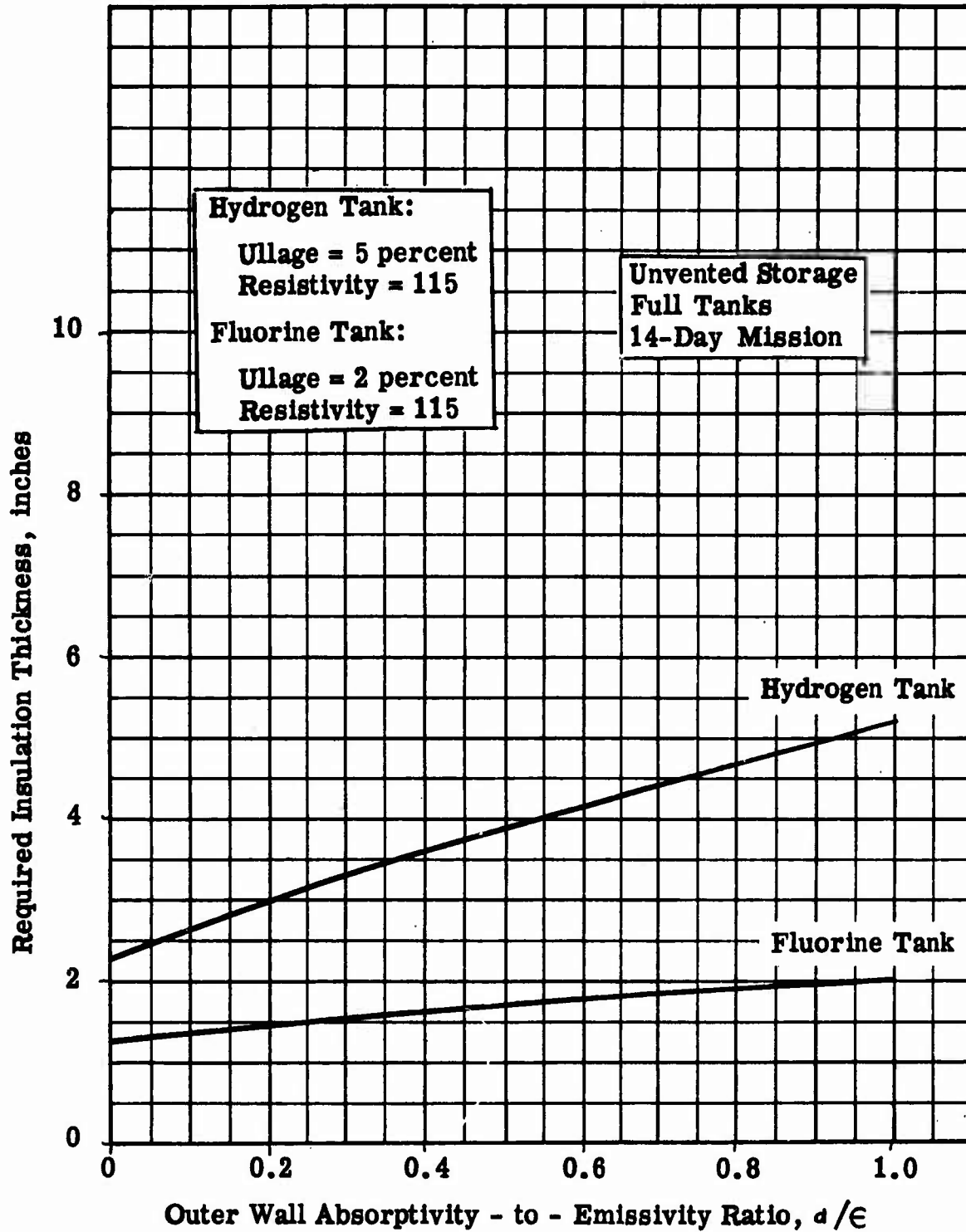


Figure 108. Required Insulation Thickness as a Function of Outer Wall Absorptivity - to - Emissivity Ratio for the  $LF_2/LH_2$  Vehicle on a 14-Day Mission

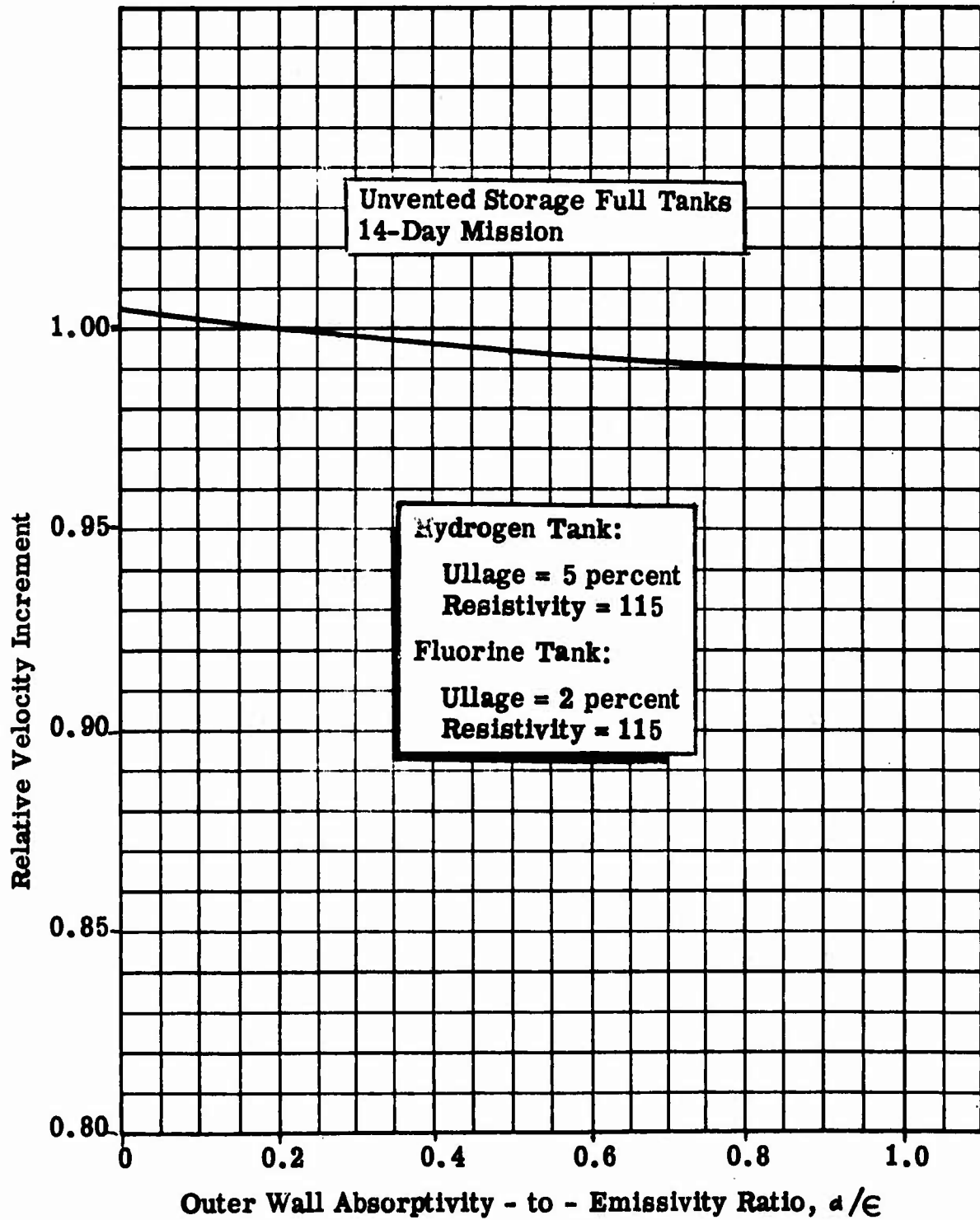


Figure 109 Vehicle Performance as a Function of Outer Wall Absorptivity - to - Emissivity Ratio for the  $LF_2/LH_2$  Vehicle on a 14-Day Mission

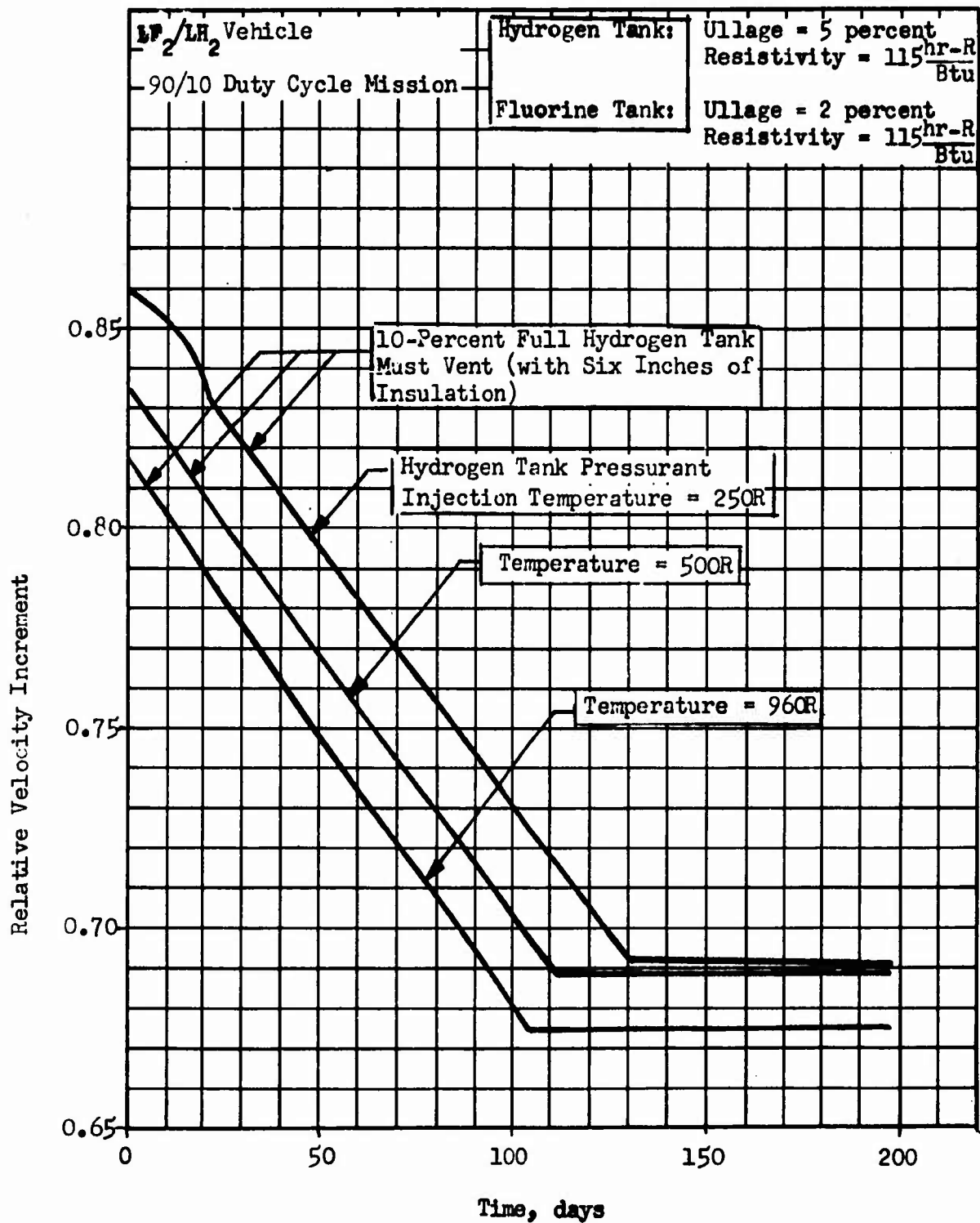


Figure 110. Performance of LF<sub>2</sub>/LH<sub>2</sub> Vehicle with Different Hydrogen Tank Pressurant Temperatures

- (U) The  $\Delta V$  performance for a 90/10 duty cycle of the  $LF_2/LH_2$  vehicle is shown in Fig. 111 as a function of the pressure at which the hydrogen pressurant is vented. The hydrogen pressurant injection temperature is 250 R, and a 14-day coast period is assumed. The  $LF_2$  tank is not vented because the 500 R helium injection temperature does not result in an excessive vapor pressure rise.
- (U) The maximum number of day's storage with perfect insulation, with 6 inches of insulation, and the maximum number of days for unvented storage are shown in Fig. 112 as a function of pressurant vent pressure. The two lower curves indicate the coast times, after venting to the specified value immediately after the first firing, which could be accomplished without exceeding the 58 psia NPSP limit. The storage time, after the first burn and venting, which would result in complete depletion of the  $LH_2$  by venting, is shown by the upper curve. The vapor pressure of the hydrogen immediately before the first firing is 23 psia, therefore vent pressures below this value are not shown. The gain in performance from decreasing the pressurant injection temperature from 960 R to 250 R is 5 percent (Fig. 110) and the gain from venting pressurant for 250 R injection temperature is 3 percent (Fig. 111).

e. Effect of Tank Venting

- (U) The method of tank venting used in calculating the vehicle performance conserves the oxidizer by use of the vented hydrogen. However, for vehicles using a constant engine mixture ratio (i.e., no propellant utilization system) this conservation of oxidizer may actually penalize the performance because this excess weight must be carried through the propulsive maneuver. That is, the oxidizer will not deplete as rapidly as the fuel (from venting) and some oxidizer will be left after the fuel tank has been emptied. An advantage of thermally conditioning the oxidizer tank however is the greater safety of not venting fuel and oxidizer simultaneously.
- (U) Venting the ullage gas directly to space has the advantage of not requiring a thermal conditioning system, thus saving inert weight. Another possibility would be the use of the vented gases to cool the vehicle shroud. This cooling would be accomplished by flowing the gases through tubes in the vehicle wall before venting them to space. The radiation from the shroud could be reduced considerably by this method. The effect upon the  $\Delta V$  performance and required insulation would be similar to that shown for the variation in the  $\alpha/\epsilon$  ratio, since the net result would be to reduce the vehicle equilibrium temperature. Some weight penalty however would be incurred with use of the cooling system.
- (U) An alternative to continuous venting is venting to the required vapor pressure immediately before a firing. Preconditioning in this way however has the disadvantage of increasing response time.

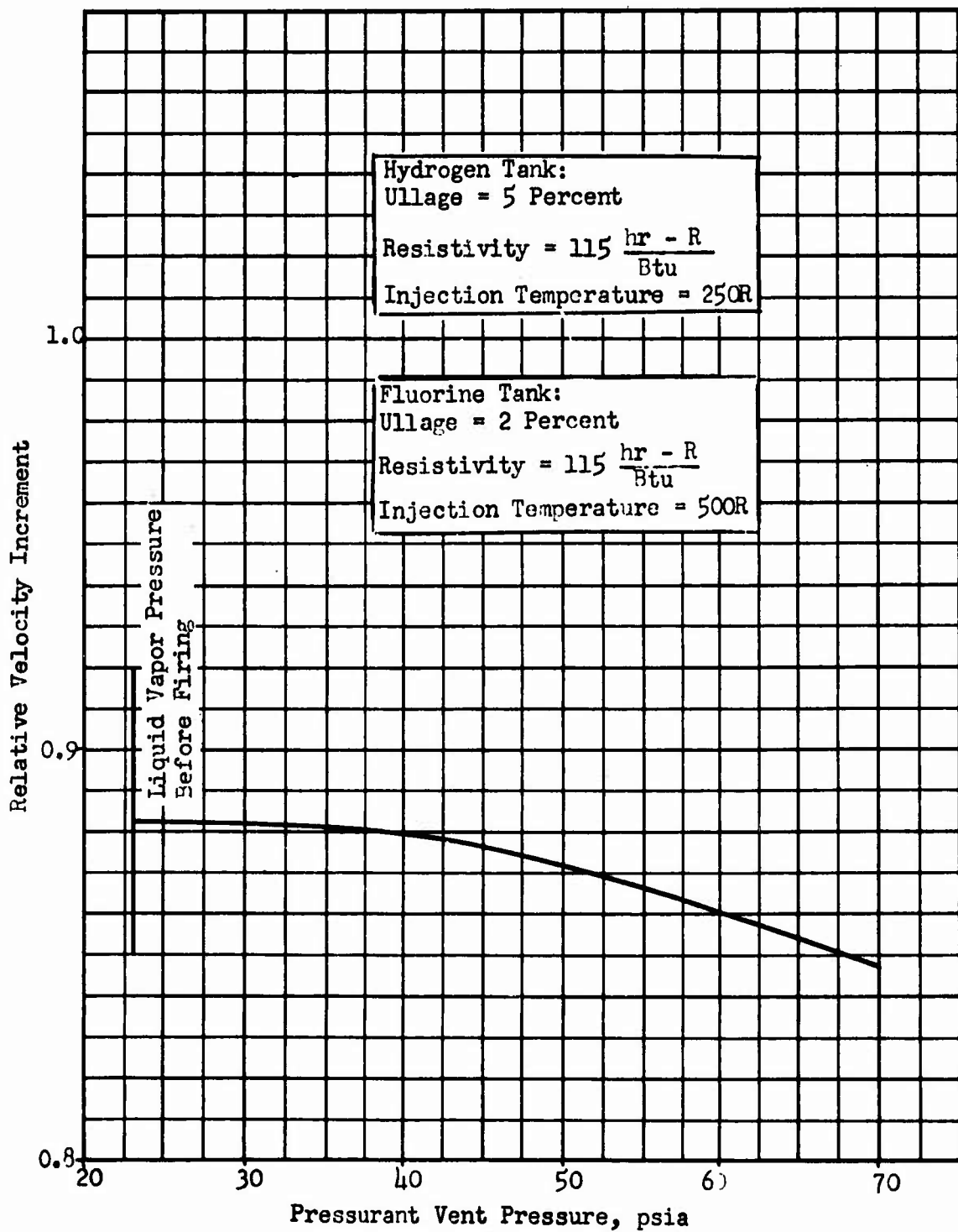


Figure 111. Vehicle Performance for a 14-Day Mission as a Function of Pressurant Vent Pressure for  $\text{LF}_2/\text{LH}_2$  Vehicle

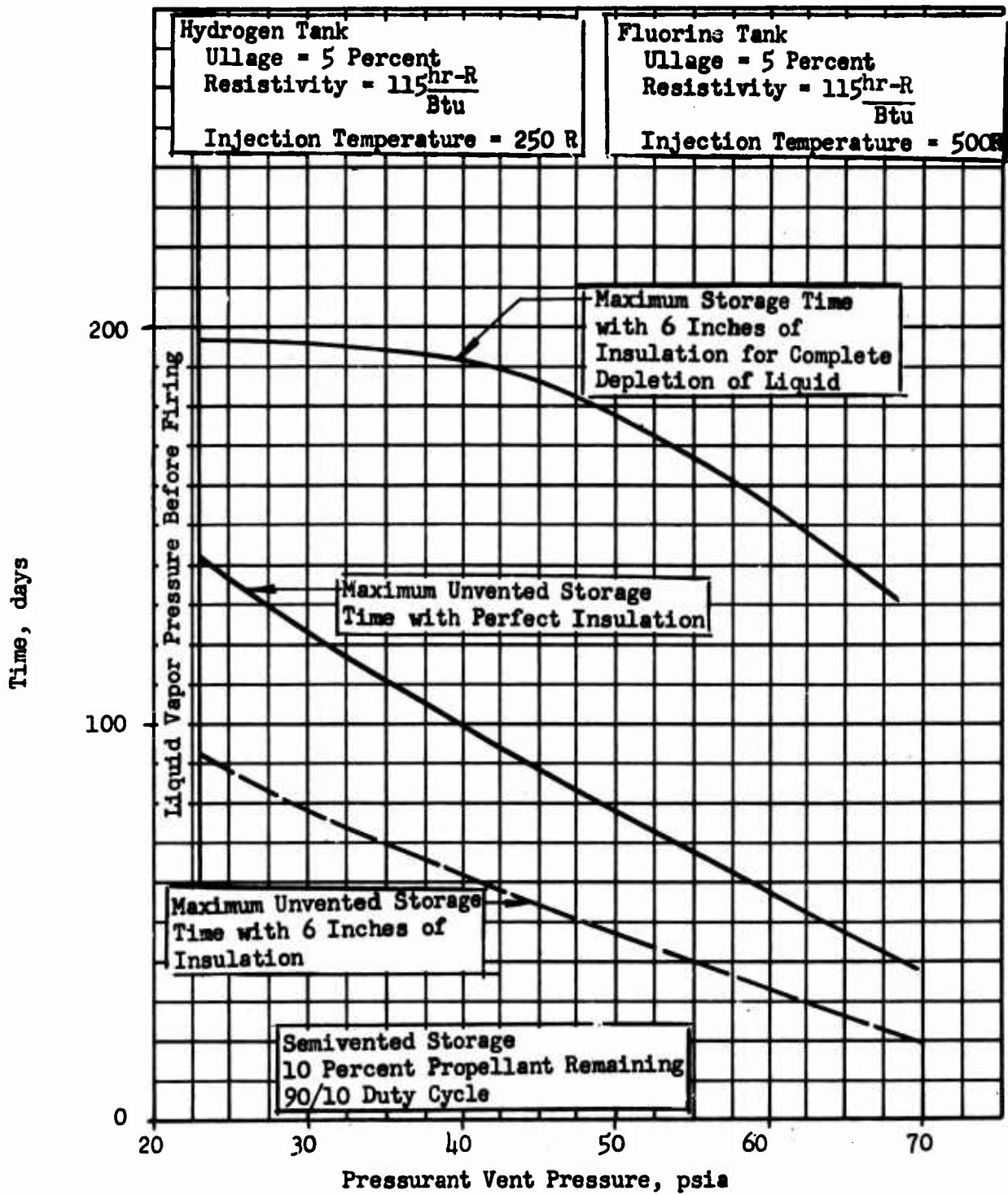


Figure 112. Storage Time Limits as a Function of Pressurant Vent Pressure

# CONFIDENTIAL

## f. Effect of Propellant Utilization Systems

- (U) The venting of hydrogen before the venting of oxidizer indicates that a propellant utilization system could improve vehicle performance. To evaluate the usefulness of a propellant utilization system, a  $\text{LF}_2/\text{LH}_2$  vehicle with an initial tank mixture ratio of 10:1 was used. The engine operating mixture ratio was allowed to vary between 10:1 and 13:1. No inert weight penalty was assigned to the propellant utilization system device, however, tank and insulation weight effects were included.
- (U) The  $\Delta V$  performance of this vehicle is shown in Fig. 113 and 114 compared to the nominal vehicle. For the full tank mission (Fig. 113) the nominal vehicle achieves higher performance for storage times less than 28 days because the 13:1 tanked mixture ratio results in a lower inert weight. The vehicle with a propellant utilization system has higher  $\Delta V$  capability for all times greater than 28 days. The very slow decrease of  $\Delta V$  of the propellant utilization system vehicle after venting of hydrogen begins indicates that the mixture ratio has been adjusted to use all of the fluorine. The maximum mixture ratio of 13:1 occurs at 400 days; and after this time, the performance decreases rapidly similar to that of the nominal vehicle. This comparison is for 5-percent ullage. Larger ullages would provide longer storage prior to the use of the propellant utilization system. With 15-percent ullage and a propellant utilization system, the vehicle could coast for almost 600 days before residual fluorine effects performance.
- (U) For the 90/10 duty cycle mission, (Fig. 114) the propellant utilization system vehicle obtains higher  $\Delta V$  performance for all times less than 150 days. This improvement of performance is obtained because the system adjusts for the vaporization of hydrogen by the pressurant. Higher ullages would have somewhat lower performance but would still show improvement.

## g. Effect of Tank Ullage

- (U) The oxidizer tank ullage was fixed for purposes of this study, since it is a small quantity. The hydrogen ullage was chosen so that the vehicle with full tanks would achieve a design coast time of 14 days without venting. The required insulation thickness for the hydrogen tanks to prevent venting are shown in Fig. 115 as a function of ullage for full and 10-percent full tanks for a 14-day mission for the  $\text{LF}_2/\text{LH}_2$  vehicle. The maximum unvented storage time is shown in Fig. 116 as a function of ullage for the full and 10-percent-full tanks. The larger ullages penalize the 10-percent tank storage but improve the full tank storage. At 5-percent ullage, the storability of both full and 10-percent full tanks is the same.

## h. Effect of Propellant Loading

- (C) The vehicle propellant loading may change for two reasons, the payload could be changed from the present 2000 pounds, and the vehicle gross weight could be increased. The effect of both payload and gross weight can be seen by analyzing the effect of propellant loading.

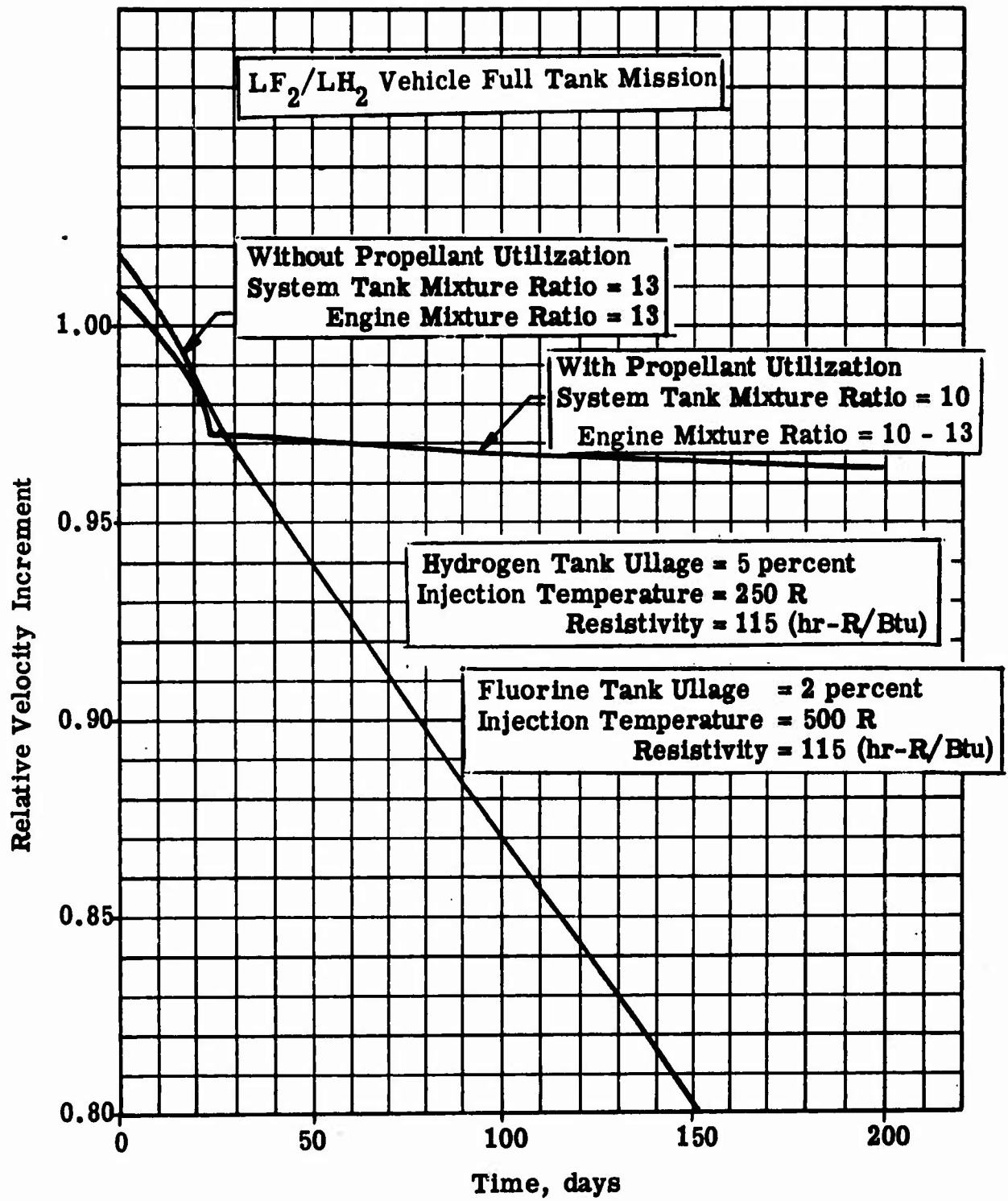


Figure 113. Performance Comparison of LF<sub>2</sub>/LH<sub>2</sub> Vehicle with and Without a Propellant Utilization System

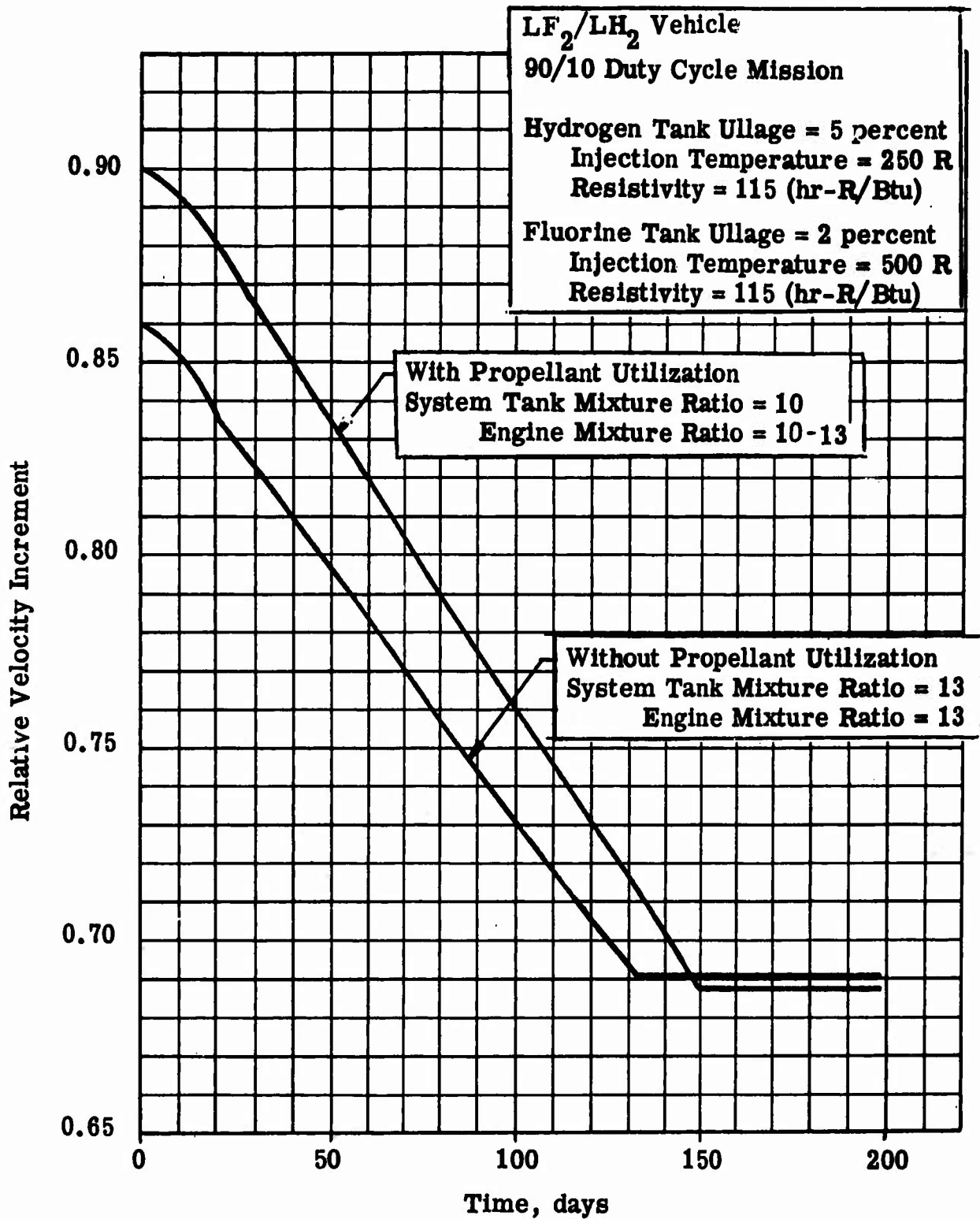


Figure 114 . Performance Comparison of LF<sub>2</sub>/LH<sub>2</sub> Vehicle With and Without a Propellant Utilization System

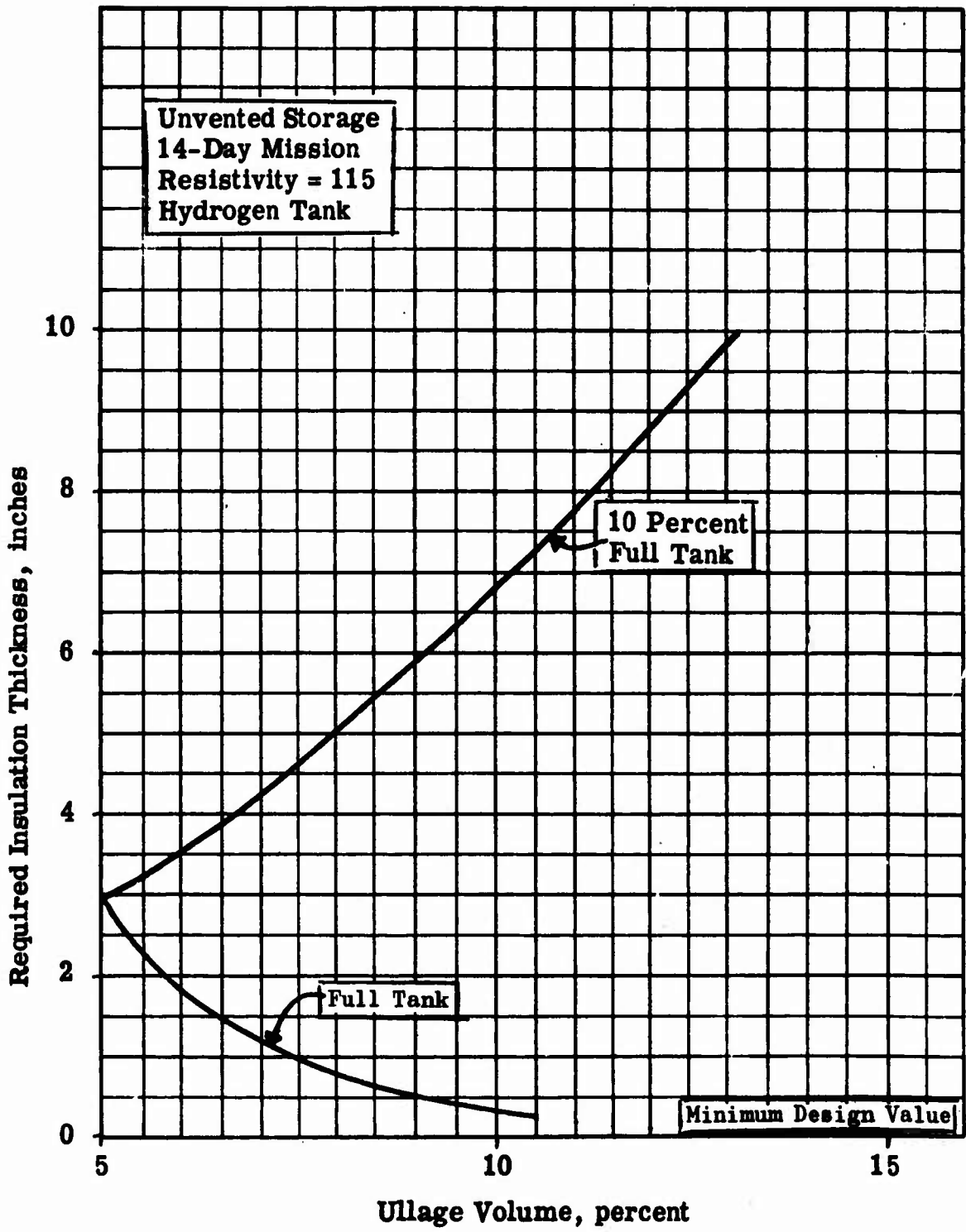


Figure 115. Required Insulation as a Function of Ullage for the  $LF_2/LH_2$  Vehicle on a 14-Day Mission

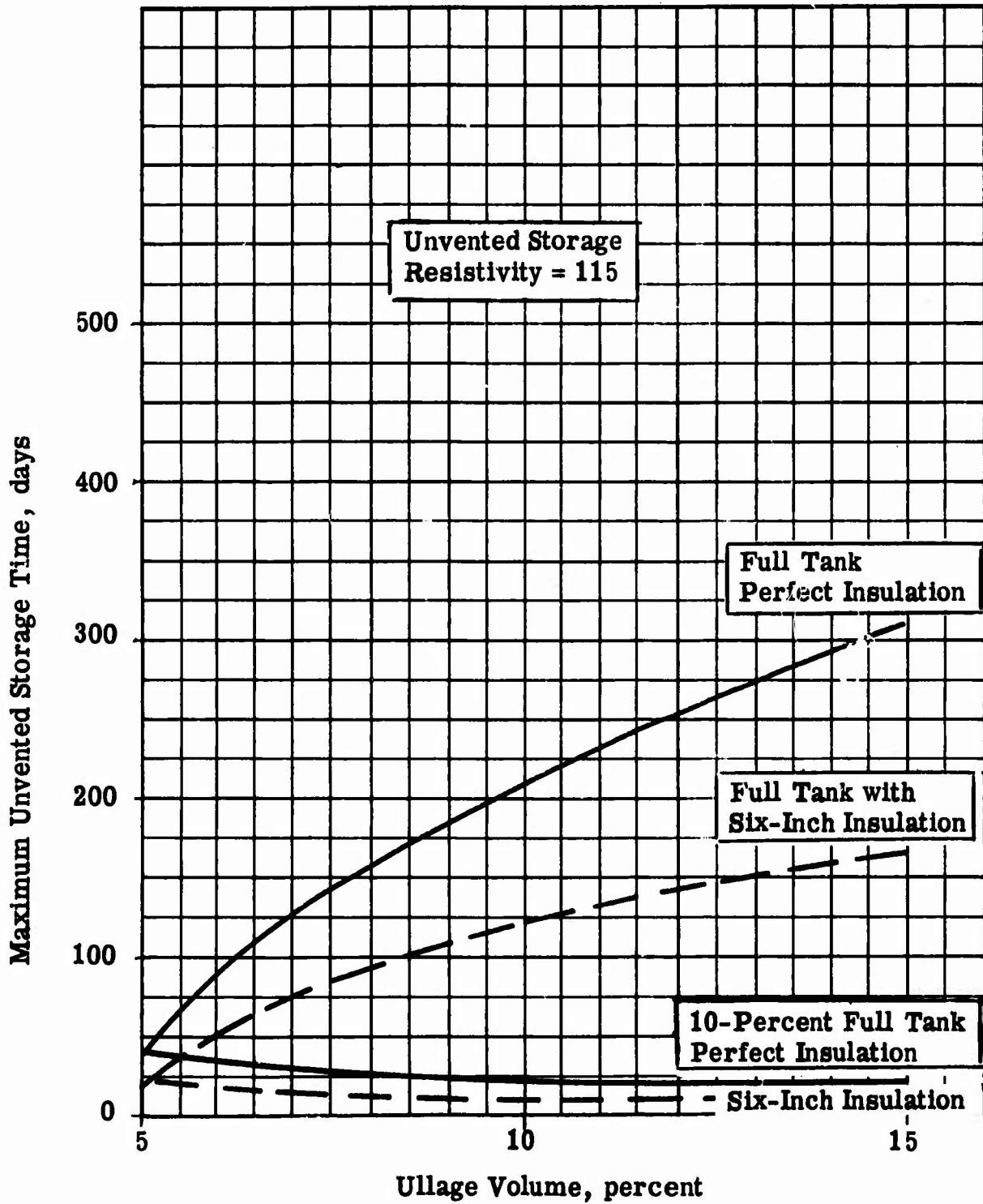


Figure 116 . Maximum Unvented Storage Time for  $LF_2/LH_2$  Vehicle Hydrogen Tank as a Function of Ullage Volume

# CONFIDENTIAL

(C) The required insulation thicknesses for the hydrogen tank and fluorine tank of the  $LF_2/LH_2$  vehicle are shown in Fig. 117 as a function of propellant weight. The 14-day mission with the 90/10 duty cycle was used for the parametric analysis. The values corresponding to 2000- and 5000-pound payloads for gross weights of 20,000 and 35,000 pounds are located on the curves. The maximum unvented storage time for the 90/10 duty cycle is shown in Fig. 118 for various propellant loadings. The full tanks will vent at the same time or later. Increasing propellant loading improves the storability of the larger volume-to-area ratio associated with increased propellant weight. The heat leak through wall to tank connections does not increase significantly with propellant weight and therefore the effect of this heat leak becomes smaller with increasing propellant weight.

i. Effect of Slush Hydrogen

(U) The use of a mixture of hydrogen liquid and solid (slush) is attractive for long storage duration missions since the latent heat of fusion of the solid can be used to absorb much of the external heat input early in the mission. However, for a vehicle which may be required to fire as soon as it is placed in orbit, the use of slush hydrogen could penalize the system since the solid is unusable by the engine. The use of slush would increase the ground hold time. If the vehicle is to remain in orbit for an extended period before firing, or if the pumps and feed system can be designed to run with a mixture of solid and liquid hydrogen, the use of slush hydrogen should be considered.

j. Sensitivity of Design Point

(U) The nominal vehicle design represents a sound choice in the storage system design concept. Other storage methods such as the use of slush hydrogen, pressurant venting, shroud cooling and propellant utilization systems could give performance gains for long-term missions but only at the expense of added complexity and cost. The sensitivity of the nominal design to the variations considered is small enough that its performance will not be very much lower than that of a vehicle optimized for a specific mission.

k. New Technology Areas

(U) Since the propellant storage comparison makes use of devices that are not yet developed, and since the storability of the cryogenic vehicles could be improved by advanced methods, a number of specific areas of new technology development can be cited as being of importance.

These areas are:

1. Thermodynamic Venting and Thermal Conditioning. The use of vented hydrogen to cool the fluorine tank requires development of a number of devices and controls. A tradeoff study may be necessary to determine the most advantageous method.

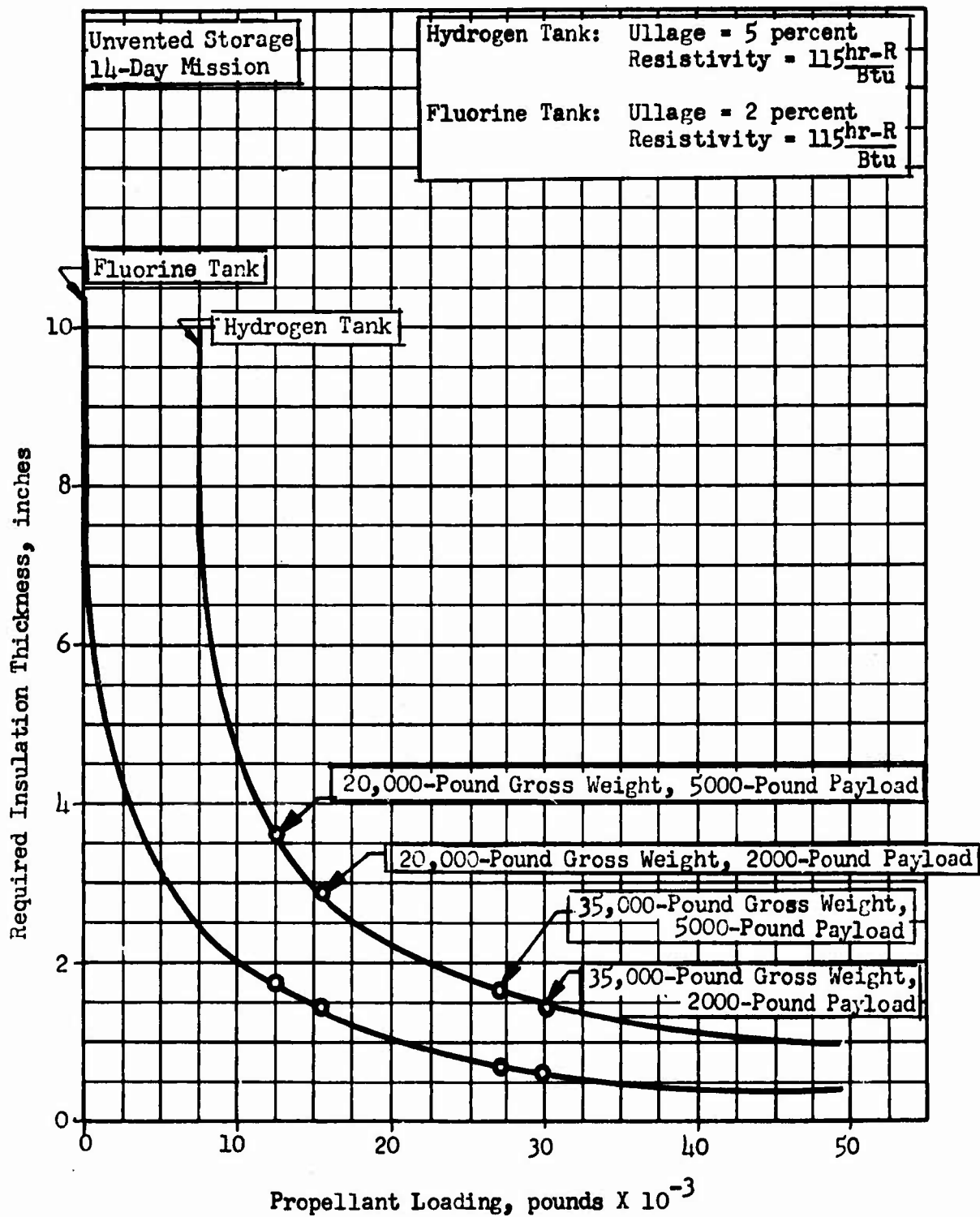


Figure 117. Required Insulation Thickness for 14-Day Mission as a Function of Propellant Loading

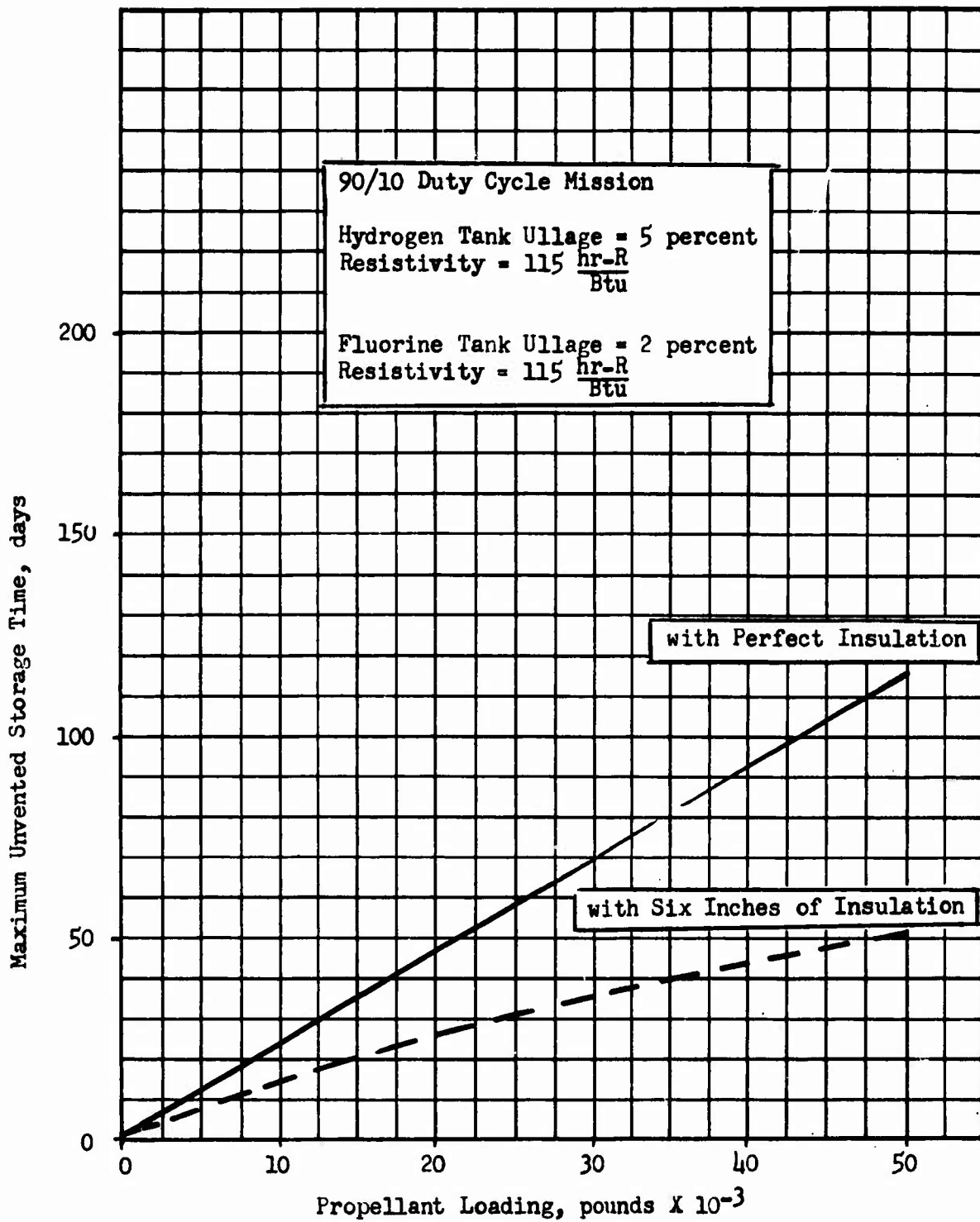


Figure 118. Maximum Unvented Storage Time as a Function of Propellant Loading for Perfect Insulation and for Six Inches of Insulation for F<sub>2</sub>/H<sub>2</sub> Vehicle

2. Propellant Utilization System. Methods of improving the measurement of instantaneous tank mixture ratio warrants further effort.
3. Thermal Isolation of Propellant Tanks. The high resistivity value of wall-to-tank connections used in this study depends upon the development of effective propellant line heat blocks. Other new methods such as detachable lines could improve the propellant storability.
4. Reduction of Pressurant Effects in Hydrogen Tank. The vaporization of liquid hydrogen by hot pressurant is a major cause of  $\Delta V$  loss in multiple firing missions. Methods of reducing these effects should be investigated.

# CONFIDENTIAL

## SECTION VI

### (C) CONCLUSIONS

1. Larger launch vehicles such as growth versions of Titan III and Saturn IB result in higher optimum gross weights for the MSPS with corresponding significantly higher maneuvering  $\Delta V$  capabilities.
2. Larger MSPS payloads result in higher optimum gross weights for the MSPS.
3. For a given MSPS payload size, a single MSPS gross weight and thrust level may be selected to yield near optimum (maximum) orbital  $\Delta V$  capabilities with each of the launch vehicles considered.
4. A compromise MSPS gross weight and thrust level may be selected which would accommodate either the 2000- or 5000 pound payloads with a small  $\Delta V$  penalty for each payload.
5. For most cases of launch vehicles and payloads, the  $\Delta V$  gains obtained with suborbital firing are slight (0 to 3 percent). For the nominal Titan III-C and Saturn IB launch vehicles, however, the 5000 pound payload  $LF_2/LH_2$  MSPS achieves significant increases in  $\Delta V$  (14 percent) with suborbital burn and increased gross weight.
6. The orbital residence time of the  $LF_2/LH_2$  MSPS can be greatly extended beyond the previous 14 day requirement with only slight degradation of performance.
7. Propulsion systems using  $LF_2/LH_2$  maintain their performance superiority over  $LO_2/LH_2$  and  $N_2O_4/N_2H_4$ -UDMH(50-50) systems for orbital storage periods greater than 2 years.

# CONFIDENTIAL

## APPENDIX I

### MSPS MISSION PERFORMANCE EXCHANGE FACTORS

- (c) Exchange factors to determine the effect of variations in the MSPS inert weight and specific impulse are presented in Fig. 119 and in Table XLI. Inert weight gain factors for the various MSPS vs gross weights are shown in Fig. 119. For the 36,000-pound gross weight LF<sub>2</sub>/LH<sub>2</sub> MSPS, 1 pound of increased structure weight costs 2.6 fps of  $\Delta V$  for the 2000-pound payload and 1.7 fps of  $\Delta V$  for the 5000-pound payload. The 52,000-pound gross weight LF<sub>2</sub>/LH<sub>2</sub> MSPS loses 2.3 fps for a 1-pound increase in structure weight with the 2000-pound payload, and 1.6 fps with the 5000-pound payload. A chart of  $\Delta V/I_s$  gain factors is shown in Table XLI for the two selected MSPS gross weights associated with each launch vehicle.

CONFIDENTIAL

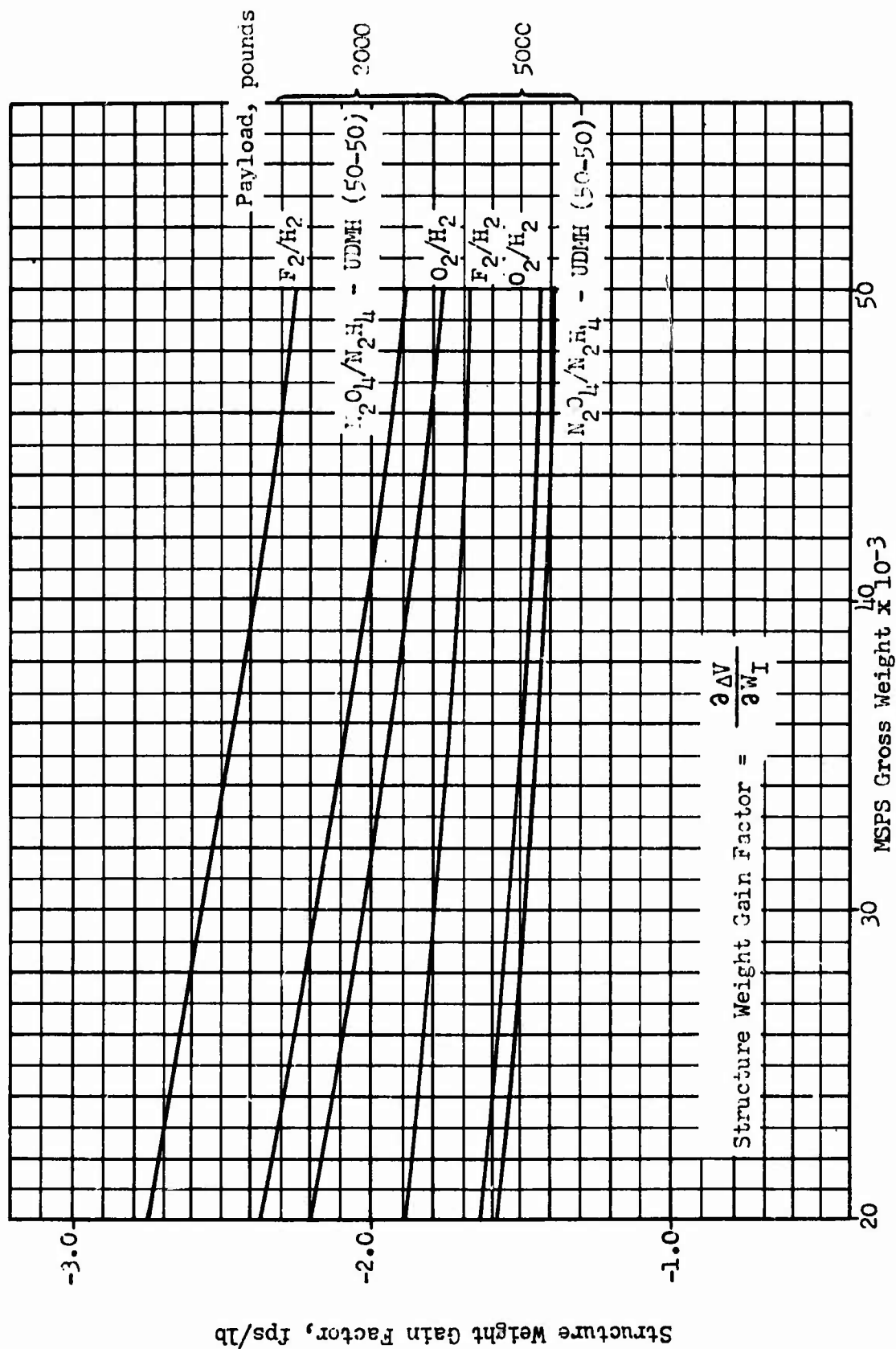


Figure 119. Effect of Structure Weight Change on  $\Delta V$  Capability for 2000-pound and 5000-pound Payloads

CONFIDENTIAL

# CONFIDENTIAL

TABLE XLI

SPECIFIC IMPULSE GAIN FACTORS  
( $\Delta V$  in ft/sec per second of  $I_g$ )

<u>Launch Vehicle</u>	Gross Weight, pounds			
	36,000		52,000	
	Payload Weight, pounds			
	2000	5000	2000	5000
Nominal Titan III-C	51.6	38.5	51.0	39.8
Titan III-C with 7-Segment 120-inch solids	56.7	43.9	55.6	45.6
Titan III-C with 3- Segment 156-inch solids	58.9	56.0	61.6	50.7
Nominal Saturn I-B	56.8	43.9	56.2	45.4
Saturn I-B with Minuteman Strap-Ons	58.8	46.2	59.9	49.0

## APPENDIX II

### A SURVEY OF HIGH PERFORMANCE THERMAL INSULATION

- (U) As a part of a Maneuvering Space Propulsion System study, the physical properties of presently available types of high performance super insulation were reviewed. Auxiliary considerations such as fabrication, application, and durability were also considered. The use of the various insulations in a Maneuvering Propulsion System is discussed and insulation designs for cryogenic and storable propellant combinations for the Maneuvering Propulsion System are chosen.

#### 1. PHYSICAL PROPERTIES OF SUPERINSULATIONS

- (U) There are at present a number of superinsulations available. The most widely used types are made up of multiple layers of highly reflective material which act as radiation shields and which may be separated by a low conductivity spacing material. The designs of some of the most promising superinsulations are shown in Table XLII. The important properties of some of these materials are given in Table XLIII for application at  $LF_2$ ,  $LO_2$ , and  $LH_2$  temperatures with the warm side at 400R temperature; and for application at  $N_2O_4/N_2H_4$  - UDMH temperatures.

- (U) The product of density and conductivity given in Table XLIII is a measure of the actual weight of insulation necessary to reduce the heat flux to a given value. That is,

$$q = k \frac{A}{L} \Delta T$$

$$L = k \frac{A \Delta T}{q}$$

$$W_I = \rho AL = \rho k \frac{A^2 \Delta T}{q} \propto \rho k$$

TABLE XLII

DESIGN OF SUPERINSULATIONS

(U) Mylar and Paper

The Mylar and paper insulation is composed of alternating layers of 0.25-mil Mylar, aluminized on two sides, and 2.8-mil Dexiglas paper. Both the Mylar and paper have excellent resistance to tearing, Ref.10.

(U) Foil and Paper

The foil and paper insulation is similar to the Mylar and paper but uses 0.25 mil aluminum foil in place of the Mylar. The foil has a tendency to tear under boost-type loadings, Ref. 10.

(U) NRC-2 Type

NRC-2 is made up of layers of Mylar which have been aluminized on one side and crinkled to reduce contact points. The Mylar resists tearing, Ref. 10 and 11.

(U) Dimplar

Dimplar is made up of alternating sheets of smooth doubly aluminized Mylar and dimpled doubly aluminized Mylar. The Mylar resists tearing, Ref. 11 and 12.

(U) Linde

The Linde superinsulation is made of alternating layers of aluminum foil and fiber spacers and has good resistance to tearing, Ref. 13.

TABLE XLIII

## PROPERTIES OF SUPERINSULATION

Insulation	Conductivity Btu/ft-R-hr	Density lb/ft <sup>3</sup>	Product, <sup>4</sup> Btu-lb/ft <sup>4</sup> - R-hr
LH <sub>2</sub> Temperature			
LMSC Mylar and Paper	0.75 x 10 <sup>-5</sup>	4.5	3.4 x 10 <sup>-5</sup>
LMSC Foil and Paper	0.75 x 10 <sup>-5</sup>	5.7	4.3 x 10 <sup>-5</sup>
NRC-2 Type	2 x 10 <sup>-5</sup>	1.5	3 x 10 <sup>-5</sup>
Dimplar	4.0 x 10 <sup>-5</sup>	1.0	4.0 x 10 <sup>-5</sup>
Linde	1 x 10 <sup>-5</sup>	7.5	7.5 x 10 <sup>-5</sup>
LF <sub>2</sub> - LO <sub>2</sub> Temperature			
LMSC Mylar and Paper	1 x 10 <sup>-5</sup>	4.5	4.5 x 10 <sup>-5</sup>
LMSC Foil and Paper	1 x 10 <sup>-5</sup>	5.7	5.7 x 10 <sup>-5</sup>
NRC-2 Type	2.7 x 10 <sup>-5</sup>	1.5	4 x 10 <sup>-5</sup>
Dimplar	5.5 x 10 <sup>-5</sup>	1.0	5.5 x 10 <sup>-5</sup>
Linde	1.5 x 10 <sup>-5</sup>	7.5	11.3 x 10 <sup>-5</sup>
N <sub>2</sub> O <sub>4</sub> /N <sub>2</sub> H <sub>4</sub> -UDMH(50-50)			
LMSC Mylar and Paper	3.5 x 10 <sup>-5</sup>	4.5	1.6 x 10 <sup>-4</sup>
LMSC Foil and Paper	3.5 x 10 <sup>-5</sup>	5.7	2 x 10 <sup>-4</sup>
NRC-2 Type	3.5 x 10 <sup>-5</sup>	1.5	0.53 x 10 <sup>-4</sup>
Dimplar	9.9 x 10 <sup>-5</sup>	1.0	0.99 x 10 <sup>-4</sup>
Linde	4.5 x 10 <sup>-5</sup>	7.5	3.4 x 10 <sup>-4</sup>

## 2. FABRICATION TECHNIQUES

- (U) Present design considerations (Ref. 10) favor insulation which is easily removable. Some designs require fixed insulation, however, the fabrication of fixed insulation is dependent upon the exact design and will not be discussed here. Removable insulation can be fabricated in panels which are nearly independent of vehicle design. These panels are generally made of layers of superinsulation fastened to a fabric backing.
- (U) The two presently accepted (Ref. 10) methods of attaching the multilayer insulation to the backing are button-type with nylon thread or teflon studs and shingle type with glued ends (Fig. 120). The nylon thread has lower thermal conductance but for thick insulations the teflon stud gives better structural integrity. The end glued layers have higher conductivity than the button method.

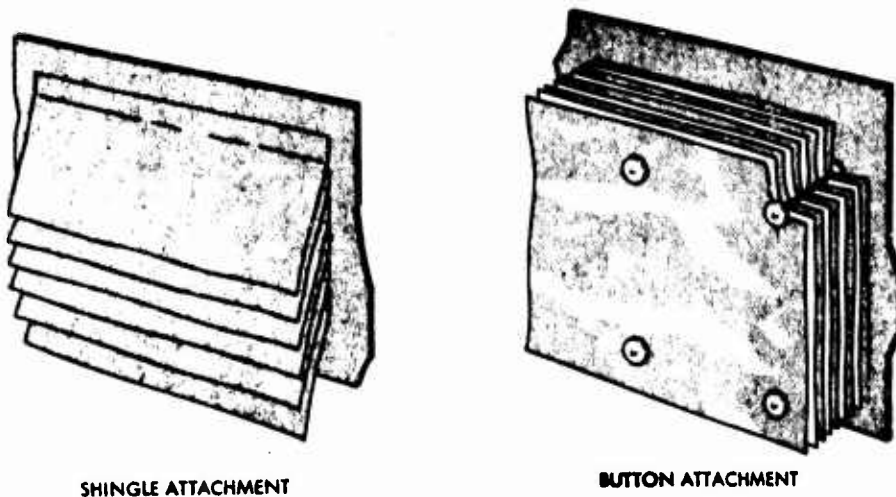


Figure 120. Methods of Attachment

- (U) The panels can be fastened to the tank by Velcro Fasteners to insure ease of removal. One half the fastener is attached to the wall and the other half is sewn to the panel backing. The use of Velcro fasteners is illustrated in Fig. 121.

## 3. INSTALLATION TECHNIQUES

- (U) The major criteria in the choice of the installation method for high performance insulation are given in Table XLIV (Ref. 11). The weighting given to each of the design considerations depends upon the propellants, thermal environment, mission and mission duration.

TABLE XLIV

DESIGN REQUIREMENTS

1. Allow leak checking of tank.
2. Minimize boiloff during ground hold.
3. Eliminate liquefaction of air during ground hold.
4. Avoid condensation of water on insulation.
5. Minimize consumption of helium.
6. Provide thermal protection during boost.
7. Withstand rapid depressurization.
8. Allow rapid degassing.
9. Resist degrading effects of leaks.
10. Provide thermal protection in space.

Press to fasten,  
peel to remove.  
(Fasteners are reusable.)

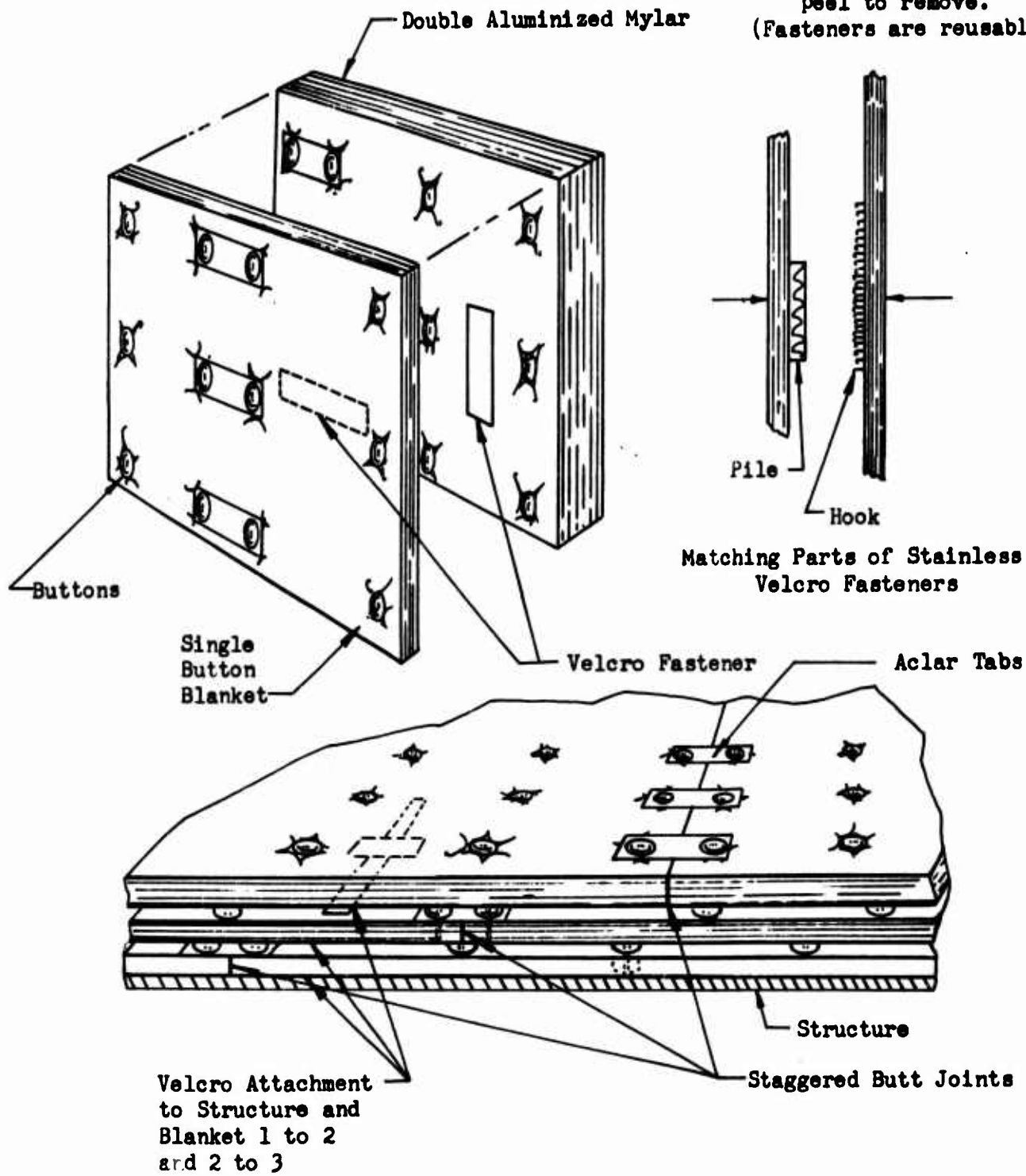


Figure 121. Cross Section of Three Installed Button Blankets

- (U) Some designs based upon these criteria are shown in Fig. 122 (Ref. 11); the way in which the designs meet the criteria is given in Table XLV. Since some of the designs use a substrate material (Fiberglass felt batting in the examples), the properties of some of the materials presently in use as substrates are given in Table XLVI (Ref. 10 and 11).

#### 4. INSULATION AT PENETRATIONS

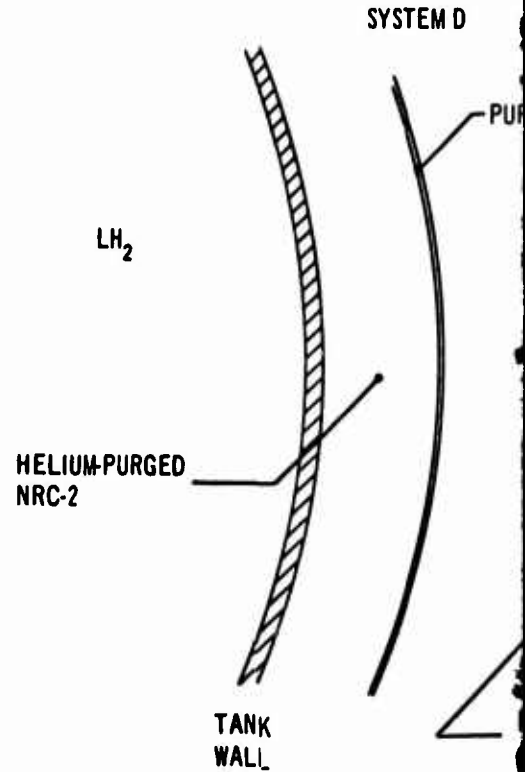
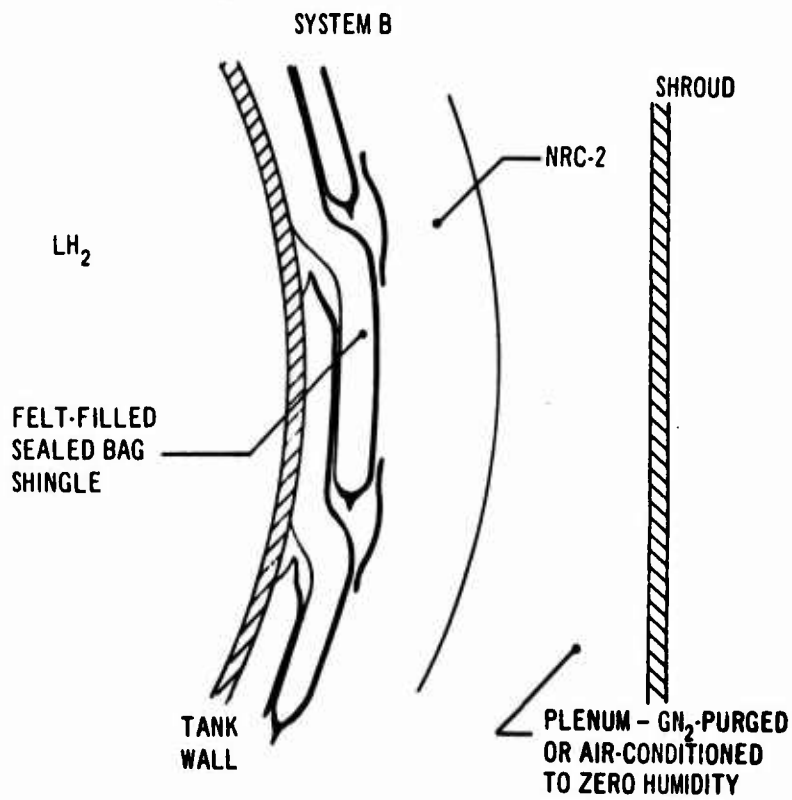
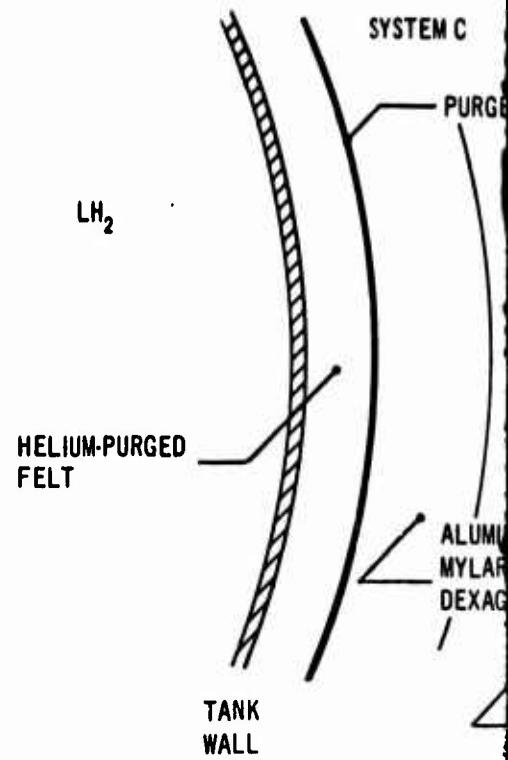
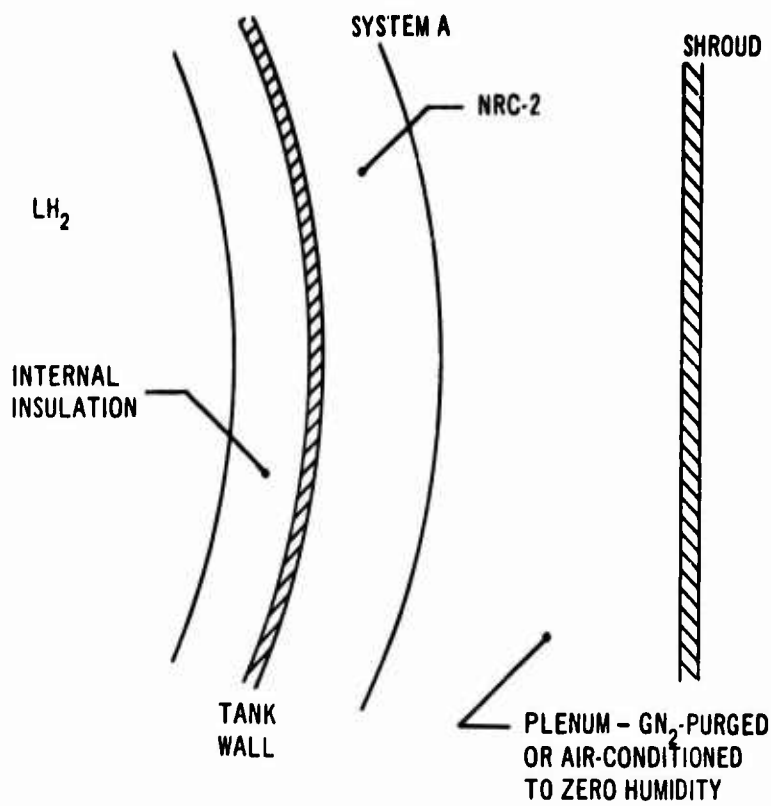
- (U) There are two presently accepted methods of joining tank insulation to the insulation around fittings entering or attached to the tank. The first, which gives performance equal to that of unbroken insulation, is to weave the two insulations together layer by layer. The second method is to butt both insulations to a low conductivity collar surrounding the pipe. This type of installation allows about twice the heat flux of the woven type but is simpler to fabricate. The heat flux of both types is generally much smaller than the heat flux through the penetration (pipe or support) itself.

#### 5. USE OF HIGH-PERFORMANCE INSULATION IN A MSPS

- (U) Although a complete optimization of a high-performance insulation system for a Maneuvering Space Propulsion System would include a wide variety of mission and cost effects, a representative system can be chosen which, thermally, would perform almost identically to an optimum system. The weight and cost of the chosen system might vary from those of an optimum system, but the weight variation should be minor.

##### a. Cryogenic Propellants

- (U) In choosing an insulation design for the maneuvering propulsion application, some of the criteria shown in Table XLIV can be de-emphasized. In particular, the requirements of minimizing boiloff and of conserving helium can be minimized by using closed recirculating systems and short ground hold times. The use of helium purge without a substrate or complicated sealing system provides the lightest design to prevent liquefaction of air and condensation of water on the tanks. Thermal protection during boost, while important for short duration missions, can be de-emphasized for long term missions. The last four design requirements of the table are met by all the superinsulations considered.
- (U) Some additional considerations can also be added to the basic requirements. The first of these is ease of installation. Panel type construction is probably the most easily installed and also meets design requirements of leak checking. The stud construction of the panel type fulfills another consideration - that of structural integrity. This consideration also favors tank mounting over shroud mounting.
- (U) The design system chosen based upon the design requirements and considerations discussed is System E of Fig. 122, with NRC-2 type insulation and no substrate. The entire vehicle is purged with helium while on the ground.



Insulation Systems



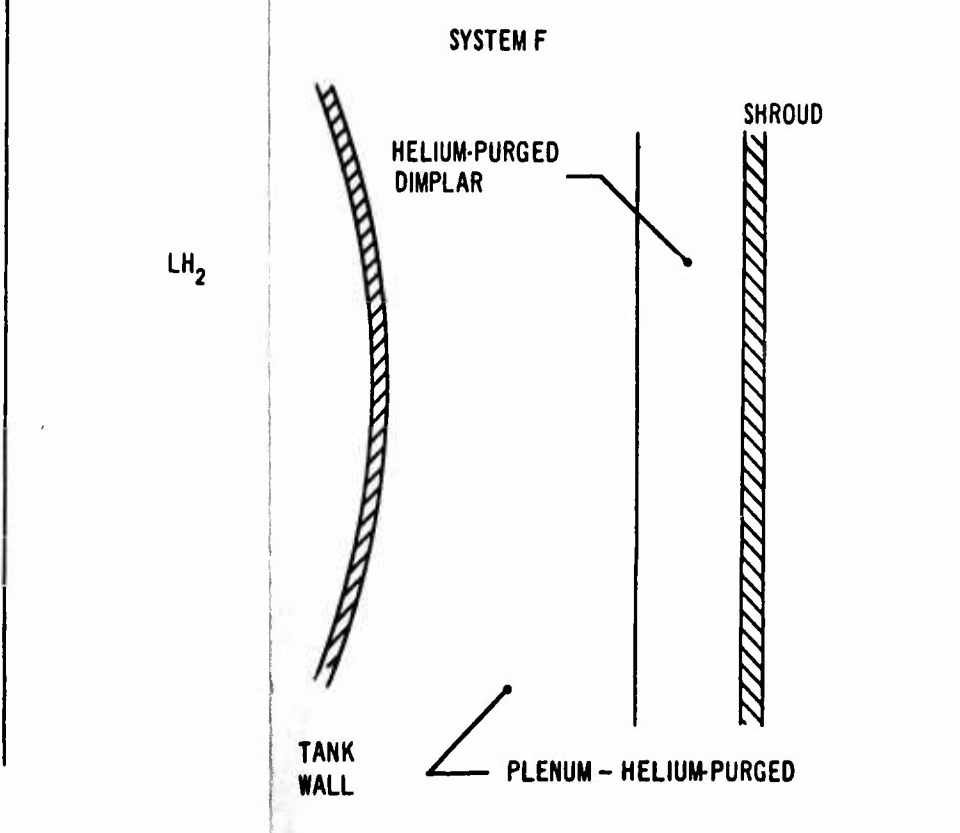
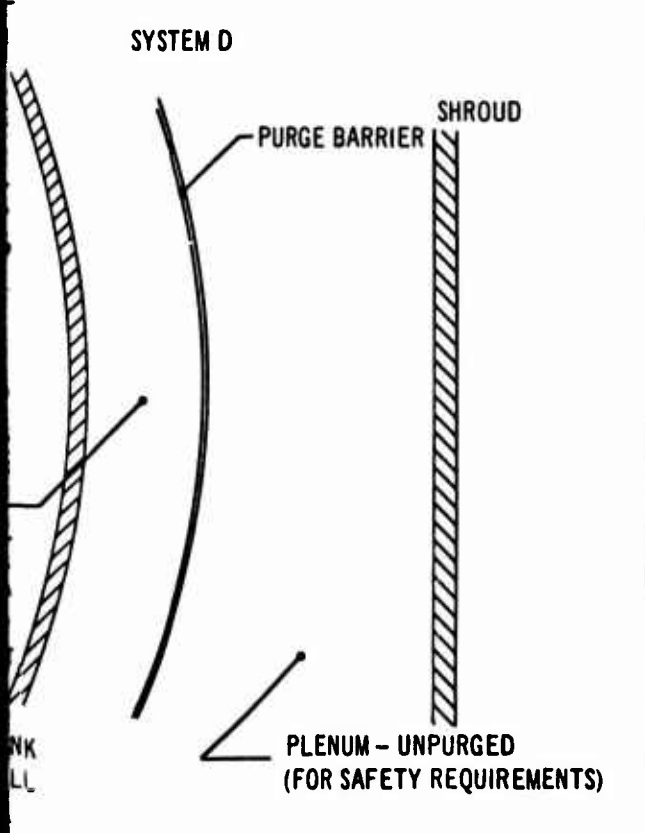
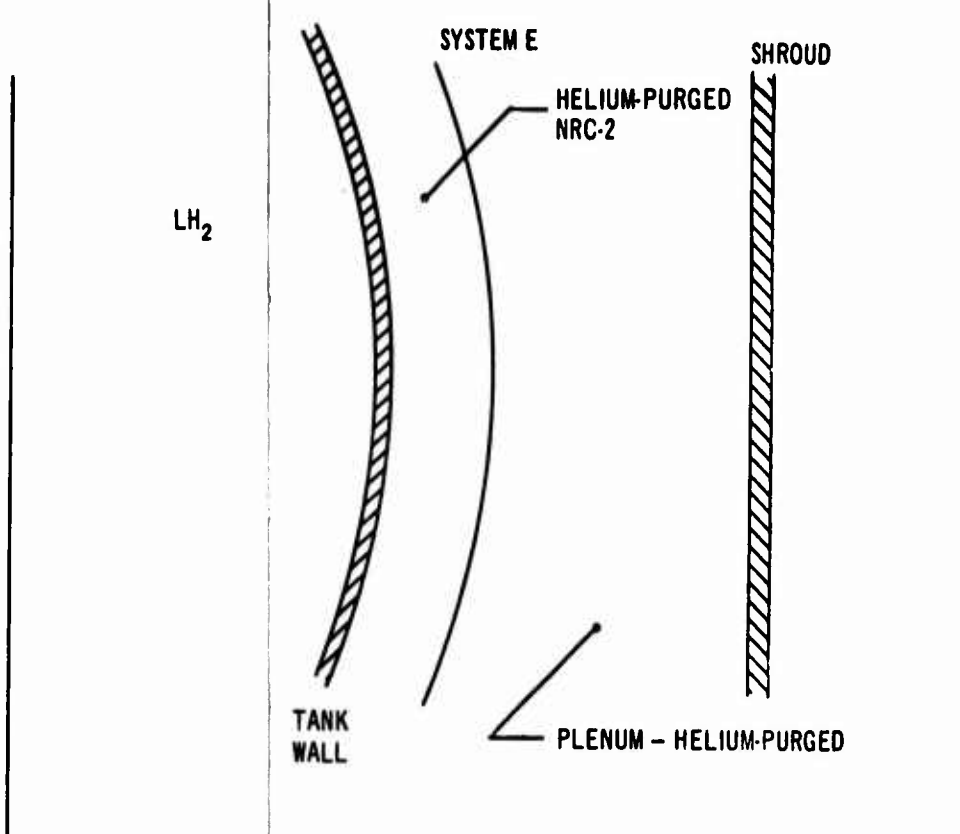
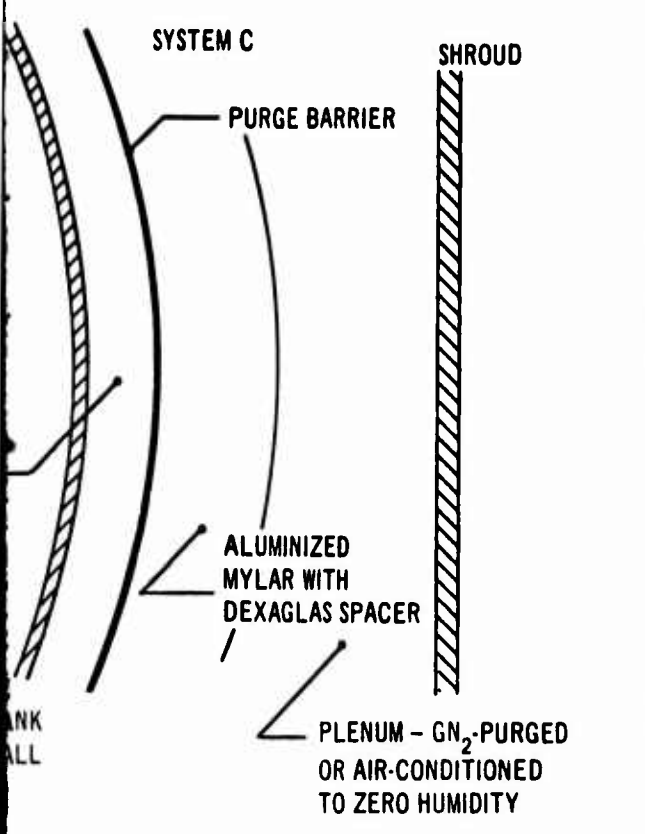


Figure 122. Insulation Systems

2

TABLE XLV  
INSULATION SYSTEMS

Design Requirements	A	B	C	D	E	F
Provide thermal protection in space	NRC-2	NRC-2	Aluminized Mylar and Dextraglas spacers	NRC-2	NRC-2	Damplar
Eliminate liquifaction or air during ground hold	Internal insulation	Felt and air-filled sealed bag	Helium-purged felt	Helium purge for NRC-2	Helium purge interstage	Helium purge for interstage
Withstand rapid depressurization	Insulation blanket design	Insulation blanket design	Insulation blanket design	Vent insulation blankets	Insulation blanket design vent interstage	Vent interstage insulation blanket design
Allow rapid degassing	Insulation blanket design	Insulation blanket design	Insulation blanket design	Vent or slit purge membrane	Insulation blanket design	Insulation blanket design
Minimize consumption of Helium	Does not use Helium	Does not use Helium	Recirculated Helium	Recirculated Helium	Recirculated Helium	Recirculated Helium
Provide thermal protection during boost	GN <sub>2</sub> in insulation plus internal insulation	GN <sub>2</sub> in insulation plus sealed bag	Helium in felt GN <sub>2</sub> in insulation	Helium in insulation	Helium in insulation	Helium in insulation
Minimize boiloff during ground hold	GN <sub>2</sub> in insulation plus internal insulation	GN <sub>2</sub> in insulation plus sealed bag	Helium in felt GN <sub>2</sub> in insulation	Helium in insulation	Helium in insulation	Helium in insulation
Avoid condensation of water on insulation	GN <sub>2</sub> interstage purge	GN <sub>2</sub> interstage purge	GN <sub>2</sub> interstage purge	Insulation in purged envelope	Helium purge for interstage	Helium purge for interstage
Allow leak checking of tank	Tank wall warm, use noncryogenic	Insulation removable	Insulation removable	Leak check before instillation	Insulation removable	Insulation not on tanks
Resist degrading effects of leaks	Blanket design, internal insulation is added leak barrier	Leaks confined beneath sealed bags	Leaks confined to felt by purge barrier	Blanket design	Blanket design	Insulation not on tanks

TABLE XLVI

SUBSTRATE MATERIAL PROPERTIES

Substrate	Conductivity, Btu/ft-R-hr	Density, lb/ft <sup>3</sup>
<b>LH<sub>2</sub> Temperatures</b>		
Helium Filled Fiberglass Felt Batting	0.015	0.5 to 4
Neon Filled Fiberglass Felt Batting	0.01	0.5 to 4
Nitrogen Filled Fiberglass Felt Batting	0.001 to 0.13	0.5 to 4
Cryopumped Polyurethane Foam	0.0015 to 0.0025	2 to 4
<b>LF<sub>2</sub>-LO<sub>2</sub> Temperatures</b>		
Helium Filled Fiberglass Felt Batting	0.04	0.5 to 4
Neon Filled Fiberglass Felt Batting	0.015	0.5 to 4
Nitrogen Filled Fiberglass Felt Batting	0.001 to 0.13	0.5 to 4
Cryopumped Polyurethane Foam	0.005 to 0.007	2 to 4

The NRC-2 type insulation was chosen because of its low  $\rho k$  product, however several of the other insulations would have comparable weight for the same thermal protection.

- (U) The selected method of fastening the insulation to the tank walls is described in Fig. 121. The panels of removable superinsulation are attached to the Dacron fabric backing with nylon threads. These panels are fastened to the tank by velcro fasteners for ease of removal. One half of the fastener is attached to the tank wall and the other half is sewn to the panel backing.

b. Earth Storable Propellants

- (U) Earth storable propellants, when used in a space environment, may need insulation to prevent freezing. The design requirements of Table XLIV that pertain to ground hold can be eliminated for the earth storable propellants. Since the propellants are at ambient temperature, there can be no boiloff, air liquefaction or water condensation. Also, since the vehicle skin temperature can be kept close to the propellant temperature, the rapid degassing properties of helium are not necessary and the helium purge can be eliminated.
- (U) As with the cryogenics, the panel type construction mounted on the tank appears to be preferable to other designs and the NRC-2 type insulation should provide the lightest system. The design chosen is similar to that of System E of Fig. 122 without the helium purge gas.

## APPENDIX III

### INTERNAL HEATING EFFECTS

#### 1. UNVENTED STORAGE

- (U) For unvented storage the propellants (liquid and vapor) fill the entire tank and have a constant mass. Therefore, the thermodynamic process followed by the propellant in a tank undergoing heat input is a constant-density process. This process can be analyzed with the use of a temperature-entropy (T-S) diagram using lines of constant density, constant enthalpy, and constant pressure.
- (U) As the heat is input to the tank, the enthalpy of the tank and its contents increases by an amount equal to the heat input. If the heat is considered to be distributed uniformly throughout the tank, the temperature and pressure in the tank can be found directly. For example, if the only content of the tank is propellant, the temperature and pressure after a particular heat addition by external sources can be found by moving along a constant density line from the initial temperature, pressure and enthalpy to the new enthalpy, which is simply the sum of the initial enthalpy and the heat input. The new temperature and pressure can then be read directly from the chart.
- (U) If there are other gases or liquids present in the tank, the heat input is divided among the tank and its contents, raising the enthalpies of all. In this case, an iterative procedure is necessary to calculate the final enthalpy of the tank and the contents, such that the final temperature of each is the same and the change in total enthalpy in the tank is equal to the heat input.
- (U) The problem of calculating the tank pressure, propellant vapor pressure, and amount of propellant vaporized for a given heat input by external sources can be separated into two parts: The calculation of the initial conditions; density, temperature, enthalpy, before heat input occurs; and the analysis of the constant density process from these initial conditions.
- (U) The conditions that exist before the constant-density heat addition process can be calculated by an energy and mass balance within the tank. This balance must take into account the previous history of the tank, including
  1. All previous heat input by external sources
  2. All heat and mass input by prepressurants
  3. All heat and mass input by pressurants
  4. All heat and mass removal by venting or propellant burn.

The following assumptions are necessary for the energy balance:

1. The tank comes to complete temperature equilibrium, there is no temperature stratification.
2. The tank comes to equilibrium so quickly that there is no heat input to the tank from external sources during the process.
3. There is no heat or mass loss from the tank during the process.

- (U) After the initial conditions have been found, the conditions in the tank, at any stage of storage having heat input only by radiation or conduction, can be calculated as a series of equilibrium stages. As heat is input, the propellant (liquid and vapor) undergoes a constant density process (i.e., total tank volume and mass of propellant remain constant even though the volume and mass of either the liquid or vapor portions may change). Any pressurant gases, however, do not have a constant volume and so do not have a constant density. Since the heat addition has been assumed to occur in a series of equilibrium stages, the enthalpy,  $h_p$ , of the propellant can be calculated at any later time from the conditions at the equilibrium starting point. An iteration must be made to obtain the energy division between the various constituents. To calculate the total pressure, the partial pressures of all the gases within the tank must be known. The pressure of the propellant vapor is known from the point on the T-S diagram. However, since the densities of the other gases are not constant and are not at saturation, the pressures must be calculated. This can be done by finding the volume occupied by the gases. Since all the gases occupy the same volume and have the same temperature and since the weight of each is known, the densities and pressures can be calculated.

## 2. VENTED STORAGE

- (U) Vented storage differs from unvented storage in the thermodynamic process followed by the propellant. In vented storage, the propellant has nearly constant temperature and pressure. The vapor pressure may change in vented storage if gases other than propellant vapor are present. This change occurs because venting depends upon the total tank pressure, which is the sum of the partial pressures of all the gases in the tank. The calculation of the equilibrium conditions after a firing is more difficult than for the equivalent unvented case.
- (U) As heat is input to the tank, liquid is vaporized and gases are vented. The amount of vaporization is determined by the heat of vaporization of the liquid at the tank temperature. If there are other gases in the tank, the partial pressure of these gases will decrease. (because some are vented and because the liquid volume decreases). The vapor pressure of the liquid must increase to open the vent valve, therefore the temperature must increase. This process can be approximated by a series of constant density heat inputs and adiabatic expansions. The calculation again consists of the two steps: (1) finding the initial conditions, and (2) finding the subsequent path from these initial conditions. A perfect liquid-vapor separator for venting is assumed.
- (U) The conditions that exist following venting but before the constant-density heat addition process cannot be calculated by an energy and mass balance because some of the energy and mass were vented to space. However, by making some assumptions, such a balance can be used as a step in finding the initial conditions. The assumptions which are necessary for performing the calculations are:

1. The vent valve opens immediately upon reaching the vent pressure.
2. There is no heat input from external sources during the decay process.
3. All venting is adiabatic.

Again, the previous history of the tank must be considered as an input to the calculations.

The calculations involved in the vented storage for finding the equilibrium conditions are the same as for the unvented case with the initial densities and enthalpies of the gases reduced by the adiabatic expansion to the reduced tank pressure. Actually the tank pressure fluctuates between a minimum and a maximum which are determined by the vent valve settings. Since the initial densities (and therefore weights) of the gases are now known, the tank can be allowed to come to equilibrium as in unvented storage. The propellant will then follow a constant-density process until its vapor pressure is high enough to bring the total pressure to the vent pressure. Venting will then occur reducing the tank pressure to the minimum pressure (the pressure at which the vent valve closes).

### 3. PRESSURANT GAS HEAT INPUT

- (U) To find the effect of the heat input by the pressurants, an energy balance must be performed. Basically, the method assumes that the materials within a propellant tank come to uniform equilibrium instantaneously after a firing. The method of finding this equilibrium state depends upon whether the tank is vented or unvented. However, both methods depend upon the conservation of mass and energy. For the energy balance calculations, the previous history of the tank must be considered; therefore, the heat inputs from external sources prior to a firing must be included in the calculation. The effects of external and internal heat sources therefore are not additive, but interact to make each possible duty cycle a separate case. The details of the energy balance calculations are described in the discussion of the unvented storage method.

#### APPENDIX IV

##### THERMAL HEAT SHORT ANALYSIS FOR THE $LF_2/LH_2$ VEHICLE

- (U) The heat conduction paths from the vehicle wall to the propellant tanks are the feed, fill and vent propellant transfer lines and the supports holding the tanks in position. By varying the material, length and area of these wall-to-tank connections, a variety of thermal resistances can be found. Several designs and their corresponding thermal resistances are discussed here and variations of these designs are suggested to obtain higher resistance. The design chosen in Ref. 4 is also included.
- (U) The supports for all the designs are the same, hollow fiberglass tubes 1.5 inches in diameter with a 0.003-inch wall. The supports of the oxidizer tank are 9.1 inches long; those of the hydrogen tank are 16.25 inches long.
- (U) The various heat leak models are compared for the line lengths, conductivities, cross-sectional areas, diameters, wall thicknesses, and thermal resistance in Tables XLVII through L. Differences in thermal conductivities reflect different references; those used in this study are averaged from the integrated values given in WADD 60-56.
- (U) Model A has aluminum propellant lines for compatibility with the aluminum tanks. The lines are assumed to be empty of propellants.
- (U) Model B is the design generated for Ref. 4. The propellant lines are of stainless steel and the hydrogen line has a fiberglass and stainless steel heat block. The lines contain liquid and vapor.
- (U) Model C is the design selected to determine the heating rates used in the analysis. The design is similar to Model B but some of the line sizes and lengths have been changed because of the final stage design analysis presented in Ref. 4.
- (U) Model D is similar to Model C with several design changes made to improve the thermal resistance. The major change is the disconnecting of the fill line before launch.
- (U) Those lines which contain heat blocks may be of either aluminum or stainless steel since the line above the heat block is liquid filled. The heat block itself is vapor filled. The lines above the heat blocks are assumed to be insulated against radiation from the walls.

TABLE XLVII

FEED LINES

Model	A	B	C	D
<b>Hydrogen Tank</b>				
Material	Aluminum	Heat Block	Heat Block	Heat Block
Length, feet	2.3	0.5	1.0	2.0
Diameter, inches	3.0	3.0	3.0	3.0
Wall, inches	0.03	0.01	0.01	0.01
Thermal Conductivity, Btu/hr-R-ft	140.0	8.0	5.6	5.6
Resistivity, hr-R/Btu	7.8	160.0	440.0	880.0
<b>Oxidizer Tank</b>				
Material	Aluminum	Stainless	Heat Block	Heat Block
Length, feet	14.0	1.0	1.0	2.0
Diameter, inches	3.0	3.0	3.0	3.0
Wall, inches	0.03	0.03	0.01	0.01
Thermal Conductivity, Btu/hr-R-ft	120.0	8.0	5.6	5.6
Resistivity, hr-R/Btu	56.0	60.0	640.0	1280.0

TABLE XLVIII

## VENT LINES

Model	A	B	C	D
<b>Hydrogen Tank</b>				
Material	Aluminum	Stainless	Stainless	Stainless
Length, feet	3.0	2.0	3.0	6.0
Diameter, inches	3.0	2.0	2.0	1.0
Wall, inches	0.03	0.03	0.02	0.02
Thermal Conductivity, Btu/hr-R-ft	140.0	8.0	5.6	5.6
Resistivity, hr-R/Btu	10.2	160.0	600.0	2400.0
<b>Oxidizer Tank</b>				
Material	Aluminum	Stainless	Stainless	Stainless
Length, feet	2.0	1.25	2.0	4.0
Diameter, inches	3.0	2.0	2.0	1.0
Wall, inches	0.03	0.03	0.02	0.02
Thermal Conductivity, Btu/hr-R-ft	120.0	8.0	5.6	5.6
Resistivity, hr-R/Btu	8.0	120.0	400.0	1600.0

TABLE XLIX

FILL LINES

Model	A	B	C	D
<b>Hydrogen Tank</b>				
<b>Material</b>	<b>Aluminum</b>	<b>Stainless</b>	<b>Stainless</b>	<b>Detached</b>
<b>Length, feet</b>	1.0	1.0	1.0	--
<b>Diameter, inches</b>	3.0	3.0	2.0	--
<b>Wall, inches</b>	0.03	0.03	0.02	--
<b>Thermal Conductivity, Btu/hr-R-ft</b>	140.0	8.0	5.6	0
<b>Resistivity, hr-R/Btu</b>	3.4	60.0	200.0	0
<b>Oxidizer Tank</b>				
<b>Material</b>	<b>Aluminum</b>	<b>Stainless</b>	<b>Stainless</b>	<b>Detached</b>
<b>Length, feet</b>	1.0	1.0	1.0	--
<b>Diameter, inches</b>	3.0	3.0	2.0	--
<b>Wall, inches</b>	0.03	0.03	0.02	--
<b>Thermal Conductivity, Btu/hr-R-ft</b>	120.0	8.0	5.6	--
<b>Resistivity, hr-R/Btu</b>	4.0	60.0	200.0	--

TABLE L

TOTAL THERMAL RESISTIVITY  
(HR-R/BTU)

Model	Hydrogen Tank	Fluorine Tank
A	2.0	2.5
B	30.0	36.0
C	115.0	115.0
D	640.0	640.0

## APPENDIX V

### TEMPERATURE CONTROL SURFACES FOR USE IN EARTH ORBITAL ENVIRONMENT

- (U) One of the major parameters in the thermal analysis of a Maneuvering Space Propulsion System is the ratio of the solar absorptivity to infrared emissivity ( $\alpha/\epsilon$ ) of the vehicle outer wall. A variety of outer wall coatings is available (Ref. 12 and 14) to provide almost any  $\alpha/\epsilon$  surface. The radiative properties of a number of these materials are reviewed in order to provide a basis for the design choices presented in this report.
- (U) The material chosen for the outer wall coating of a Maneuvering Space Propulsion System must be compatible with the aluminum wall material, must withstand boost phase heating and abrasion, must be unaffected by a wide temperature range in space, and must remain useful after long-term exposure to electromagnetic and particle radiation effects in space.
- (U) A number of materials which appear to meet these requirements (Ref. 12 and 14) are listed in Table LI with their ratio of solar absorptivity to infrared emissivity ( $\alpha/\epsilon$ ). The  $\alpha/\epsilon$  value shown is the value measured after the materials were exposed to a simulated space environment including exposure to ultraviolet radiation.
- (U) Using these coatings or a combination of them, any  $\alpha/\epsilon$  value between 0.185 and 6.0 can be obtained. By covering different fractions of a vehicle's surface with two or more of these coatings, almost any desired outer wall temperature within the range 340 R to 800 R can be obtained in near-Earth orbit.

TABLE LI

## RADIATION PROPERTIES OF COATINGS

<u>Wall Coating</u>	<u>Ratio of Solar Absorptivity to Infrared Emissivity</u>
Gold on Magnesium	6.0
Mystik Tape	2.4
Black Kemacryl	1.03
Aluminum Paint	0.85
White Kemacryl	0.31
LMSC Ematal ( $K_2Y_iO(C_2O_4)_2$ )	0.65
LMSC Lithafrax	0.32
LMSC Ultrox	0.22
LMSC Synthetic, $li Al Si O_4$	0.29
RTD Anodized Aluminum	0.37
LMSC Thermatrol 6A-100 Silicone	0.28
American Cyanamid S7094-3	0.31
American Cynamid S7094-4	0.34
MANE $Ti O_2$ - Acrylic	0.39
IITRI Z-93	0.20
IITRI S-13	0.23
DAC $Ti O_2$ Epoxy	0.22
DAC White Porcelain Enamel	0.21
DAC Synthetic Spodumene in Sodium Silicate	0.20
DAC Zinc Oxide in Potassium Silicate	0.19
DAC Zirconium Silicate in Potassium Silicate	0.185

# CONFIDENTIAL

## APPENDIX VI

### SELECTION OF HYDROGEN PRESSURANT INJECTION TEMPERATURE

- (U) Subsequent to the completion of the study of Ref. 4 an error in the calculated heat content of the expulsion pressurant gases was noted. The actual heat content of the expulsion pressurant is greater than originally predicted by a factor of about 2 and 1.4 for the LH<sub>2</sub> and LF<sub>2</sub> pressurants, respectively. These factors are equal to the respective collapse factors for each tank. The computer program which was used to evaluate the tank pressure histories during coast failed to account for the additional heat transfer into the propellants as reflected by the collapse factors. In other words, while the pressurant requirements were properly calculated based on the appropriate collapse factor, the heat content of the pressurant was based on a collapse factor of 1 for each tank. Consequently, a correct accounting of the pressurant heat content results in higher heat transfer into the propellant as the gases are cooled subsequent to an engine burn phase than initially calculated. This results in more propellant evaporation and higher tank pressures during the coast phase for the 90/10 duty cycle
- (C) The above error was corrected in the program and the most thermally critical duty cycle was re-evaluated. The duty cycle chosen was the 90/10 cycle with a payload to 5000 pounds. In this duty cycle, 90 percent of the propellant is used immediately after the vehicle reaches orbit. Following a 14-day coast, the remaining propellant is then used. The 5000 pound payload was used instead of 2000 pounds since the propellant load is lowest for the 5000 pound payload case. This results in a higher heat input per pound of propellant than for the 2000 pound payload vehicle.
- (U) The initial re-evaluation was for the final configuration of the vehicle described in Ref. 4. This vehicle used 25 sheets of NRC-2 insulation on the LH<sub>2</sub> tank and 60 sheets on the LF<sub>2</sub> tank. The pressurant inlet temperatures were 1000 R and 500 R for the LH<sub>2</sub> and LF<sub>2</sub> tanks, respectively. Nominal effective thermal resistivities of 44 R/Btu for the LH<sub>2</sub> tank and 34 R/Btu for the LF<sub>2</sub> tank were used in this and subsequent calculations. A re-analysis of this vehicle with the corrected pressurant heat content revealed that the hydrogen tank had to be vented during the 14-day coast while the LF<sub>2</sub> tank did not. Therefore, subsequent analysis was restricted to determining the combination of insulation thickness and pressurant inlet temperature which would allow the 90/10 mission to be flown over a 14-day period without venting.
- (U) Figure 123 is a plot of total LH<sub>2</sub> boiloff due to orbit heating and/or propellant conditioning prior to the last burn as a function of pressurant inlet temperature. These curves were based on a collapse factor variation with temperature as defined in Vol. III of Ref. 4. It can be seen from these curves that boiloff cannot be prevented with up to 180 sheets of insulation at an inlet temperature of 1000 R. Additional sheets would not prevent venting since the predominant heat load into the propellant comes

from the pressurant gases and not from the vehicle sidewall as the insulation is increased. It is apparent from Fig. 123 that the only practical way of further reducing the heat transfer into the LH<sub>2</sub> is to reduce the pressurant inlet temperature.

- (U) To determine the optimum pressurant inlet temperature for the LH<sub>2</sub> tank, the vehicle performance was plotted as a function of pressurant temperature. This plot is shown in Fig. 124. By crossplotting the no-vent (or no boiloff) conditions of Fig. 123 on Fig. 124, a no-vent region may be generated as shown in Fig. 124. From the envelope of this region, an optimum pressurant temperature of about 175 R to 200 R is established in conjunction with 100 to 120 sheets of insulation. It is interesting to note the relative insensitivity of vehicle performance with variation in temperature and amount of insulation. Also, it is noteworthy that slightly higher performance may be achieved if venting was allowed.
- (U) The possibility of cooling the hydrogen gas from 1000 R to 200 R by employing a heat exchanger in the LH<sub>2</sub> inlet line at a point downstream of the turbopump was discussed in Ref. 4. This approach appears feasible and it should be possible to obtain gaseous hydrogen from the engine system at 200 R for LH<sub>2</sub> tank pressurization.

CONFIDENTIAL

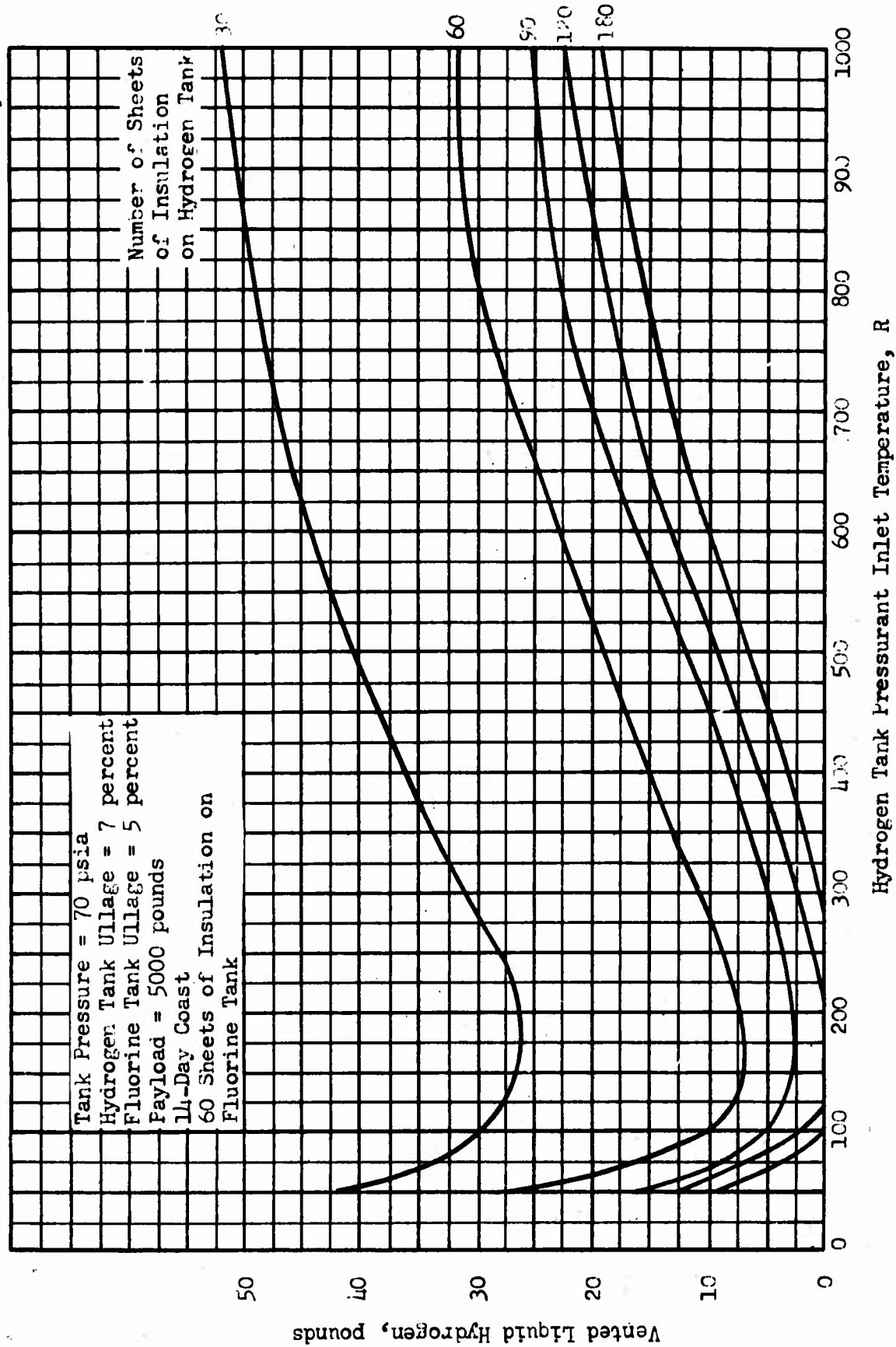


Figure 123. Effects of Hydrogen Pressurant Temperature and Insulation on Hydrogen Boiloff for 90/10 Duty Cycle

CONFIDENTIAL 271

CONFIDENTIAL

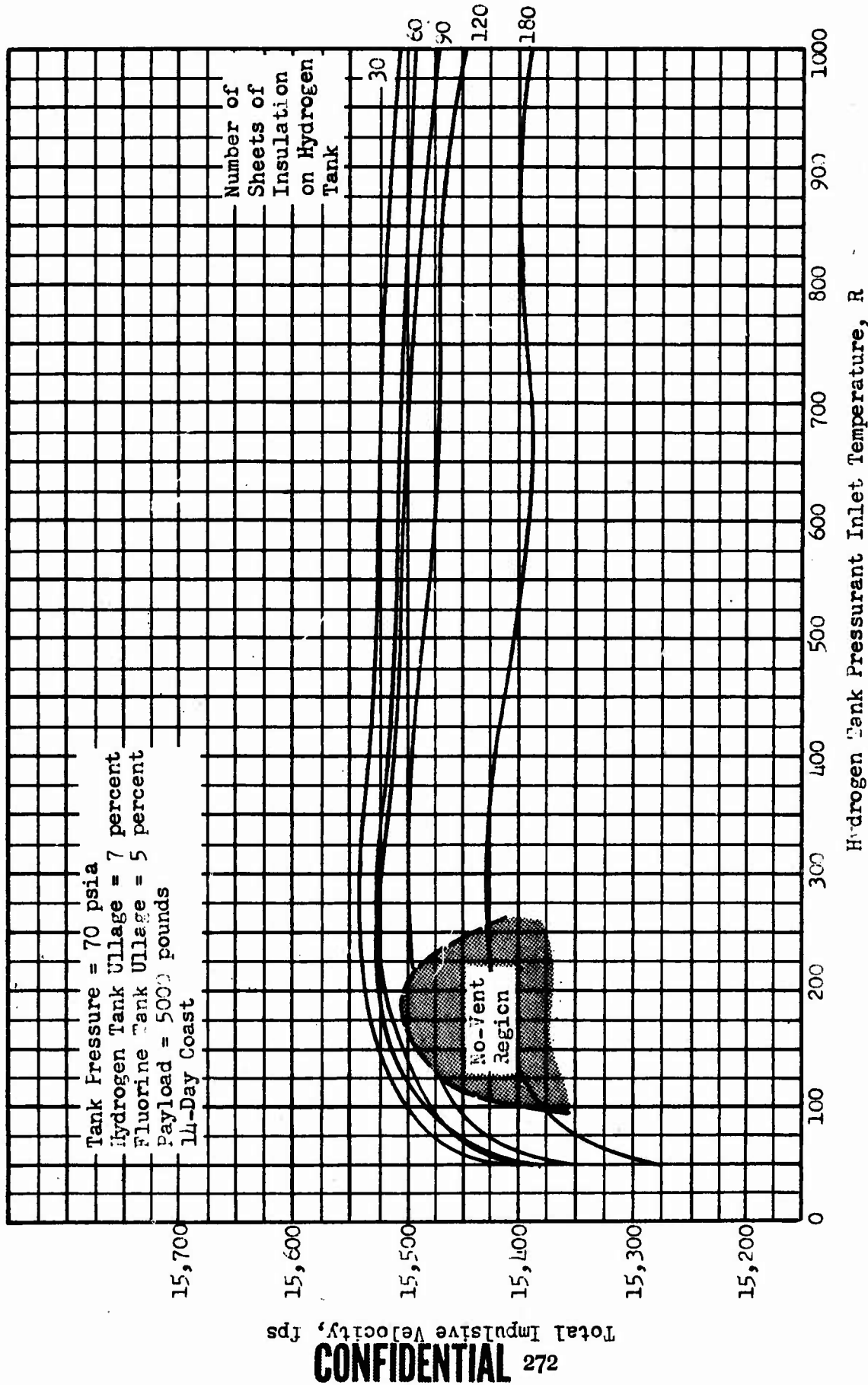


Figure 12. Hydrogen Tank Pressurant Inlet Temperature and Insulation Optimization, 90/10 Duty Cycle

CONFIDENTIAL 272

## APPENDIX VII

### THERMAL CONDITIONING SYSTEM

- (U) Direct venting of the propellant ullage in low-g environments leads to loss of helium pressurant gas and excessive loss of liquid hydrogen by entrainment. Such losses can be reduced and effective tank pressure control realized if liquid hydrogen is withdrawn from the tank, expanded, and then vaporized by extracting heat from the bulk propellant.
- (U) The basic function of the liquid propellant thermal conditioning system is to maintain positive pressure control in the liquid hydrogen tank during low-g coast periods in space flight when location of the gas ullage region is somewhat uncertain. This positive control is accomplished through the combined use of three and possibly four basic hardware units:
  - Liquid removal unit
  - Expansion unit
  - Heat exchanger unit
  - Mixer unit
- (U) The liquid removal unit provides a sufficient mass transfer rate of liquid hydrogen to the expansion unit and heat exchanger so that the total enthalpy change results in adequate heat removal from the propellant. Since the volumetric ratio of saturated vapor to liquid hydrogen is 43 (at a liquid hydrogen temperature of 37.7 R), the thermal conditioning system must have a liquid removal unit design for providing liquid in a near zero-g environment. Use of a single phase liquid hydrogen during venting prevents loss of the helium pressurant gas.
- (U) The expansion unit lowers the pressure of the incoming liquid, subcooling it below the bulk temperature of the remaining liquid in the tank. This temperature drop provides the necessary thermal driving potential for operation of the heat exchanger.
- (U) The heat exchanger unit may be located inside the tank or on the tank wall. By warming and converting the subcooled liquid to a saturated or superheated vapor, heat may be removed or intercepted. More than one heat exchanger may be connected in series and located at various tank hot spots.
- (U) A mixer unit may be required; specifically if the thermal conditioning system employs a compact heat exchanger located in the propellant tank. Since gravity-forced convection is absent at zero-g, heat transfer would be limited to the conduction mode. Consequently, fluid currents should be made to flow over the heat exchanger to increase the heat transfer rates by forced convection and maintain positive pressure control throughout the tank. It is also possible that cooled propellant drawn throughout the heat exchanger and discharged along the tank walls may effect suppression of vapor bubbles formation by ensuring a sufficiently large heat

transfer coefficient to remove, by forced convection, all heat entering through the tank wall. In the event that bubbles are generated on the tank wall at points of high local heating the mixer will serve to aid in the removal or detachment of vapor bubbles from the wall.

- (U) On the basis of these system functional requirements, a number of liquid propellant thermal conditioning system concepts have been defined, to provide a basis for component parametric data development and component matching requirements. These concepts are shown in Fig. 125. In some, a capillary standpipe is used to position the liquid so that it always covers the inlet tube to the expansion valve. This component can be used with either an on-tank or a bulk-fluid heat exchanger, with or without a mixer. Also shown are systems employing a wicking material as the liquid removal unit. This device also can be used with either heat exchanger, with or without a mixer. If no mixer is used to continuously flow liquid hydrogen past the wick, then the latter must be placed near enough to the tank bottom that it can be refilled during the next to last engine firing. Thus, its placement is dependent upon the mission expulsion profile. A third type of liquid removal unit is a dynamic liquid-vapor separator. Although dynamic liquid-vapor separators have been previously evaluated for vapor vent systems and found to be inefficient, it appears possible to design such a device for efficient liquid extraction. This type of liquid removal unit would probably be integral with bulk fluid heat exchanger. One conceptual thermal conditioning system is shown with no mixer; this system is considered possible only with a tank-wall heat exchanger and a continuously operating system. The heat exchanger should be designed to intercept all the heat before it gets into the tank, which implies a concentration of coils at points of high heat flux.
- (U) These systems serve to identify the components that require analysis. A list of the important parameters for each of these components is shown in Table LII. The results of such an analysis would permit determination of the optimum grouping of the components and system performance for specified mission requirements.
- (U) The proper utilization of a typical thermal conditioning system on the  $LH_2$  tank can result in a non-vented oxidizer tank. That is, the  $GH_2$  after leaving the  $LH_2$  tank heat exchanger can be used to cool the oxidizer tank, thereby eliminating the requirement of oxidizer tank venting. The required operational cycles for maintaining  $LH_2$  tank pressure control determine the oxidizer tank heat exchange and insulation systems necessary to ensure thermal compatibility within the oxidizer tank. Subcooling of the oxidizer should present no particular problems. The oxidizer tank insulation system can be altered and optimized to limit the amount of subcooling. If the cycle could potentially result in freezing the oxidizer, by-pass controls could be utilized on the oxidizer tank heat exchanger. At no time should the oxidizer tank govern the operation of the  $LH_2$  tank thermal conditioning system. Such a procedure would represent inefficient operation through unnecessary subcooling of the  $LH_2$ . The  $LH_2$  tank pressure control should govern the optimization of the oxidizer insulation and heat exchanger systems.

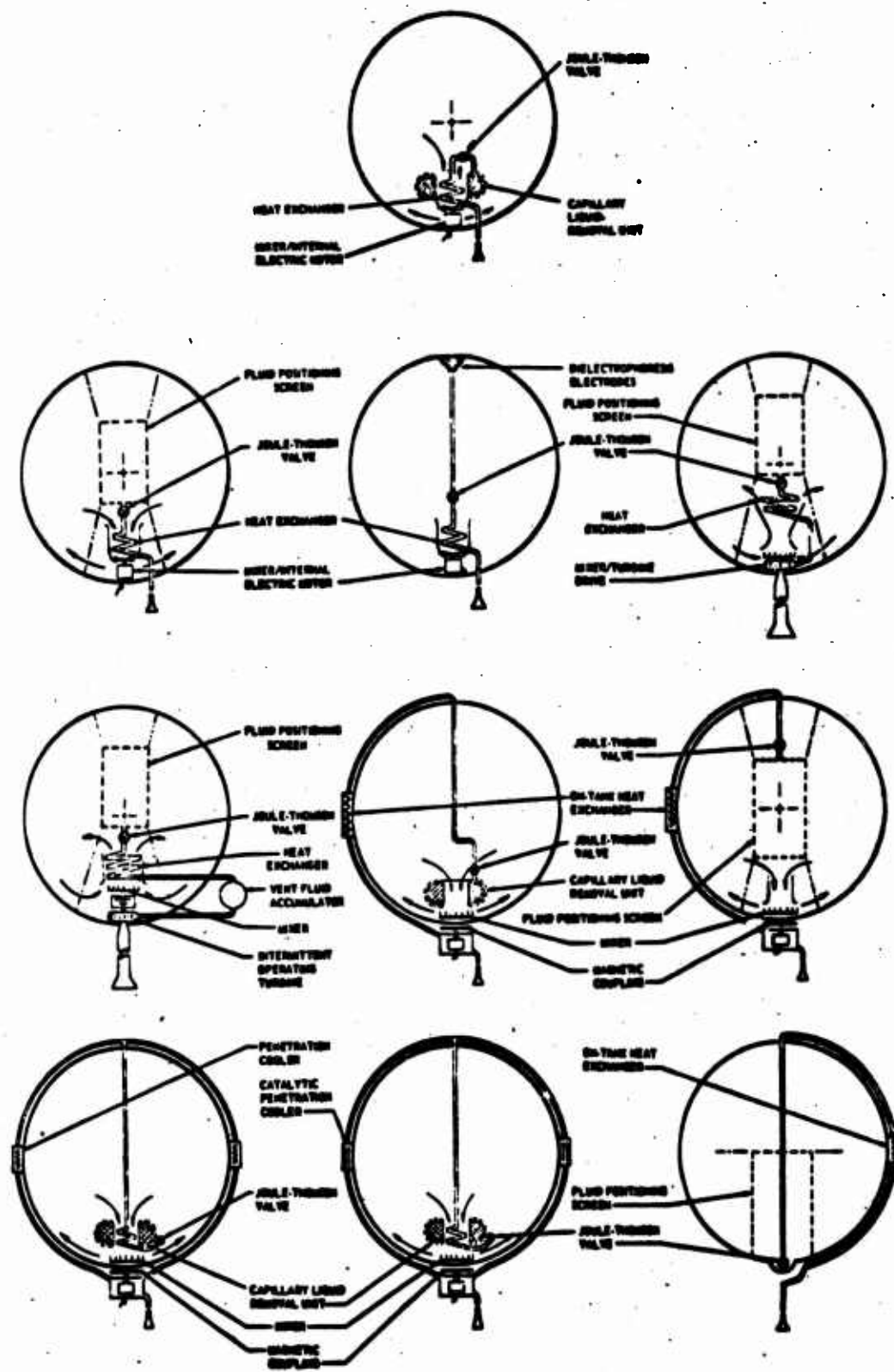


Figure 125. Conceptual Thermal Conditioning Systems

**TABLE LII**  
**COMPONENT PARAMETERS**

Component	Dependent Parameter	Independent Parameter
Liquid Removal Units Capillary Standpipe	Minimum dimensions  Weight	Minimum ullage volume Tank diameter  Tank diameter Tank height Tank volume Minimum ullage
Wicking Device	Minimum pull-through dimension  Weight	Capillary pressure drop fluid surface velocity  Maximum radius Minimum pull-through dimension Material density
Dynamic Separator	Weight Dimensions Power	Inlet fluid quality Vent flow rate Separation efficiency
Dielectrophoretic Device	Number of electrodes  Weight	Voltage Electrode spacing Ullage volume  Vehicle size Electrode spacing Voltage Vehicle acceleration
Expansion Units Valves	Maximum temperature differential Vent fluid quality into heat exchanger  Weight Size	Valve pressure drop    Pressure drop Vent fluid flow rate Tank pressure
Turbines	Weight Diameter Power output  Efficiency	Vent fluid flow rate Inlet pressure Turbine pressure ratio Efficiency  Speed Reynolds number

TABLE LII (Continued)

Component	Dependent Parameter	Independent Parameter
Heat Exchanger Units On-Tank Heat Exchanger	Cold side heat transfer coefficients Vent fluid pressure drop  Tube attachment spacing  Weight	Vent fluid flow rate Tube size Fluid quality Fluid pressure  Tank thickness Maximum heat flux  Tube size Tank radius Maximum heat flux Expansion fluid temperature drop Tank pressure
Compact Heat Exchanger	Warm side coefficients  Weight Dimensions  Vent fluid pressure drop	Circulation velocity  Vent fluid flow rate Total heating rate Pressure drop Inlet quality Circulation velocity  Vent fluid flow rate Inlet quality Heat exchanger flow volume
Impeller	Efficiency  Weight Diameter Power input	Speed Reynolds number  Bulk fluid circulation rate Bulk fluid quality Efficiency
Wall Jet	Jet velocity Heat transfer coef. Bubble size Shroud weight	Reynolds number Frohde number Vehicle acceleration Tank size
Drive Units Electric Motors	Diameter Weight	Power output Motor type
Turbine	Same data as for expansion turbine	Expansion turbine data

## APPENDIX VIII

### CORRELATION OF CALCULATED PROPELLANT BOILOFF RATES WITH TEST DATA

- (U) A number of simulated environmental tests have been performed by the General Electric Company upon cryogenic propellant tanks of approximately the same size and configuration as those of the nominal MSPS. These results were reported in Ref. 15. Although the tank supports and insulation were of a different type than those selected for the analysis presented in this report, the heat leak rates through these were found to be comparable to the selected MSPS design. In addition the feed and fill lines were similar to those used in the analysis and the overall heat input rates were in the same range as those determined in the analysis presented in this report.
- (U) The tanks were orientated with one side constantly facing the solar simulator. This represents a maximum heat input. The test program was conducted with  $\text{LN}_2$  as the cryogen and the results of these tests were used to predict the boiloff rates for several cryogenic rocket propellants. The results are shown in Table LIII.
- (U) These results are similar to the calculated values given in the text of this report for the hydrogen tanks of the selected cryogenic vehicles and for the oxygen tank of the  $\text{LO}_2/\text{LH}_2$  vehicle. For example, the calculated boiloff rate for the 8-foot diameter  $\text{LH}_2$  tank of the  $\text{LF}_2/\text{LH}_2$  vehicle was 27.8 percent/year, that of the 10-foot diameter  $\text{LH}_2$  tank of the  $\text{LO}_2/\text{LH}_2$  vehicle was 17.7 percent/year. The calculated boiloff rate of the oxygen tank of the  $\text{LO}_2/\text{LH}_2$  vehicle was 1.4 percent/year for a 7-foot diameter tank. There is reasonable agreement between the results of the analysis presented in this report and the predicted values of propellant boiloff rates determined from the General Electric Co. test program. The advanced design concepts and thicker insulation incorporated in the thermal model would account for the indicated differences.
- (U) As further correlation of the analytical predictions, the percent loss of propellant per day found by General Electric Company for an 8-foot tank are shown in Fig. 126 and 127 for various vehicle orientations (projected tank area ratio). The test numbers compare very well with the calculated loss rate of 0.106 percent/day based on use of an insulation thickness (3 inches) which corresponds to that of the test tank. The thermal model for the analysis actually was insulated with six inches of NRC-2 and had a boiloff rate of 0.076 percent/day. This comparison supports the analysis presented in this report and indicates that reasonable design concepts were incorporated in the thermal model.

TABLE LIII

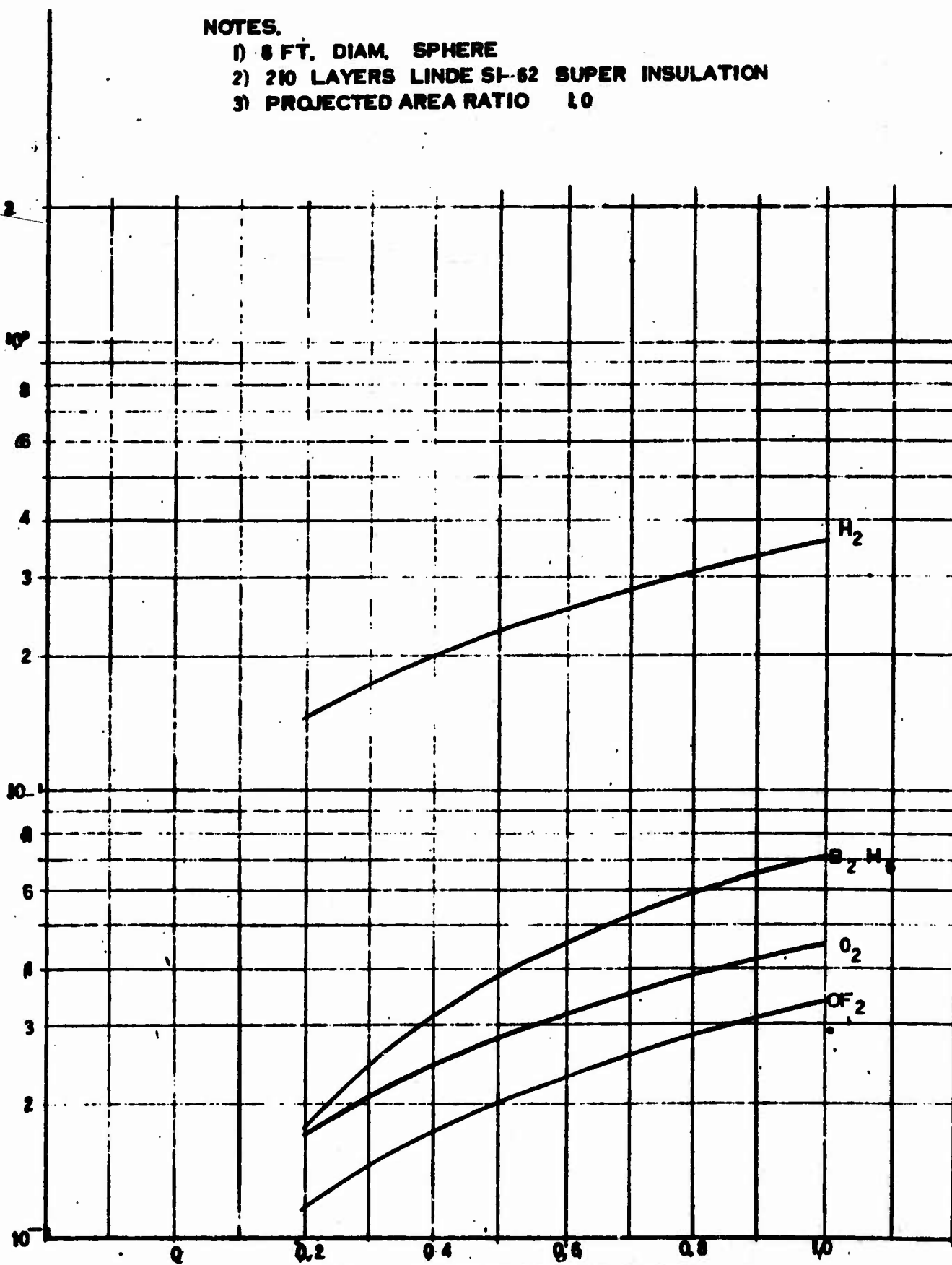
STORAGE CHARACTERISTICS OF SELECTED  
CRYOGENIC PROPELLANTS

Propellant	Tank Diameter, feet	Percent Boil- off Per Year
Hydrogen	10	27.3
	15	10.9
	20	6.9
Diborane	10	3.7
	15	1.4
	20	0.9
Oxygen	10	3.3
	15	1.3
	20	0.8
Oxygen Difluoride	10	2.3
	15	0.9
	20	0.6

NOTES.

- 1) 8 FT. DIAM. SPHERE
- 2) 210 LAYERS LINDE SI-62 SUPER INSULATION
- 3) PROJECTED AREA RATIO 1.0

PERCENT LOSS OF ORIGINAL PROPELLANT MASS PER DAY



$\alpha/\epsilon$ , MICROMETEOROID SHIELD

Figure 126. Boiloff Rate vs  $\alpha/\epsilon$

NOTES.

- 1) 8 FT. DIAM. SPHERE
- 2) 210 LAYERS LINDE SI-62 SUPER INSULATION
- 3) PROJECTED AREA RATIO 0.5

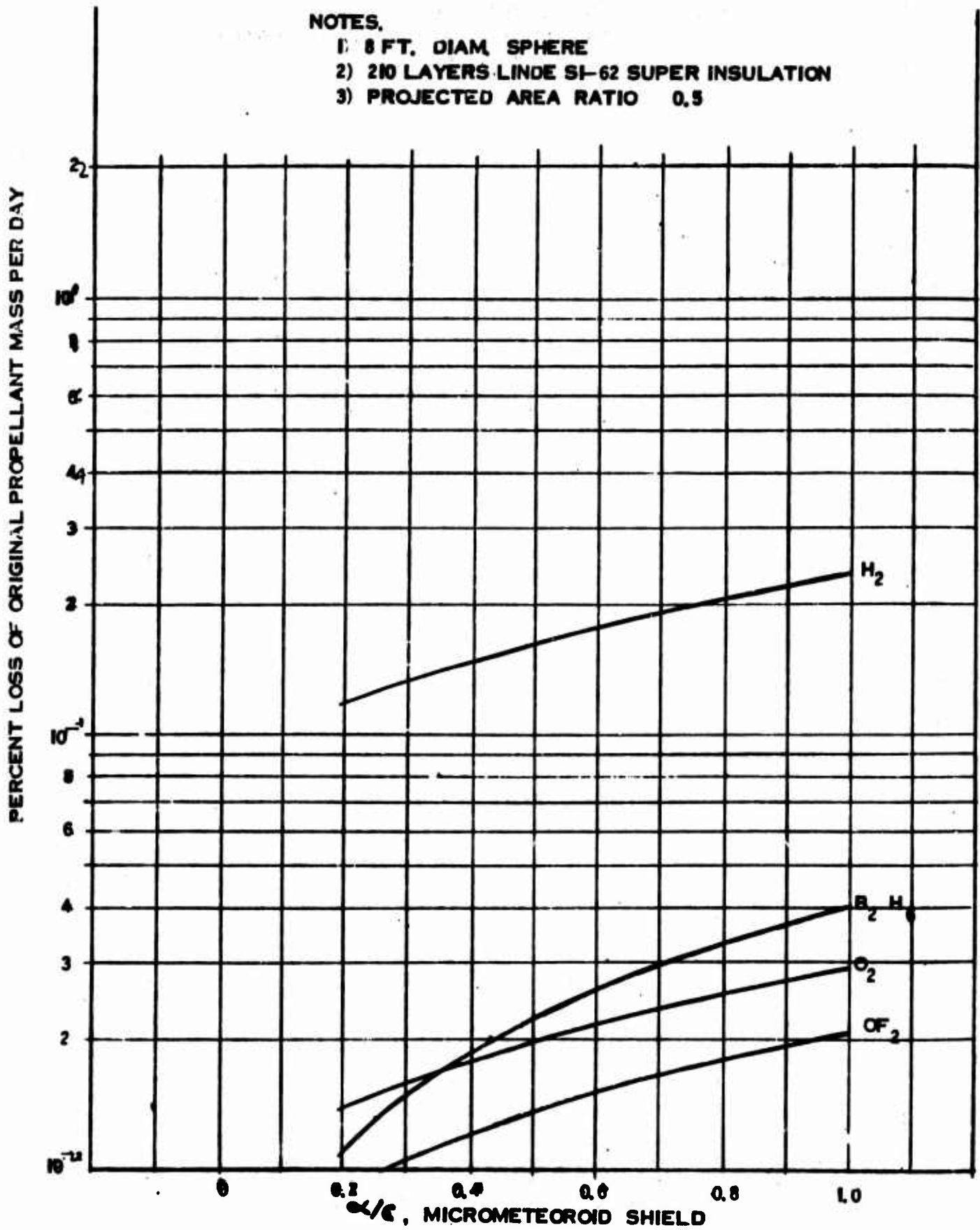


Figure 127. Boiloff Rate vs  $\alpha/\epsilon$

# CONFIDENTIAL

## REFERENCES

1. Vehicle Description and Mission Definition Data Book, Preliminary Draft, Saturn I-B/Centaur Joint Contractors Working Group, 10 August 1965
2. AFRPL-TR-65-252, Vol. IV, Maneuvering Satellite Propulsion System Optimization Study, Rocketdyne, a Division of North American Aviation, Inc., Canoga Park, California, April 1966, Secret
3. AFRPL-TR-65-252, Vol. II, Book II, Maneuvering Satellite Propulsion System Optimization Study, Confidential
4. AFRPL-TR-65-252, Vol. III, Maneuvering Satellite Propulsion System Optimization Study, Confidential
5. R-5940-2, Advanced Aerodynamic Spike Configurations, Third Quarterly Progress Report, Contract AF04(611)-9948, Rocketdyne, a Division of North American Aviation, Inc., Canoga Park, California, April 1965, Confidential
6. AFRPL-TR-65-174, Final Report - Large Centerbody High Area Ratio Annular Nozzle of Minimum Length, Rocketdyne, October 1965, Confidential
7. R-5375, Optimization of Operating Conditions for Manned Space Craft Engines, Final Report, Vol. III, Contract No. NAS7-164, Rocketdyne, November 1963.
8. Petrozzi, P. J. and L. E. Dean, Physical Properties of Liquid Propellants, Report No. LRP 178, Aerojet-General Corporation, Sacramento, California, 13 July 1960.
9. R-3999, Investigation of Cooling Problems at High Chamber Pressure, Final Report for Period 9 April 1962 to 8 January 1963, Rocketdyne, May 1963
10. LMSC-A742593, Vol. VI, Design of High Performance Insulation Systems, Lockheed Missiles and Space Company, Sunnyvale, 20 August 1965
11. DAC SM-53108, A Systems Approach to HPI or 'Why Trade a Headache for an Upset Stomach?', Missile and Space Systems Division Douglas Aircraft Company, Santa Monica, June 1966
12. AF04(611)-10750, System Effects on Propellant Storability and Vehicle Performance, Douglas Aircraft Company Huntington Beach, May 1965 - February 1966
13. Lindquist, C. R. Linde Company Super Insulation Applied to Space Vehicles, 1 December 1962
14. AF33(615)-1634, Temperature Control Coatings for Cryogenic Temperature Substrates, Lockheed Missiles and Space Company, Sunnyvale, March 1966
15. AF04(611)-9078, Propellant Storability in Space, General Electric Company, Philadelphia, May 1963 - June 1964

**CONFIDENTIAL**

Security Classification

DOCUMENT CONTROL DATA - R&D		
<i>(Security classification of title, body of abstract and indexing annotation must be entered when the overall report is classified)</i>		
1. ORIGINATING ACTIVITY (Corporate author) Rocketdyne, a Division of North American Aviation, Inc., 6633 Canoga Avenue, Canoga Park, California		2a. REPORT SECURITY CLASSIFICATION <b>CONFIDENTIAL</b>
		2b. GROUP 4
3. REPORT TITLE ADVANCED THRUST CHAMBER FOR SPACE MANEUVERING PROPULSION, TASK I SYSTEM STUDIES FINAL REPORT		
4. DESCRIPTIVE NOTES (Type of report and inclusive dates) Final Report, September 1966		
5. AUTHOR(S) (Last name, first name, initial) Pauckert, R. P.		
6. REPORT DATE 15 November 1966	7a. TOTAL NO. OF PAGES 303	7b. NO. OF REFS 15
8a. CONTRACT OR GRANT NO. AF04(611)-11617	8a. ORIGINATOR'S REPORT NUMBER(S) R-6730	
b. PROJECT NO.	8b. OTHER REPORT NO(S) (Any other numbers that may be assigned this report) AFRPL-TR-66-301	
c.		
d.		
10. AVAILABILITY/LIMITATION NOTICES In addition to security requirements which must be met, this document is subject to special export controls and each transmittal to foreign governments or for- eign nationals may be made only with prior approval of AFRPL, Edwards, Calif. 93523		
11. SUPPLEMENTARY NOTES	12. SPONSORING MILITARY ACTIVITY Air Force Rocket Propulsion Laboratory Edwards Air Force Base, California	
13. ABSTRACT The previous study results of Contract AF04(611)-10745 are extended to investigate the capabilities of increased gross weight Maneuvering Space Propul- sion Systems (MSPS) using $LF_2/LH_2$ , $LO_2/LH_2$ , and $N_2O_4/N_2H_4$ -UDMH(50-50) propellants. The range of stage gross weights considered was based on the payload capabilities of Titan III-C and Saturn I-B and several growth versions of these launch vehicles. Maneuvering space propulsion system gross weights ranging from 20,000 to 50,000 pounds were shown to result in velocity increment capabilities up to 29,000 ft/sec for the 2000-pound payload $LF_2/LH_2$ system. The concentric aerody- namic spike/bell engine configuration was selected for the $LF_2/LH_2$ and $LO_2/LH_2$ system design thrust levels investigated. The configuration selected for the $N_2O_4/N_2H_4$ -UDMH(50-50) consisted of one larger primary bell nozzle engine and two small secondary bell nozzle engines. The orbit storage life capabilities of the three propellant combinations were determined and compared for a 20,000-pound- gross weight stage. The $LF_2/LH_2$ system provided higher $\Delta V$ capabilities than the other propellants for orbital storage times up to 2 years with full propellant tanks. The $\Delta V$ advantage for the $LF_2/LH_2$ systems is also maintained when mission duty cycles result in partial propellant loads for the major portion of the storage duration. (C)		

DD FORM 1473  
JAN 64

**CONFIDENTIAL**  
Security Classification

14. KEY WORDS	LINK A		LINK B		LINK C	
	ROLE	WT	ROLE	WT	ROLE	WT
Propulsion System Advanced Engines Space Vehicles System Performance Propellant Storage						

**INSTRUCTIONS**

1. **ORIGINATING ACTIVITY:** Enter the name and address of the contractor, subcontractor, grantee, Department of Defense activity or other organization (*corporate author*) issuing the report.
- 2a. **REPORT SECURITY CLASSIFICATION:** Enter the overall security classification of the report. Indicate whether "Restricted Data" is included. Marking is to be in accordance with appropriate security regulations.
- 2b. **GROUP:** Automatic downgrading is specified in DoD Directive 5200.10 and Armed Forces Industrial Manual. Enter the group number. Also, when applicable, show that optional markings have been used for Group 3 and Group 4 as authorized.
3. **REPORT TITLE:** Enter the complete report title in all capital letters. Titles in all cases should be unclassified. If a meaningful title cannot be selected without classification, show title classification in all capitals in parenthesis immediately following the title.
4. **DESCRIPTIVE NOTES:** If appropriate, enter the type of report, e.g., interim, progress, summary, annual, or final. Give the inclusive dates when a specific reporting period is covered.
5. **AUTHOR(S):** Enter the name(s) of author(s) as shown on or in the report. Enter last name, first name, middle initial. If military, show rank and branch of service. The name of the principal author is an absolute minimum requirement.
6. **REPORT DATE:** Enter the date of the report as day, month, year; or month, year. If more than one date appears on the report, use date of publication.
- 7a. **TOTAL NUMBER OF PAGES:** The total page count should follow normal pagination procedures, i.e., enter the number of pages containing information.
- 7b. **NUMBER OF REFERENCES:** Enter the total number of references cited in the report.
- 8a. **CONTRACT OR GRANT NUMBER:** If appropriate, enter the applicable number of the contract or grant under which the report was written.
- 8b, 8c, & 8d. **PROJECT NUMBER:** Enter the appropriate military department identification, such as project number, subproject number, system numbers, task number, etc.
- 9a. **ORIGINATOR'S REPORT NUMBER(S):** Enter the official report number by which the document will be identified and controlled by the originating activity. This number must be unique to this report.
- 9b. **OTHER REPORT NUMBER(S):** If the report has been assigned any other report numbers (*either by the originator or by the sponsor*), also enter this number(s).
10. **AVAILABILITY/LIMITATION NOTICES:** Enter any limitations on further dissemination of the report, other than those

imposed by security classification, using standard statements such as:

- (1) "Qualified requesters may obtain copies of this report from DDC."
- (2) "Foreign announcement and dissemination of this report by DDC is not authorized."
- (3) "U. S. Government agencies may obtain copies of this report directly from DDC. Other qualified DDC users shall request through \_\_\_\_\_."
- (4) "U. S. military agencies may obtain copies of this report directly from DDC. Other qualified users shall request through \_\_\_\_\_."
- (5) "All distribution of this report is controlled. Qualified DDC users shall request through \_\_\_\_\_."

If the report has been furnished to the Office of Technical Services, Department of Commerce, for sale to the public, indicate this fact and enter the price, if known.

11. **SUPPLEMENTARY NOTES:** Use for additional explanatory notes.

12. **SPONSORING MILITARY ACTIVITY:** Enter the name of the departmental project office or laboratory sponsoring (*paying for*) the research and development. Include address.

13. **ABSTRACT:** Enter an abstract giving a brief and factual summary of the document indicative of the report, even though it may also appear elsewhere in the body of the technical report. If additional space is required, a continuation sheet shall be attached.

It is highly desirable that the abstract of classified reports be unclassified. Each paragraph of the abstract shall end with an indication of the military security classification of the information in the paragraph, represented as (TS), (S), (C), or (U).

There is no limitation on the length of the abstract. However, the suggested length is from 150 to 225 words.

14. **KEY WORDS:** Key words are technically meaningful terms or short phrases that characterize a report and may be used as index entries for cataloging the report. Key words must be selected so that no security classification is required. Identifiers, such as equipment model designation, trade name, military project code name, geographic location, may be used as key words but will be followed by an indication of technical context. The assignment of links, rules, and weights is optional.